

UNIVERSITY OF CALIFORNIA

Los Angeles

**Critical Percolation, Universality, and  $SLE_6$**

A dissertation submitted in partial satisfaction  
of the requirements for the degree  
Doctor of Philosophy in Mathematics

by

Guo-Ying Lei

(a.k.a. Helen K. Lei)

June 2010



The dissertation of Guo–Ying Lei (a.k.a. Helen K. Lei) is approved.

---

Joseph A. Rudnick

---

Benjamin Sudakov

---

Terence (Chi–Shen) Tao

---

Lincoln Chayes, Committee Chair

University of California, Los Angeles

June 2010

## DEDICATION

As I do not see the compilation of this dissertation representing any fundamental change in my intellectual life, I can only understand this to be an opportunity to pause in my academic endeavors to express my most heartfelt gratitude to all who helped me along the way. As such, this and the more formal acknowledgements that follow are indeed the most important parts of this manuscript.

I am most fortunate to have always had people in my life to teach me to place my humanity above all else, for after all, I like to believe that the best mathematics is a result of neither ego nor genius, but simply the very human desire to understand, and be understood. I would not be where I am today without my family, friends, and let me not forget the kindness of strangers, to remind me to never lose heart and that we were all strangers once....

THIS MANUSCRIPT IS DEDICATED TO  
ALL OF MY TEACHERS,  
IN THE BROADEST SENSE OF THE WORD.

# Contents

<b>List of Figures</b>	<b>vi</b>
<b>Acknowledgements</b>	<b>x</b>
<b>Vita</b>	<b>xiv</b>
<b>Publications</b>	<b>xv</b>
<b>Abstract of the Dissertation</b>	<b>xvi</b>
<i>Bibliography</i> . . . . .	xvii
<b>I Introduction</b>	<b>1</b>
I.1 Critical Percolation and Properties . . . . .	3
I.2 The Scaling Limit and Cardy's Formula . . . . .	5
I.3 Site Percolation on the Triangular Lattice . . . . .	7
I.4 Other Models and Universality . . . . .	8
I.5 Convergence to $\text{SLE}_6$ . . . . .	10
I.6 Uniform Continuity of Crossing Probabilities . . . . .	12
I.7 Guide to the Manuscript . . . . .	12
<i>Bibliography</i> . . . . .	15

<b>II Random Cluster Models on the Triangular Lattice</b>	<b>19</b>
II.1 Introduction . . . . .	20
II.2 Generalized Star–Triangle Relations: Percolation . . . . .	23
II.3 Generalized Star–Triangle Relations: Random Cluster Measure . . . . .	35
II.4 Conclusion . . . . .	51
<i>Bibliography</i> . . . . .	52
 <b>III Cardy’s Formula for Certain Models of the Bond–Triangular Type</b>	 <b>58</b>
III.1 Introduction . . . . .	59
III.2 Bond–Triangular Lattice Problems . . . . .	64
III.3 Paths and Path Designates . . . . .	74
III.4 Convergence to Cardy–Carleson Functions . . . . .	100
III.5 Conclusion . . . . .	124
III.6 Appendix 1: Harris–FKG Properties and Criticality . . . . .	126
III.7 Appendix 2: Equivalence of the Cardy–Carleson Functions . . . . .	130
<i>Bibliography</i> . . . . .	143
 <b>IV Discrete Approximations and Extraction of Cardy’s Formula for General Domains</b>	 <b>147</b>
IV.1 Introduction . . . . .	148
IV.2 The Carathéodory Minimum . . . . .	150
IV.3 Interior Approximations . . . . .	153

IV.4 Sup-Approximations . . . . .	158
IV.5 Verification of Boundary Values for $u, v, w$ . . . . .	167
<i>Bibliography</i> . . . . .	177
<b>V Convergence to <math>SLE_6</math></b>	<b>181</b>
V.1 Introduction . . . . .	182
V.2 Conformal Invariance of the Scaling Limit . . . . .	184
V.3 Properties of Typical Explorer Paths . . . . .	205
V.4 The Model . . . . .	219
<i>Bibliography</i> . . . . .	238
<b>VI Restricted Uniform Continuity of Crossing Probabilities</b>	<b>243</b>
VI.1 Preliminaries . . . . .	245
VI.2 Properties of Slits Under Consideration . . . . .	246
VI.3 Statement and Proof of Main Result . . . . .	257
VI.4 Corollaries to the Main Result . . . . .	285
<i>Bibliography</i> . . . . .	288

# List of Figures

II.1	Phase diagram for percolation problem on the triangular lattice; variable $s$ suppressed. The line $a = e$ is the self-dual line. The curve $ae = 2s^2$ separates the regions with and without positive correlations. Within the region of positive correlations, $a > e$ is the percolation phase, $a < e$ non-percolating with exponential decay of connectivities and percolation of the <i>dual</i> model. These phases are divided by the self-dual line, where there is no percolation of either type and critical behavior is observed. Some of these results may be extended out of the region of positive correlations by monotonicity. . . . .	32
III.1	Bond percolation as a hexagon tiling problem: (a) Typical bond configuration on the triangular lattice. (b) Amalgamation into relevant connected objects. (c) Associated tiling problem using hexagons and split hexagons.	65

III.2	Correspondence between eight configurations on (up-pointing) triangles and five hexagon configurations. All four configurations which fully connect the triangle map to the single, fully yellow, hexagon with total weight $a$ . Empty configuration has probability $e$ and maps to the fully blue hexagon. The three single bond configurations lead to split hexagons, each carrying probability $s$ . Note that not all the possible ways of splitting a hexagon appears: Images obtained from the above three by reflections in the $x$ -axis are not present. . . . .	67
III.3	A flower. . . . .	69
III.4	In a triggering configuration (three yellows, two of which are contiguous) a split hexagon is forbidden. The iris is pure yellow or pure blue with conditional probabilities one-half. . . . .	71
III.5	A circumstance leading to asymmetry in conditional color switching. . .	86
III.6	A case with $ \diamond  = 1$ and $ \mathcal{D}  = 3$ . . . . .	89
III.7	All paths transmit through the iris. . . . .	93
IV.1	Violation of condition ii) in Definition IV.3.1, which would lead to incorrect (limiting) boundary values. . . . .	156
IV.2	Masking and intermixing of boundary values. . . . .	159
IV.3	A case where the limiting domains does not contain a component present in approximating domains. Due to frequent self-touching, such (limiting) domains are in fact typical of $\text{SLE}_6$ . . . . .	162
IV.4	The domain $\mathcal{V}_n$ , etc. . . . .	164
IV.5	Failure to continue $\mathcal{P}$ to $\mathcal{P}_r$ inside $B(a)$ . . . . .	167

V.1	Atypical behavior of $\mu_\varepsilon$ curves. . . . .	210
V.2	A jump of magnitude $l$ occurring in the vicinity of the prime end $c$ . . .	214
V.3	The three allowed “split” states of the hexagon. Note that these correspond to single bond occupancy events in the corresponding up-pointing triangle in the bond-triangular lattice percolation problem. . . . .	220
V.4	The setup for the definition of the Exploration Process. . . . .	223
V.5	“Multistep” procedure by which the Exploration Process gets through a mixed hexagon. . . . .	225
VI.1	Atypical behavior of $\mu_\varepsilon$ curves . . . . .	248
VI.2	Division of configurations containing a left-right blue crossing for $R_1$ into cases. . . . .	261
VI.3	Reduction of case 3 to case 2. . . . .	262
VI.4	Scenarios where it is easy to reduce to the highest crossing. . . . .	264
VI.5	Case where $\beta_0$ is manifesting the conditions of case 2 but a higher crossing may not be. . . . .	265
VI.6	The region $\mathbb{B}$ and $\mathbb{B}^c$ – the unconditioned region. . . . .	270
VI.7	Outcome of Claims 1 and 2. . . . .	271
VI.8	Multiply connected domain. . . . .	272
VI.9	The point $\gamma^*$ . . . . .	273
VI.10	$\gamma(t^*)$ cannot be trapped between $\gamma_1$ and $\gamma_2$ . . . . .	274
VI.11	$\gamma_2$ pseudo-pods. . . . .	276
VI.12	Two possible orientations of blue pseudo-pods. . . . .	277
VI.13	Scenario where $\gamma_2$ “hides” behind $\gamma_1$ . . . . .	279
VI.14	Final RSW construction to continue crossing. . . . .	281

## ACKNOWLEDGEMENTS

What follows represent joint work with I. Binder and L. Chayes, so it goes without saying that none of this would have been possible without them. My advisor Lincoln Chayes has been with me from the very beginning and never gave up, on me or on our projects.

I have had an especially long and very colorful association with the UCLA Math Department, where since the Fall of 2001 I have taken/TAed/sat in 57 quarter courses and attended many seminars. In the last couple of years I spent quite a bit of time working in the Applied Math Room.

Across from the UCLA Math Department lies the Institute for Pure and Applied Mathematics (IPAM) which has played a defining role in my research career thus far. I was officially in residence at IPAM during the Spring of 2007, and unofficially attended parts of the Optimal Transport program in the Spring of 2008 and the Kinetic Transport program in the Spring of 2009. I have also enjoyed the three wonderful weeks spent at Lake Arrowhead culminating and reunion conferences in the Spring of 2007 and the Winters of 2008 and 2009. Indeed, a lot of my research thus far, including projects not collected in this thesis, had their origins in these IPAM programs.

Away from UCLA, I wish to acknowledge the hospitality of Georgia Institute of Technology and the University of Toronto – which I visited more than once – during my research visits, and the two Oberwolfach conferences I have attended, in the summers of 2006 and 2009. I also made short visits to the University of Cambridge, University of Southern California and California Institute of Technology, as well as attending the 93rd and 103rd Statistical

Mechanics Meetings at Rutgers University.

Lastly, I would like to thank Stas Smirnov, for his beautiful proof of Cardy's Formula for site percolation, which is what led me to pursue most of the research collected herein. I have meandered a bit in my mathematical interests since the work in [12] and [13], but I will always consider myself very fortunate to have found a mathematical home in such a rich area.

Financially I was supported by the VIGRE fellowship during my first couple of years, by the NSF over most summers, and by the Graduate Research Mentorship Program and the Dissertation Year Fellowship Program in the last two years (detailed acknowledgements appear below).

Almost each of the works that are compiled here has benefitted from discussions with other mathematicians. Their names appear here in alphabetical order (detailed acknowledgements again appear below): Marek Biskup, John Garnett, Jonathan Handy, Stas Smirnov, Christoph Thiele, Wendelin Werner. Also, I would like to thank one of our referees for a previous version of what is now Chapter V, for pointing out a mistake in our original proof of continuity of crossing probabilities (now in Chapter VI) and making some helpful comments, and for suggesting that we reorganize the paper to separate out model specifics from a general proof of convergence.

Bibliographical information and acknowledgements for relevant chapters:

- Chapter II is a version of *Random Cluster Models on the Triangular Lattice*, joint with L. Chayes. Appeared in Journal of Statistical Physics **122**, no. 4, 647–670 (2006).

**Acknowledgements:** This research was supported by the NSF grant DMS–0306167.

- Chapter III is a version of *Cardy’s Formula for Certain Models of the Bond-Triangular Type*, joint with L. Chayes. Appeared in Reviews in Mathematical Physics **19**, no. 5, 51–565 (2007).

**Acknowledgements:** We would like to acknowledge useful conversations with Jonathan Handy, Marek Biskup, John Garnett, and Christoph Thiele concerning the uniqueness of the functions  $h_{\mathcal{A}}$ ,  $h_{\mathcal{B}}$  and  $h_{\mathcal{C}}$  on the basis of the existing boundary conditions. This work was in part supported by NSF under the grant DMS-0306167.

- Chapter IV is a version of *On Convergence to  $SLE_6$  II: Discrete Approximations and Extraction of Cardy’s Formula for General Domains*, joint with I. Binder and L. Chayes. Submitted to Journal of Statistical Physics.

**Acknowledgements:** The authors are grateful to the IPAM institute at UCLA for their hospitality and support during the *Random Shapes*

*Program* (where this work began). The conference was funded by the NSF under the grant DMS-0439872. I. B. was partially supported by the NSERC under the DISCOVER grant 5810-2004-298433. L. C. was supported by the NSF under the grant DMS-0805486. H. K. L was supported by the NSF under the grant DMS-0805486 and by the *Dissertation Year Fellowship Program* at UCLA.

The authors would also like to thank Wendelin Werner for useful discussions which took place during the Oberwolfach conference *Scaling Limits in Models of Statistical Mechanics* and which led to the present approach.

- Chapter V is a version of *On Convergence to  $SLE_6$  I: Conformal Invariance for Certain Models of the Bond-Triangular Type*, joint with I. Binder and L. Chayes. Submitted to Journal of Statistical Physics.

**Acknowledgements:** The authors are grateful to the IPAM institute at UCLA for their hospitality and support during the *Random Shapes Program* (where this work began). The conference was funded by the NSF under the grant DMS-0439872. I. B. was partially supported by the NSERC under the DISCOVER grant 5810-2004-298433. L. C. was supported by the NSF under the grants DMS-0306167 and DMS-0805486. H. K. L was supported by the NSF VIGRE grant, and the *Graduate Research Mentorship Program* and the *Dissertation Year Fellowship Program at UCLA*.

The authors would like to thank John Garnett for various pertinent conversations and would like to express their gratitude to Stas Smirnov for *numerous* conversations and consultations. The authors would also like to thank Wendelin Werner for some useful discussions.

# VITA

November 6, 1983	Born, Chongqing, China
Winter 2005	B. S., Mathematics University of California Los Angeles, California
2005 – 2006	Teaching Assistant Department of Mathematics, UCLA
Spring 2007	Random Shapes Program IPAM, Los Angeles, California
Fall 2007 & Winter 2008	Teaching Assistant Department of Mathematics, UCLA
2008 – 2009	Graduate Research Mentorship Program Department of Mathematics, UCLA
2009 – 2010	Dissertation Year Fellowship Department of Mathematics, UCLA

## PUBLICATIONS

Chayes, L., and Lei, H. K. (2006). *Random Cluster Models on the Triangular Lattice*. *Journal of Statistical Physics* **122**, no. 4, 647–670.

Chayes, L., and Lei, H. K. (2007). *Cardy's Formula for Certain Models of the Bond-Triangular Type*. *Reviews in Mathematical Physics* **19**, no. 5, 511–565.

Kim, I. C., and Lei, H. K. (2010). *Degenerate Diffusion With a Drift Potential: A Viscosity Solutions Approach*. *Discrete and Continuous Dynamical Systems* **27**, no. 2, 767–786.

# ABSTRACT OF THE DISSERTATION

## Critical Percolation, Universality, and $SLE_6$

by

Guo-Ying Lei (a.k.a. Helen K. Lei)

Doctor of Philosophy in Mathematics

University of California, Los Angeles, June, 2010

Professor Lincoln Chayes, Chair

Since the introduction of the Schramm–Löwner–Evolution (SLE) in 2000 ([25]), tremendous progress has been made in rigorously understanding the scaling limits of various 2D critical statistical mechanics models in two dimensions (see [22]). The starting point of understanding the scaling limit of a 2D critical lattice model is to consider the model on a bounded domain  $\Omega \subset \mathbb{R}^2$  and find a suitable observable at the discrete level which satisfies some discrete analyticity or harmonicity condition; these sorts of properties translate into

some interior analyticity statement in the continuum limit and, together with establishment of suitable boundary values, leads to conformal invariance in the continuum limit. For percolation, the appropriate observable is the crossing probability – conjectured to converge to the so-called Cardy’s Formula in the continuum. In [13], Smirnov established conformal invariance of critical site percolation on the triangular lattice (in the scaling limit) by considering a triplet of observables related to crossing probability. However, Smirnov’s proof takes advantage of the complete symmetry in the case of site percolation on the triangular lattice, and the triplet observables do not easily adapt themselves to percolation on other lattices.

This dissertation, representing joint work with L. Chayes and I. Binder (see [12], [13], [4], [5], [6]), contains construction of a non-trivial class of models for which we establish Cardy’s Formula and, following the approach outlined in [22], establishes convergence to  $SLE_6$  for the law of the interface, thus establishing some limited statement of *universality*. In the course of (and in addition to) accomplishing this, we obtain some results which may find applicability to other percolation models: 1) We show how to extract Cardy’s Formula given some interior analyticity statement (this requires some treatment of the discretization procedure in relation to retrieval of suitable boundary values) for a general class of domains; 2) our convergence to  $SLE_6$  proof is applicable for any percolation model satisfying reasonable assumptions *and* for which Cardy’s Formula can be established; 3) we obtain some (almost) uniform estimates on crossing probabilities which may contribute to establishing some statement of rate of convergence to  $SLE_6$ .

# Bibliography

- [1] I. Binder, L. Chayes, and H. K. Lei. *On Convergence to  $SLE_6$  II: Discrete Approximations and Extraction of Cardy's Formula for General Domains*. Submitted.
- [2] I. Binder, L. Chayes, and H. K. Lei. *On Convergence to  $SLE_6$  I: Conformal Invariance for Certain Models of the Bond-Triangular Type*. Submitted.
- [3] I. Binder, L. Chayes, and H. K. Lei. *Restricted Uniform Continuity of Crossing Probabilities in Slit Domains*. Unpublished manuscript.
- [4] L. Chayes and H. K. Lei. *Random Cluster Models on the Triangular Lattice*. *Journal of Statistical Physics* **122**, no. 4, 647–670 (2006).
- [5] L. Chayes and H. K. Lei. *Cardy's Formula for Certain Models of the Bond-Triangular Type*. *Reviews in Mathematical Physics* **19**, no. 5, 51–565 (2007).
- [6] O. Schramm. *Scaling Limits of Loop-Erased Random Walks and Uniform Spanning Trees*. *Israel Journal of Mathematics*, **118**, 221-288 (2000).

- [7] S. Smirnov. *Critical Percolation in the Plane: Conformal Invariance, Cardy's Formula, Scaling Limits*. C. R. Acad. Sci. Paris Sr. I Math. **333**, 239–244 (2001).

Also available at <http://www.math.kth.se/~stas/papers/percras.ps>.

- [8] S. Smirnov. *Towards Conformal Invariance of 2D Lattice Models*. Proceedings of the International Congress of Mathematicians, Madrid, Spain, 2006.

# Chapter I

## Introduction

Phase transition is a ubiquitous natural phenomenon, the simplest example being that of the transition from a liquid phase to a gaseous one, or the ferromagnetic transition. At a more refined level, phase transitions can be either discontinuous or continuous, characterized by exponential and power law decay of correlations, respectively. Continuous transitions especially display very interesting behavior near the transition point, also called the critical point: Many quantities of physical interest are found to satisfy a power law of the form  $|T - T_c|^{-\omega}$ , where  $T_c$  is the critical parameter, and  $\omega$  is some scaling exponent. In 2D, assuming various analytical properties of the scaling limits of such models, physicists have made many predictions on critical behavior, including exact values of scaling exponents. It is also expected that some universal behavior should hold: The same model on different lattices should converge to the same conformally invariant limit.

The mathematical description of such models involve putting a parameter dependent probability measure on the space of all possible configurations. The

setup is as follows: Start with some domain  $\Omega \subset \mathbb{R}^2$  with two marked boundary points  $a$  and  $b$ , consider the lattice model at criticality on some discretization  $\Omega_\delta$  of  $\Omega$ , and take the mesh size  $\delta$  to zero. Often, if the model is considered with suitable boundary conditions, then a distinguishing curve which runs from  $a$  to  $b$ , called the *interface*, naturally arises in any configuration. These curves then generate, through the underlying probability measure, a measure on curves. O. Schramm suggested ([25]) that the limits of such  $\mu_\delta$  are given by a one parameter family of laws on random curves,  $\text{SLE}_\kappa$ , which can be described as follows: Let us consider the curves  $\gamma(t)$  to be growing from 0 to  $\infty$  on the upper half plane, and let  $g_t$  be the conformal map from  $\mathbb{H} \setminus \gamma_t$  to  $\mathbb{H}$ , then  $g_t$  satisfies

$$\partial_t g_t(z) = \frac{2}{g_t(z) - \sqrt{\kappa} B_t}, \quad g_0(z) = z$$

where  $B_t$  is the standard Brownian motion. The SLE's are characterized by two properties: 1) conformal invariance and 2) Markov property. These two properties can be easily described: Let  $\mu$  denote the law of SLE curves, then if  $(\Omega, a, b)$  and  $(\Omega', a', b')$  are domains with two marked boundary points and  $\varphi : \Omega \rightarrow \Omega'$  is a conformal map, then conformal invariance requires that

$$\varphi(\mu(\Omega, a, b)) = \mu(\varphi(\Omega), \varphi(a), \varphi(b)).$$

On the other hand, the Markov property states that

$$\mu(\Omega, a, b) |_{\gamma[0,t]} = \mu(\Omega \setminus \gamma[0,t], \gamma(t), b),$$

i.e., the law conditioned on an initial portion of the curve is the same as the law in the domain formed by deleting the same initial portion of the curve.

There has been much mathematical progress establishing the convergence to SLE of various models: See [18, 20, 13, 23].

As explained in [18] and [22], in order to prove convergence, what is required is 1) some *a priori* estimates which ensure the limiting measure (whose existence is guaranteed by the Banach–Alaoglu Theorem) is supported on sufficiently nice curves and 2) to find a good observable at the discrete level for a sufficiently general class of domains and establish convergence and conformal invariance of the observable, and 3) finally use the corresponding continuum observable to pin down the value of  $\kappa$  (thus uniquely specifying the limiting measure). The properties of the specific model under consideration feature heavily in the first two items and conformal invariance is encoded in some discrete analyticity or harmonicity of the relevant observable. Especially in the cases of statistical mechanics models ([13, 23]), nice properties of the corresponding observables actually follow from non-trivial combinatorial arguments at the discrete level. Once convergence to SLE has been established, using SLE one can recover information of interest about the model, e.g., computation of critical exponents (see [24]).

## I.1 Critical Percolation and Properties

The focus of the present manuscript is on critical percolation models, which we now describe: Consider some regular lattice structure, e.g., the bond square lattice or hexagonal tiling of  $\mathbb{R}^2$ . We let each bond, site, or tile be blue with probability  $p$  and otherwise yellow, with probability  $1 - p$ , independently; this

induces a measure on the space of all possible configurations. It is well known that there is a non-trivial, lattice dependent critical value  $p_c$  such that a vertex is connected to infinity by a blue path with positive probability if and only if  $p > p_c$ . For classical percolation results we allude to in the present section and elsewhere, we refer the reader to [8] and [10].

In 2D, there is a suitably defined notion of a dual lattice and a dual percolation problem. E.g., for bond percolation on the square lattice, the dual sites are placed in the middle of faces of the direct lattice and we declare a dual edge to be yellow if and only if the direct edge it crosses is yellow. The square lattice is self-dual: The dual lattice is a shift of the original lattice, and corresponding to a parameter value  $p$  is a parameter  $p^*$  on the dual lattice, and, finally, we denote by  $p_{sd}$  the point where  $p = p^*$ . A similar notion of duality works for the hexagonal tiling problem, and here the direct and dual lattices actually coincide. Due to overwhelming symmetry, we actually have  $p_c = p_{sd} = 1/2$  for both bond percolation on the square lattice and hexagonal tiling.

It is the case that we have exponential decay of blue correlations (i.e., the probability that two sites  $x$  and  $y$  are connected by a blue path decays like  $e^{-\xi|x-y|}$ ) in the subcritical case, and by duality the same statement for yellow in the supercritical case. By contrast, at criticality there is power law decay of correlations for both species: The probability of a monochrome connection between  $x$  and  $y$  can be bounded from above and below by the distance between them raised to some power. There are also scale-invariant bounds on crossing probabilities: There are upper and lower bounds for the crossing probability of

a  $L$  by  $\gamma L$  rectangle which only depend on  $\gamma$ , and not  $L$ . (Again, this is true for both blue and yellow crossings.) Further, such scale invariant estimates can be “stitched” together to derive scale invariant bounds on existence of blue (or yellow) rings in an annulus: Typically, we have two scales  $\eta < \delta$  and set up  $\log(\delta/\eta)$  annuli; the probability that there exists a ring in each annulus is uniformly bounded below by  $\alpha$ , independently. Therefore the probability there does not exist a ring in any annulus tends to zero as  $\eta/\delta \rightarrow 0$ . These are the so-called Russo–Seymour–Welsh (RSW) estimates, which is a basic tool in deriving *a priori* estimates on (mathematical) quantities derived from critical percolation.

Now suppose we are interested in the behavior near criticality. If we assume that the relevant quantities of interest, for example the probability a site is connected to infinity, the average finite cluster size, or the typical radius of a cluster, behave like  $(p - p_c)$  raised to some power, then using non-rigorous methods scaling relations had been derived and numerical values for the various exponents conjectured. Also, these exponents are expected to be *universal*, which for examples means that they should be lattice independent. Kesten in [17] rigorously showed that to understand near critical behavior, it is enough to study the critical problem: In particular, to compute all the relevant exponents, it is enough to compute the one-arm and two-arm exponents at criticality.

## I.2 The Scaling Limit and Cardy's Formula

The idea is then to start with a bounded domain  $\Omega$ , tile it with a lattice at scale  $\varepsilon$  and perform percolation at the critical value. We would then like to study the limit as  $\varepsilon \rightarrow 0$ . We may envision e.g.  $\varepsilon = 1/N$ , so that we obtain information about large scale behavior by studying the limit.

To obtain “full” information, we at least need some stochastic object in the limit. The simplest such object, as alluded to earlier, is the (law of the) interface. Recall that we start with a domain  $\Omega \subset \mathbb{R}^2$  with two marked boundary points  $a$  and  $c$ , which divides the boundary into two parts. If we color one part blue and the other yellow, then given any percolation configuration there is indeed an interface running from  $a$  to  $c$ . We can also think of the interface as the external boundary of the biggest blue cluster connected to a certain piece of the boundary, so really the exact location of  $a$  and  $c$  is immaterial. (Understanding the interface is the first step in an iterative process to understand the full configuration in the scaling limit, which we shall not address in the present manuscript; the interested reader may consult [7] on this matter.) We can also think of the interface as a (realization of a) very simple process: We start at one corner and reveal say hexagons one by one by flipping a coin, then either turn left or right depending on the color of the hexagon revealed; this will be referred to as the *Exploration Process*. Since everything is independent, these two descriptions are the same, and in either the static or dynamic description, one can note that we have the domain Markov property: The law of the interface conditioned on an initial portion is the same as the law of the interface if we started in the slit domain formed by the corresponding

curve segment.

However, to establish convergence to the corresponding SLE – which turns out to be  $\text{SLE}_6$  for percolation – we still must obtain conformal invariance from the model. A convenient observable turns out to be crossing probability: Let us now consider a simply connected domain with four marked boundary points, i.e., a conformal rectangle, and look at the probability of say a left right blue crossing. Crossing probabilities are believed to be conformally invariant and given by *Cardy's Formula* [11] (derived from conformal field theory considerations and assuming conformal invariance) in the limit . If we conformally map  $(\Omega, a, b, c, d)$  to  $(\mathbb{H}, 1 - x, 1, \infty, 0)$  (here  $a, b, c, d \in \partial\Omega$  are the marked points and  $\mathbb{H}$  denotes the upper half plane), then Cardy's Formula takes the explicit form

$$F(x) := \frac{\int_0^x (s(1-s))^{-2/3} ds}{\int_0^1 (s(1-s))^{-2/3} ds}.$$

The idea is then to determine this *one* observable, but for *all* domains (see [18, 22]). It is worth noting, for aesthetic reasons if nothing else, that this ideology is in complete resonance with the Markov property: Starting with a simply connected domain and running the interface (*any* interface) up till some time  $t$ , we may learn the conditional distribution up till that time by considering the corresponding slit domain. Indeed, our proof of convergence to  $\text{SLE}_6$  ([4, 5]) – which follows the strategic initiative in [22], takes exactly this approach.

### I.3 Site Percolation on the Triangular Lattice

The first result on convergence of percolation to  $\text{SLE}_6$  is due to Smirnov in [13] – and completed by [8], restricted to site percolation on the triangular lattice and Jordan domains. (There is no explicit assumption on the type of domains under consideration in [13], but the result of [8] is restricted to Jordan domains.)

The relevant observable for percolation, introduced in [13], is a function related to the crossing probability: Let us add a marked point to the boundary so that now the boundary is divided into three pieces  $\mathcal{B}_i, i = 1, 2, 3$ . Then we define the function  $u^{(i)}(z)$  to be the probability of a blue crossing from  $\mathcal{B}_{i-1}$  to  $\mathcal{B}_{i+1}$ , separating  $z$  from  $\mathcal{B}_i$  (here addition is done modulo 3). These are the now called *Cardy–Carleson–Smirnov* functions.

The discrete derivatives of the functions  $u^{(i)}$  correspond to certain configurations which are easy to describe and due to complete color switching symmetry, a rather ingenious combinatorial bijection between the (configurations contributing to the) discrete derivative of  $u^{(i)}$  in one lattice direction with the discrete derivative of  $u^{(i-1)}$  and  $u^{(i+1)}$  in other lattice directions is constructed, which then implies (approximate) discrete versions of Cauchy–Riemann equations.

These relations imply that  $F := u_1 + e^{2\pi i/3}u_2 + e^{-2\pi i/3}u_3$  converges (as the lattice spacing tends to zero) to an analytic function. With appropriate determination of boundary values, Beffara [4] observed that the limiting  $F$  is in fact the unique conformal map from  $\Omega$  to the equilateral triangle with vertices at  $\{1, e^{2\pi i/3}, e^{-2\pi i/3}\}$ . If we evaluate  $u^{(i)}$  at a boundary point, then

we indeed obtain the (limiting) crossing probability of a conformal rectangle, and, by Carleson's observation, this corresponds to Cardy's Formula.

## I.4 Other Models and Universality

The proof of the interior analyticity statement for Cardy's Formula in [13] requires, at first glance, exact combinatorial identities and hence takes tremendous advantage of the exact symmetries of the model for hexagonal tiling, and consequently does not immediately work for any other lattice (including the square bond percolation problem, which also has  $p_c = 1/2$ , but lacks the property that the direct and dual lattices coincide).

There were some efforts and results for other models (see [9, 10]), however, the critical models considered therein were, at long distance, already demonstrably equivalent to the hexagonal tiling model from which they were evolved. This deviates somewhat from the original spirit of scaling and universality – a central dogma for the theory of critical phenomena since the 1960's: It is supposed that one can infer the critical exponents of a given lattice model via the universality class to which it belongs, i.e., one ought to learn about such properties of the lattice model from the continuum limit, and not vice versa.

In [13], building on results from [12], we instead construct a non-trivial class of locally correlated models evolved from *bond* percolation on the triangular lattice and establish Cardy's Formula for such models (for a restricted class of domains). We may represent such models as a hexagonal tiling with some hexagons allowed to be colored half blue and half yellow and here by

local correlation we mean that neighboring hexagons are not colored independently – in contrast to the hexagonal tiling studied in [13] – but hexagons separated by two or more lattice spacings are configured independently. The original hexagonal tiling can be obtained as the degenerate case when the local correlation is set to zero.

The underlying idea behind the construction of the models in [13] is that instead of requiring color symmetry at the level of a single hexagon, we look for color symmetry at a slightly larger scale, with the goal of utilizing some version of the Cardy–Carleson–Smirnov functions to establish Cardy’s Formula. Having constructed a satisfactory self–dual model with some color–symmetry, we then show that the resulting self–dual models satisfy the typical critical properties and correlation inequalities. However, perhaps surprisingly, in addition to the complications and intricacies of the models themselves, new ideas and generalizations are required: A stochastic element vis–à–vis whether paths are considered disjoint or not has to be introduced to successfully establish some version of interior analyticity for *modified* functions  $\tilde{u}, \tilde{v}, \tilde{w}$  which are now expectations of random variables instead of probabilities of events. We then estimate away e.g., the difference  $|u - \tilde{u}|$  via percolation estimates as the scaling limit is taken.

## I.5 Convergence to $\text{SLE}_6$

The statement of some universality, however, is not complete until we show that (the law of the interface of) our models from [13] also converges to  $\text{SLE}_6$ .

While the proof of convergence to  $\text{SLE}_6$  is already sketched in [13] and later completed in [8], it is not clear that the proof easily applies to models other than hexagonal tiling. Perhaps more pertinently, we wish to provide a proof of convergence (in [5]) along the lines of the [22], which, as explained at the end of §I.2, requires consideration of a more general class of domains than Jordan domains, which is the setting of [8].

Let us now expound on the last point. Let us be informal: At the discrete level (i.e., lattice spacing is not yet zero), it is not terribly difficult to see that if  $(\Omega, a, b, c, d)$  is a conformal rectangle,  $C_\varepsilon$  denotes the crossing probability from  $[a, b]$  to  $[c, d]$  at the  $\varepsilon$ -scale,  $\Omega_\varepsilon$  denotes  $\Omega$  with some suitable discretization and  $\mathbb{X}_{[0,t]}^\varepsilon$  denotes the interface up to some time  $t$  (parametrized in some reasonable fashion), then

$$C_\varepsilon(\Omega_\varepsilon, a, b, c, d \mid \mathbb{X}_{[0,t]}^\varepsilon) = C_\varepsilon(\Omega_\varepsilon \setminus \mathbb{X}_{[0,t]}^\varepsilon, \mathbb{X}_t^\varepsilon, b, c, d). \quad (\text{I.1})$$

This equation translates into the statement that  $C_t^\varepsilon := C_\varepsilon(\Omega \setminus \mathbb{X}_{[0,t]}^\varepsilon, \mathbb{X}_t^\varepsilon, b, c, d)$  is a martingale. If it can be demonstrated that limits can be taken and we obtain in the continuum a corresponding *conformally invariant* martingale, then we will have captured both defining properties of SLE.

Upon closer examination, we realize that it is a non-trivial task to remove all  $\varepsilon$ 's from (VI.7). Indeed, in addition to  $C_\varepsilon$ , one must also make sense of how the discretizations  $\Omega_\varepsilon$  converge to  $\Omega$  and how  $\mathbb{X}_{[0,t]}^\varepsilon$  converges to a continuum curve. As for the latter, we have from a result of [2] that (informally speaking) we have  $\mathbb{X}_{[0,t]}^\varepsilon$  converges to some continuum  $\mathbb{X}_{[0,t]}$  in the sup-norm for curves (which is given as the infimum over parametrization of the usual supremum norm for functions). Thus – especially in light of the exposition in [14], one

way to take the desired limit of (VI.7) is to provide a proof of Cardy’s Formula where the domain is approximated by “sup–approximations”: Some portions of the boundary of the domain may be approximated by curves converging to them in the sup–norm.

This line of reasoning leads us to investigate in more detail the question of discretization in relation to proving Cardy’s Formula. Here the key issue is extraction of boundary values (recall that Cardy’s Formula can be retrieved as boundary value of the Cardy–Carleson–Smirnov functions): Given discrete functions  $u_\varepsilon$  on  $\Omega_\varepsilon$  which are converging to  $u$  on  $\Omega$ , how do we guarantee that we can extract the appropriate boundary values for  $u$ ? It is worth emphasizing here that in order to establish Cardy’s Formula we must achieve pre–specified limiting boundary values on various pieces of the boundary. We resolve such issues in [4] by considering the situation from a complex analytic viewpoint. As a result we can indeed obtain Cardy’s Formula for arbitrary domains (due to specific technicalities of the models in [13], we can only establish Cardy’s Formula there for domains with boundary Minkowski dimension less than two) and take the limit of (VI.7).

Finally, we point out that the convergence proof in [5] is applicable for any percolation model satisfying reasonable assumptions (these critical properties are informally axiomatized in [5]) and for which Cardy’s Formula can be established. It is in fact also the case that a lot of the arguments and results of [4] would also go through for any reasonable model. The *interior analyticity statement* required to prove Cardy’s Formula is, without a doubt, the most elusive – and perhaps illusive as well – item in endeavors along these lines.

## I.6 Uniform Continuity of Crossing Probabilities

Let us conclude by mentioning a relatively “elementary” result on some uniform continuity of crossing probabilities, which gives power-law (i.e.,  $C\varepsilon^\alpha$  for some  $\alpha$ ) estimates. This result may also be used to establish (VI.7) (although it is too strong). Further, by translating the (limiting) crossing probability into information about the driving function, this result may contribute to some proof of rate of convergence to  $\text{SLE}_6$ . Finally, we caution the reader that this last chapter (chapter VI) contains non-rigorous discussions and the arguments therein are perhaps far from optimal and not tight.

## I.7 Guide to the Manuscript

The rest of the manuscript will then be a compilation of [12, 13, 4, 5, 6], in the order as listed. There will be much redundancies and inconsistencies of notations, for which the author apologizes in advance. The discussions in §I.4 – I.6 represent some summary of the results contained in the above-mentioned references. Some additional remarks on the contents:

- §II.2 contains percolation results which will be later used in the construction of the “flower” model in [13].
- §II.3 concerns random cluster models and should be skipped for readers only interested in percolation.

- §III is rather long. The main percolation contents are in §III.2 and §III.3 up to §III.3.2, culminating in establishing criticality for the “flower” models constructed. Correlation inequalities for these models can be found in §III.6 and §V.4.3.
- The rest of §III concerns color switching, etc., necessary to establish Cardy’s Formula for the “flower” models for piecewise smooth domains. Much of the arguments have a combinatorial/discrete probabilistic flavor. The establishment of Cauchy–Riemann type relations and discrete contour integration arguments are in §III.4.2 and §III.4.3.
- The interior analyticity statement necessary to establish Cardy’s Formula result is extended to domains with boundary Minkowski dimension less than two in §V.4.4. The result in §IV then allows one to rigorously extract Cardy’s Formula for such general domains for the “flower” models.
- §IV features complex analysis and invokes RSW estimates to establish (limiting) boundary values.
- §V.3 involves percolation estimates to establish properties of a typical limiting interface and also deals with crosscuts around prime ends in order to obtain tightness for general domains. (We note that conformal invariance of crossing probabilities is in fact utilized to show that there are no double visits to the boundary (Lemma V.3.8).)
- §V.2 contains discussions of typical critical properties and collects results to prove convergence to  $\text{SLE}_6$  given such properties and Cardy’s Formula.

§V.2.4 contains some SLE arguments, including *a priori* estimates and showing that it is possible to reparametrize by Löwner parametrization (Corollary V.2.9).

# Bibliography

- [1] M. Aizenman and A. Burchard. *Hölder Regularity and Dimension Bounds for Random Curves*. Duke Math. J. **99**, no. 3, 419–453 (1999).
- [2] M. Aizenman, J. T. Chayes, L. Chayes, and C. M. Newman. *Discontinuity of the Magnetization in One-Dimensional  $1/|x - y|^2$  Ising and Potts Models*. J. Stat. Phys. **77**, 351–359 (1994).
- [3] V. Beffara. *Cardy’s Formula on the Triangular Lattice, the Easy Way*. Universality and Renormalization, vol. 50 of the Fields Institute Communications, 39–45 (2007).
- [4] I. Binder, L. Chayes, and H. K. Lei. *On Convergence to  $SLE_6$  II: Discrete Approximations and Extraction of Cardy’s Formula for General Domains*. Submitted.
- [5] I. Binder, L. Chayes, and H. K. Lei. *On Convergence to  $SLE_6$  I: Conformal Invariance for Certain Models of the Bond-Triangular Type*. Submitted.
- [6] I. Binder, L. Chayes, and H. K. Lei. *Restricted Uniform Continuity of Crossing Probabilities in Slit Domains*. Unpublished manuscript.

- [7] F. Camia, C. M. Newman. *Two-Dimensional Critical Percolation: The Full Scaling Limit*. Comm. in Math. Phys. **268**, no. 1, 1–38 (2006).
- [8] F. Camia, C. M. Newman. *Critical Percolation Exploration Path and  $SLE_6$ : A Proof of Convergence*. Probability Theory and Related Fields, **139**, 1432–2064 (2007).
- [9] F. Camia, C. M. Newman and V. Sidoravicius. *Cardy’s Formula for Some Dependent Percolation Models*. Bull. Braz. Math. Soc. (N. S.), **33**, 147–156 (2002).
- [10] F. Camia, C. M. Newman and V. Sidoravicius. *A Particular Bit of Universality: Scaling Limits of Some Dependent Percolation Models*. Comm. Math. Phys. **246**, 311–332 (2004).
- [11] J. Cardy. *Critical Percolation in Finite Geometries*. J. Phys. A, **25**, L201–L206 (1992).
- [12] L. Chayes and H. K. Lei. *Random Cluster Models on the Triangular Lattice*. Journal of Statistical Physics **122**, no. 4, 647–670 (2006).
- [13] L. Chayes and H. K. Lei. *Cardy’s Formula for Certain Models of the Bond-Triangular Type*. Reviews in Mathematical Physics **19**, no. 5, 51–565 (2007).
- [14] G. Grimmett. *Percolation*. Grundlehren der Mathematischen Wissenschaften 321, Springer–Verlag, Berlin, second edition, 1999.
- [15] G. Grimmett. *The Random-Cluster Model*. Grundlehren der Mathematischen Wissenschaften 333, Springer–Verlag, Berlin, 2006.

- [16] H. Kesten. *Percolation Theory for Mathematicians*. Boston, Basel, Stuttgart: Birkhauser (1982).
- [17] H. Kesten. *Scaling Relations for 2D-Percolation*. *Comm. Math. Phys.* **109**, 109–156 (1987).
- [18] G. F. Lawler, O. Schramm, W. Werner. *Conformal Invariance of Planar Loop-Erased Random Walks and Uniform Spanning Trees*. *Ann. Probab.* **32** no. 1B, 939–995 (2004).
- [19] O. Schramm. *Scaling Limits of Loop-Erased Random Walks and Uniform Spanning Trees*. *Israel Journal of Mathematics*, **118**, 221-288 (2000).
- [20] O. Schramm and S. Sheffield. *Harmonic Explorer and its Convergence to  $SLE_4$* . *Ann. Probab.* **33**, 2127–2148 (2005).
- [21] S. Smirnov. *Critical Percolation in the Plane: Conformal Invariance, Cardy's Formula, Scaling Limits*. *C. R. Acad. Sci. Paris Sr. I Math.* **333**, 239–244 (2001).  
Also available at <http://www.math.kth.se/~stas/papers/percras.ps>.
- [22] S. Smirnov. *Towards Conformal Invariance of 2D Lattice Models*. Proceedings of the International Congress of Mathematicians, Madrid, Spain, 2006.
- [23] S. Smirnov. *Conformal invariance in random cluster models. I. Holomorphic fermions in the Ising model*. To appear in *Ann. Math.*
- [24] S. Smirnov and W. Werner. *Critical Exponents for Two-Dimensional Percolation*. *Math. Res. Lett.* **8**, 729–744 (2001).

- [25] W. Werner. *Lectures on Two-Dimensional Critical Percolation*.  
arXiv:0710.0856

# Chapter II

## Random Cluster Models on the Triangular Lattice

**Abstract:** We study percolation and the random cluster model on the triangular lattice with 3-body interactions. Starting with percolation, we generalize the star–triangle transformation: We introduce a new parameter (the 3-body term) and identify configurations on the triangles solely by their connectivity. In this new setup, necessary and sufficient conditions are found for positive correlations and this is used to establish regions of percolation and non-percolation. Next we apply this set of ideas to the  $q > 1$  random cluster model: We derive duality relations for the suitable random cluster measures, prove necessary and sufficient conditions for them to have positive correlations, and finally prove some rigorous theorems concerning phase transitions.

**Keywords:** percolation, random cluster models, Potts models, star–triangle relations, FKG inequalities

## II.1 Introduction

The study of duality relations for  $2D$ -Potts systems is not a new topic. Indeed, it is older than the model itself in the sense that [21] and [2] provided special cases long before the general Potts spin-systems were formulated. While we will not dwell on the historical aspects of this subject, it is worth remarking that this line of study has had immeasurable impact on the entirety of two-dimensional statistical mechanics. Notwithstanding, the usual derivations of duality for Potts models (see [36] and references therein) suffer in three respects which we will describe in increasing order of importance:

- (I) There are informal aspects to many of the derivations and thus some effort – presumably small – would be needed to elevate these derivations to the status of mathematical theorems.

- (II) The various standard techniques, which include mapping to vertex models or the introduction of dual-spin variables in the form of constraints, do not include all relevant values of parameters. In particular, the dual-constraints approach only makes sense for integer  $q \geq 2$ . It is only as an afterthought that duality relations for continuous  $q$ 's are inferred from the analytic structure of the formulas produced for the integer  $q$ 's.

While we do not necessarily regard these two issues as being of great urgency, the third issue is considered to be pertinent both by mathematicians and physicists.

- (III) The result of a typical duality relation is the identification of the free energies at dual parameter values. Hence, as concerns the subject of *phase transitions* one is always left with an unsatisfactory provisional statement: *If*

there is but a single non-analyticity, *then* this must occur at the self-dual point.

It should be remarked that this third issue is certainly not “academic”. In particular, in the so called  $rs$ -models, which are generalizations of the Ashkin–Teller and/or the  $q$ -state Potts models (with  $q = r \times s$ ) there is a self-dual line through an intermediate phase where, apparently, nothing of interest transpires; c.f. [32], [26] and [9].

As an alternative to the “usual methods”, it is possible to establish duality via *graphical representations*, in particular the FK-representation [15], whereby the duality shows up on the level of the representation itself. Duality in this context is akin to (and a generalization of) the elementary sort of duality found in Bernoulli percolation. Hence, using percolation based techniques, genuine irrefutable statements can be made concerning the presence of phase transitions at points of self-duality. For example, on the square lattice, duality of the random cluster models has been used to establish rather sharp theorems concerning their phase structures [3], [11].

In this work we will study the  $q$ -state Potts models – and their associated random cluster representations – on the triangular lattice. For these problems, the derivation is considerably more intricate than the square lattice; one must first go through the intermediate honeycomb lattice. The inevitable consequence of this contortion is the production of extra correlations in the dual model. In the language of spin-systems, these correlations translate into the phrase “three body interactions” but we iterate that the phenomenon is quite general and occurs even for percolation ( $q = 1$ ). Well known exceptions to

this rule are (i) The Ising spin–system at all couplings and (ii) A special point, called the star–triangle point, where by a miracle, the correlations in the dual model vanish. Since the star–triangle point is also a point of self–duality, it is readily identified as the transition point. However, to the authors’ knowledge, it is only for the case of percolation ([33], [34]) that a rigorous theorem along these lines has been established.

The perspective of this work is that since we are generically stuck with the additional correlations after duality, then they should be in the model from the outset. We find that with the additional freedom of “three body interactions”, duality becomes a straightforward map in a two–dimensional space that has a self–dual *curve* of fixed points. One of the points on this curve – and of no particular significance – is the star–triangle point. This general picture has been known (and under appreciated) for quite some time: Duality relations on the level of free energies are derived in [36] using the methods of [5] – here for integer  $q \geq 2$ . Additional results along these lines are obtained in [35], [37] and [4] via relations to vertex models. A cornerstone of the former work is a graphical expansion akin to what is developed here. However, in these works the representation was only employed as an auxiliary device. The full potential for relating percolation phenomena in the graphical representations to phase transitions (as defined by other means) and the use of the interplay between direct and dual representations to elucidate this phenomena was not exploited.

From the perspective of rigorous analysis, a significant problem emerges at the outset. In particular, the sorts of additional correlations introduced

are not necessarily *positive* correlations. E.g. for the spin-systems, the extra interactions are, as often as not, antiferromagnetic. While this may or may not alter the nature of the transition, it is an enormous technical obstacle since nearly all probabilistic arguments concerning systems of this sort are based on the positivity of correlations. To overcome these difficulties, we must introduce a reduced state space for the graphical models wherein positive correlations can be re-established. Notwithstanding, our techniques do not cover the entirety of the self-dual curve but this could in principle be accomplished by an extension of our scheme. Further, to avoid technical complications we deal exclusively with the isotropic case whenever possible: *A priori*, all three edges of the triangle have the same probability of being occupied. One might also, with some effort, extend various results proved here to the anisotropic cases.

The remainder of this paper is organized as follows: In section two, we examine the case of percolation where the necessity of introducing local correlations is underscored. Here the star-triangle duality is generalized and relatively complete results for the phase diagram are derived. In section three, we study this problem for the  $q > 1$  random cluster models. The duality of [35] and [4] are derived by graphical methods and we characterize the conditions for positive correlations. Finally, in section four, we show that in the region where correlations are positive, there is a phase transition (or at least critical behavior) at all points of self-duality.

## II.2 Generalized Star–Triangle Relations: Percolation

### II.2.1 The Classical Star–Triangle Situation

In order to motivate our work, we first briefly describe the classical star-triangle relation. As mentioned above, we will treat the isotropic case, so let  $p$  be the probability that a bond is occupied. Now on any given triangle there are eight possible configurations; we denote their respective probabilities by  $e$  (empty),  $s$  (single),  $d$  (double) and  $a$  (full). Thus, for example,  $s = p(1-p)^2$ . Under the usual sort of planar duality, the triangular lattice problem becomes a problem on the honeycomb lattice where we could also associate a bond probability e.g.  $p^\star = 1-p$ . Considering only connectivity properties and integrating out the central vertex returns us to a problem on the triangular lattice (but with the triangles inverted). Using  $e^\star$ ,  $s^\star$ ,  $d^\star$  and  $a^\star$  to denote probabilities of the corresponding configurations, we easily arrive at

$$e^\star = p^3 + 3p^2(1-p), \tag{II.1}$$

$$s^\star = p(1-p)^2, \tag{II.2}$$

$$3d^\star + a^\star = (1-p)^3. \tag{II.3}$$

Ostensibly, one would like to define a  $p^\star$  such that the right hand sides of (II.1), (II.2), and (II.3) are, respectively,  $(1-p^\star)^3$ ,  $p^\star(1-p^\star)^2$  and  $(p^\star)^3 + 3(p^\star)^2(1-p^\star)$ . However, for general  $p \in (0, 1)$ , this cannot be done – there are just too many equations. Explicitly, if we try to force this sort of duality, this in turn forces  $p$  to a particular value which, in fact, is the one for which  $p = p^\star$ . To see this,

if we substitute (II.1) into (II.2) we get, in the variables  $R = p/(1 - p)$  and  $R^* = p^*/(1 - p^*)$ , the equation  $RR^*(R^* + 3) = 1$ . But the similar procedure on (II.3) and (II.2) gets us  $RR^*(R + 3) = 1$  thence any non-trivial solution requires  $R = R^*$ . At  $p^* = p$ , we see that  $p$  must satisfy:

$$p^3 - 3p + 1 = 0, \tag{II.4}$$

which is of course the self-dual point of the classic star-triangle relation.

## II.2.2 Introduction of Correlations

Overall, the above situation is clearly *not* suitable for the development of a general theory of duality. Clearly, if we wish to salvage this situation, the next step would be to put in some sort of correlations. A manageable way to implement correlations – which has its analogs in physical systems, c.f. subsection II.3.1 – is to introduce correlations within triangles but to keep separate triangles independent. (Here, of course, we refer only to “up-pointing” triangles; configurations on the “down-pointing” triangles will be determined from the former.)

A secondary consequence of the above duality experiment (on a single triangle) is the observation that, when the rinse cycle is finished, the dual model does not really distinguish between the double and full configurations. This is due to the fact that all we track are connectivities between sites and, in both situations, the triangle is fully connected.

In this spirit, we might as well confine all of our attention to the three types of configurations listed in (II.1), (II.2), and (II.3); e.g., we *define* our

model to have only five configurations on each triangle, namely empty, three singles and a full. So (in the fully isotropic case) we have five parameters:  $e$ ,  $s$  and  $a$  with  $e + 3s + a = 1$ . We state without proof the following proposition concerning this model on the triangular lattice:

**Proposition II.2.1.** *Consider the model on the triangular lattice in which configurations on the up-pointing triangles are independent and confined to empty, singles and full with respective probabilities  $e$ ,  $s$  and  $a$ . Then this model is dual to the model with parameters  $e^*$ ,  $s^*$  and  $a^*$  which are given by*

$$e^* = a \tag{II.5}$$

$$s^* = s \tag{II.6}$$

$$a^* = e \tag{II.7}$$

*In particular, the condition for self-duality is just  $a = e$ .*

We make a simple observation which will be useful in the next subsection:

**Corollary II.2.2.** *For the parameters  $a$ ,  $e$  as above and for  $r \in [0, 1]$ , the curve  $a + e = r$  is invariant under the  $*$ -map.*

In order to translate all of this into a statement about percolation properties of the model we will need to establish some FKG-type properties of the system. Since separate up-pointing triangles are independent this amounts to a problem on a single triangle. Here, unfortunately, we must prove the result for the anisotropic case as it will be needed later. First we need some basic definitions.

**Definition II.2.3.** Let  $\Omega$  be a probability space with probability measure  $P$ . Let  $A \subset \Omega$  be an event and let  $\omega \in \Omega$ . Then the *indicator function*  $\mathbf{1}_A$  is defined by

$$\mathbf{1}_A(\omega) = \begin{cases} 1 & \text{if } \omega \in A, \\ 0 & \text{otherwise.} \end{cases}$$

If  $f$  is a function on  $\Omega$ , then  $\mathbf{E}(f)$ , the *expectation* (or mean value) of  $f$  is defined to be

$$\mathbf{E}(f) = \int_{\Omega} f(\omega) dP(\omega).$$

Finally, we say the functions  $f$  and  $g$  have *positive correlations* if

$$\mathbf{E}(fg) \geq \mathbf{E}(f)\mathbf{E}(g).$$

**Theorem II.2.4.** *Consider the above described 5-state system realized as bond configurations on a triangle: Let  $[\mathcal{S}]_1$ ,  $[\mathcal{S}]_2$  and  $[\mathcal{S}]_3$  denote the events that the three various sides of the triangle are the sole bonds occupied with  $[\mathcal{A}]$  and  $[\mathcal{E}]$  denoting the full and empty configurations. Let  $\nu$  denote a measure on this system and let us denote the respective probabilities of the above-mentioned by  $s_1$ ,  $s_2$ ,  $s_3$ ,  $a$  and  $e$ . It is assumed without loss of generality that  $s_1 \geq s_2 \geq s_3$ . Then the necessary and sufficient condition for  $\nu$  to have positive correlation is*

$$ae \geq s_1(s_2 + s_3)$$

**Proof:** To prove the necessity of the condition  $ae \geq s_1(s_2 + s_3)$ , note that if  $f(s_1) = 0$ ,  $f(s_2) = 1 = f(s_3) = 1$ ,  $f(a) = 1$  and  $f(e) = 0$ , and  $g(s_1) = 0$ ,  $g(s_2) = g(s_3) = 1$ ,  $g(a) = 1$  and  $g(e) = 0$ , then  $\mathbf{E}(fg) \geq \mathbf{E}(f)\mathbf{E}(g)$  gives

exactly that  $ae \geq s_1(s_2 + s_3)$ . For sufficiency, we aim to show that

$$\mathbf{E}(fg) - \mathbf{E}(f)\mathbf{E}(g) \geq 0 \tag{II.8}$$

To simplify matters we first note that (II.8) is not changed by adding constants to  $f$  and  $g$ . Thus we may assume that  $f$  and  $g$  are overall non-negative and (by subtracting  $f(E)$  and  $g(E)$  respectively) vanish on the lowest configuration. Similarly, the truth or falsehood of (II.8) is unaffected by the scaling of  $f$  and  $g$  so we may as well assume that  $f([\mathcal{A}]) = g([\mathcal{A}]) = 1$ .

Next let  $\sigma$  be a permutation on three letters such that

$$f([\mathcal{S}]_{\sigma_1}) \geq f([\mathcal{S}]_{\sigma_2}) \geq f([\mathcal{S}]_{\sigma_3})$$

. Then we are down to six parameters: for convenience let  $x_1, x_2, x_3$  denote  $f([\mathcal{S}]_{\sigma_1}), f([\mathcal{S}]_{\sigma_2}),$  and  $f([\mathcal{S}]_{\sigma_3}),$  respectively. Similarly define  $y_1, y_2,$  and  $y_3$  for  $g$ . We assume that some of these parameters are non-trivial, for otherwise the theorem is already proved.

Next we observe that any increasing function is automatically positively correlated with  $\mathbf{1}_{[\mathcal{A}]}$ , the indicator of the top configuration. Indeed (with all of our simplifications enforced),  $\mathbf{E}(\mathbf{1}_{[\mathcal{A}]}g) = a$ , whereas  $\mathbf{E}(\mathbf{1}_A)\mathbf{E}(g) = a\mathbf{E}(g)$ , which is smaller. Thus, the quantity  $\mathbf{E}(fg) - \mathbf{E}(f)\mathbf{E}(g)$  will decrease if we subtract from  $f$  the function  $\lambda\mathbf{1}_A$  with  $\lambda > 0$ . However, in order to keep  $f$  increasing, the most we can subtract is  $\lambda = 1 - \max\{x_1, x_2, x_3\} = 1 - x_1$ , by assumption. Thus, after this subtraction and more rescaling, we have that  $x_1 = 1$ .

Similar considerations show that  $\min\{x_1, x_2, x_3\} = 0$ . To see this one first observe that  $g$  is always positively correlated with the function  $1 - \mathbf{1}_{[\mathcal{E}]}$ .

Then subtracting from  $f$  the function  $x_3(1 - \mathbf{1}_{[\mathcal{E}]})$  (where by assumption  $x_3 = \min\{x_1, x_2, x_3\}$ ) and rescaling again gives the desired conclusion.

Given all these simplifications, we now have  $\mathbf{E}(fg) = a + s_{\sigma_1}y_1 + s_{\sigma_2}x_2y_2$  and  $\mathbf{E}(f)\mathbf{E}(g) = (a + s_{\sigma_1} + s_{\sigma_2}x_2)(a + s_{\sigma_1}y_1 + s_{\sigma_2}y_2 + s_{\sigma_3}y_3)$ . Since the goal is to show that  $\mathbf{E}(fg) \geq \mathbf{E}(f)\mathbf{E}(g)$ , we may assume that  $y_1 = 0$  and  $y_3 = 1$ , since the coefficient of  $y_1$  in  $\mathbf{E}(f)\mathbf{E}(g)$  is smaller than in  $\mathbf{E}(fg)$  and  $y_3$  does not even occur in  $\mathbf{E}(fg)$ .

Next one can check that  $f$  is positively correlated with  $\mathbf{1}_{[\mathcal{S}]_{\sigma_2}} + \mathbf{1}_{[\mathcal{S}]_{\sigma_3}} + \mathbf{1}_{[\mathcal{A}]}$ : To see this observe that  $\mathbf{E}((\mathbf{1}_{[\mathcal{S}]_{\sigma_2}} + \mathbf{1}_{[\mathcal{S}]_{\sigma_3}} + \mathbf{1}_{[\mathcal{A}]})f) = (x_2s_{\sigma_2} + a)(s_{\sigma_2} + s_{\sigma_3} + a + s_{\sigma_1} + e)$  whereas  $\mathbf{E}(f)\mathbf{E}(\mathbf{1}_{[\mathcal{S}]_{\sigma_2}} + \mathbf{1}_{[\mathcal{S}]_{\sigma_3}} + \mathbf{1}_{[\mathcal{A}]}) = (xs_{\sigma_2} + a + s_{\sigma_1})(s_{\sigma_2} + s_{\sigma_3} + a)$ , so the difference is  $ae - s_{\sigma_1}(s_{\sigma_2} + s_{\sigma_3})$ , which is positive by hypothesis. It is also easy to check that  $g - y_2(\mathbf{1}_{\mathcal{S}_{\sigma_2}} + \mathbf{1}_{\mathcal{S}_{\sigma_3}} + \mathbf{1}_{\mathcal{A}})$  is still increasing. Also, note that if  $y_2$  was equal to one before the subtraction, then after the subtraction  $g \equiv 0$  and again the conclusion of the theorem holds trivially, so we may as well assume  $y_2 \neq 1$ . As before, Subtracting and renormalizing, we acquire  $y_2 = 0$ , which immediately implies that  $x_2 = 1$  since that maximizes  $\mathbf{E}(f)\mathbf{E}(g)$  without changing  $\mathbf{E}(fg)$ .

To summarize we are down to  $f([\mathcal{E}]) = g([\mathcal{E}]) = 0$ ,  $f([\mathcal{S}]_{\sigma_3}) = g([\mathcal{S}]_{\sigma_1}) = g([\mathcal{S}]_{\sigma_2}) = 0$ ,  $f([\mathcal{S}]_{\sigma_1}) = f([\mathcal{S}]_{\sigma_2}) = g([\mathcal{S}]_{\sigma_3}) = 1$ , and  $f([\mathcal{A}]) = g([\mathcal{A}]) = 1$ , so for positive correlation we need

$$a \geq (a + s_{\sigma_1} + s_{\sigma_2})(a + s_{\sigma_3}),$$

which is true if  $ae \geq s_{\sigma_3}(s_{\sigma_1} + s_{\sigma_2})$ . The right hand side is clearly maximized when  $\sigma_3 = 1$  (since by assumption  $s_1$  is the maximum of  $s_1, s_2$ , and  $s_3$ ), and we obtain  $ae \geq s_1(s_2 + s_3)$  as claimed.  $\square$

**Remark (a).** It is clear that the standard FKG technology does not extend to the present case. Indeed, if we view our system as  $\{0, 1\}^3$ , but restrict our attention to measures which assigns weight zero to the double edge configurations, then it is obvious that the FKG lattice condition *fails* for any such measure. On a slightly more subtle level, regarding  $\{[\mathcal{A}], [\mathcal{S}]_1, [\mathcal{S}]_2, [\mathcal{S}]_3, [\mathcal{E}]\}$  as simply a partially ordered set with lattice structure given by  $X \vee Y = \inf\{Z | X \preceq Z \text{ and } Y \preceq Z\}$  and  $X \wedge Y = \sup\{Z | Z \preceq X \text{ and } Z \preceq Y\}$ , it is not hard to see that the FKG lattice condition holds whenever  $ae \geq s_1 s_2$ . This is in apparent contradiction with (the necessity part of) Theorem (II.2.4). However, the connection between the lattice condition and positive correlation hinges on the fact that the lattice satisfies distributivity, which is a property that our lattice lacks, as  $[\mathcal{S}]_1 = [\mathcal{S}]_1 \wedge ([\mathcal{S}]_2 \vee [\mathcal{S}]_3) \neq ([\mathcal{S}]_1 \wedge [\mathcal{S}]_2) \vee ([\mathcal{S}]_1 \wedge [\mathcal{S}]_3) = [\mathcal{E}]$ .

**Remark (b).** We observe that  $ae \geq 2s^2$  implies that  $a^*e^* \geq 2(s^*)^2$  by (II.5), (II.6), and (II.7), so the \*-map takes the region of positive correlation into itself.

**Remark (c).** It is noted that for independent bonds, at density  $p$ , the condition  $ae \geq 2s^2$  is well-satisfied. But supposing we write

$$e = (1 - p)^3(1 - t), \tag{II.9}$$

$$s = p(1 - p)^2(1 - t), \tag{II.10}$$

and

$$a = (p^3 + 3p^2(1 - p))(1 - t) + t \tag{II.11}$$

(as we will have occasion to do when we discuss magnetic systems) and again consider, with the obvious interpretations, our old eight configurations. Then

it is clear that the correlations between bonds are positive if and only if  $t \geq 0$ . However, our condition  $ae \geq 2s^2$  is satisfied for values of  $t$  which are considerably negative.

### II.2.3 Phase Diagram

**Theorem II.2.5.** *Consider the correlated percolation model on the triangular lattice as defined previously which has parameters  $e$ ,  $s$  and  $a$ ; the parameters are described by points in the  $ae$ -plane. Supposing that  $ae \geq 2s^2$ , then in the region*

$$a + e > r_0 \equiv \frac{2\sqrt{2}}{3 + 2\sqrt{2}},$$

*the following hold*

- (1) *The region  $a > e$  has a (unique) infinite cluster.*
- (2) *The region  $a < e$  has no infinite cluster and is characterized by exponential decay of correlations.*
- (3) *The line  $a = e$  has no infinite cluster of either type but power law (lower bounds) on the decay of correlations.*

*These results are summarized in Figure 1.*

**Proof** (sketch): We will be brief since the major ingredients are transcriptions with minimal modifications of the well-known results from standard percolation theory. Our setup will be as follows: we will fix the value of  $a+e$ , denoting this by  $r$ , and write  $a = \lambda r$ ,  $e = (1 - \lambda)r$ ,  $0 \leq \lambda \leq 1$ . We will denote by  $\lambda_c(r)$  the (purported) threshold above which there is percolation (Notwithstanding, we do not “yet” know that there will be percolation even if  $\lambda = 1$ ). Notice by

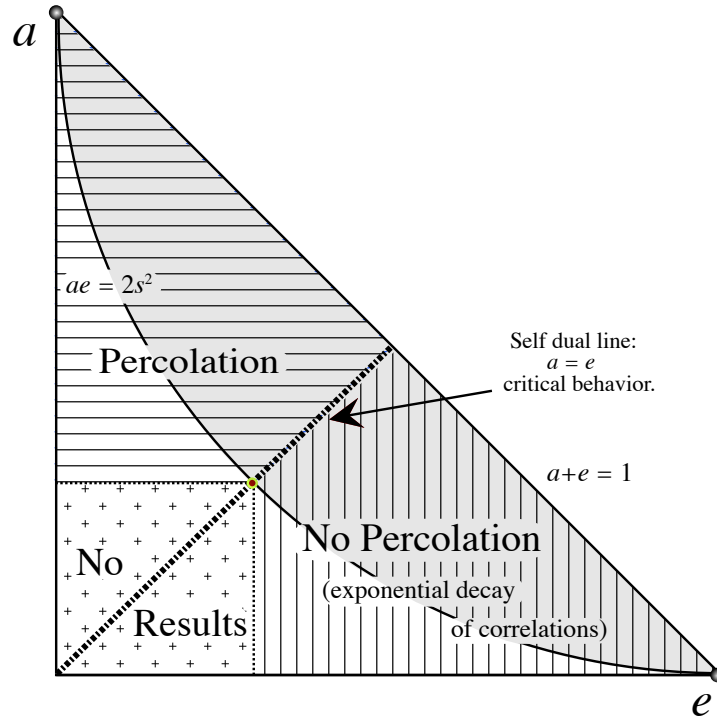


Figure II.1: Phase diagram for percolation problem on the triangular lattice; variable  $s$  suppressed. The line  $a = e$  is the self-dual line. The curve  $ae = 2s^2$  separates the regions with and without positive correlations. Within the region of positive correlations,  $a > e$  is the percolation phase,  $a < e$  non-percolating with exponential decay of connectivities and percolation of the *dual* model. These phases are divided by the self-dual line, where there is no percolation of either type and critical behavior is observed. Some of these results may be extended out of the region of positive correlations by monotonicity.

Proposition (II.2.1) and its corollary that, in these circumstances, the duality takes  $\lambda$  to  $1 - \lambda$ .

Our first claim is that the result on the exponential decay of connectivities below threshold applies whenever  $r > 0$  [24],[25]. The starting point is the adaptation of Russo’s formula [29] to the current situation. For an increasing event  $\mathcal{A}$ , a triangle  $t$  is pivotal if, when empty, the event  $\mathcal{A}$  does not occur but if fully occupied then it does. Denoting by  $\mathbf{P}_{r,\lambda}$  the probability measure with parameters  $a = \lambda r$ , etc, and  $\mathbf{E}_{r,\lambda}$  for the corresponding expectation, the modification of Russo’s formula is easily shown to be

$$\frac{\partial \mathbf{P}(\mathcal{A})}{\partial \lambda} = r \mathbf{E}_{r,\lambda}(|\delta \mathcal{A}|),$$

where  $|\delta \mathcal{A}|$  denotes the number of pivotal triangles for the event  $\mathcal{A}$ .

Next, we denote by  $A_n$  the event that the origin is connected by occupied bonds to the boundary of a “ball” of radius  $n$ . It is clear that the basic “chain of sausages” picture holds in this context (with paths of bonds replaced by clusters of triangles) and at the endpoint of each sausage, a pivotal triangle. We note that for the present setup two events are said to occur *disjointly* if they are determined on the configurations in disjoint sets of triangles. Thus, using the more general Reimer’s inequality [27] in place of the van den Berg–Kesten inequality one can follow the standard derivations to obtain

$$\mathbf{E}_{r,\lambda}(|\delta A_n|) \geq \frac{n}{\sum_{k=1}^n \mathbf{P}_{r,\lambda}(A_k)} - \text{const.}$$

Thereafter, some tedious analysis shows that if at some  $\lambda_0$ ,  $\mathbf{P}_{r,\lambda_0}(A_n) \rightarrow 0$  then for all  $\lambda < \lambda_0$ ,  $\exists \Psi > 0$  such that  $\mathbf{P}_{r,\lambda}(A_n) \leq e^{-\Psi(\lambda,r)n}$ ; in particular there

is exponential decay of connectivities. However, standard 2D arguments show that once the direct model has rapid decay of correlations, the dual model percolates. (E.g, if there is no connection between points on the  $x$ -axis with  $x < -L$  and points with  $x > +L$  than some dual point with  $x$ -coordinate in the vicinity of the gap is connected to infinity).

Using duality this immediately implies that  $\lambda_c \leq 1/2$ : Any other possibility would imply percolation of the dual model at values of  $\lambda$  greater than  $1/2$  which, by duality, implies percolation at  $\lambda$ -values less than  $1/2$ , contradicting the possibility of any other possibility.

For general values of parameters, the results of [6] apply which rules out the possibility of multiple infinite clusters (of the same type). In the region of positive correlation ( $r \geq r_0$ ) the results of [12] and [18] (see also the proof by Zhang, 1988, unpublished) demonstrates that infinite clusters of the opposite type cannot coexist. This implies that there cannot be percolation of either type on the self-dual line, i.e. that  $\lambda_c \geq 1/2$  so that  $\lambda_c = 1/2$ .

Finally, to prove power law lower bounds on the decay of correlations, we observe that for appropriate rectangles of length-scale  $L$ , there is either a left-right crossing by the direct bonds or a up-down crossing by the dual bonds, so that without loss of generality the crossing probabilities are of order unity uniformly in  $L$ . Standard arguments (see e.g. Theorem 2 in [11]) can then be used to demonstrate power law lower bounds.  $\square$

**Remark.** Our assumptions of positive correlations and that  $s_1 = s_2 = s_3$  are the ingredients needed to use the Zhang (and [12], [18]) arguments. Without these assumptions we cannot mathematically rule out the possibility of per-

colation *before* or *at* the self-dual point with unique infinite clusters of both types. In the independent case, coexisting clusters were ruled out in [16] using direct (Kesten–style) arguments. It is conceivable that these arguments could be modified to the present case but we make no specific claims. Nevertheless, some of the isotropic results can be extended outside the regions of positive correlations by domination arguments:

**Corollary II.2.6.** *In the region  $a > r_0/2$ ,  $e < r_0/2$  the relevant (percolative) conclusions of Theorem II.2.5 hold while in the region  $a < r_0/2$ ,  $e > r_0/2$  the relevant non-percolative conclusions of Theorem II.2.5 hold.*

**Proof:** Consider a point with parameters  $a > r_0/2$ ,  $e < r_0/2$  which is not covered in the previous theorem. Such a point can be joined by a horizontal line to a point in the percolative region described in Theorem II.2.5. For all intents and purposes, the new measure is obtained from the known percolative measure by replacing empty triangles with singly occupied triangles: Explicitly, the measure in question stochastically dominates a measure with the stated percolative properties. The conclusion follows since the two claims about the regions  $a > e$ ,  $a + e > r_0$  may be phrased in terms of the events:

- (1) The existence (wp1) of an infinite cluster and
- (2) Uniqueness of said cluster.

The first is manifestly increasing while the second is equivalent to the absence of an infinite cluster of the dual type, hence also increasing. The region  $a < r_0/2$ ,  $e > r_0/2$  is handled similarly. □

## II.3 Generalized Star–Triangle Relations: Random Cluster Measure

### II.3.1 Graphical Weights and Spin Systems

We start in this subsection with the random cluster models – a generalization of the usual random cluster models which features interactions among certain triples of sites. Here we will confine attention only to triples which constitute three vertices of an up pointing triangle.

The random-cluster models are defined by four parameters,  $e$ ,  $s$ ,  $a$ , and  $q$ , and are given formally by

$$W(\omega) \propto q^{c(\omega)} s^{|\mathcal{S}(\omega)|} a^{|\mathcal{A}(\omega)|} e^{|\mathcal{E}(\omega)|} \quad (\text{II.12})$$

where  $\omega$  is a bond configuration,  $|\mathcal{S}(\omega)|$  denotes the number of triangles with solely one side occupied and  $|\mathcal{A}(\omega)|$  denotes the number of triangles with all three vertices connected, and  $|\mathcal{E}(\omega)|$  the number of empty triangles. It may be assumed, without loss of generality, that  $a + 3s + e = 1$ . Of course as usual the above only makes sense in finite volumes with particular boundary conditions; infinite volume problems are extracted via limits. However, as far as we are concerned, boundary conditions only enter through the definition of  $c(\omega)$ ; once we establish the basic monotonicity properties of the model, there are natural dominations in both volume and the various parameters  $s$ ,  $a$  and  $e$ . Then, the passage to infinite volume follows the exactly the same lines as for the usual random-cluster model. Indeed, as far as these general matters are concerned we refer the reader to [17] (see also [8] and [7]) where the issues

have been discussed in some detail.

It is also clear (see the above mentioned citations) that for integer  $q$  greater than one, this random-cluster model is the graphical representation of a (formal) Potts Hamiltonian with two and three site interactions:

$$-\beta\mathcal{H} = \sum_{\langle x,y,z \rangle} J(\delta_{\sigma_x\sigma_y} + \delta_{\sigma_y\sigma_z} + \delta_{\sigma_x\sigma_z}) + \kappa\delta_{\sigma_x\sigma_y\sigma_z}, \quad (\text{II.13})$$

where the sum is over all generic up-pointing triangles. We assume that  $J$  is positive but there is, as of yet, no restriction concerning the parameter  $\kappa$ .

For completeness, a quick derivation proceeds as follows: Let  $\Lambda$  denote a finite collection of (up-pointing) triangles and  $\mathcal{H}_\Lambda$  the restriction of  $\mathcal{H}$  to  $\Lambda$  with free boundary conditions, and  $Z_\Lambda$  the corresponding partition function. Then,

$$Z_\Lambda = \sum_{\sigma_\Lambda} e^{-\beta\mathcal{H}_\Lambda} = \sum_{\sigma_\Lambda} \prod_{\langle x,y,z \rangle \in \Lambda} (S\delta_{\sigma_x\sigma_y} + 1)(S\delta_{\sigma_y\sigma_z} + 1)(S\delta_{\sigma_x\sigma_z} + 1)(1 + g\delta_{\sigma_x\sigma_y\sigma_z}),$$

where  $S = e^J - 1$  and  $g = e^\kappa - 1$ , and again with no stipulation about the sign of  $g$ . Multiplying everything out, we get

$$Z_\Lambda = \sum_{\sigma_\Lambda} \prod_{\langle x,y,z \rangle \in \Lambda} [1 + S(\delta_{\sigma_x\sigma_y} + \delta_{\sigma_y\sigma_z} + \delta_{\sigma_x\sigma_z}) + A\delta_{\sigma_x\sigma_y\sigma_z}],$$

where  $A = 3S^2 + g(1+S)^3$ , which we *now* stipulate to be positive. Notice that we have deliberately failed to distinguish terms corresponding to products of two, versus three Kronecker deltas. Opening up the product and identifying graphical terms in the usual fashion we perform the trace to obtain

$$Z_\Lambda = \sum_{\omega} q^{c(\omega)} S^{|S(\omega)|} A^{|\mathcal{A}(\omega)|}, \quad (\text{II.14})$$

where  $\omega$  denotes a bond configuration restricted to five possibilities on each triangle as described in the previous section. Since everything is positive, the objects in the above summand represent *weights* for the configurations  $\omega$ . For convenience, we can multiply the above by an overall (irrelevant) factor and then, by suitable redefinitions of parameters, we have our weights in the form of (II.12).

We remark that the more standard decomposition into eight configurations per triangle would, as can be checked, lead to positive correlations if and only if  $g \geq 0$ . Indeed,  $g/(1+g)$  corresponds exactly to the parameter  $t$  which was discussed in equations (II.9)-(II.11). As we will show in Theorem II.3.4 below, the present system provides a great deal more leeway.

**Remark.** Finally, it is worth a reminder that as far as the spin systems are concerned, most quantity's relevance can be read directly from the graphical problem [1], [13]. In particular (at least in the realm of positive correlations), percolation is synonymous with magnetization, while the absence of percolation implies unicity among the possible limiting Gibbs states.

### II.3.2 Duality Relations and Self-Dual Curve

**Theorem II.3.1.** *For the random cluster measure as defined in the previous section, the duality relations are given by*

$$\frac{s^*}{e^*} = \left( \frac{qs}{a} \right)$$

and

$$\frac{a^*}{e^*} = \left( \frac{q^2 e}{a} \right).$$

The self dual curve, obtained in the above by setting  $a = a^*$ ,  $e = e^*$  and  $s = s^*$  is then

$$a = qe.$$

**Remark.** We note that the above corresponds exactly to equation (15) in [35].

**Proof (sketch):** To derive the duality relations, we make use of Euler's formula, which, as usual, has to be interpreted in the context of specific boundary conditions. And here we have the additional step of integrating out the middle spin to return to the triangular lattice. However, with careful consideration of the situation at the boundary, dual measures may be identified in finite volume. Specifically, if  $\Lambda$  consists of nothing more than  $N$  connected up-pointing triangles with free boundary conditions, then the dual model will consist of the corresponding down-pointing triangles with fully wired boundary conditions. Other scenarios at the boundary can be treated in a similar fashion; we will be content to proceed formally. But before we begin there is yet another technical difficulty: Our three-body interactions do not distinguish between triangles with two or three edges occupied; in order to use Euler's formula we must take this into account, so we set the convention that all three-body interactions have all three edges occupied. Now, finally, we have:

$$\begin{aligned} W(\omega) &= q^{c(\omega)} s^{|\mathcal{S}(\omega)|} a^{|\mathcal{A}(\omega)|} e^{|\mathcal{E}(\omega)|} \\ &\propto q^{l(\omega)} \left(\frac{s}{q}\right)^{|\mathcal{S}(\omega)|} \left(\frac{a}{q^3}\right)^{|\mathcal{A}(\omega)|} e^{|\mathcal{E}(\omega)|}. \end{aligned}$$

Thus if  $\omega^\star$  is the standard dual (on the hexagonal lattice) we have:

$$W(\omega) \propto q^{c(\omega^\star)} \left(\frac{s}{q}\right)^{|\mathcal{S}(\omega^\star)|} \left(\frac{a}{q^3}\right)^{|\mathcal{A}(\omega^\star)|} e^{|\mathcal{E}(\omega^\star)|},$$

where  $|e(\omega^\star)|$  corresponds to the number of empty triads, etc. Finally, integrating out all middle spins, we obtain:

$$\begin{aligned} W(\omega) &\propto q^{c(\omega^*)} \left(\frac{s}{q}\right)^{|\mathcal{S}(\omega^*)|} \left(\frac{a}{q^2}\right)^{|\mathcal{E}(\omega^*)|} e^{|\mathcal{A}(\omega^*)|} \\ &\propto q^{c(\omega^*)} \left(\frac{qs}{a}\right)^{|\mathcal{S}(\omega^*)|} 1^{|\mathcal{E}(\omega^*)|} \left(\frac{eq^2}{a}\right)^{|\mathcal{A}(\omega^*)|}. \end{aligned}$$

Here we have used the fact that the empty configuration on the triad has four connected components while that on the triangle when the middle vertex is integrated out has only three, so we must compensate a factor of  $q$  for each  $\mathcal{E}(\omega^\star)$ , yielding the  $q^{-2}a$ . The weights are now in the form of equation (II.14). Derivation of the self-dual curve is now straightforward.  $\square$

Simple algebra now gives:

**Corollary II.3.2.** *For  $\lambda \geq 0$ , the regions  $ae \geq \lambda s^2$  are invariant under the  $\ast$ -map.*

### II.3.3 Positive Correlation

Our proof of positive correlations will concern  $N$  triangles with configurations of the type described and measures determined by the weights given in (II.12). For the purposes of this proof, we make no restrictions on the geometry of the triangles: they need not represent a subset of the triangular (or any other planar) lattice. In general, sites can belong to any number of triangles, but if a pair of sites belong to two distinctive triangles, the associated bonds can appear twice. In addition, we will need to consider different sorts of boundary conditions on our  $N$  triangles; these will, generically, be denoted by  $\Gamma$ . These

$\Gamma$  conditions are the identification of sets of points which are considered to be “preconnected” (even if no bonds are present). In particular, the specification of  $\Gamma$  provides us with a precise notion of  $c(\omega)$  and, for all intents and purposes, determines the geometry of the collection.

**Definition II.3.3.** Fix  $a, e, s$  with  $a + 3s + e = 1$ . Let  $\Lambda$  be a fixed set of vertices in the triangular lattice corresponding to  $M$  triangles which we label  $t_1, t_2, \dots, t_M$ . Let  $\mathcal{T}_M \equiv \{[\mathcal{E}], [\mathcal{S}]_1, [\mathcal{S}]_2, [\mathcal{S}]_3, [\mathcal{A}]\}^M$  denote the set of configurations on  $\{t_1, t_2, \dots, t_M\}$ . Let  $\Gamma$  denote an arbitrary wiring on  $\Lambda$ , then for  $\omega \in \mathcal{T}_M$ ,

$$W_\Lambda^\Gamma(\omega) \propto q^{c(\omega, \Gamma)} e^{|\mathcal{E}(\omega)|} s^{|\mathcal{S}(\omega)|} a^{|\mathcal{A}(\omega)|}, \quad (\text{II.15})$$

where  $c(\omega, \Gamma)$  now denotes the number of connected components determined by the wiring  $\Gamma$  as well as the configuration  $\omega$ . Now for  $N \leq M$ , and  $\omega \in \mathcal{T}_N$ , we let

$$\mu_N^\Gamma(\omega) \propto W_\Lambda^\Gamma(\omega, \underbrace{[\mathcal{E}], \dots, [\mathcal{E}]}_{M-N \text{ times}}),$$

denote the measure on those  $N$  triangles obtained from the corresponding weight.

**Remark.** The main thing to remember from the above definition is that we are working with some *a priori*  $\Lambda$  and *all* the vertices of  $\Lambda$  are taken into account in the term  $c(\omega, \Gamma)$ ; this will become important later in the section when the structure of the weights actually come into play. Needless to say, we will be interested (for the purposes of induction) in an  $N$  which may be envisioned as far smaller than  $M$ ; indeed, for finite  $M$  there is no difficulty with the immediate passage  $M \rightarrow \infty$ .

**Theorem II.3.4.** *Let  $\mu_N^\Gamma$  denote the measures as described above with  $q \geq 1$  and  $ae \geq 2s^2$ . Then for all  $N$  and all wiring boundary conditions  $\Gamma$ , these measures have positive correlations.*

The idea is to proceed by induction on the number of triangles  $N$  which we regard as embedded in the larger space of  $M$  triangles,  $N - M$  of which are automatically empty. We will need the strong inductive hypothesis that  $\mu_{N-1}^\Gamma$  has positive correlations for *all* possible wirings  $\Gamma$ . For the case  $N = 1$ , there are clearly only five possible outside wirings: no vertices are connected, the vertices corresponding to side one (respectively two and three) are connected, and finally all three vertices are connected; we denote these wirings by  $\mathcal{E}$ ,  $\mathcal{S}_1$ ,  $\mathcal{S}_2$ ,  $\mathcal{S}_3$ , and  $\mathcal{A}$ , respectively. The all wired case, namely  $\mu_1^{\mathcal{A}}$  is exactly the case proved in Theorem II.2.4. Let us quickly dispense with another example,  $\mu_1^{\mathcal{S}_1}$ . Here we see

$$\mu_1^{\mathcal{S}_1}([\mathcal{S}]_1) = zs.$$

Meanwhile, for  $k = 2, 3$ ,

$$\mu_1^{\mathcal{S}_1}([\mathcal{S}]_k) = z\frac{s}{q},$$

and finally

$$\mu_1^{\mathcal{S}_1}([\mathcal{A}]) = z\frac{a}{q}, \quad \mu_1^{\mathcal{S}_1}([\mathcal{E}]) = ze,$$

where we use the notation  $[\mathcal{A}]$ ,  $[\mathcal{S}]_1$ ,  $\dots$ ,  $[\mathcal{E}]$  to denote the relevant corresponding events and  $z$  is a normalization constant. The necessary inequality  $\mu_1^{\mathcal{S}_1}([\mathcal{A}])\mu_1^{\mathcal{S}_1}([\mathcal{E}]) \geq \mu_1^{\mathcal{S}_1}([\mathcal{S}]_1)(\mu_1^{\mathcal{S}_1}([\mathcal{S}]_2) + \mu_1^{\mathcal{S}_1}([\mathcal{S}]_3))$  follows readily from  $ae \geq 2s^2$  provided  $q \geq 1$ . The other cases are just as easily demonstrated and we may consider the base case to be established.

We make use of two key ideas in the forthcoming inductive proof. The first is a generalized version of the lattice condition. Indeed, whenever the underlying space is the product of linearly ordered spaces, the lattice condition is entirely equivalent to the minimalist version:

$$\frac{\nu(\eta, a, b)}{\nu(\eta, a, b')} \geq \frac{\nu(\eta, a', b)}{\nu(\eta, a', b')}, \quad (\text{II.16})$$

where the  $a$ 's and  $b$ 's represent the configuration at any two coordinates,  $\eta$  is all other coordinates and  $a \geq a'$  and  $b \geq b'$ . Crucial to our argument is that despite the absence (or inapplicability) of the full lattice condition, an analogue of (II.16) nevertheless holds. The second key idea is a slight generalization of Proposition 2.22 in [22] which is the statement that a convex combination of two measures with positive correlations itself has positive correlations if one of the measures FKG dominates the other. We state and prove these as our next two lemmas below.

**Lemma II.3.5.** *Let  $\mu_N^\Gamma$  be defined as above with  $q \geq 1$ . Then an analogue of (II.16) holds for  $\mu_N^\Gamma$ , provided the separate increases pertain to different triangles. E.g., if  $\mathbb{T}_{N-2}$  is the configuration on the first  $N - 2$  triangles, and we have  $T_{N-1}, T'_{N-1}, T_N, T'_N$  as configurations on the last two triangles with  $T_{N-1} \succeq T'_{N-1}$  and  $T_N \succeq T'_N$ , then*

$$\frac{\mu_N^\Gamma(\mathbb{T}_{N-2}, T_{N-1}, T_N)}{\mu_N^\Gamma(\mathbb{T}_{N-2}, T_{N-1}, T'_N)} \geq \frac{\mu_N^\Gamma(\mathbb{T}_{N-2}, T'_{N-1}, T_N)}{\mu_N^\Gamma(\mathbb{T}_{N-2}, T'_{N-1}, T'_N)}.$$

**Proof:** Examining the ratios in the statement above, a quick glance at (II.15) reveals that all the “prefactors” cancel on both sides of the purported inequality, leaving only the  $q$ -dependent terms. Since  $q > 1$ , the above amounts to a

special case of

$$C(\omega \vee \eta) + C(\omega \wedge \eta) \geq C(\omega) + C(\eta),$$

which has been proved in complete generality in numerous places (e.g. [1]).  $\square$

**Lemma II.3.6.** *Let  $(\mathcal{H}, \succeq_{\mathcal{H}})$  and  $(\mathcal{K}, \succeq_{\mathcal{K}})$  be finite partially ordered sets. Let  $\mu$  be a probability measure on  $\mathcal{H}$  and for each  $\eta \in \mathcal{H}$ , let  $\nu_{\eta}$  be a probability measure on  $\mathcal{K}$ . It is supposed that  $\mu$  has positive correlations, that for each  $\eta$ , the measure  $\nu_{\eta}$  has positive correlations and furthermore, if  $\eta_1 \succeq \eta_2$ , then  $\nu_{\eta_1} \underset{FKG}{\geq} \nu_{\eta_2}$ . Then*

$$\nu(-) \equiv \sum_{\eta \in \mathcal{H}} \mu(\eta) \nu_{\eta}(-)$$

*has positive correlations.*

**Proof:** Let  $f$  and  $g$  be increasing functions on  $\mathcal{K}$ . Then

$$\begin{aligned} \mathbf{E}_{\nu}(fg) &= \sum_{\omega \in \mathcal{K}} \nu(\omega) f(\omega) g(\omega) \\ &= \sum_{\eta \in \mathcal{H}} \mu(\eta) \mathbf{E}_{\nu_{\eta}}(fg) \\ &\geq \sum_{\eta \in \mathcal{H}} \mu(\eta) \mathbf{E}_{\nu_{\eta}}(f) \mathbf{E}_{\nu_{\eta}}(g). \end{aligned}$$

It is observed from the hypothesis that  $\mathbf{E}_{\nu_{\eta}}(f)$  and  $\mathbf{E}_{\nu_{\eta}}(g)$  are increasing in  $\eta$  and the result follows from the positive correlation of  $\mu$ .  $\square$

Now let us informally proceed with an inductive proof. In what is to follow we assume that  $f$  and  $g$  are increasing functions on  $N$  triangles,  $\mathbb{T}_{N-1}$  always denotes the configuration on the first  $N-1$  triangles and  $T_N \in \{[\mathcal{A}], \dots, [\mathcal{E}]\}$  a generic state of the  $N^{\text{th}}$  triangle. We condition on the state of the last triangle,

and according to Bayes' formula, we get

$$\mu_N^\Gamma(-) = \sum_{T_N} \mu_{N|\Delta_N}^\Gamma(T_N) \mu_N^\Gamma(-|T_N),$$

where  $\mu_{N|\Delta_N}^\Gamma$  is the restriction of  $\mu_N^\Gamma$  to the last triangle.

As far as the first  $N - 1$  triangles are concerned, we can apply the inductive hypothesis to conclude that the measures  $\mu_N^\Gamma(-|T_N)$  has positive correlations, since the conditioning, along with  $\Gamma$ , give us *some* wiring scenario for these triangles. So (appealing to Lemma (II.3.6)) we will be done if we can show that (i)  $\mathbf{E}_N^\Gamma(f|T_N)$  and  $\mathbf{E}_N^\Gamma(g|T_N)$  are increasing in  $T_N$  (i.e.  $\mu_N^\Gamma(-|T_N) \underset{\text{FKG}}{\geq} \mu_N^\Gamma(-|T'_N)$  whenever  $T_N \succeq T'_N$ ), and (ii) the measure  $\mu_{N|\Delta_N}^\Gamma$  has positive correlation. These are the topics of yet the next two lemmas.

**Lemma II.3.7.** *Let  $f$  and  $T_N$  be as described and define*

$$F_{T_N} = \mathbf{E}_N^\Gamma(f|T_N).$$

*Then  $F_{T_N}$  is an increasing function.*

**Proof:** Suppose  $T_N \succeq T'_N$ . Then we note that, as in the standard argument, Lemma (II.3.5) implies that

$$\phi(\mathbb{T}_{N-1}) = \frac{\mu_N^\Gamma(T'_N)}{\mu_N^\Gamma(\mathbb{T}_{N-1}, T'_N)} \frac{\mu_N^\Gamma(\mathbb{T}_{N-1}, T_N)}{\mu_N^\Gamma(T_N)} \quad (\text{II.17})$$

is an increasing function of  $\mathbb{T}_{N-1} = (T_1, \dots, T_{N-1})$ . We aim to show that

$$\mathbf{E}_N^\Gamma(f|T_N) \geq \mathbf{E}_N^\Gamma(f|T'_N).$$

We have

$$\begin{aligned} \mathbf{E}_N^\Gamma(f|T_N) &= \sum_{\mathbb{T}_{N-1}} f(\mathbb{T}_{N-1}, T_N) \frac{\mu_N(\mathbb{T}_{N-1}, T_N)}{\mu_N(T_N)} \\ &\geq \sum_{\mathbb{T}_{N-1}} f(\mathbb{T}_{N-1}, T'_N) \frac{\mu_N(\mathbb{T}_{N-1}, T_N)}{\mu_N(T_N)}, \end{aligned}$$

since  $f$  is increasing and  $T_N \geq T'_N$ . Now the last expression can be rewritten as

$$\sum_{\mathbb{T}_{N-1}} f(\mathbb{T}_{N-1}, T'_N) \frac{\mu_N^\Gamma(\mathbb{T}_{N-1}, T'_N)}{\mu_N^\Gamma(T'_N)} \phi(\mathbb{T}_{N-1}) = \mathbf{E}_N^\Gamma(f\phi|T'_N),$$

which by induction is greater than or equal to  $\mathbf{E}_N^\Gamma(f|T'_N)\mathbf{E}_N^\Gamma(\phi|T'_N)$ . Thus, concatenating the above expressions, we have

$$\begin{aligned} \mathbf{E}_N^\Gamma(f|T_N) &\geq \mathbf{E}_N^\Gamma(f|T'_N)\mathbf{E}_N^\Gamma(\phi|T'_N) \\ &= \left( \sum_{\mathbb{T}_{N-1}} f(\mathbb{T}_{N-1}, T'_N) \frac{\mu_N^\Gamma(\mathbb{T}_{N-1}, T'_N)}{\mu_N^\Gamma(T'_N)} \right) \left( \sum_{\mathbb{T}_{N-1}} \frac{\mu_N^\Gamma(\mathbb{T}_{N-1}, T_N)}{\mu_N^\Gamma(T_N)} \right) \\ &= \mathbf{E}_N^\Gamma(f|T'_N), \end{aligned}$$

since  $\sum_{\mathbb{T}_{N-1}} \frac{\mu_N^\Gamma(\mathbb{T}_{N-1}, T_N)}{\mu_N^\Gamma(T_N)} = 1$ . □

**Lemma II.3.8.** *Let  $\mu_{N|\Delta_N}^\Gamma$  denote the measure  $\mu_N^\Gamma$  as described above restricted to the  $N^{\text{th}}$  triangle. Then  $\mu_{N|\Delta_N}^\Gamma$  has positive correlation.*

**Proof:** We will again make use of Lemma II.3.6, so we write

$$\mu_{N|\Delta_N}^\Gamma(-) = \sum_{\mathcal{B}} \mu_N^\Gamma(\mathcal{B}) \mu_{N|\Delta_N}^{\mathcal{B}}(-), \quad (\text{II.18})$$

where  $\mathcal{B}$  represents the total wiring conditions outside the  $N^{\text{th}}$  triangle due to the initial wiring condition  $\Gamma$  and the outside configurations,  $\mathbb{T}_{N-1}$ . However, the overall effect of  $\Gamma$  and  $\mathbb{T}_{N-1}$  is to produce one of the five types of wiring on a single triangle – a situation with which we are familiar – and henceforth we may assume  $\mathcal{B} \in \{\mathcal{A}, \mathcal{I}_1, \mathcal{I}_2, \mathcal{I}_3, \mathcal{E}\}$ .

We note that for each  $\mathcal{B}$ ,  $\mu_{\Delta_N}^{\mathcal{B}}$  has positive correlations (the subject of the base case). Next, we claim that  $\mathcal{B} \succeq \mathcal{B}'$  implies that  $\mu_N^{\mathcal{B}} \geq \mu_N^{\mathcal{B}'}$ . This follows from the observation that less wiring on the outside produces more

factors of  $q^{-1}$  for the weights of the higher configurations (see the Remark after Definition (II.3.3)). Explicitly, it can be checked that for  $\mathcal{B} \succeq \mathcal{B}'$ ,

$$\mu_N^{\mathcal{B}'} \propto D \mu_N^{\mathcal{B}},$$

where  $D$  (which depends on  $\mathcal{B}'$  and  $\mathcal{B}$ ) is a decreasing function of  $T_N$ . Thus we have verified two of the three hypotheses of Lemma (II.3.6).

We are down to the last hypothesis; here we will need to write  $\mu_N^\Gamma(\mathcal{B})$  in a more explicit form. Note that by induction  $\mu_{N-1}^\Gamma(\mathcal{B})$  has positive correlations, so we seek some relationship between  $\mu_N^\Gamma(\mathcal{B})$  and  $\mu_{N-1}^\Gamma(\mathcal{B})$ . To do this we must exploit the “almost” product structure of the weights (II.15) from which our measures came. So we first let  $Z_{N-1}(\mathcal{B})$  denote the *weight* of observing  $\mathcal{B}$ , before the introduction of the  $N^{\text{th}}$  triangle, and let  $Z_{N-1}^T = \sum_{\mathcal{B}} Z_{N-1}(\mathcal{B})$  denote the overall normalization factor, so that  $\lambda_{\mathcal{B}} \equiv Z_{N-1}(\mathcal{B})/Z_{N-1}^T = \mu_{N-1}^\Gamma(\mathcal{B})$ . Next we may write  $Z_{N-1}(\mathcal{B}) = \sum_{\mathbb{T}_{N-1}} \mathbf{1}_{\mathbb{T}_{N-1} \cup \Gamma = \mathcal{B}} W_\Lambda^\Gamma(\mathbb{T}_{N-1})$ , where  $W_\Lambda^\Gamma(\mathbb{T}_{N-1})$  is the weight of observing the configuration  $\mathbb{T}_{N-1}$  as given by (II.15). Similarly, if  $Z_N(\mathcal{B})$  denotes the weight of observing  $\mathcal{B}$  given the  $N^{\text{th}}$  triangle, then

$$Z_N(\mathcal{B}) = \sum_{\mathbb{T}_{N-1}} \mathbf{1}_{\mathbb{T}_{N-1} \cup \Gamma = \mathcal{B}} \left( \sum_{T_N} W_\Lambda^\Gamma(\mathbb{T}_{N-1}, T_N) \right).$$

Comparing the previous two expressions and referring back to Definition (II.3.3), it is not difficult to see that

$$Z_N(\mathcal{B}) = n_{\mathcal{B}} Z_{N-1}(\mathcal{B}),$$

where (up to a factors of  $e$ )  $n_{\mathcal{E}} = (\frac{a}{q^2} + \frac{3s}{q} + e)$ ,  $n_{\mathcal{S}_i} = (\frac{a}{q} + s + \frac{2s}{q} + e)$ , and  $n_{\mathcal{A}} = (a + 3s + e)$  – which happens to be one. Thus, letting  $Z_N^T = \sum_{\mathcal{B}} Z_N(\mathcal{B})$ ,

we arrive at

$$\mu_N^\Gamma(\mathcal{B}) = \frac{Z_N(\mathcal{B})}{Z_N^T} = \frac{Z_{N-1}^T}{Z_N^T} \lambda_{\mathcal{B}} n_{\mathcal{B}}.$$

It is noted that the factor  $Z_{N-1}^T/Z_N^T$  is independent of the wiring  $\mathcal{B}$ ,  $T_N$ , etc. Thus by Theorem (II.2.4) all we need to show is that  $(n_{\mathcal{A}} \lambda_{\mathcal{A}})(n_{\mathcal{E}} \lambda_{\mathcal{E}})$  exceeds  $n_{\mathcal{J}_1} \lambda_{\mathcal{J}_1} (n_{\mathcal{J}_2} \lambda_{\mathcal{J}_2} + n_{\mathcal{J}_3} \lambda_{\mathcal{J}_3})$  – or whatever ordering combination maximizes the latter object. To this end, let  $\sigma$  be a permutation on three letters such that  $\lambda_{\mathcal{J}_{\sigma_1}} \geq \lambda_{\mathcal{J}_{\sigma_2}}$  and  $\lambda_{\mathcal{J}_{\sigma_1}} \geq \lambda_{\mathcal{J}_{\sigma_3}}$ . Our last hypothesis will be verified if we can show that

$$(n_{\mathcal{E}} \lambda_{\mathcal{E}})(n_{\mathcal{A}} \lambda_{\mathcal{A}}) \geq (n_{\mathcal{J}_{\sigma_1}} \lambda_{\mathcal{J}_{\sigma_1}})(n_{\mathcal{J}_{\sigma_2}} \lambda_{\mathcal{J}_{\sigma_2}} + n_{\mathcal{J}_{\sigma_3}} \lambda_{\mathcal{J}_{\sigma_3}}).$$

To this end, we first observe that the induction hypothesis implies  $\lambda_{\mathcal{A}} \lambda_{\mathcal{E}} \geq \lambda_{\mathcal{J}_{\tau(1)}} (\lambda_{\mathcal{J}_{\tau(2)}} + \lambda_{\mathcal{J}_{\tau(3)}})$  for any permutation on three letters  $\tau$ : On general grounds this is true because of the similarity between the outside wiring space and the inside configuration space. But, to proceed formally, let  $f$  and  $g$  be the increasing functions of the outside wiring such that  $f(\mathcal{E}) = g(\mathcal{E}) = 0$ ,  $f(\mathcal{A}) = g(\mathcal{A}) = 1$ ,  $f(\mathcal{J}_{\tau(1)}) = 1 - g(\mathcal{J}_{\tau(1)}) = 1$  and  $f(\mathcal{J}_{\tau(i)}) = 1 - g(\mathcal{J}_{\tau(i)}) = 0$ ,  $i = 2, 3$ . Then by the fact that  $\mu_{N-1}$  has positive correlation, we indeed get  $\lambda_{\mathcal{A}} \lambda_{\mathcal{E}} \geq \lambda_{\mathcal{J}_{\tau(1)}} (\lambda_{\mathcal{J}_{\tau(2)}} + \lambda_{\mathcal{J}_{\tau(3)}})$ . On the basis of this inequality we only need that  $n_{\mathcal{A}} n_{\mathcal{E}} \geq n_{\mathcal{J}_{\sigma_1}}^2$  (since  $n_{\mathcal{J}_{\sigma_1}} n_{\mathcal{J}_{\sigma_1}} = n_{\mathcal{J}_{\sigma_1}} n_{\mathcal{J}_{\sigma_2}} = n_{\mathcal{J}_{\sigma_1}} n_{\mathcal{J}_{\sigma_3}}$ ), i.e. we need that,

$$(a + 3s + e) \left( \frac{a}{q^2} + \frac{3s}{q} + e \right) \geq \left( \frac{a}{q} + s + \frac{2s}{q} + e \right)^2.$$

Now if one multiplies and compares terms, one has an expression which involves  $(q - 1)$  times a quantity which is “easily positive”.

We have verified all three hypotheses of Lemma (II.3.6) and can therefore

conclude that  $\mu_{N|\Delta_N}^\Gamma$  has positive correlation. □

**Proof of Theorem (II.3.4):** As already remarked, we will (again) use Lemma II.3.6. Explicitly, we apply Lemma (II.3.6) with

$$\mathcal{H} = \{[\mathcal{A}], [\mathcal{S}]_1, \dots, [\mathcal{E}]\}$$

(corresponding to configurations on the  $N^{\text{th}}$  triangle) and  $\mu = \mu_{N|\Delta_N}^\Gamma$ , and  $\mathcal{H} = \{[\mathcal{A}], [\mathcal{S}]_1, \dots, [\mathcal{E}]\}^N$  (corresponding to configurations on all  $N$  triangles) and  $\nu_\eta = \mu_N^\Gamma(-|\eta)$ . The three hypotheses of the Lemma are verified by the induction hypothesis and Lemmas II.3.7 and II.3.8. □

We conclude this section with a brief discussion on infinite-volume limits: In the region of positive correlations, more wiring leads to a higher measure. Thus, for free boundary conditions (the restrictions of) measures increase with increase volume and for fully wired boundary conditions, they decrease. So, for a nested sequence of volumes which exhaust the lattice, well-defined infinite-volume limits – which are independent of sequence – exist. Furthermore, as mentioned earlier, wired and free measures may be dually identified in finite volume. Thus, in turn, we may identify the dual of the infinite volume free measure as the wired measure and vice versa.

## II.3.4 Phase Transitions

In this subsection, we establish results on phase transitions in the  $q$ -state Potts/random cluster models under consideration. Here, unlike in the percolation case, we cannot establish with certainty whether the transition is

continuous or discontinuous. Moreover, for the continuous cases, our statements will be considerably weaker than our Theorem II.2.5 since much of the technical artillery (e.g. the van den Berg-Kesten inequalities) do not apply. In particular, in the continuous case, we cannot even prove that the percolation/magnetization transition actually occurs on the self-dual line. Nevertheless, critical *behavior* is established for self-dual points which are also points of continuity, the subject of our first proposition:

**Proposition II.3.9.** *Consider the random cluster model on the triangular lattice as defined by (II.12) and satisfying  $ae \geq 2s^2$ . Then at any self-dual point  $a = qe$  which is a point of continuity of the bond density the following hold: (1) The percolation probability vanishes and (2) there are power law lower bounds on the correlation functions.*

**Proof:** Much of the proof can be transcribed directly from our proof of Theorem II.2.5 and as for the rest, similar arguments have appeared before ([3], [11]), so we will be succinct. The first statement follows from the results in [19] which, under the conditions of positive correlations and 2D symmetries, forbids coexisting infinite clusters of the opposite types. Thus, in any realization, there is either no percolation of either type or there are separate states (depending on how the infinite-volume limit was constructed) which have and don't have percolation. However, this latter happenstance, by appeal to Strassen's Theorem [30] implies that the distinctive states have different bond densities which would imply a discontinuity in the bond density. For the second statement, routine arguments which may be traced back to [1] imply that the limiting random cluster measure is unique and therefore may be identified with the

dual measure; on this basis the rest of the argument follows mutatis mutandis from the proof of Theorem II.2.5 for percolation (again see [11]).  $\square$

Finally we show that in the region of positive correlation, any discontinuity in bond density must occur on the self-dual curve:

**Proposition II.3.10.** *Consider the random cluster model on the triangular lattice as defined by (II.12) and satisfying  $ae \geq 2s^2$ . Then any discontinuity in the bond density must occur on the self-dual curve as given by  $a = qe$ .*

**Proof:** Our proof is a variation of the one found in [3]; here we unfortunately do not have a convenient family of curves which are nicely preserved under the duality relations. We will work with  $A$  and  $S$  parameters given in (II.14); suppose at  $(A_0, S_0)$  – with  $A_0 > 2S_0^2$  – we have a discontinuity in the bond density. Let  $\lambda \geq 1$  and consider the curve  $C \equiv \{(2\lambda S_0^2, S_0) : \lambda \geq 1\}$ . We note that along  $C$  the measure is FKG increasing with increasing  $\lambda$ . Next let  $\lambda^{SD}$ ,  $\lambda^P$  and  $\lambda^D$  denote the corresponding values of  $\lambda$  at which the curve  $C$  intersects the self-dual curve, the percolation threshold, and the discontinuity, respectively. We aim to show that  $\lambda^{SD} = \lambda^P = \lambda^D$ .

Let  $C_l$  denote the part of  $C$  which is below the self-dual curve and similarly let  $C_u$  denote the part of  $C$  which is above the self-dual curve. Since it is not the case that  $(C_l)^* = C_u$ , we need to define two new curves to work with: Let  $C_y = C_l \cup (C_l)^*$  and  $C_p = C_u \cup (C_u)^*$ , and we parametrize  $C_y$  by  $\lambda_y$  and  $C_p$  by  $\lambda_p$  with the requirement that  $\lambda = \lambda_y$  on  $C_l$  and  $\lambda = \lambda_p$  on  $C_u$  (and extending in the obvious fashion). We remark that with these parametrizations,  $C_y$  and  $C_p$  are FKG increasing in  $\lambda_y$  and  $\lambda_p$  by duality (or by explicit computation): E.g., on  $C_y \cap C_l$  the measures are clearly FKG increasing; on the other hand, this

implies the measures corresponding to the *dual* parameters – these lie on  $(C_l)^*$  and are parametrized by  $\lambda_y \geq \lambda_y^{SD}$  – are *decreasing* in  $\lambda_y$  for  $\lambda_y \leq \lambda_y^{SD}$ , and hence increasing in  $\lambda_y$  for  $\lambda_y \geq \lambda_y^{SD}$ . Now if we let  $\lambda_y^D$ ,  $\lambda_y^{SD}$  and  $\lambda_y^P$  denote the corresponding values of  $\lambda_y$  at which the curve  $C$  intersects the self-dual curve, the percolation threshold and (should it exist) the discontinuity, respectively. Similarly we define  $\lambda_p^D$ ,  $\lambda_p^{SD}$  and  $\lambda_p^P$  for  $C_p$ . Then  $\lambda_y^{SD} = \lambda_p^{SD} = \lambda^{SD}$ .

First we show that  $\lambda^P \geq \lambda^{SD}$ : If this is not the case, then for  $\lambda^{SD} > \lambda > \lambda^P$  the direct model is percolating in the wired state. Note that this  $\lambda$  corresponds to a  $\lambda_y$  in our new parametrization. At the dual value,  $\lambda_y^*$ , we would then have dual percolation in the state with free boundary conditions. However, the dual model in the wired state at parameter  $\lambda$  “dominates” the dual model in the free state at parameter  $\lambda_y^*$ , and hence there is dual *and* direct percolation at  $\lambda$  (e.g. in the wired state), which is a contradiction of [19]. Next we can easily show that  $\lambda^P \leq \lambda^D$ : This is because a discontinuity in the bond density implies non-uniqueness of the limiting measure and hence, ultimately, percolation. Finally, we must have  $\lambda^D \leq \lambda^{SD}$ : Towards a contradiction assume that  $\lambda^D > \lambda^{SD}$ ; this implies that  $\lambda_p^D$  actually exists and is equal to  $\lambda^D$ . Next note that the same argument that showed  $\lambda^P \leq \lambda^D$  also shows  $\lambda_p^P \leq \lambda_p^D$ . Since we have a discontinuity in the direct model if and only if we have a discontinuity in the dual model, we have another discontinuity at  $\lambda_p^* < \lambda_p^{SD} \leq \lambda_p^P$ , a contradiction.  $\square$

## II.4 Conclusion

We have described a Potts/random cluster model on the triangular lattice with three-body correlations. By introducing a reduced state space, the duality relations are easily derived. It is noted, in the context of spin systems, that the purely ferromagnetic region of parameters is *not* mapped into itself under duality. More generally, in the  $q \geq 1$  random cluster models, when we consider the full state space, the region which has positive correlations is not mapped into itself. However, for the reduced case, necessary and sufficient conditions for positive correlations are derived which are invariant under duality and include a larger portion of the original parameter space. Under the conditions of positive correlations, for percolation and for values of  $q$  where there are discontinuities, it is proved that the transition occurs at the self-dual point; if there is no discontinuity, self-dual points admit critical behavior. On the basis of exact solutions [4] it has been argued that the dividing line is  $q = 4$ , similar to the situation on the square lattice. The advantage of the current random cluster formulation is that this hypothesis can be tested numerically using cluster methods; e.g., the algorithms in [13], [23] and [10] can be readily adapted. While we have no reason to doubt the results in [4] in this case, for a related model with three-body interactions on the square lattice, there is some evidence pointing to the reduction of the dividing  $q$ . In any case, although we will not discuss details, it should at least be possible to prove that for large  $q$  there is a discontinuous transition. Here certain modifications will be needed to adapt the methods of reflection positivity to the present case, which may very well be the subject of a later paper.

# Bibliography

- [1] M. Aizenman, J. T. Chayes, L. Chayes, and C. M. Newman. *Discontinuity of the Magnetization in One-Dimensional  $1/|x - y|^2$  Ising and Potts Models*. J. Stat. Phys. **77**, 351-359 (1994).
- [2] J. Ashkin and E. Teller. *Statistics of Two-Dimensional Lattices with Four Components*. Phys. Rev. **64**, 178–184 (1943).
- [3] T. Baker and L. Chayes. *On the Unicity of Discontinuous Transitions in the Two-Dimensional Potts and Ashkin-Teller Models*. Jour. Stat. Phys. **93**, 1-15 (1998).
- [4] R. J. Baxter, N. H. V. Temperley and S. E. Ashley. *Triangular Potts Model at Its Transition Temperature, and Related Models*. Proc. R. Soc. **A 358**, 535-539 (1978).
- [5] Theodore W. Burkhardt. *Applications of an Exact Duality-Decimation Transformation for Two-Dimensional Spin Systems on a Square Lattice*. Physical Review B. **20** no. 7, 2905-2913 (1979).
- [6] R. M. Burton and M. Keane. *Density and Uniqueness in Percolation*. Comm. Math. Phys. **121** no. 3, 501–505 (1989).

- [7] J. T. Chayes and L. Chayes. *The Correct Extension of the Fortuin-Kasteleyn Result to Plaquette Percolation*. Nuclear Physics **B235**, 19-23 (1983).
- [8] L. Chayes. *Percolation and Ferromagnetism on  $\mathbb{Z}^2$ : the  $q$ -state Potts Cases*. Stochastic Processes and Their Applications **65**, 209-216 (1996)
- [9] L. Chayes and J. Machta. *Graphical Representations and Cluster Algorithms I. Discrete spin systems*. Physica A **239**, 542-601 (1997).
- [10] L. Chayes and J. Machta. *Graphical Representations and Cluster Algorithms II*. Physica A **254**, 477-516 (1998).
- [11] L. Chayes and K. Shtengel. *Critical Behavior for 2D Uniform and Disordered Ferromagnets at Self-Dual Points*. Comm. Math. Phys. **204**, 353-366 (1999).
- [12] E. Domany and E. K. Riedel. *Two-Dimensional Anisotropic  $N$ -Vector Models*. Phys. Rev. B **19**, 5817-5834 (1979).
- [13] R. G. Edwards and A. D. Sokal. *Generalization of the Fortuin-Kasteleyn-Swendsen-Wang Representation and Monte Carlo Algorithm*. Phys. Rev. D. **38**, 2009-2012 (1988).
- [14] Essam and Syskes. *Dimensional Crossover in Selective Site Percolation*. J. Math. Phys. **5**, 1117-27 (1964).
- [15] C. M. Fortuin and P. W. Kasteleyn. *On the Random-Cluster Model. I. Introduction and Relation to Other Models*. Physica **57**, 536-564 (1972).

- [16] G. Grimmett. *Percolation*. Berlin, New York: Springer Verlag (1999).
- [17] G. Grimmett. *Potts models and random-cluster models with many-body interactions*. J. Stat. Phys. **75**, 67–121 (1994).
- [18] A. Gandolfi, G. Grimmett, and L. Russo. *On the Uniqueness of the Infinite Open Cluster in the Percolation Model*. Comm. Math. Phys. **113**, 549-552 (1988).
- [19] A. Gandolfi, M. Keane, and L. Russo. *On the Uniqueness of the Infinite Cluster in Dependent Two-Dimensional Site Percolation*. Annals of Prob. **16**, 1147-1157 (1988).
- [20] D. Kim and R. I. Joseph. *Exact Transition Temperature of the Potts Model With  $q$  States Per Site for the Triangular and Honeycomb Lattices*. J. Phys. C. **7**, L167 (1974).
- [21] H. A.Kramers and G. H. Wannier. *Statistics of the Two-Dimensional Ferromagnet. I*. Phys. Rev. (2) **60**, 252-262 (1941).
- [22] T. M. Liggett. *Interacting Particle Systems*, Berlin, New York: Springer Verlag (2005).
- [23] J. Machta, Y. S. Choi, A. Lucke, T. Schweizer, and L. V. Chayes. *Invaded Cluster Algorithm for Equilibrium Critical Points*. Phys. Rev. Lett. **75**, 2792-2795 (1995).
- [24] M. V. Menshikov. *Coincidence of Critical Points in Percolation Problems*. Soviet Mathematics Doklady **33**, 856-859 (1986).

- [25] M. V. Menshikov, S. A., Molchanov, and A. F. Sidorenko. *Percolation Theory and Some Applications*. Itogi Nauki i Techniki, Series of Probability Theory, Mathematical Statistics, Theoretical Cybernetics **24**, 53-110 (1986).
- [26] C. E. Pfister. *Phase Transitions in the Ashkin-Teller Model*. J. Stat. Phys. **29**, 115-118 (1982).
- [27] D. Reimer. *Proof of the vanden Berg-Kesten Conjecture*. Combin. Probab. Comput. **9** no. 1, 27-32 (2000).
- [28] L. Russo. *A Note on Percolation*. Z. Wahrscheinlichkeitstheorie und Verw. Gebiete **43** no. 1, 39-48 (1978).
- [29] L. Russo. *On the Critical Percolation Probabilities*. Zeitschrift für Wahrscheinlichkeitstheorie und Verwandte Gebiete **56**, 229-237 (1981).
- [30] V. Strassen. *The Existence of Probability Measures with Given marginals*. Ann. Math. Statist. **36**, 423-439 (1965).
- [31] R. H. Swendsen and J. S. Wang. *Nonuniversal Critical Dynamics in Monte Carlo Simulations*. Phys. Rev. Lett. **58**, 86-88 (1987).
- [32] F. J. Wegner. *Duality Relation Between the Ashkin-Teller and the Eight-Vertex Model*. J. Phys. C **5**, L131-132 (1972).
- [33] John C. Wierman. *Bond Percolation On Honeycomb and Triangular Lattices*. Adv. in Appl. Probab. **13** 298-313 (1981).

- [34] John C. Wierman. *A Bond Percolation Critical Probability Determination Based On the Star-Triangle Transformation*. J. Phys. A. **17**, 1525-1530 (1984).
- [35] F. Y. Wu and K. Y. Lin. *On the Triangular Potts Model With Two- and Three-Site Interaction*. J. Phys. A **13**, 629-636 (1980).
- [36] F. Y. Wu. *The Potts Model*. Rev. Mod. Phys. **54**, 235-268 (1982).
- [37] F. Y. Wu and R. K. P. Zia. *Critical Point of a Triangular Potts Model With Two- and Three-Site Interactions*. Journal of Physics A. **14**, 721-727 (1981).

# Chapter III

## Cardy's Formula for Certain Models of the Bond–Triangular Type

**Abstract:** We introduce and study a family of 2D percolation systems which are based on the bond percolation model of the triangular lattice. The system under study has local correlations, however, bonds separated by a few lattice spacings act independently of one another. By avoiding explicit use of microscopic paths, it is first established that the model possesses the typical attributes which are indicative of critical behavior in 2D percolation problems. Subsequently, the so called Cardy–Carleson functions are demonstrated to satisfy, in the continuum limit, Cardy's formula for crossing probabilities. This extends the results of S. Smirnov to a non-trivial class of critical 2D percolation systems.

**Keywords:** Universality, Conformal invariance, Cardy’s formula, Critical percolation.

## III.1 Introduction

### III.1.1 Introductory Remarks

In recent years, tremendous progress has been made towards understanding the (limiting) behavior of critical 2D percolation models; much of this is contained in the works of [14], [2], [16], [11]. However, with very few exceptions, e.g. long distance behavior of certain multi-arm correlations [11], [1], [10], all results have been confined to the site percolation model on the triangular lattice and scaling limits thereof. Indeed, as uncovered by Smirnov [14], on this particular lattice, there is a miraculous local  $120^\circ$  symmetry that facilitates the passage to the continuum. Needless to say, an underlying theme behind “invariant critical behavior” is some notion of *universal* behavior for the limiting model. Unfortunately, the problem of extending Smirnov’s result to other well-known 2D percolation models has, so far, proved illusive. Here we present some limited progress towards these goals by establishing that in addition to the site problem on the triangular lattice, Cardy’s formula holds for a modified bond problem on the triangular lattice.

We remark that in [3] and [4], some steps in this direction have already been taken. However, the critical models considered therein were, at long distance, demonstrably equivalent to the triangular site model from which they were evolved. In particular, the asymptotic behavior of the connectivity functions

and the cluster size distributions can be bounded above and below by their counterparts from the independent model on the triangular site lattice. Thus the mere existence of “ $\eta$ ” and “ $\delta$ ” for the independent site model (implied by [14], [2], [16], [11]) gives this for free in the models of [3] and [4]. This deviates somewhat from the original spirit of scaling and universality: it is supposed that one can *infer* the critical exponents of a given lattice model via the universality class to which it belongs.

The work of the present note is in rather closer adherence to the above-mentioned order of reasoning. We construct a model based more on triangular bond percolation than site percolation. (For technical as well as aesthetic reasons, local correlations between neighboring bonds will be introduced, but all events separated by three or more lattice spacings are independent.) While perhaps obvious on the level of heuristics, critical behavior of the model requires verification; indeed this constitutes a non-trivial fraction of the work. When this is achieved – around the end of Section 2 – one has a fairly standard-looking percolation-like model, not particularly distinguished from the myriad of critical 2D percolation models which one presumes is equivalent, in the scaling limit, to the limit obtained from the site model on the triangular lattice. We remark, however, that before the advent of this work, and as likely as not in its aftermath, this will be among the less well-known models of critical 2D percolation. Notwithstanding a derivation for this model, which parallels the derivation in [14], is obtained for universal – and conformally invariant – behavior of the limiting crossing probabilities.

### III.1.2 Background and Smirnov's Proof

In [14], a conformal invariant was found for critical site percolation on the triangular lattice that amounts to the conformal invariance of certain crossing probabilities and a verification of Cardy's formula [5]. These properties allow the unique determination of the scaling limit [17] via a connection to  $\text{SLE}_6$ . As our general strategy follows closely that of [14], we include here a short discussion on [14] and set up some general notation – before launching into the specifics of our problem in the next section. We will be succinct since most of what we say here can be found in the first part of [14].

Let  $\Lambda$  denote a piecewise smooth domain which is the conformal image of a triangle. We denote the portions of the boundaries corresponding to the sides of the triangle by  $\mathcal{A}$ ,  $\mathcal{B}$  and  $\mathcal{C}$ , and the associated vertices by  $e_{AB}$ ,  $e_{BC}$  and  $e_{CA}$  respectively. The sequence  $(\mathcal{A}, e_{AB}, \mathcal{B}, e_{BC}, \mathcal{C}, e_{CA})$  should be regarded as counterclockwise ordered.

Let  $h_A$ ,  $h_B$  and  $h_C$  denote the linear and hence harmonic functions defined on the unit equilateral triangle with vertices at  $z = 0$ ,  $z = 1$  and  $z = \frac{1}{2} + i\frac{\sqrt{3}}{2}$ :

$$h_A = 1 - \left(x + \frac{1}{\sqrt{3}}y\right), \quad h_B = x - \frac{1}{\sqrt{3}}y, \quad h_C = \frac{2}{\sqrt{3}}y.$$

Notice that  $h_A$  vanishes on one of the boundaries (the  $\mathcal{A}$  boundary) and is equal to one at the vertex  $e_{BC}$ , and similarly for  $h_B$  and  $h_C$ . Let  $h_{\mathcal{A}}$ ,  $h_{\mathcal{B}}$  and  $h_{\mathcal{C}}$  denote the corresponding functions under the appropriate conformal transformation which takes the above-mentioned triangle into  $\Lambda$ . Note that the boundary conditions, including the vertices are preserved under this transformation. Obviously, even after the transformation, these three functions are

not independent, e.g. they add to one. More importantly, they form a “harmonic triple”; i.e. the functions

$$h_{\mathcal{A}} + \frac{i}{\sqrt{3}}(h_{\mathcal{B}} - h_{\mathcal{C}}), \quad h_{\mathcal{B}} + \frac{i}{\sqrt{3}}(h_{\mathcal{C}} - h_{\mathcal{A}}), \quad h_{\mathcal{C}} + \frac{i}{\sqrt{3}}(h_{\mathcal{A}} - h_{\mathcal{B}})$$

are all analytic.

**Definition III.1.1.** Let  $\Lambda$  and  $\mathcal{A}$ , etc. be as above and consider the intersection of  $\Lambda$  with the triangular site lattice with spacing  $N^{-1}$ . Let us consider critical percolation on this lattice – sites are blue or yellow with probability  $\frac{1}{2}$  and, for  $z \in \Lambda$ , define  $\mathcal{U}_N(z)$  to be the event that there is a path from  $\mathcal{A}$  to  $\mathcal{B}$  which separates  $z$  from  $\mathcal{C}$ . Similarly we define  $\mathcal{V}_N$  and  $\mathcal{W}_N$  cyclically. We note that for each of the  $u$ ,  $v$  and  $w$  there are in fact two objects to consider, namely a blue version of the event and a yellow version, but we will not let these details detract us from this informal discussion; similarly one should also define, with a bit of precision, the definition of the boundaries  $\mathcal{A}$ ,  $\mathcal{B}$  and  $\mathcal{C}$  in accord with the lattice–approximation of  $\Lambda$ ). We let  $u_N$ ,  $v_N$  and  $w_N$  be the probabilities of the events  $\mathcal{U}_N$ ,  $\mathcal{V}_N$  and  $\mathcal{W}_N$ , respectively and consider the limits of these functions as  $N \rightarrow \infty$  (if the limit indeed exists).

The seminal result of the work by Smirnov [14] is that as  $N \rightarrow \infty$ , each of these functions converge to the appropriate  $h_{\mathcal{A}}$ ,  $h_{\mathcal{B}}$  or  $h_{\mathcal{C}}$  mentioned above. We note that on the equilateral triangle these  $h$ ’s (by definition) satisfy the Cardy–Carleson Formula and therefore they satisfy Cardy’s formula on any conformal domain.

Next we say a few words about the strategy for the proof of this theorem. The lattice functions, which satisfy the same boundary conditions as the

continuum  $h$ 's, are shown to converge, at least subsequentially. Appropriate combinations of the limiting functions are demonstrated to be analytic, the key ingredient being a verification of the Cauchy condition for a (relatively) arbitrary contour. Boundary conditions and some uniqueness arguments completely specify the limiting functions.

The crucial ingredient which underpins the entire scheme is the existence of a set of Cauchy–Riemann type equations – referred to as *Cauchy–Riemann relations* – which equate various directional derivatives of  $u_N$ ,  $v_N$  and  $w_N$  at the *discrete* level. In particular, the difference between any one of these functions at neighboring lattice sites has a probabilistic interpretation or, more precisely, may be expressed as the difference of two probabilities. Both the positive and negative pieces of these derivatives are shown to be exactly equal to nearby counterparts of an appropriate member of the triple of functions. Roughly speaking, (and here we refer the reader to the original reference [14] or to Section 3 of the present note), the keynote of the strategy is “color switching”. Indeed, the derivative pieces turn out to be the probability of three paths emanating from the three boundaries and converging at the point where the derivative is taken. The colors of the paths determine which particular function the derivative piece should be associated with. Hence changing a path color changes the function and this amounts to a Cauchy–Riemann relation. The ability to freely switch the colors of paths – which is not common among the standard critical percolation models – is an inherent symmetry of the triangular site percolation model at criticality.

The major technical obstacle to a proof of Cardy’s Formula for any other

system is to circumvent or modify appropriately the color switching property. The tack of this paper is along the latter course. For our model we define a stochastic class of events known as *path designates* and we meticulously enforce detailed criteria for which paths are to be considered. It turns out that this requires the introduction of a host of auxiliary random variables which provide “permissions” for exceptions to the usual conventions of (self-avoiding) paths. Furthermore, the random variables occasionally deny the existence of paths notwithstanding their appearance in the percolation configuration. The end result is that a modified version of color switching symmetry is locally restored and an analogue of Smirnov’s Cauchy–Riemann relations can be established. Thereafter we can use a nearly identical contour-based argument to prove convergence of  $u_N$ ,  $v_N$  and  $w_N$  to the limiting  $h$ ’s.

## III.2 Bond–Triangular Lattice Problems

### III.2.1 Preliminary Discussion

We start with a brief recapitulation of the perspective on the usual bond-triangular lattice problems that was introduced in [6]. Normally one considers the model where edges of the triangular lattice are independently declared to be occupied with probability  $\lambda \in (0, 1)$  and otherwise – with probability  $(1 - \lambda)$  – they are vacant. Typically, the problems of interest are concerned with sets of sites connected by occupied bonds; paying heed only to the induced connectivity properties of the underlying sites, it is clear that the bond description provides more information than is actually needed. Indeed, fo-

cusing attention on a single triangle we see that out of the grande total of eight possible occupied/vacant edge configurations, there are only five distinguished outcomes: all sites connected, a pair of sites connected (which has three distinctive instances) and none of the sites connected.

Thus, as far as percolation problems are concerned, we might as well just consider the problem where these five configurations are all that can be exhibited on a given triangle. Furthermore, the structure of the full lattice allows the partition of the underlying space into disjoint triangles, e.g. the up-pointing triangles, wherein each triangle independently exhibits one of the above mentioned five configurations.

Needless to say, the configurations may still be represented by occupied and vacant bonds but, on up-pointing triangles, the original event of exactly two occupied bonds is identified with the full (three-bond) configuration. From this perspective, it is natural – and actually helpful – to consider the general problem where the Bernoulli parameters are *not* entangled by an underlying independent bond structure. Thus we assign probabilities  $a$  for all-bond event,  $e$  for the empty event and  $s$  for the three singles;  $a + e + 3s = 1$ . It is noted that in the context of the  $q$ -state Potts model and the random cluster model of which this is the  $q = 1$  version, this enlargement of the problem amounts to the addition of three-body interactions in the Hamiltonian. Under the star-triangle transformation, up-pointing triangles are replaced by superimposed down-pointing triangles and the parameters  $a$  and  $e$  get swapped, at least for  $q = 1$ . For more details see [6]. But of immediate relevance to the subject of *site* percolation on the triangular lattice (and all of its associated advantageous

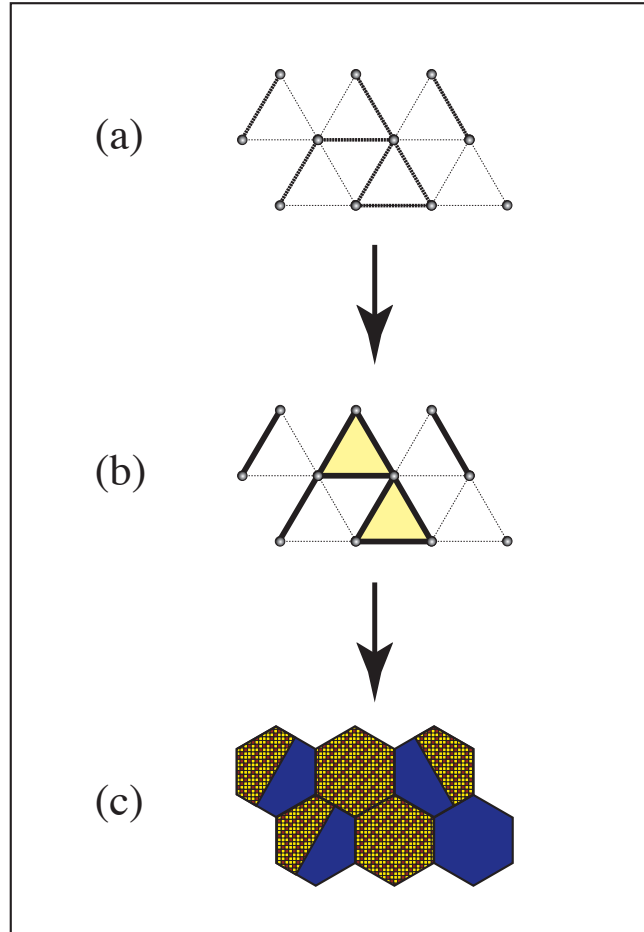


Figure III.1: Bond percolation as a hexagon tiling problem: (a) Typical bond configuration on the triangular lattice. (b) Amalgamation into relevant connected objects. (c) Associated tiling problem using hexagons and split hexagons.

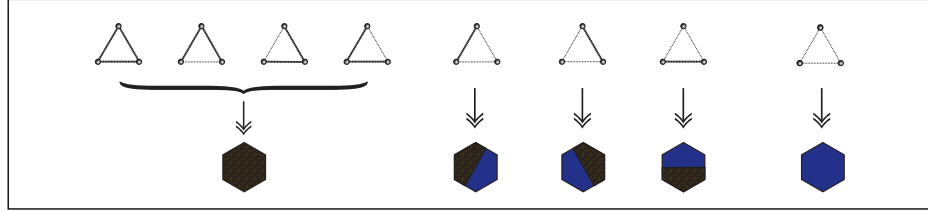


Figure III.2: Correspondence between eight configurations on (up-pointing) triangles and five hexagon configurations. All four configurations which fully connect the triangle map to the single, fully yellow, hexagon with total weight  $a$ . Empty configuration has probability  $e$  and maps to the fully blue hexagon. The three single bond configurations lead to split hexagons, each carrying probability  $s$ . Note that not all the possible ways of splitting a hexagon appears: Images obtained from the above three by reflections in the  $x$ -axis are not present.

attributes) is the observation that for  $s = 0$ , the above model on up-pointing triangles is this site model with triangles playing the rôle of the sites.

As far as the present work is concerned, the crucial benefit of this “packaged triangular” description is the realization of these problems vis-à-vis hexagonal tilings. Starting at the  $s = 0$  limit – the site model – we may replace each up-pointing (and/or superimposed, dual, down-pointing  $*$ ) triangle with a hexagon. The hexagons tile the plane and, as is well-known from the site triangular model, exhibit the correct neighborhood connectivity relations, where, of course, connectivity is defined by the sharing of an edge.

The bond model and its dual are now represented by a tile coloring problem: we color the hexagon blue if the corresponding up-pointing triangle is empty and yellow if it is all-bonds. Yellow connectivity in the hexagon language corresponds to bond connectivity in the direct model while the connections between blue hexagons designate the connectivity properties of the dual model.

As it turns out, a representation along these lines remains valid for  $s > 0$ . We map single bond events associated with the original bond problem into hexagons that have been split along the diagonals connecting the midpoints of opposing edges and coloring them half–yellow and half–blue. It is easy to check that this can be done in a consistent fashion so that the single bond events are faithfully represented, where two hexagons are now considered connected if they share either a full edge or half an edge (see Figure III.1).

A few remarks on symmetry are in order. First we note that only three of the six possible split hexagons occur. This restriction breaks (microscopic) color symmetry for the models under consideration (see Figure III.2). The tiling model with all six split hexagons present (which enjoys full yellow–blue symmetry) can presumably be handled by a direct extension of [14] but does not correspond to any realistic scenario in the language of the bond model. Nevertheless, the set of three split hexagons do enjoy some symmetry of another sort: if we orient the hexagons so that two of the edges are parallel to the  $y$ –axis (as in all the figures) then the restricted set of three split hexagons does enjoy a reflection symmetry through the  $y$ –axis as well as the two axes at  $\pm 120^\circ$  to the  $y$ –axis. As far as the  $x$ –axis and the other two axes are concerned, there is the more restrictive symmetry of reflection followed by color reversal.

### III.2.2 Setup, Definitions and the Model

We begin with a (more formal) recapitulation of the generalized triangular bond lattice problem in the hexagonal language, as it forms the basis of the model we will eventually study. Consider a hexagonal tiling of the plane; to be

definitive, the hexagons are oriented so that two of the edges are parallel to the  $y$ -axis. With reference to the underlying bond model, the direct model will consist of up-pointing triangles and hence the superimposed down-pointing triangles constitute the “dual” lattice under the star-triangle transformation. The color yellow will correspond to the direct model and blue to the dual model. We call a hexagon which has only one color *pure* and we call a hexagon which has two colors *mixed*; the allowed mixed configurations are illustrated in Figure III.2.

Using the hexagonal representation described in the last subsection, let  $a$ ,  $s$  and  $e$  (with  $a + e + 3s = 1$ ) denote the probabilities that a hexagon is pure yellow, mixed (one of three ways) or pure blue. Occasionally, for the sake of clarity, we will use  $y$  and  $b$  instead of  $a$  and  $e$ , which allows for effective tracking of various terms in up and coming formulae. On general grounds [6], the critical condition is simply  $a = e$ , which, as far as the pure hexagons are concerned, is the point of yellow-blue symmetry. The usual independent bond model is just the curve in the  $a$ - $e$  plane  $a = \lambda^3 + 3\lambda^2(1 - \lambda)$ ,  $e = (1 - \lambda)^3$ ; where this curve hits the line  $a = e$  is the star-triangle point. We point out that this means for each value of  $a = e$ , we have a one parameter family, parametrized by  $s$ , of critical percolation models. However, this is not the full story. It turns out that we can appeal to FKG type inequalities (positive correlations) if and only if  $ae \geq 2s^2$  [6] and, since this will prove necessary on occasion, we restrict ourselves to this range of parameters.

The full problem as described is, unfortunately, beyond our present capabilities. In

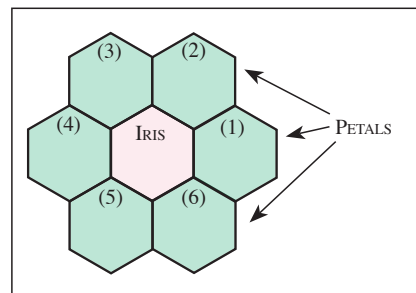


Figure III.3: A flower.

this paper, we will study a one parameter family of models which is on the one hand simpler than the full bond triangular lattice problem but on the other hand highlights some of the difficulties one encounters extracting continuum limits on lattices other than the triangular site lattice. Our model is derived from the above by limiting the set of hexagons that are allowed to exhibit mixed configurations and introducing yet more local correlations. Specifically, our efforts are focused on specific local arrangements of hexagons which we now describe.

**Definition III.2.1.** We define a *flower* to be a hexagon together with its six neighboring hexagons. The central hexagon is called the *iris* and the outer hexagons are called the *petals* which are labeled 1 through 6 (and occasionally designated by other integers modulo 6), starting from the one directly to the right of the iris. See Figure III.3.

For technical – and complicated – reasons, this work will be limited by restrictions on which hexagons are (and under what circumstances a hexagon is) allowed to exhibit the mixed states. In particular, we envision a number of irises, whose flowers are disjoint, together with a background of *filler sites*. It is only the irises of the flowers which are allowed to exhibit the mixed hexagons. In infinite volume we ultimately require the placement of the irises to have a periodic structure with  $60^\circ$  symmetries, but we will not invoke this proviso till considerably later on. For finite volumes, the specifics are as follows.

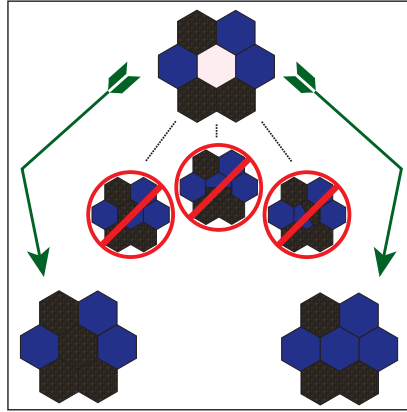


Figure III.4: In a triggering configuration (three yellows, two of which are contiguous) a split hexagon is forbidden. The iris is pure yellow or pure blue with conditional probabilities one-half.

**Definition III.2.2.** Consider a domain  $\Lambda \subset \mathbb{C}$  which is tiled by hexagons and which we assume, for once and all, to be simply connected. We identify  $\Lambda$  with the set of hexagons tiling it. We say that  $\Lambda_{\mathfrak{F}}$  is a *floral arrangement* of  $\Lambda$  if certain designated hexagons of  $\Lambda$ , the irises, satisfy the following two criteria:

- No iris is a boundary hexagon of  $\Lambda$ .
- There are at least two non-iris hexagons between each pair of irises.

Note that this means that the flowers associated with each iris are disjoint and are not “broken across” the boundary of  $\Lambda$ .

We now give a general description of our model:

**Definition III.2.3.** Let  $\Lambda$  be a domain with floral arrangement  $\Lambda_{\mathfrak{F}}$ .

- Any background filler sites, as well as the petal sites, must be  $Y$  (pure yellow) or  $B$  (pure blue), each with probability  $\frac{1}{2}$ . In most configurations

of the petals, we allow each iris to exhibit one of five states:  $Y$ ,  $B$ , or the three mixed states  $\alpha$  (horizontal split),  $\beta$  ( $120^\circ$  split) and  $\gamma$  ( $60^\circ$  split). Each mixed state occurs with probability  $s$  and each pure state with probability  $a = \frac{1}{2}(1 - 3s)$ .

- The exceptional configurations, which we call *triggers*, are configurations where there are three yellow petals and three blue petals with exactly one pair of yellow (and hence one pair of blue) petals contiguous. Under these circumstances, the iris is restricted to a pure form, i.e., blue or yellow with probability  $\frac{1}{2}$ .

All petal arrangements are independent, all flowers are configured independently, and these in turn are independent of the background filler sites (if any). The resulting measure on these hexagon configurations will be denoted by  $\mu$ .

For fixed  $\Lambda_{\mathfrak{F}}$ , a *configuration*  $\omega \in \Omega_{\Lambda_{\mathfrak{F}}}$  is an assignment of yellow or blue to all the petals in  $\Lambda_{\mathfrak{F}}$  and an assignment of one of the five types to each iris, in accordance with Definition V.4.1. Connectivity in  $\omega$  is defined in the natural fashion; specifically, the notion of e.g. blue connectivity may be defined as the usual  $\mathbb{R}^2$  connectivity of (the closure of) the region that has been colored blue.

### III.2.3 Scaling Limit and Statement of Main Theorem

Percolation in our model is defined by considering a sequence of floral arrangements

$$\Lambda_{\mathfrak{F}_1}^{(1)}, \dots, \Lambda_{\mathfrak{F}_k}^{(k)}, \dots$$

with  $\Lambda^{(j)} \subset \Lambda^{(j+1)}$ ;  $\Lambda^{(j)} \nearrow \mathbb{C}$  and the  $\Lambda_{\mathfrak{F}_k}$ 's *consistent* in the sense that all the irises of  $\Lambda_{\mathfrak{F}_j}$  are in  $\Lambda_{\mathfrak{F}_{j+1}}$ . Then (pertinent to the extended model with differing parameters for pure blue and pure yellow hexagons) we say there is percolation of yellow's if some fixed point belongs to an infinite cluster of yellow with positive probability and similarly for blue's. However, not surprisingly, it turns out that the model under consideration has no percolation (here is one instance in which we are forced to invoke our  $60^\circ$  symmetry) and, as we will later demonstrate, the model exhibits all the well-known properties which are indicative of criticality in a 2D percolation problem (Theorem III.3.10).

To state our main result we need to introduce some minimal notation (more details to come in Section III.4) and describe how the scaling limit is taken. Let  $\mathcal{D} \subset \mathbb{C}$  denote a domain with piecewise smooth boundary which is conformally equivalent to a triangle. The boundaries and relevant prime ends will be denoted by  $\mathcal{A}, \dots, e_{BC}$ . We let  $\tilde{\Lambda}_{\mathfrak{F}_N}$  denote an approximate discretization of  $\mathcal{D}$  with lattice spacing  $N^{-1}$  in accord with Definition III.2.2. The version of  $\tilde{\Lambda}_{\mathfrak{F}_N}$  rescaled to unit size will be denoted by  $\Lambda_{\mathfrak{F}_N}$ . It is required that the  $\Lambda_{\mathfrak{F}_N}$ 's are consistent in the fashion described above. The limiting floral arrangement will be denoted by  $\Lambda_{\mathfrak{F}_\infty}$ .

We write  $z \in \Lambda_{\mathfrak{F}_N}$  if  $z$  is a vertex of a hexagon in  $\Lambda_{\mathfrak{F}_N}$ . For  $z \in \Lambda_{\mathfrak{F}_N}$  we define the discrete function  $\mathcal{U}_N^B(z)$  to be the indicator function of the event that there is a blue path connecting the  $\mathcal{A}$  and  $\mathcal{B}$  boundaries which separates  $z$  from  $\mathcal{C}$ . We let  $u_N^B(z) = \mathbb{E}(\mathcal{U}_N^B(z))$ , with similar definitions for  $v$  and  $w$  and yellow paths. We extend these functions in some suitable fashion off the lattice sites. Then for  $\mathcal{Z} \in \mathcal{D}$  (unscaled), define  $U_N^B(\mathcal{Z}) = u_N^B(Nz)$ .

Our main result, convergence to the Cardy–Carleson functions, can now be stated:

**Theorem III.2.4.** *For the model as defined in Definition V.4.1, with setup and notation as just described, under the conditions that*

$$a^2 \geq 2s^2$$

*and that  $\Lambda_{\mathfrak{F}_\infty}$  is periodic and has  $60^\circ$  symmetry, we have*

$$\lim_{N \rightarrow \infty} U_N^B = h_\ell,$$

*with similar results for  $V_N^B$  and  $W_N^B$ . The yellow versions of all of these functions converge to the same corresponding limiting functions.*

The key to all these considerations are the long–distance and local connectivity properties of the model. This subject, along with the necessary deviations from the usual percolation scenarios is the content of the forthcoming section.

## III.3 Paths and Path Designates

### III.3.1 Paths

We start with a description of the paths we will be considering. First we give a general definition for the usual notions of an allowed path and then describe exceptions in particular cases. Under normal circumstances, a *path* is a sequence of hexagons  $(h_1, \dots, h_M)$  where  $h_k$  and  $h_j$  are neighbors (sharing an edge in common) if  $|j - k| = 1$ . Additional rules may be implemented

concerning *hexagon self-avoidance*, i.e. forbidding multiple usage of the same hexagon ( $h_1, \dots, h_M$  are all distinct) and *close encounters* ( $h_k$  and  $h_j$  neighbors with  $|j - k| > 1$ ). In most circumstances these supplementary conditions are immaterial; if there is a “path” from  $h_1$  to  $h_M$  with close encounters and multiple hexagon usage then there is a subsequence of these hexagons which forms the requisite path with neither close encounter nor multiple hexagon usage. In this work, we will make use of all these phenotypes. However, in various circumstances, it will be necessary that our paths represent *cuts*. Thus we do not consider a sequence of hexagons ( $h_1, \dots, h_M$ ) to constitute a path unless successive interfaces between adjacent hexagons can be joined by a finite number of straight line segments which (in the continuum) culminate in a non-self-crossing path. In particular, if the collection  $\{h_1, \dots, h_M\}$  has the appearance of a path with a loop, one ordering is permitted, while the other – which would force the straight line segments to cross – is not considered legitimate.

Hence in any configuration of pure hexagons, there are blue and yellow paths. With the injection of mixed hexagons into the picture, the necessary modifications are obvious; note the proviso that in a colored path with mixed elements, the relevant portions of successive hexagons are required to share at least *half* an edge in common. More precisely, here is a definition.

**Definition III.3.1.** Let  $(h_1, \dots, h_M)$  denote a path and  $\omega$  a configuration in some  $\Lambda_{\mathfrak{G}}$ . We will say that the path is a *blue transmit* in  $\omega$  if each of  $h_1, \dots, h_M$  is either pure blue or, if  $h_j$  is mixed, the blue part of  $h_j$  shares at least half an edge with both  $h_{j-1}$  and  $h_{j+1}$  and thereby connects  $h_{j-1}$  to  $h_{j+1}$ . Similarly

for a *yellow transmit*.

Typically – as was evidently the case in [14] – on any path, multiple usage is forbidden and close encounters are indulged. We remark that these normally inconsequential provisos are only slightly important in the definition of the events  $\mathcal{U}_N(z)$ ,  $\mathcal{V}_N(z)$  and  $\mathcal{W}_N(z)$  (cf. Definition III.1.1), but they become essential when it comes to the derivatives of their probabilities. In particular, as to the definitions of the paths satisfying these events we will occasionally forbid touches and (as sort of a compensation) we will occasionally allow multiple usage. These exceptions will be stochastically implemented according to the details of the local configuration.

**Remark III.3.2.** We remark that there are certain self-avoiding paths which, by the standards of the pure model, would not be called self-avoiding. Indeed, consider a horizontal blue transmit across a flower with the iris in the  $\alpha$ -state (horizontal split, blue on top). If the next hexagon in the path sequence is petal 6, so that the sequence is now [4; iris; 1; 6], the path has the appearance of a redundant visit to petal 1. However, due to the mixed nature of the iris, it is seen that in fact all the hexagons specified are necessary for the connection between petal 4 and petal 1. The preceding example illustrates that it is just the blue parts of the path that have to be self-avoiding, which is a property directly inherited from the “correct” notions of self-avoiding in the underlying bond model. These phenomena lead to some interesting scenarios whereby the geometric structure of a self-avoiding path sometimes does and sometimes does not reveal the underlying state of the iris.

### III.3.2 Path Designates

A key technical device in this work is to replace the usual (i.e. full) description of paths with partial information to arrive at a set of objects called *path designates*. By the usual abuse of notation, we will use the phrase path designate to describe both events and geometric objects. With regards to the latter a path designate is, for all intents and purposes, a collection of paths. So, for pedagogical purposes, let us start with a microscopic path and describe which path designate it belongs to. Consider the portion of the path that intersects a particular flower. In the simplest case, the path only visits the flower once and thus there is an *entrance petal* and an *exit petal*. In contrast to the microscopic description where it must be specified how the path got between these “ports”, we leave these details unsaid. Similarly, with multiple visits to a single flower, the first entrance and exit petals, the second entrance and exit petals, etc. must all be specified. This must be done for *all* flowers and on the region complementary to the flowers (if any) the path must be entirely specified. Note that, with only slight loss of generality, path designates do not begin or end on irises. A formal definition is as follows:

**Definition III.3.3.** (Path Designate) Let  $\Lambda_{\mathfrak{F}}$  denote a floral arrangement. A *path designate* in  $\Lambda$  from  $h_0$  to  $h_{K+1}$  is a sequence

$$[H_{0,1}, (\mathcal{F}_1, h_1^e, h_1^x), H_{1,2}, (\mathcal{F}_2, h_2^e, h_2^x), H_{2,3}, \dots, (\mathcal{F}_K, h_K^e, h_K^x), H_{K,K+1}]$$

where  $\mathcal{F}_1, \dots, \mathcal{F}_K$  are flowers in  $\Lambda_{\mathfrak{F}}$ ,  $h_j^e$  and  $h_j^x$  are (entrance and exit) petals in the  $j^{\text{th}}$  flower and, for  $1 \leq j \leq K-1$ ,  $H_{j,j+1}$  is a path in the complement of flowers which connects  $h_j^x$  to  $h_{j+1}^e$ . Further,  $H_{01}$  is a path in the complement

of flowers from  $h_0$  to  $h_1^e$  and similarly  $H_{K,K+1}$  is a path from  $h_K^x$  to  $h_{K+1}$  in the complement of flowers. We note that in the above definition, not all flowers have to be distinct:  $h_j^e$  could equal  $h_j^x$  – i.e. the flower is visited at a single petal and, depending on the floral arrangement, the  $H_{j,j+1}$ 's could be vacuous. However, we shall assume, with negligible loss of generality, that all of the explicitly mentioned hexagons (i.e., the collection of hexagons which constitute the paths  $H_{j,j+1}$  along with the entrance and exit hexagons) in a path designate are used only once.

Of course, for percolation problems the only matter of importance is the realization of underlying paths. Thus the following is obviously relevant:

**Definition III.3.4.** (Realization of a Path Designate) Let  $\mathcal{P}$  denote a path designate. We let  $\mathcal{P}_B$  denote the event that for all  $j$ , all hexagons in the path  $H_{j,j+1}$  as well as  $h_j^e$  and  $h_j^x$  are blue and there is a blue connection in  $\mathfrak{F}_j$  between  $h_j^e$  and  $h_j^x$ . A similar definition holds for the event  $\mathcal{P}_Y$ .

**Remark III.3.5.** Clearly the event  $\mathcal{P}_B$  means that the designate  $\mathcal{P}$  is “achieved” (or “transmitted”) by an underlying blue path. However, there is no guarantee that the underlying blue path has reasonable self-avoidance properties. Indeed, it may be the case that the path is inundated with close encounters; in particular, entrance and exit hexagons may be used in a seemingly redundant way. These matters will be of no concern and in our derivations we will be dealing exclusively with path designates and the events that various transmissions along these designates are achieved.

We begin with a preliminary demonstration of how the path designates

might allow us to implement microscopic color switching. In particular, and of seminal importance for the present model, is the following:

**Lemma III.3.6.** *Let  $\Lambda_{\mathfrak{F}}$  denote a floral arrangement and let  $\mathbf{r}, \mathbf{r}'$  denote points (hexagons) in  $\Lambda_{\mathfrak{F}}$  which are not irises. Let  $K_{\mathbf{r}\mathbf{r}'}^B$  denote the event of a blue transmission between  $\mathbf{r}$  and  $\mathbf{r}'$ , and similarly for  $K_{\mathbf{r}\mathbf{r}'}^Y$ . Consider the model as described in Definition V.4.1 and let  $\kappa_{\mathbf{r}\mathbf{r}'}^B = \mathbb{P}(K_{\mathbf{r}\mathbf{r}'}^B)$  with a similar definition for  $\kappa_{\mathbf{r}\mathbf{r}'}^Y$ . Then*

$$\kappa_{\mathbf{r}\mathbf{r}'}^B = \kappa_{\mathbf{r}\mathbf{r}'}^Y.$$

Before the proof of Lemma III.3.6 we will need a preliminary lemma, and, of course, some further definitions.

**Definition III.3.7.** Let  $\mathcal{F}$  denote a flower and  $\mathcal{D}$  a collection of petals. Let  $T_{\mathcal{D}}^B$  denote the event that all the petals in  $\mathcal{D}$  are blue and that they are blue connected within the flower. Let  $T_{\mathcal{D}}^Y$  denote a similar event with blue replaced by yellow.

**Lemma III.3.8.** *For all  $\mathcal{D}$ ,*

$$\mathbb{P}(T_{\mathcal{D}}^B) = \mathbb{P}(T_{\mathcal{D}}^Y).$$

**Proof:** Let  $\eta$  denote a configuration on the petals and  $\bar{\eta}$  the color reverse of  $\eta$ . Clearly, it is enough to show that (for all  $\eta$ )

$$\mathbb{P}(T_{\mathcal{D}}^B \mid \eta) = \mathbb{P}(T_{\mathcal{D}}^Y \mid \bar{\eta}).$$

It may be assumed without further discussion that all petals in  $\mathcal{D}$  are already blue in  $\eta$  (otherwise both sides of the previous equation are zero). If  $\mathcal{D}$  is

already blue connected in  $\eta$  then there is nothing to prove. If  $\eta$  is a trigger, then there is also nothing to prove because of full color symmetry. In general  $\mathcal{D}$  cannot have more than three components. In the case of three, if none of these have been connected in  $\eta$  then the only possibility is the alternating configuration which, as can easily be checked, requires a pure iris to achieve full connectivity. We are thus down to two separate components in  $\eta$  which need to be connected through the iris.

To be specific, let us study the blue version of this problem. For all intents and purposes, the only cases that need be considered are the ones where  $\eta$  has two non-adjacent blue petals (which need to be connected through the iris) and all other petals yellow. Now, it turns out that either the blue petals are blue connected through the iris or the complementary “yellow” sets are yellow connected through the iris – a micro-environment duality. To dispense with the present case, we invoke (and not for the last time) the fact that for two non-adjacent petals of the same color, there is one and only one mixed hexagon which permits the successful transmission of their color. Thus, for all the cases where  $\eta$  has exactly two usable blue petals we have

$$\mathbb{P}(T_{\mathcal{D}}^B \mid \eta) = b + s$$

with a similar result for  $\mathbb{P}(T_{\mathcal{D}}^Y \mid \bar{\eta})$ . But now, by the above-mentioned duality, any other (non-trigger) two-component case which involves more than just two usable petals of the same color has probability given by  $a + 2s$ .  $\square$

**Remark III.3.9.** We will, formally, have to consider cases involving several sets; e.g.,  $\mathcal{D}_1, \mathcal{D}_2, \dots, \mathcal{D}_k$  and  $T_{\mathcal{D}_1 \dots \mathcal{D}_k}^Y$ , the event that all the relevant  $\mathcal{D}'$ s are

yellow connected sets, but not necessarily all connected to each other. Due to the limitations of the flower size, it is seen that any case with  $k \geq 3$  is trivial or reduces to  $k < 3$ . The only non-trivial case with  $k = 2$  is exemplified by the problem where  $\mathcal{D}_1$  consists of two petals separated by another petal and  $\mathcal{D}_2$  a single petal separated from both of these by yet another petal – the alternating configuration. Here either  $\eta$  reduces this back to a single- $\mathcal{D}$  problem or, if all the other petals are blue, the desired result (transmission color symmetry) follows from the previous observation that each binary transmission through the iris is permitted by exactly one mixed hexagon for both yellow and blue. We therefore consider the multi-set version of Lemma III.3.8 to be proved.

**Proof of Lemma III.3.6:** Let  $\mathbf{r}$  and  $\mathbf{r}'$  denote two non-iris points in  $\Lambda_{\mathfrak{F}}$ . We first observe that the event of a blue transmission between  $\mathbf{r}$  and  $\mathbf{r}'$  is also the event that there exists a  $\mathcal{P}$  beginning at  $\mathbf{r}$  and ending at  $\mathbf{r}'$  such that  $\mathcal{P}_B$  occurs. In particular, letting  $\Pi_{\mathbf{r}\mathbf{r}'}$  denote the collection of all path designates beginning at  $\mathbf{r}$  and ending at  $\mathbf{r}'$ , we have

$$\kappa_{\mathbf{r}\mathbf{r}'}^B = \mathbb{P}\left(\bigcup_{\mathcal{P} \in \Pi_{\mathbf{r}\mathbf{r}'}} \mathcal{P}_B\right) \quad (\text{III.1})$$

and similarly for  $\kappa_{\mathbf{r}\mathbf{r}'}^Y$ . Noting that  $|\Pi_{\mathbf{r}\mathbf{r}'}| < \infty$ , we will handle the likes of (III.1) via an inclusion-exclusion argument. Let us first demonstrate that for any  $\mathcal{P}$ ,

$$\mathbb{P}(\mathcal{P}_Y) = \mathbb{P}(\mathcal{P}_B).$$

Indeed, we write

$$\mathcal{P} = [H_{\mathbf{r}\mathbf{1}}, (\mathcal{F}_1, h_1^e, h_1^x), H_{12}, (\mathcal{F}_2, h_2^e, h_2^x), H_{23}, \dots, (\mathcal{F}_K, h_K^e, h_K^x), H_{K\mathbf{r}'}],$$

where  $\mathbf{r}$  is used to denote the hexagon at  $\mathbf{r}$ , etc. Assuming for simplicity that each flower is used only once, the formula for  $\mathbb{P}(\mathcal{P}_B)$  is given by the product along successive terms:

$$\mathbb{P}(\mathcal{P}_B) = \left(\frac{1}{2}\right)^{|H_{\mathbf{r},1}|} \mathbb{P}(T_{\{h_1^e, h_1^x\}}^B) \left(\frac{1}{2}\right)^{|H_{1,2}|} \dots \mathbb{P}(T_{\{h_k^e, h_k^x\}}^B) \left(\frac{1}{2}\right)^{|H_{\mathbf{K},\mathbf{r}'|}.$$

By Lemma III.3.8, all terms are the same when  $B$  is replaced by  $Y$ . In more generality – for the case of a single path – various pairs or triples of transmission terms which actually involve the same flower must be treated in one piece. E.g., if  $\mathfrak{F}_\ell = \mathfrak{F}_j$  and, say,  $h_\ell^e = h_\ell^x$  while  $h_j^e \neq h_j^x$  which is in turn distinct from  $h_\ell^e$ , then we would replace  $\mathbb{P}(T_{\{h_\ell^e\}}^B)\mathbb{P}(T_{\{h_j^e, h_j^x\}}^B)$  by  $\mathbb{P}(T_{\{h_\ell^e, \{h_j^e, h_j^x\}\}}^B)$ . In any case, by Lemma III.3.8 and Remark III.3.9, each term in the expression for blue transmission is equal to the corresponding term in the expression for yellow transmission.

The general term in an inclusion–exclusion expansion will be of the form:

$$\pm \mathbb{P}((\mathcal{P}_1)_B \cap (\mathcal{P}_2)_B \cap \dots \cap (\mathcal{P}_\ell)_B).$$

These terms will be handled in a manner similar to the single path case. Indeed, first we will need an overall term representing the amalgamation of all the outside hexagons (if any); this will be  $\frac{1}{2}$  to some power, which will be the same for yellow as for blue. Then, for each flower which appears in any of the relevant designates, we will need to multiply in a blue transmission probability to ensure that all the relevant entrance hexagons are connected to their corresponding exit hexagons, i.e. a term of the form  $\mathbb{P}(T_{\mathcal{D}_1, \mathcal{D}_2, \dots, \mathcal{D}_m}^B)$ . However, by Lemma III.3.8 and Remark III.3.9, these blue transmission probabilities are, once again, the same as they are for yellow. Thus, down to the level of each

term in inclusion–exclusion, we have equality and the lemma is proved.  $\square$

The preceding is entirely general provided the floral arrangement adheres to the criteria spelled out in Definitions III.2.2 and V.4.1. We augment this with some additional stipulations in order to obtain:

**Theorem III.3.10.** *Consider the model as described in Definition V.4.1 with the periodicity and  $60^\circ$  symmetry assumptions discussed in the paragraph prior to Definition III.2.2 and with the additional proviso that  $a^2 \geq 2s^2$ . Then the model exhibits all the typical properties of a 2D percolation model at criticality:*

- *There is no percolation of either the blue or yellow connected clusters.*
- *Crossings of squares and rectangles have probabilities uniformly bounded above and below independent of scale (but dependent on their aspect ratio).*
- *In any annulus of the form  $S_L \setminus S_{\lambda L}$ , where  $S_L$  is a square of scale  $L$  centered at the origin and  $\lambda \in (0, 1)$  with probability bounded uniformly (in  $L$ ) above and below, there is a yellow ring and/or a blue ring separating the outer boundary of  $S_L$  from the origin.*
- *The probability of a connection between a fixed site and any other site a distance  $n$  away is bounded above by an inverse power of  $n$ .*
- *The probability of a connection between two distant sites is bounded above and below by a power of their separation.*

**Proof:** In essence all of the above follows from Russo–Seymore–Welsh ([12], [13]) type arguments, which extend a lower bound on the probability of short

way crossings of rectangles to lower bounds on the probabilities of crossing *longer* rectangles; of crucial importance will be the fact that the ultimate bounds are uniform in  $L$ . For these types of arguments an essential ingredient is, ostensibly, the Harris–FKG property. It turns out that full monotonicity properties for the measure do not hold, however, as will be proved later, Lemma III.6.2 in the Appendix, a restricted form of the Harris–FKG property holds for all paths and path type events. This lemma is proved under the proviso that  $a^2 \geq 2s^2$ . Thus as far as RSW lemmas are concerned, we are free to use these sorts of correlation inequalities.

In point of fact, we will not use the argument of either the above references, but will rely on the methods of Lemma 6.1 in [8]. A necessary input for Lemma 6.1 in [8] is bounds on the crossing probabilities of rectangles with aspect ratios not terribly different from unity. We start with the establishment of a uniform bound on the probability of “easy” way crossings of rectangles with an aspect ratio of approximately  $2 : \sqrt{3}$ . (We note here that due to the microscopic structure of the hexagonal lattice and the occasional necessity to cut out irises at the boundary, there will be rough edges to the rectangles and to other shapes which are to follow. These and future similar issues are not terribly important and will not be mentioned explicitly.) The following, we assume, is standard for models with  $60^\circ$  symmetry:

Consider a large hexagon, of scale  $L$ , which is oriented in the same way as in Section III.2.2; i.e. with a set of edges parallel to the  $y$ -axis. Without loss of generality, we assume that  $L$  is commensurate with the period of the tiling and that the vertical line which splits this hexagon in half is a line of symmetry for

the model. Let us discuss the event of a yellow connection between, say, the left edge and one of its second-neighbor edges. Our first claim is that if this event has a probability of order unity independent of  $L$ , then any connection between any pair of edges has a similar sort of bound. Indeed, by  $120^\circ$  symmetry this is manifestly true for the triad of next-neighbor faces anchored on the left side, and the opposite triad follows from reflection symmetry through the  $y$ -axis. It is not hard to see that when all second-neighbor edges have probabilities of order unity of being connected, then (here we use the Harris-FKG property) any pair of edges are connected with a probability of order unity. However, once these probabilities are established for yellow, then by Lemma III.3.6, the same holds for blue – and vice versa. Thus let us proceed with the event in question.

If this event fails, then at least one of two dual blue events of a similar type must occur and/or a blue connection between the appropriate pair of opposing edges. In the former case, we are done by the above-mentioned color symmetry. In the latter case (blue success with opposing edges), by employing an  $120^\circ$  symmetry and taking the intersection of two such opposing edge events, we get, by the Harris-FKG property, the desired sort of connection (albeit in blue). Having established the preliminary claims, it turns out that all we have use for is a horizontal crossing between the opposing edges. Inscribing the hexagon in a rectangle with the above stated aspect ratio, we are finished with the horizontal problem.

For the vertical problem we first reorient the big hexagon so that two edges are parallel to the  $x$ -axis. We may now proceed in almost the identical

fashion, except that whereas in the previous argument, we employed the simple symmetry of  $y$ -reflections, here we employ the reflection through the  $x$ -axis combined with color reversal, which, as mentioned earlier, is another inherent symmetry of the model. However, after this spurious color reversal, we may restore the original color by appeal to Lemma III.3.6.

We have gathered the following ingredients as inputs for Lemma 6.1 in [8]: lower bounds on vertical and horizontal crossing probabilities of suitable rectangles (the requisite aspect ratios must, as it turns out, have a product that is not in excess of  $3/2$ ) Harris–FKG properties for paths, and symmetry with respect to reflections through lines parallel to the  $y$ -axis. One may follow the steps in Lemma 6.1 of [8], modifying and abridging when appropriate.

Once we have vertical and horizontal crossings of long rectangles, the establishment of power law bounds, rings in annuli, etc. follow – with the help of Harris–FKG properties – standard 2D percolation arguments. We remark that some of these properties (e.g. the power law lower bounds) but unfortunately not the crucial ones, can be established without the benefit of the RSW lemmas. □

### III.3.3 Color–Switching Lemmas

In the previous subsection, where paths were free to wander throughout the relevant domain, complete parity between yellow and blue was established. However, as can be gleaned from the introduction, it will be necessary to establish this sort of equivalence in the presence of pre-existing blue or yellow paths; e.g. the probability of a yellow/blue path connecting a pair of sets  $A$  and

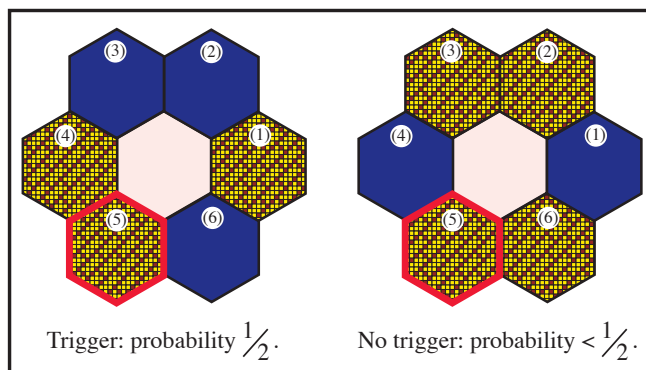


Figure III.5: A circumstance leading to asymmetry in conditional color switching.

$B$  in the presence of – and disjoint from – other paths connecting other sets. While there is no doubt of such parity in the long view (i.e. in a statistical sense on a large length scale), on the microscopic scale, yellow–blue equivalence will break down, as the following example demonstrates.

**Example III.3.11.** As an example consider the probability that petals 2, 3 and 6 are connected in the complement of petal 5 – which is conditioned to be yellow. If the connection is achieved by going through the petals (without using 5) the yellow and blue transmission probabilities are the same. However, on the transmissions through the iris, the probability of petals 2, 3 and 6 being blue and connected in the complement of petals 1, 4 and 5 (all of which are yellow) is  $\frac{1}{2}$  since this is a triggering situation. On the other hand, the situation with all petal colors (save the one that is conditioned, i.e. petal 5) reversed gives that the probability of a yellow connection between 2, 3 and 6 is only  $y + s < \frac{1}{2}$ .

Our cure for these microscopic difficulties will be, in essence, to define

away our problems. Indeed, in the up and coming we will establish some results concerning transmissions through flowers with conditioned petals. These transmissions are supposed to represent the construction of path segments in the presence of segments of other paths where all paths under consideration are meant to be disjoint. We may therefore restore yellow–blue parity *at the microscopic level* by relaxing the strict conventions which apply to disjoint paths. In particular, while “disjoint” paths usually are interpreted as allowing the paths to touch while not sharing hexagons, here we will implement a special set of rules which permits some exceptions. These will typically be denoted by a  $*$ , and the definition is as follows:

**Definition III.3.12.** Let  $\diamond$  denote a configuration on a proper subset of the petals of a flower. For  $\mathcal{D}$  a set of petals (or a collection of sets of petals, c.f. Remark III.3.9) on the complement of  $\diamond$ , we consider the events  $T_{\mathcal{D},\diamond}^B$  and  $T_{\mathcal{D},\diamond}^Y$  defined by

$$T_{\mathcal{D},\diamond}^B = \{\omega \mid \mathcal{D} \text{ is blue and all connected up in the complement of } \diamond\},$$

and similarly for  $T_{\mathcal{D},\diamond}^Y$ . The  $*$ -*transmissions*, denoted by  $T_{\mathcal{D},\diamond}^{B*}$  and  $T_{\mathcal{D},\diamond}^{Y*}$  are events defined on a larger space. Letting  $\eta_\diamond$  denote the full petal configuration, we have for each flower  $\mathfrak{F}_k$  a collection  $\mathcal{X}^k$  of 3-valued random variables  $X_{\mathcal{D},\diamond}^k \in \{O, Y, B\}$ . Focusing on a single flower, with  $\mathcal{D}$  and  $\diamond$  fixed, and denoting the random variable by  $X$  (notwithstanding that there are, literally, thousands of these objects), we have,

$$\text{if } X = O, \text{ then: } T_{\mathcal{D},\diamond}^{B*} = T_{\mathcal{D},\diamond}^B \text{ and } T_{\mathcal{D},\diamond}^{Y*} = T_{\mathcal{D},\diamond}^Y.$$

However, if  $X = \text{B}$ , then

$$T_{\mathcal{D}, \diamond}^{B*} \cap \{X = \text{B}\} = \{\omega \mid \mathcal{D} \text{ is blue and all connected up}$$

possibly using the blue petals of  $\diamond\} \cap \{X = \text{B}\}$

and

$$T_{\mathcal{D}, \diamond}^{Y*} \cap \{X = \text{B}\} = \{\omega \mid \mathcal{D} \text{ is yellow and all connected up}$$

without touching any yellow petals of  $\diamond\} \cap \{X = \text{B}\}$ .

Similar definitions hold for when  $X = \text{Y}$  with the roles of the transmission colors reversed. We remind the reader that in case  $\mathcal{D}$  refers to multiple sets, the connections need not be disjoint. It is observed that for certain  $\diamond$  and  $\mathcal{D}$ , some of the above may be vacuous; this is an extreme case of a seminal point which will be exploited later. We will call an assignment of these conditional probabilities (for the values of  $X$ ) a set of *\*-rules* and the corresponding transmissions *\*-transmissions*.

Our microscopic rebalancing will be broken down into two lemmas, ordered by conceptual difficulty. The first deals exclusively with the cases where the iris is not involved in the conditioning and the second where it is. The conceptual difference is that in the latter cases, the nature of the hexagon at the iris itself may change. Fortunately, in these latter set of circumstances there are only a limited number of possibilities to consider.

**Lemma III.3.13.** *Let  $\mathfrak{F}$  denote a flower and  $\diamond$  a partial configuration on the petals – with all petals in  $\diamond$  being yellow. Then for  $X_{\mathcal{D}, \diamond} \in \{\text{O}, \text{Y}, \text{B}\}$ , consider the *\*-transmissions*  $T_{\mathcal{D}, \diamond}^{Y*}$  as defined in Definition III.3.12. Then there are joint laws for the  $X_{\mathcal{D}, \diamond}$ 's such that*

$$\mu(T_{\mathcal{D}, \diamond}^B) = \mu^*(T_{\mathcal{D}, \diamond}^{Y*}),$$

where  $\mu^*$  denotes the joint probability measure on the flower configurations and  $\mathcal{X}^k$  with marginal  $\mu$ . Similar results hold with the role of yellow and blue reversed and, in case  $\diamond$  has petals of both colors,  $*$ -probabilities for the  $*$ -transmissions of the two colors are equal:

$$\mu^*(T_{\mathcal{D},\diamond}^{B*}) = \mu^*(T_{\mathcal{D},\diamond}^{Y*}),$$

**Proof:** We will in fact prove the stronger statement

$$\mu^*(T_{\mathcal{D},\diamond}^{Y*} \mid \eta_\diamond) = \mu(T_{\mathcal{D},\diamond}^B \mid \bar{\eta}_\diamond), \quad (\text{III.2})$$

where  $\bar{\eta}_\diamond$  denotes the color reverse on the complement of  $\diamond$ . The above implies the desired result because the *petal* configurations are provided by independent Bernoulli statistics. We need not discuss trivial cases when the configuration of  $\eta$  does not provide the necessary yellow petals of  $\mathcal{D}$ . Furthermore, with the exception of a single configuration, i.e. the alternating configuration, it turns out that without loss of generality, we may regard the yellow petals of  $\eta$  that are contiguous to  $\mathcal{D}$  as part of  $\mathcal{D}$ .

We therefore do a case by case analysis, starting with the situation where  $\diamond$  is but a single petal (which, without loss of generality, we have assumed to be yellow). If on the complement of  $\diamond$  there are five yellow petals in  $\eta_\diamond$  then there is nothing to prove, and with four yellow petals, essentially nothing to prove. Indeed, assuming those four petals are not contiguous, there is either the three and one split or the two and two split. The desired result for the two and two split follows from symmetry (the blue petal *must* be diametrically opposed to the conditioned petal which implies that the line joining them is an axis of reflection/color reverse symmetry). The three and one splits follow similarly

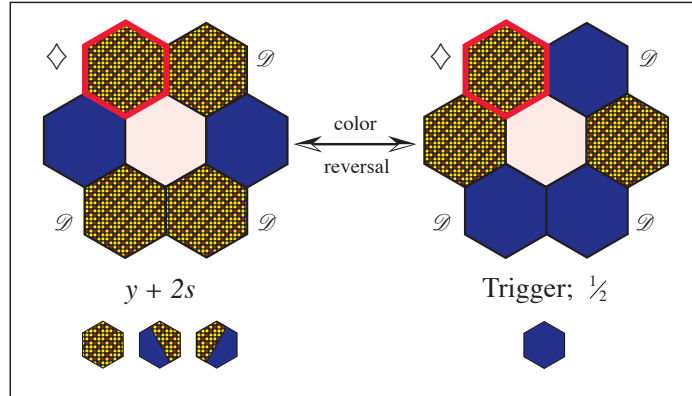


Figure III.6: A case with  $|\diamond| = 1$  and  $|\mathcal{D}| = 3$ .

from this inherent reflection/color reverse symmetry. E.g. if the conditioned hexagon is petal 3 and the blue petals are at  $\pm 1$ , then transmission equality follows from the symmetry of reflection through the  $x$ -axis followed by reversal of *all* colors.

The three petal cases – those which are non-trivial – are initially ominous looking, but can be easily handled with the added flexibility of implementing special rules. First we discuss the more serious cases where two of the three petals are contiguous. Whenever we have both the frozen petal and the pertinent trio in  $\eta_\diamond$  all yellow, triggers can only occur in the color reverse  $\bar{\eta}_\diamond$ . Under these conditions, the relevant (conditional) blue transmission probabilities will all be  $\frac{1}{2}$ . As for the yellow transmissions – where there is no trigger – the result will be either  $y + s$  or  $y + 2s$ , neither of which is  $\frac{1}{2}$ . However, in the  $y + s < \frac{1}{2}$  cases, where yellow would have the lower transmission probability, we may stochastically implement permission to share the conditioned petal. As can be readily checked, since there are four (out of six) active petals in play, the extra

petal is always in position to enhance the transmission probability. Indeed, in certain cases, the implementation of the sharing automatically creates the desired connection and in the other cases it boosts the transmission probability up to  $y + 2s > \frac{1}{2}$ . Thus, allowing sharing with the appropriate probability (e.g. probability  $\frac{1}{2}$  in the latter mentioned cases), we restore balance. To deal with the cases where yellow has the *a priori* higher transmission probability, first observe that since we have three yellow petals which are not contiguous, one of them must be adjacent to the conditioned petal. We may therefore implement the rule forbidding close encounters with the appropriate probability, which happens to be  $s/(2y + 4s)$ . This is illustrated in Figure III.6.

Finally, to finish the cases with a single petal in  $\diamond$  along with three yellow petals in the complement, we discuss the alternating configuration. First note that the placement of petals precludes the possibility of triggers in either  $\eta_\diamond$  or  $\bar{\eta}_\diamond$ . Further we note that here are the only instances where  $\mathcal{D}$  may consist of multiple sets, where some transmission is actually needed. Suppose then that  $\mathcal{D} = \{\mathcal{D}_1, \mathcal{D}_2\}$ , where  $\mathcal{D}_1$  consists of a single petal and  $\mathcal{D}_2$  the other two. Then  $\mathcal{D}_1$  is already connected and there is only one mixed mechanism to hook up  $\mathcal{D}_2$ , so the cost is  $y + s$  which is the same as the blue transmission problem. On the other hand, there may be several  $\mathcal{D}'_i$ 's involved implying that a successful transmission of all of them requires all three yellow petals to be connected; in this case the only mechanism available is the pure yellow state in the iris. Finally, for completeness, there is the case of a single  $\mathcal{D}$  consisting of two of the petals while the third one is incidental. This differs only formally from the  $\mathcal{D}_1, \mathcal{D}_2$  case.

For  $\eta_\diamond$  containing two yellow petals in the complement of  $\diamond$ , there would be nothing to prove were it not for the advent of the triggering phenomena. Indeed, all transmissions could only use a unique mixed hexagon and hence the probabilities would be just  $y + s = b + s$ . However, unfortunately, the case of two yellow petals plus a conditioned yellow would often lead to triggering situations, boosting this probability to  $\frac{1}{2}$ . Here we implement the appropriate dosage of no close encounter rules as before.

The cases where  $\diamond$  consists of more than one petal are similar (or trivial). At the level of conditional transmissions, given  $\eta_\diamond$ , the full petal configuration, these cases appear to be identical to the ones above with the rôle of the additional petals of  $\diamond$  played by petals of  $\eta_\diamond$  which happen to be the wrong color to aid transmission. Notwithstanding, these problems are *not* isomorphic, because of the advent of triggering in the comparisons of  $\eta_\diamond$  versus  $\bar{\eta}_\diamond$ . Nevertheless, the mechanisms exploited to handle to single petal problems do apply in the cases where  $\diamond$  has more than one petal. Indeed, all that was needed to handle the single petal case was the explicit verification that the single petal of  $\diamond$  was in a position to influence the transmission. Obviously, this will still be true in the multiple petal cases. We see no merit in explicit calculations for these additional cases and therefore consider the proof to be completed.  $\square$

We now turn attention to cases where the conditioned hexagons include the iris. Fortunately, the analogue of the above lemma, in its full generality, is certainly not necessary. Indeed, it is important to realize that these exercises are tailored for situations where the conditioned hexagons in  $\diamond$  are, in fact,

segments of paths. These considerations drastically cut down the number of problems – essentially to a single case, which we prove in the following:

**Lemma III.3.14.** *Let  $\mathfrak{F}$  denote a flower and  $\diamond$  a specification of at least two petals and partial information about the iris with the property that a connection between two yellow petals of  $\diamond$  must be taking place through the iris. Let  $\mathcal{D}$  denote another set of petals on  $\mathfrak{F}$  which is disjoint from  $\diamond$  and let  $T_{\mathcal{D},\diamond}^B$  be defined as before. Let  $X_{\mathcal{D},\diamond}^\circ$  denote a  $\{0,1\}$  valued random variable and  $T_{\mathcal{D},\diamond}^{Y,*}$  the event that  $\mathcal{D}$  is yellow connected such that: If  $X_{\mathcal{D},\diamond}^\circ = 1$ , usage of the iris is permitted, but, if  $X_{\mathcal{D},\diamond}^\circ = 0$ , usage of the iris is forbidden. Then for  $b \geq s$ , there are joint laws such that*

$$\mu(T_{\mathcal{D},\diamond}^B) = \mu^*(T_{\mathcal{D},\diamond}^{Y,*}),$$

where by abuse of notation from Lemma III.3.13,  $\mu^*$  denotes the appropriate joint distribution. Similar results hold with the role of yellow and blue reversed and, in case  $\diamond$  has petals of both colors,  $*$ -probabilities for the  $*$ -transmissions of the two colors are equal.

**Remark III.3.15.** In the non-trivial implementation of the above result, a clear interpretation of the above scenario is that the pure iris is shared by both “paths”. We adhere to this interpretation.

**Proof:** As in the Proof of Lemma III.3.13, we will prove the analogue of Equation III.2. Due to the stipulation that  $\diamond$  must contain a yellow transmission through the iris, if the requisite transmission in  $\diamond$  is between diametrically opposed hexagons, the (conditional) blue transmission will occur automatically and there is basically nothing to prove. Indeed, the hexagons in  $\diamond$  plus the

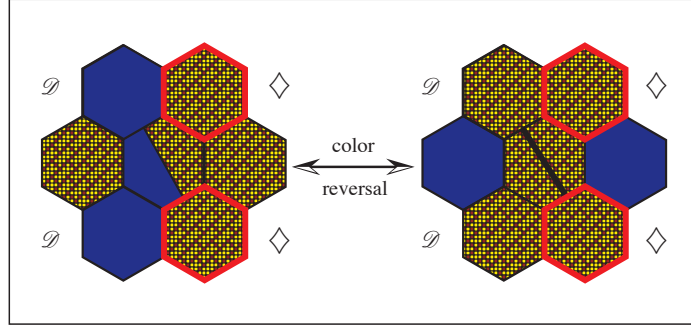


Figure III.7: All paths transmit through the iris.

iris divide the remaining petals into two halves and, by micro-environment duality (c.f. remark following Lemma III.3.17), there cannot be a blue connection between these two halves. Evidently the only possible blue transmissions under consideration will be between adjacent petals. In these cases we simply set  $X_{\mathcal{D},\diamond}^{\circ} = 0$ .

Thus, the only non-trivial case is when there are two petals in  $\diamond$  separated by one unit with the appropriate mixed iris providing the required connection along with a pair of blue hexagons which are adjacent to this pair. While perhaps not obvious in a verbal description, a look at Figure III.7 shows that it is nevertheless true that the same mixed hexagon provides the requisite connection for  $\mathcal{D}$ . Thus, in the presence of such an  $\eta$ , the conditional probability is

$$\mu(T_{\mathcal{D},\diamond}^B | \eta) = \frac{s}{y + s}.$$

On the other hand, in  $\bar{\eta}_{\diamond}$ , the only possibility for achieving the requisite yellow transmissions is when the iris is pure yellow which necessitates  $X_{\mathcal{D},\diamond}^{\circ} = 1$ . Here

we get

$$\mu^*(T_{\mathcal{D},\diamond}^{Y*} \mid X_{\mathcal{D},\diamond}^{\circ} = 1, \bar{\eta}_{\diamond}) = \frac{y}{y+s},$$

so if we adjust the conditional probability for  $X_{\mathcal{D},\diamond}^{\circ} = 1$  to  $s/y$ , then the desired result is achieved.  $\square$

**Remark III.3.16.** It is important for later purposes to emphasize certain cases where the random variables do *not* come into play:

1. The random variables  $X_{\mathcal{D},\diamond}$  are really defined conditional on the configuration  $\eta_{\diamond}$ , i.e. the entire petal configuration. This has the following consequences: If the petal configuration is such that the required connection between say petal  $x$  and  $y$  has already occurred, then  $X_{\mathcal{D},\diamond} \equiv 0$ . For later reference, we call such transmissions *predetermined* transmissions.

2. Our random variables are designed to punish or reward transmissions of the same color as the set being conditioned on and thereby level the playing field compared to transmissions of a different color. In particular, if  $\mathcal{D}$  is blue and  $\diamond$  is all yellow (or vice versa), then the random variables do not affect the transmission.

We now recast the previous results in a form which is more pertinent for later use.

**Lemma III.3.17.** *Let  $\Gamma_b$  be a blue path and let  $\Gamma_y$  be a yellow path. Let  $x$  and  $y$  be two points. Then the probability of a  $*$ -transmission from  $x$  to  $y$  in the “complement” of  $\Gamma_y$  and  $\Gamma_b$  is the same in yellow as it is in blue. Here, complementary  $*$ -transmission denotes, depending on the values of the auxiliary random variables and the relevant colors involved, the possibility of leeway*

*provided for the sharing of hexagons and/or adherence to no close encounter rules, as discussed in Lemmas III.3.13 and III.3.14.*

**Proof:** In light of the preceding two lemmas, all that is needed is an argument (involving inclusion–exclusion) along the lines used in the proof of Lemma III.3.6. We may follow the reasoning used therein *mutatis mutandis*.  $\square$

**Remark III.3.18.** We have made no stipulation about the path type of  $\Gamma_b$  and  $\Gamma_y$ . E.g. self–avoiding, no close encounters, etc. However, it turns out to be the case that if  $\Gamma_y$  and/or  $\Gamma_b$  were supposed to be self–avoiding in the strongest sense – hexagon self–avoiding and no close encounters, then the presence of our additional transmissions do not change this property. Indeed, the only mechanism for local changes in e.g. the path  $\Gamma_y$  is the transmutation of a mixed iris to a pure iris or vice versa. Ostensibly, this could “change” the required use of a mixed iris in a path segment such as [3, 4, (mixed horizontal iris), 1] (in yellow) to a path where the use of 4 is redundant when the iris “turns” pure (c.f. Remark III.3.2). However, under these and similar circumstances, the blue part of the iris, cannot, by micro–environment duality, be used to connect anything that cuts across the yellow path and the remaining petals of the flower, if used at all, will be automatically connected. Hence, should the path  $\Gamma_y$  have segments of this type, it will never be the case that the  $*$ –rules permit a change of the iris type.

The following is of not immediate use but will be important later on. We include the result here because the proof follows along the lines of what has preceded.

**Lemma III.3.19.** *Let  $\mathfrak{F}$  be a flower and let  $\diamond$  and  $\mathcal{D}$  be as in Definition III.3.12 and suppose that  $a^2 \geq 2s^2$ . Then the probability of  $\mathcal{D}$  being all of one color and connected in the same color conditioned on  $\diamond$  – even with the  $*$ -rules enforced – is no bigger than the same probability in the unconditioned case, e.g.*

$$\mu^*(T_{\mathcal{D},\diamond}^{B*}) \leq \mu(T_{\mathcal{D}}^B).$$

*In particular, consider the event  $\tilde{T}_{\mathcal{D},\diamond}^{B*}$  which is similar to  $T_{\mathcal{D},\diamond}^{B*}$ , but where the right to close encounters is never withheld. Then*

$$\mu^*(\tilde{T}_{\mathcal{D},\diamond}^{B*}) \leq \mu(T_{\mathcal{D}}^B),$$

*and similarly with  $B$  replaced by  $Y$ .*

**Proof:** We discuss first the cases where  $\diamond$  does not include the iris. We note that all situations where  $\mathcal{D}$  consists of multiple sets do not actually involve the extra degrees of freedom provided by the random variable, so we in fact get the desired result immediately; usually as a strict inequality, i.e. when the sites in  $\diamond$  are in a position to participate in the necessary connections. Thus we may assume without loss of generality that  $\mathcal{D}$  consists of two components which must be connected. Let  $\square$  denote an alternative configuration to  $\diamond$  (on the same subset) and  $\eta_{\square}$  the full configuration on all the petals. Clearly it is enough to show

$$\sum_{\square, \eta_{\square}} \mu(\eta_{\square}) \mu(T_{\mathcal{D}}^B | \eta_{\square}) \geq \sum_{\eta_{\diamond}} \mu(\eta_{\diamond}) \mu^*(\tilde{T}_{\mathcal{D},\diamond}^{B*} | \eta_{\diamond}). \quad (\text{III.3})$$

We divide into two cases, the first and more serious of which is when  $\mathcal{D}$  contains next neighbor sites separated by a site which is not in  $\mathcal{D}$ . However, if the site

separating  $\mathcal{D}$  is in  $\diamond$ , the result is trivial: Confining attention only to those configurations on “the other side” of  $\mathcal{D}$ , which, given the condition in  $\diamond$ , would require a transmission, the difference between the left and right hand side is, at best, proportional to a  $(b + 2s)$  for the transmissions with permissions, versus a  $\frac{1}{2}(b + s) + \frac{1}{2}$  times the same proportionality constant for the unconditioned case. We may thus assume that the separating petal is not in  $\diamond$  and, obviously, since the terms in which it is blue contribute equally to the left and right side of Eq. (III.3), we may as well assume that this separating petal is yellow.

We first consider the possibility that  $\mathcal{D}$  contains more than just the two “ports” in question, i.e. magnitude of  $\mathcal{D}$  is bigger than or equal to 3. If  $|\mathcal{D}| \geq 4$  – and there is no automatic transmission – then the conditional transmissions will be  $(a + 2s)$  for both yellow and blue and therefore the  $*$ -rules do not even come into play. Thus we have, for all  $\square$  configurations,

$$\mu(T_{\mathcal{D}}^B | \eta_{\square}) \geq \mu^*(T_{\mathcal{D},\diamond}^{B*} | \eta_{\diamond}), \quad (\text{III.4})$$

whenever  $\eta_{\diamond} = \eta_{\square}$  on the complement of the conditioned set. Now, turning to cases where  $|\mathcal{D}| = 3$ , since  $\mathcal{D}$  only has two components, the extra port must be contiguous to one of the other two. The unconditioned case will be unity with probability  $\frac{1}{4}$  (both petals not yet accounted for are blue),  $\frac{1}{2}$  with probability  $\frac{1}{4}$  (both yellow which leads to a triggering situation), and otherwise  $(a + 2s)$ . On the other hand, the conditional situation can at best get  $(a + 2s)$ , which is smaller than the preceding combination.

We are down to the central cases we must consider:  $|\mathcal{D}| = 2$  and the two petals of  $\mathcal{D}$  are separated by a single yellow petal. The unconditioned case

(under the above mentioned conditions) yields a grand total of:

$$G_T = \frac{1}{8} \left[ 1 + 2 \cdot \frac{1}{2} + 2(b + s) + 3(b + 2s) \right], \quad (\text{III.5})$$

where the various terms in the parenthesis are in obvious accord with each of the eight configurations. Now we partition the remaining cases according to the size of  $\diamond$ . If  $|\diamond| = 3$ , there is, in essence, nothing to prove unless there is a triggering situation. Indeed, without triggers, the blue transmission probabilities (given  $\eta_\diamond$ ) and the yellow transmission probabilities (given  $\bar{\eta}_\diamond$ ) are identical and no  $*$ -rules would be implemented. In the triggering situations, the best scenario for the conditional probability is  $\frac{1}{2}$ , which is easily exceeded by  $G_T$ .

We are down to the case where  $|\diamond| = 2$ . If the two petals in  $\diamond$  are not contiguous, this, for all intents and purposes, reduces to the case where  $|\diamond| = 3$ . Indeed, the best scenario for the conditioned problem is a trigger, which leads to  $\frac{1}{2} \leq G_T$ . For the remaining cases, we must treat separately the situations where both petals of  $\diamond$  are blue and when there is one blue and one yellow (we remind the reader that we need never consider the case where  $\diamond$  is entirely yellow in a blue transmission, c.f. Remark III.3.16). In the case where  $\diamond$  is entirely blue, as far as the conditional transmission is concerned, when the unaccounted for petal is blue, there is no triggering and, at best,  $(b + 2s)$ ; when the remaining petal is yellow, one gets  $(a + s)$  (in both  $\eta_\diamond$  and  $\bar{\eta}_\diamond$  hence no rules are implemented). Thus we are looking at equal admixtures of  $(a + s)$  and  $(a + 2s)$ , which is less than  $G_T$ . Now, the final  $|\diamond| = 2$  situation:  $\diamond$  contains one yellow petal and one blue; we remind the reader that the two petals of  $\diamond$  are contiguous. Summing over  $\eta$ , here we find equal admixtures of  $\frac{1}{2}$  and

$(a + 2s)$  for the conditioned case; the second case is self-explanatory, the first case could directly be a trigger, or be an alternating configuration whose color reverse is a trigger. In any case, a casual tally shows that  $G_T \geq \frac{1}{4} + \frac{1}{2}(a + 2s)$  and so we are done with  $|\diamond| = 2$ .

We now turn to the consideration of  $|\diamond| = 1$ , in which case this petal, wherever it may be located, is certainly blue. If  $\diamond$  is contiguous with one of the ports, there will be a triggering scenario with probability  $\frac{1}{4}$  (which is an enhancement over the color reverse) and to the rest of the configurations we assign  $(a + 2s)$ . However, we contend that  $\frac{1}{4} \cdot \frac{1}{2} + \frac{3}{4}(a + 2s)$  does not exceed  $G_T$ ; this time, finally, due to the inequality  $b \geq s$ . Finally, if  $\diamond$  is perched right between the two ports (on the “big” side), then in the non-triggering scenario, both unaccounted for petals of  $\eta$  must be yellow, the color reverse of which does not even lead to triggering, therefore actually does worse than when the  $\diamond$  was contiguous with one of the ports.

The very last case to consider is where the two ports of  $\mathcal{D}$  lie at opposite ends of the flower. Borrowing from the previous next-nearest neighbor case, we may as well assume that these are the only petals of  $\mathcal{D}$ . First the unconditioned probability ought to be computed. As can be explicitly verified, along one route to connect  $\mathcal{D}$  around the iris, the addition of either hexagon will already improve the probability to  $y + 2s$ ; unfortunately, a single hexagon on the other side does nothing. However, for this case of  $\mathcal{D}$ , by running the gamut of possibilities on the “good” and “bad” approaches, we still obtain

$$\sum_{\square, \eta_{\square}} \mu(\eta_{\square}) \mu(T_{\mathcal{D}}^B | \eta_{\square}) = \frac{1}{4} + \frac{3}{4} \left( \frac{1}{4} + \frac{1}{4}(b + s) + \frac{1}{2}(b + 2s) \right).$$

It is noticed that the term in parenthesis is in excess of  $(b + 2s)$ , thus, even if  $\diamond$

is concentrated on one side of the “transmission line” – which would produce a  $\frac{1}{4}$  similar to the one in the above display; in every configuration in which there is no direct transmission, the conditional probability still does not exceed  $(b + 2s)$  and we are done.

Finally, we discuss the circumstances where  $\diamond$  includes information about the irises. While intricate arguments along the above lines are almost certainly possible, these problems are easily handled under the proviso  $b^2 \geq 2s^2$  – which is anyway implemented later for entirely different reasons. Indeed, the only non-trivial cases, the ones discussed in the proof of Lemma III.3.14, are when the conditional transmissions are given by  $s/(b + s)$ . On the other hand, given that  $\mathcal{D}$  is blue, but in the absence of any other conditioning, a transmission always takes place with probability at least as big as  $b + s$ , which is greater than or equal to  $s/(b + s)$ , whenever  $b^2 \geq 2s^2$ .  $\square$

## III.4 Convergence to Cardy–Carleson Functions

### III.4.1 Introductory Remarks and More on Paths

Here we will introduce the functions,  $u_N^*$ ,  $v_N^*$  and  $w_N^*$ , which are more or less the functions with which we will work. Of course our ultimate theorem concerns the usual functions  $u_N$ ,  $v_N$  and  $w_N$  discussed in the introduction; but all of the mechanics, e.g. Cauchy–Riemann relations, contour integration, etc., hold only for the former set. We will be content with the knowledge that  $|u_N - u_N^*| \rightarrow 0$  uniformly on compact sets disjoint from the boundary (which we do not ultimately prove till the appendix) and similarly for the  $v$ ’s and  $w$ ’s.

For the purpose of what is to follow, let us introduce some concise notation.

**Notation III.4.1.** Let  $\mathcal{D} \subset \mathbb{C}$  denote a finite, open, simply connected domain with piecewise smooth boundary, which we will regard as having a diameter of order unity. The boundary of  $\mathcal{D}$  is exhausted by three disjoint (except possibly for end points) connected sets, which we denote by  $\mathcal{A}$ ,  $\mathcal{B}$  and  $\mathcal{C}$ , in counterclockwise order. We tile  $\mathcal{D}$ , including the boundary, with hexagons of scale  $N^{-1}$ , and we will freely use the notation  $\mathcal{A}$ ,  $\mathcal{B}$  and  $\mathcal{C}$  to denote the boundary hexagons corresponding to these three boundary pieces. While there may be some ambiguity as to which boundary piece a few hexagons belong to, we do not dwell on these details; it is sufficient that some choice be made which keeps these sets connected. The resulting subset of the hexagon lattice we will denote by  $\Lambda^{(N)}$  and we will place a floral arrangement  $\Lambda_{\mathfrak{F}N}^{(N)}$  inside  $\Lambda^{(N)}$  in accord with the conventions discussed in Section III.2.2. Since all of the actual labor will take place at finite  $N$ , we will, whenever possible, treat the hexagons as separated by unit distances and simply regard  $N$  as a large parameter. In particular, we use the notation  $z$  to locate vertices of the hexagon lattice; most of our  $z$ 's will be of order  $N$ .

As was the case in [14], the functions are defined on the vertices of the hexagons and smoothly extended if technically necessary. Let us focus on the  $u$ 's since the same considerations hold for  $v$ 's and  $w$ 's. We start with a definition of the standard  $u_N(z)$  in blue, which is the probability of the following event: There is a blue path from  $\mathcal{A}$  to  $\mathcal{B}$ , separating  $z$  from  $\mathcal{C}$ . To be definitive, the path must be self-avoiding but with close encounters permitted; as will be demonstrated in the appendix, such matters are inconsequential in

the large  $N$  limit. We define  $\mathcal{U}_N(z)$  to be the indicator function of the event just described. We will not be notationally specific as to whether we are talking about a blue path or a yellow path for this event; in any case, we define  $u_N(z) = \mathbb{E}[\mathcal{U}_N(z)]$ .

The function  $u_N^*(z)$  is analogous to  $u_N(z)$  in that both concern the probability of a path from  $\mathcal{A}$  to  $\mathcal{B}$  that separates  $z$  from  $\mathcal{C}$ . However, first we should emphasize that  $u_N^*$  pertains to a probability on our enlarged space and second, there are the seemingly modest differences which become very important in the (unlikely) event that the path comes close to  $z$ . In fact, at the finest level of distinction, our functions will be the expectations of random variables rather than the probabilities of events. While there are again two versions of our functions, one for yellow and one for blue, for ease of notation we will still omit specific reference to the color, and, for the sake of definitiveness, unless otherwise specified we will be talking about the blue version of these objects.

We turn to the definition of the object  $\mathcal{U}_N^*(z)$ , a random variable, which defines  $u_N^*(z)$ . In most cases,  $\mathcal{U}_N^*(z)$  is in fact the indicator of an event and  $u_N^*(z)$  the corresponding probability; we will proceed with this language and later highlight the configurations in which the random variable takes on a value other than zero or one. First and foremost,  $\mathcal{U}_N^*(z)$  indicates an event on  $\Omega_N \times \mathbb{D}^K$ , where  $\Omega_N$  is the set of percolation configurations in  $\Lambda_{\mathfrak{F}_N}^{(N)}$ ,  $K$  is the number of flowers in  $\Lambda_{\mathfrak{F}_N}^{(N)}$  and  $\mathbb{D}$  is the space corresponding to the range of the random variables  $X_{\mathcal{D},\diamond}$  and  $X_{\mathcal{D},\diamond}^\circ$ . In order for a configuration to satisfy the criterion of  $\mathcal{U}_N^*(z)$ , it is first necessary that the hexagons contain a blue path connecting  $\mathcal{A}$  and  $\mathcal{B}$  separating  $z$  from  $\mathcal{C}$ . As of yet we make no specifications

concerning the type of the path – it may contain close encounters and it may contain shared hexagons. Note that a path can be “contracted”, i.e. by cutting out loops till it is a self-avoiding, non-self-touching path. The resulting path still connects  $\mathcal{A}$  to  $\mathcal{B}$  and, if it still separates  $z$  from  $\mathcal{C}$  (which need *not* be the case) then, as we shall see, the event  $u_N^*(z)$  is automatically satisfied regardless of the auxiliary variables. It is in the grey zone between the extremes of {no separating path exists} and {a separating path exists which enjoys strict self-avoidance} where the random variables  $X_{\mathcal{D},\diamond}$  and  $X_{\mathcal{D},\diamond}^\circ$  really come into play.

In order to be concrete, we will simply give a prescription which shows whether a particular path  $(h_1, \dots, h_M)$  of blue and mixed hexagons in a configuration  $\omega$  satisfies, depending on the values of the  $X_{\mathcal{D},\diamond}$  &  $X_{\mathcal{D},\diamond}^\circ$ ’s, the event  $\mathcal{U}_N^*(z)$ . First and foremost, the underlying segments which form a “skeleton” for the blue path must constitute an actual self-avoiding path from  $\mathcal{A}$  to  $\mathcal{B}$  which separates  $z$  from  $\mathcal{C}$ . Thus, the hexagons have been ordered in such a way that the skeleton does not cross itself. Second, in the region complementary to flowers (if any), the path must obey the “conventional” rules, i.e. no sharing of hexagons permitted, self-touching allowed. We now turn to the delicate discussion of what takes place within the flowers. The best prescription is to follow the path sequentially: by and large, the first pass of the path through any flower is “free”. If the flower is never revisited, it need not be considered again, but, in case the path returns to the flower, the initial portion of the flower which had been used defines, temporarily, the set  $\diamond$ . The value of  $X_{\mathcal{D},\diamond}$  for all possible  $\mathcal{D}$ ’s is now ascertained. When the path revisits the flower, with the intention to share a hexagon of  $\diamond$ , or, encounter a hexagon of  $\diamond$ , it must

receive “permission” from the appropriate  $X_{\varrho, \diamond}$  and/or  $X_{\varrho, \diamond}^{\odot}$ . If success is achieved at this level, the new  $\diamond$  is reset by adjoining to the old  $\diamond$  the petals that had been used in the second visit; all of this in case of a possible third visit, etc. Failure on any pass through any flower renders that particular path useless for achieving the event. Notwithstanding, *all* candidate paths must be checked; if no path of  $\omega$  satisfies the geometric criterion with these permissions, then the event  $\mathcal{U}_N^*(z)$  does not occur. If at least one path satisfies all of the above criteria, then  $\mathcal{U}_N^*(z)$  is declared to have occurred. The event  $\mathcal{U}_N^*(z)$  has been defined; corresponding definitions hold for  $\mathcal{V}_N^*(z)$  and  $\mathcal{W}_N^*(z)$ .

The exceptional situations occur when  $z$  is a vertex of an iris hexagon *and* the path under consideration ostensibly goes through the iris. It is worthwhile, referring to the previous discussion, to assign a value to each path, namely zero or one, and then define  $\mathcal{U}_N^*(z)$  to be the maximum over all paths of the path value. We will continue this perspective. Let us now describe the circumstances under which the path value will be set to  $\frac{1}{2}$ : First, as alluded to,  $z$  itself must be the vertex of an iris hexagon; second, the iris must be in a mixed state; and finally, the path under consideration would lead to a value of one *if* the iris had been pure blue (and of course zero had the iris been pure yellow). Notice that depending on the particulars of the mixed state and the path, the path value can be  $\frac{1}{2}$  even when the requisite blue transmit has not literally occurred. Under these circumstances,  $\mathcal{U}_N^*(z)$  *may* take on the value  $\frac{1}{2}$ . Of course, it should be emphasized that if an alternative path exists which does not use the iris and does satisfy all the requisite permissions, then  $\mathcal{U}_N^*(z)$  will be one. Thus it is only the configurations in which the iris attached to

$z$  is *pivotal* for the relevant event that  $\mathcal{U}_N^*(z)$  can be  $\frac{1}{2}$ . These are, as is well known from [14], exactly the configurations contributing to the derivatives of the relevant functions.

As is seen from the above descriptions, it is indeed the case that anytime a self-avoiding, non-self-touching path of the right color separates  $z$  from  $\mathcal{C}$ ,  $\mathcal{U}_N^*(z) = 1$ , simply because no permissions are ever required. Thus without the advent of sharings, etc. no such paraphernalia would be necessary and we might just as well focus on the *reduced* path. However, it is crucial to our analysis that certain paths loop around in order to “capture”  $z$ . Nevertheless, the existence of certain self-avoiding, non-self-touching paths is important for conditioning/partitioning purposes. In this vein, one might envision that a path with permissions which nevertheless contain such loops may be partially reduced in this fashion, i.e. the journey “towards”  $z$  indeed has this property, with all the auxiliaries occurring in the later portion of the path. That such a rearrangement is possible is the subject of the next lemma.

**Definition III.4.2.** Consider a blue transmit in the configuration  $\omega$  which satisfies the (geometric) requirements of the event that  $\mathcal{U}_N^*(z) \neq 0$ . If this path cannot be reduced to a self-avoiding, non-self-touching path then it has loops which are essential for the fulfillment of this event. We define the *lasso* points of this path as follows: The last lasso point is a shared hexagon or a close encounter pair which is part of a relatively simple closed loop of the path with  $z$  in its interior. The next to last lasso point (if any) enjoys a similar definition, save that the loop in question passes through the last lasso point. Similarly for the earlier lasso points.

**Lemma III.4.3.** *Suppose that  $(\omega, X)$  is a configuration such that  $\mathcal{U}_N^*(z) > 0$ . Then, in  $\omega$  there is a path fulfilling the requirements of  $\mathcal{U}_N^*(z) > 0$  (i.e. connects  $\mathcal{A}$  to  $\mathcal{B}$  and separates  $z$  from  $\mathcal{C}$ ) with the property that in the part of the path from  $\mathcal{A}$  to the last lasso point necessary for the capture of  $z$ , the only points of sharing or pairs of close encounters are those which are essential for the particular path to fulfill the criterion  $\mathcal{U}_N^*(z) > 0$ . In particular this portion of the path may be regarded as having no sharings and no close encounters with itself.*

**Remark III.4.4.** We remark that while the above appears to be geometrically obvious – just cut out the necessary loops – what is at issue is that the rearranged path still has some close encounters/shared hexagons with the later portion of the path. Thus it is not *a priori* clear that the new path, with the new  $\mathcal{D}$ 's, will still have the requisite permissions. In point of fact, the stronger statement that the *full* path can be reduced to one in which all the shared hexagons and close encounters remaining are essential for the capture of  $z$  turns out to be false, as the following example shows.

**Example III.4.5.** We consider a situation – destined for a *yellow* capture of  $z$  – in which the initial incoming line to the flower is at petal 3 whereupon the path leaves the flower immediately and, after capturing  $z$ , returns to petal number 6. It then leaves again and reenters at petal 5 (thereby making a redundant loop), undergoes a diametric transmission through the iris to petal number 2 and leaves for the last time. Notice that petals 1 and 4 have not been specified, but let us assume that they are both blue. The initial condition for transmission – before the reduction – is that petals 6 and 3 are conditioned

on; however, after the reduction, we regard the reentrance – after capture – at petal 6 to be a fresh transmit to 2, where petal number 5 happens to be yellow. Thus, in the reduced version of the transmission problem,  $\diamond$  consists solely of petal 3. The reader can check that for this transmission situation, both the  $\beta$  and  $\gamma$  ( $60^\circ$  and  $120^\circ$ ) mixed hexagons will provide the requisite transmission, so the overall un-starred transmission probability would be  $(a + 2s)$ . On the other hand, the color reverse of this scenario (keeping the singleton in  $\diamond$  fixed at yellow) represents a trigger situation, so, indeed, the reduced transmission will require permissions for a close encounter with the conditioned petal at 3.

**Proof:** Any reduction of the requisite type that takes place on the complement of flowers may, obviously, be performed without discussion. We are therefore, without loss of generality, down to the consideration of paths where all loop and lasso points take place within flowers. Now suppose a flower only contains loop points whose removal does not affect the separation event. Then, as discussed previously, we claim that the required reduction may also be performed with impunity. (To recapitulate, if the reduction within the flower can be performed which then renders the path segment going through a flower as self-avoiding and non-self-touching, then, in the new path within the associated flower, no random variables need to be consulted since no permissions are actually required.)

We will consider a flower  $\mathfrak{F}$  which contains a generic lasso point of the separation event, and let  $\Gamma$  denote the (unreduced) path which actually satisfies the event. More precisely,  $\Gamma$  will enter the flower at some petal  $e_0$  and, after some meandering (possibly leaving the flower to make redundant loops) must

leave the flower at some petal  $c$  to capture  $z$ ; the petal  $c$  is defined by the condition that it is the last petal of  $\mathfrak{F}$  that  $\Gamma$  visits before capturing  $z$ , i.e. the next time  $\Gamma$  visits  $\mathfrak{F}$  it will have generated a loop with  $z$  in its interior. We therefore need to show that the part of  $\Gamma$  between  $e_0$  and  $c$  – which we denote by  $\Gamma_{\mathfrak{F}}$  – can be made strongly self-avoiding. Denoting the reduced path by  $\hat{\Gamma}_{\mathfrak{F}}$ , we need to guarantee that  $\hat{\Gamma}_{\mathfrak{F}}$  is actually a legitimate path. The cases we have to treat are the ones in which there are one or more loop points in  $\mathfrak{F} \cap \Gamma_{\mathfrak{F}}$  and for the event to be accomplished, we must make another essential non-predetermined transmission through the flower before we get to  $c$  (c.f. Remark III.3.16). We reiterate that these cases are dangerous because after the removal of the loop, the corresponding  $\diamond$  we condition on (to make the transmission) may change so it is not *a priori* clear that the random variable will still “allow” the required transmission to happen. Nevertheless, we have a fairly limited situation and we are able to ensure that the necessary transmission does indeed happen after the reduction.

We consider  $\hat{\Gamma}_{\mathfrak{F}}$  and make the following definitions for convenience. First, within the petal, the three hexagons – including the iris – which form the non-predetermined core of the transmission will be call the *transmission line*; we also denote the first petal in the path ordering of the transmission the *port* and the last petal in the transmission the *terminus*.

We start by focusing our attention on the case where no hexagon was shared. Then we have two cases corresponding to whether the port and the terminus are diametrically opposed or next nearest neighbors. We observe that  $e_0$  cannot be next to the port or the terminus, because in the former case it

would be directly connected to the port, hence in  $\hat{\Gamma}_{\mathfrak{F}}$  there is no conditioning to be spoken of so the corresponding random variable is identically 0. In the latter case, since the capture of  $z$  is purported to take place after the transmission, said transmission is not actually necessary to get to the terminus. The situation is even more trivial if the port or the terminus is equal to  $e_0$ . This implies that we are done with the case where the port and the terminus are diametrically opposed. The second geometry follows similarly:  $e_0$  cannot be on the small side of the transmission line and, indeed, can only occupy the mid petal of the large side of the transmission line. Now if  $\Gamma_{\mathfrak{F}}$  used the petal between  $e_0$  and the port at all, then we are automatically done because then in  $\hat{\Gamma}_{\mathfrak{F}}$ , we have an unconditioned transmission between the port,  $e_0$ , the petal between them and the terminus. On the other hand, if  $\Gamma_{\mathfrak{F}}$  did not use the petal between  $e_0$  and the port, then either  $\Gamma_{\mathfrak{F}} = \hat{\Gamma}_{\mathfrak{F}}$  (the iris exhibits exactly the mixed configuration connecting the port to the terminus – necessitating an eventual departure before  $e_0$  connects to the port) or the iris was pure and we have a unconditioned situation where  $e_0$  is connected directly to the terminus through the iris.

We now turn attention to the cases where there is sharing. Our first claim is that under any circumstances of multiple passes through the same flower, there cannot be more than one instance of sharing. Indeed, suppose there were two instances of sharing, then a rudimentary countings of any double sharing scenario demonstrates that at least five petals must be involved. Thus in the first pass through the flower which requires sharing, the minimal situation is one conditioned hexagon in  $\diamond$  and four petals already blue in  $\eta_{\diamond}$ . These are

precisely the circumstances which were discussed at the beginning of the proof of Lemma III.3.13 and thus no sharing is permitted on this first attempt to share. On the other hand, if two petals are conditioned on before the first sharing – so that now all remaining petals are blue – any scenario either leads to probability one transmission situations or, at worst, the scenario where there is just one mixed iris which fails to allow the desired transmission, with the same being true for the color reverse, hence no sharing again. If three or less sites are left over after the first pass, there are not enough sites left for two or more passes involving transmission through the iris.

Given the claim that there will be only one sharing we can divide into the cases where petals are being shared and where the iris itself is being shared. The later has severe constraints, since the two transmissions must be side by side (c.f. the proof of Lemma III.3.14). In a straightforward rendition where the two transmissions are anti-parallel, both transmissions are redundant in the ultimate use of the flower, since the last entrance before the transmissions and the first exit after the transmissions are neighbors. The less straightforward renditions of parallel transmissions appear to be a topological impossibility given what the rest of the path is purported to do. Nevertheless, the shortened path now has a diametric transmission with two unconditioned blue petals, one on each side of the transmission axis, and at least one more (unconditioned) petal known to be blue due to a future visit of the flower after the capture of  $z$ .

Finally, let us consider, in general terms, the (single sharing) situations where petals are shared during transmission. Here we will only make inter-

mittent reference to whether we are discussing the path before or after the reduction. First, the flower must be visited and departed from without transmission, perhaps multiple times – in order that there would be something to condition on when transmission finally occurs. We claim that for such a transmission, we need only discuss cases where the port and terminus are both separated from the conditioned set by at least one spacing. If not, the path under consideration is evidently the before path and the after path can get directly to the port or terminus thereby implying an unconditioned transmission or an unnecessary transmission, respectively. Now, for the remaining cases, it is clear that the conditioned set is but a single petal. Indeed, the geometry of conditioned site, port and terminus, is the previously discussed alternating pattern. We claim that one of the three petals which are as of yet unaccounted for must be blue since, as the reader will recollect, the path is destined to return after the capture of  $z$ . We now discuss two cases. First the iris is pure blue, in which case, once again, we are evidently referring to the path before reduction since this *can* be reduced. However, the reduced path would then have an unconditioned transmission from the conditioned site to the terminus, which requires no permissions from random variables. Otherwise, a more serious sort of transmission is taking place, evidently through a mixed iris. Under these conditions, according to the conditional distributions, there will be no sharing permitted unless, possibly, the remaining two unaccounted for sites are both yellow. The mixed type of the iris is now uniquely specified, and, due to the alternating geometry, does *not* allow the direct transmission between the conditioned petal and the terminus. But now, in as far as these

visits to the flower are concerned, the path is in fact self-avoiding and non-self-touching. Due to the constraints which led to the circumstances, there is/was no possibility for reduction, i.e. it appears that we are looking at both the before and the after path with no need for analysis.  $\square$

### III.4.2 Statement and Proof of Cauchy–Riemann Relations

In this section we will establish Cauchy–Riemann relations for the triple of functions under consideration. As was the case in [14], these are not exactly Cauchy–Riemann *equations*, but equations of a Cauchy–Riemann type between positive and negative “pieces” of the derivative, which admit a probabilistic interpretation. Notwithstanding the absence of Cauchy–Riemann *equations*, these Cauchy–Riemann relations are sufficient to exhibit Green’s Theorem type cancellations in the evaluation of the appropriate discrete contour integrals.

**Definition III.4.6.** Let  $\hat{a} = i, \hat{b} = \tau i, \hat{c} = \tau^2 i$  denote three of the six lattice directions on the hexagonal lattice, where  $\tau = \exp(\frac{2\pi i}{3})$ . For a function  $f(z)$  defined on the vertices of the hexagonal lattice and  $\eta \in \{\pm\hat{a}, \pm\hat{b}, \pm\hat{c}\}$ , as appropriate, we define the directional derivative in the usual fashion:

$$D_\eta f(z) = f(z + \eta) - f(z).$$

Let  $\mathcal{U}_N^{\text{B}*}(z), \mathcal{V}_N^{\text{B}*}(z)$  and  $\mathcal{W}_N^{\text{B}*}(z)$  denote the blue versions of the random variables described in the previous subsection and  $\mathcal{U}_N^{\text{Y}*}(z), \mathcal{V}_N^{\text{Y}*}(z)$  and  $\mathcal{W}_N^{\text{Y}*}(z)$  their yellow counterparts. We denote by  $u_N^*(z), v_N^*(z)$  and  $w_N^*(z)$  the expectation of the color neutral averages, e.g.

$$u_N^*(z) = \frac{1}{2} \mathbb{E}[\mathcal{U}_N^{\text{B}*}(z) + \mathcal{U}_N^{\text{Y}*}(z)],$$

and similarly for  $v^*$  and  $w^*$ . The *Cauchy–Riemann pieces* are the quantities

$$[u_N^*]_\eta^+ = [u_N^*(z)]_\eta^+ = \mathbb{E}[(\mathcal{U}_N^{\text{B}*}(z + \eta) + \mathcal{U}_N^{\text{Y}*}(z + \eta)) - (\mathcal{U}_N^{\text{B}*}(z) + \mathcal{U}_N^{\text{Y}*}(z))]^+]$$

$$[u_N^*]_\eta^- = [u_N^*(z)]_\eta^- = \mathbb{E}[(\mathcal{U}_N^{\text{B}*}(z + \eta) + \mathcal{U}_N^{\text{Y}*}(z + \eta)) - (\mathcal{U}_N^{\text{B}*}(z) + \mathcal{U}_N^{\text{Y}*}(z))]^-,$$

where  $(\ )^\pm$  means positive/negative part and, typically, we will suppress the  $z$  dependence. Similar definitions hold for the quantities  $[v_N^*]_\eta^\pm$  and  $[w_N^*]_\eta^\pm$ . Of course we have  $D_\eta u_N^*(z) = [u_N^*]_\eta^+ - [u_N^*]_\eta^-$ , and similarly for  $v_N^*$  and  $w_N^*$ . We note that, in reference to the above display, there could be a distinction between “the positive parts of the sum” and “the sum of the positive parts”. However, as we shall see, in any configuration where, e.g.,  $(\mathcal{U}_N^{\text{B}*}(z + \eta) - \mathcal{U}_N^{\text{B}*}(z)) > 0$ , the corresponding yellow term automatically vanishes. A statement of the Cauchy–Riemann relations is as follows:

**Lemma III.4.7.** *Consider the Cauchy–Riemann pieces as described above. Then, between  $u$  and  $v$ , these objects satisfy six Cauchy–Riemann relations, the first three of which are:*

$$[u_N^*]_{\hat{a}}^+ = [v_N^*]_{\hat{b}}^+; \quad [u_N^*]_{\hat{b}}^+ = [v_N^*]_{\hat{c}}^+; \quad [u_N^*]_{\hat{c}}^+ = [v_N^*]_{\hat{a}}^+$$

for site  $z$  which emanate the edges  $\hat{a}$ ,  $\hat{b}$  and  $\hat{c}$ . For sites emanating the edges  $-\hat{a}$ ,  $-\hat{b}$  and  $-\hat{c}$ , we have:

$$[u_N^*]_{-\hat{a}}^+ = [v_N^*]_{-\hat{b}}^+; \quad [u_N^*]_{-\hat{b}}^+ = [v_N^*]_{-\hat{c}}^+; \quad [u_N^*]_{-\hat{c}}^+ = [v_N^*]_{-\hat{a}}^+.$$

We note that

$$[u_N^*(z)]_{\hat{a}}^- = [u_N^*(z + \hat{a})]_{-\hat{a}}^+,$$

and similarly for  $\hat{b}$  and  $\hat{c}$ , so the above implies all the necessary relationships for the negative pieces. There are six corresponding equations between the

derivative pieces of the  $v$  and  $w$  functions (which implies an additional six relations between the derivative pieces of the  $w$  and  $u$  functions).

We will prove separately the cases for sites which are and are not vertices of irises.

**Proof (non-iris sites):** If neither  $z$  nor its neighbor is the vertex of any iris, the preliminary step of the proof is identical to that in [14]. Explicitly, let us consider the case of  $[u_N^*]_{\hat{a}}^+$ . Since no mixed hexagon is involved, both the blue and yellow versions correspond to the *event* that the separating path goes “below”  $z + \hat{a}$  but does not go “below”  $z$ . Hence, focusing attention on the function  $u_N^{\text{B}*}(z)$ , it is the case that the hexagons surrounding the edge  $\langle z, z + \hat{a} \rangle$  are both blue, while the one directly “below”  $z$  is yellow; we will informally refer to these three hexagons as a *triad*. Note that by this criterion (among several others) no configuration will contribute to both the positive part of the blue piece *and* the positive part of the yellow piece. Returning attention to the blue case, the yellow hexagon in the triad is the terminus of a yellow path connecting to the domain boundary  $\mathcal{C}$ ; for all intents and purposes, this path may be regarded as self-avoiding and non-self-touching. As for the former pair, we may regard these as neighbors in a legitimate blue path which starts at  $\mathcal{A}$ , goes through these two from right to left and ends at  $\mathcal{B}$ . By Lemma III.4.3 we may, without loss of generality, regard the first portion of the path, namely that which connects  $\mathcal{A}$  to the hexagon on the right of  $\langle z, z + \hat{a} \rangle$ , as self-avoiding and non-self-touching. From the perspective of the remaining blue hexagon, what is required is therefore a conditional transmission – with all rules enforced – starting at this point and ending at  $\mathcal{B}$ .

(Note also that this path may have collisions, i.e. sharings of mixed hexagons with the yellow path, but as for its *interaction* with the yellow path, of course, no permissions are required.) We will replace this transmission with the same sort of transmission in yellow, after some partitioning.

We claim, according to standard arguments, that given the existence of a self-avoiding, non-self-touching blue path from  $\mathcal{A}$  to the right hexagon of the triad *and* a yellow path from the bottom hexagon of the triad to  $\mathcal{C}$  – i.e. some sort of path from  $\mathcal{A}$  to  $\mathcal{C}$  – there is a “lowest” such path. We remark that all of the pure irises involved in these paths are of the obvious requisite type, and sometimes the mixed hexagons will be completely specified by the local geometry of the path, while in other cases it may be ambiguous. With the latter consideration, we are therefore in fact conditioning on a path event rather than an actual path. It is, however, clear that details of the configuration outside the path will in fact dictate the nature of certain irises. In particular, one can envision a scenario where had the iris been pure yellow, due to some local deviation, an alternative path would have indeed been lower; therefore this mixed iris must be of a particular type. Ostensibly we will run into a dual aspect of this situation: under certain circumstances, the newly formed yellow path will be allowed to share an iris, thereby (effectively) turning a mixed hexagon into a pure hexagon. In light of the previous consideration, while the transmission may be successful, this switching could disrupt the conditioning. However, as is not hard to see, these scenarios cannot come to pass. Indeed, we claim that if changing the status of an iris from mixed to pure produces a lower path, it must be the case that the blue portion of the

iris is, in fact, already in the region below what was previously the lowest path. To demonstrate this, one only need to appeal to the skeleton structure of the underlying path: if it is possible to lower the path by switching the blue half into a pure yellow, the closure of the symmetric difference of the lowest possible skeleton of the old path and the lowest possible skeleton of the new path forms a closed loop with the blue half of the hexagon in its interior, which concludes the demonstration. We may therefore conclude that any iris involved in the yellow portion of the lowest yellow–blue path is either frozen into a particular mixed state – with the blue portion of the hexagon inside the conditioned region and therefore inaccessible for sharing – or is of a nature such that transforming the iris into a pure yellow does not render a change in the the condition of the lowest path.

It is now clear that modulo some necessities regarding triggering possibilities of the flowers which have been traversed by these paths, the region above this “lowest” blue–yellow path is entirely unconditioned. We are therefore in a position to apply Lemma III.3.17 (which automatically accounts for the triggering scenarios) to conclude that the conditional probabilities associated with the blue version of  $[u_N^*]_{\hat{a}}^+$  and the yellow version of  $[v_N^*]_{\hat{b}}^+$  are identical. Running the same argument for the yellow version of the function  $[u_N^*]_{\hat{a}}^+$  and the blue version of the function  $[v_N^*]_{\hat{b}}^+$ , we conclude  $[u_N^*]_{\hat{a}}^+ = [v_N^*]_{\hat{b}}^+$ . The other 11 relationships, for the non–iris sites, follow from an identical argument.

**Proof (iris sites):** For convenience, we will start with the  $\hat{a}$  derivative of  $u_N^*(z)$ , assuming the iris is located directly to the right of  $\langle z, z + \hat{a} \rangle$ . We first note that in those configurations where the iris happens to be pure, the

argument is identical to the non-iris site case. So we will focus attention on configurations contributing to  $[u_N^*(z)]_{\hat{a}}^+$  in which this iris is of a mixed type. Our first case will be to compare the positive part of the  $\hat{a}$  derivative of  $u_N^*$  to the positive part of the  $\hat{c}$  derivative of  $w_N^*$ . Notice that in this case – as opposed to an  $\hat{a}$  versus  $\hat{b}$  comparison – the edges  $\langle z, z + \hat{a} \rangle$  and  $\langle z, z + \hat{c} \rangle$  are both boundary edges of the iris and hence the situation before and after the switch will be more or less equivalent. We start by considering configurations for which  $\mathcal{U}_N^*(z + \hat{a}) = 1/2$  while  $\mathcal{U}_N^*(z) = 0$ . Aside from the mixed nature of the iris, we claim this is exactly the same as the pure iris case. Indeed, the inferred value of  $\mathcal{U}_N^*(z + \hat{a})$ , were this iris blue, is supposed to be one, while the inferred value of  $\mathcal{U}_N^*(z)$  is still zero, meaning that the hexagon to the left of the  $\langle z, z + \hat{a} \rangle$  bond is indeed blue (and connected to  $\mathcal{B}$ ), and similarly the hexagon below  $z$  is yellow, etc. Now, it is only necessary to observe that changing the iris to yellow destroys the event of a separating path “below”  $z + \hat{a}$ , which is indeed seen to be the case. For this portion of the proof, we will actually do a double switch: first changing the blue path from the left hexagon to  $\mathcal{B}$  to yellow and then replacing the yellow path which connects to  $\mathcal{C}$  with a blue rendition. The former is identical to the argument of the pure case modulo that we must envision the mixed hexagon as a pure blue in order to perform the conditioning partition. Having accomplished the first switch, we claim that the second switch is identical – with the same proviso concerning the mixed hexagon and, of course, a repartitioning of the configurations according to the ordering of the new yellow–blue path connecting  $\mathcal{B}$  to  $\mathcal{A}$ . When the double procedure has been achieved, we are, manifestly, in a configuration where the

blue version of  $\mathcal{W}_N^*(z+\hat{c})$  evaluates to  $1/2$  while, still, the corresponding version of  $\mathcal{W}_N^*(z)$  is zero. Since by a rotation of the arguments at the beginning of this paragraph, these are the only such configurations contributing to (the positive part of)  $\mathcal{W}_N^*(z+\hat{c}) - \mathcal{W}_N^*(z)$  (in blue), and hence we have a bijection between the configurations contributing to the positive part of the  $\mathcal{U}_N^*$  difference (in blue) and the positive part of the  $\mathcal{W}_N^*$  difference (in blue).

Finally, starting from the same initial setup, we now compare the  $\hat{a}$  derivative of  $u_N^*(z)$  with the  $\hat{b}$  derivative in  $v^*$ . As alluded to above, this case is essentially different because the site at  $z + \hat{b}$  is actually surrounded by pure hexagons. Proceeding in the *forward* direction, we follow the steps of the pure case: that is to say, we replace the blue path emanating from the hexagon to the left of  $\langle z, z + \hat{a} \rangle$  with a yellow transmission. Let us investigate the consequences. It is clear that  $\mathcal{V}_N^*(z + \hat{c})$  indeed equals one (regardless of the iris configuration) and now we claim that  $\mathcal{V}_N^*(z) = 1/2$ . Indeed, in light of the two hexagons below and to the left of  $z$ , through which a yellow path connects  $\mathcal{B}$  to  $\mathcal{C}$ , it is clear that were the iris yellow, the yellow version of  $\mathcal{V}_N^*(z)$  would be one; however, the blue path which connects the outside of this iris to  $\mathcal{A}$  indicates that were the iris to be blue, no yellow path would separate  $z$  from  $\mathcal{A}$ . We are finished with the forward direction. The last thing to be checked is that the map we just described onto, which amounts to the statement that in any configuration where  $\mathcal{V}_N^*(z + \hat{b}) = 1$ , while  $\mathcal{V}_N^*(z) = 0$  (in yellow) is of the above described form. But here the argument runs a very close parallel to the considerations at the beginning of the previous paragraph: By assumption, the iris is in a mixed state, but even if the iris were blue, there must be a yellow

separating path to the right of  $z + \hat{c}$ , and this forces the two pure hexagons of the appropriate triad to be yellow. Envisioning the iris as yellow places a path to the right of  $z$ ; however, when this iris is blue, no such path can exist, meaning that the outside of the iris is connected to  $\mathcal{A}$  by a blue path. We have recreated the final conditions after the switch and this case is proved. All other cases are  $\{u, v, w, \text{yellow}, \text{blue}\}$  permutations and discrete rotations of the two described above. In starting with color neutral combinations we always end up (via a slightly different route than in the non-iris case) with color neutral combinations, and Cauchy–Riemann relations for these functions are established.  $\square$

### III.4.3 Contour Integration

We now wish to show that the functions  $u_N$ ,  $v_N$  and  $w_N$  converge to limiting objects which are indeed harmonic. We will do this by showing that the functions  $u_N - \tau^2 v_N$ ,  $v_N - \tau^2 w_N$  and  $w_N - \tau^2 u_N$  converge to analytic functions via Morera’s theorem. Specifically, we first compute the contour integral around a single hexagon and show that this reduces to leftover derivative pieces. These pieces are judiciously and symmetrically placed about the hexagon in such a way as to cancel leftovers from neighboring hexagons. Hence, by discrete distortions, any contour integral around a region of  $N^2$  hexagons will result in some derivative pieces around the contour which are easily shown to be small. We start with some notation and a definition.

**Notation III.4.8.** Hexagons are oriented as before, that is to say with two edges parallel to the  $y$ -axis. We label the vertices of the hexagon counter-

clockwise starting with the bottom vertex by  $z_1, z_2, z_3, z_4, z_5, z_6$ . If  $f$  is a function defined on the lattice, then we may use the notation  $f(z_i)$  or  $f_i$  to denote the value of the function at the site  $z_i$ .

**Definition III.4.9.** Let  $\mathcal{C} = \{z_1, \dots, z_n\}$  denote a contour consisting of neighboring points on the hexagonal lattice and  $f$  a complex valued function on the hexagonal lattice. Then we define the discrete contour integral via

$$\oint_{\mathcal{C}}^N f dz = \frac{1}{N} \sum_{k=1}^n [f(z_k) + f(z_{k+1})] \cdot \frac{1}{2} \cdot (z_{k+1} - z_k).$$

That is to say, in our definition, the value of  $f$  for the contour element is determined by *both* endpoints of the bond. Note that this has the advantage that integrations in the opposite directions of each contour element cancel exactly.

We remark that the factor of  $\frac{1}{N}$  is for the anticipated scaling, so that the above display should be understood in the spirit of a contour whose length is of order  $N$ . In the forthcoming lemma, we will deal with small scale contours so, to avoid introduction of additional notation, we transfer the  $N$  to the other side of the equation:

**Lemma III.4.10.** *Let  $\partial H$  denote the contour which is the boundary of a hexagon in accord with Notation III.4.8. Then*

$$N \oint_{\partial H}^N [u_N^*(z) - \tau^2 v_N^*(z)] dz = i(\alpha_H + \tau \beta_H + \tau^2 \gamma_H),$$

where  $\alpha_H, \beta_H$  and  $\gamma_H$  are real numbers that represent sums of derivative pieces of  $u_N^*$ . Furthermore, these functions have a tiling symmetry in the sense that e.g. the quantity  $\alpha_H$  associated with a particular hexagon  $H$  is cancelled by the

sum of the corresponding quantities  $\alpha_{\tilde{H}}$  for all hexagons  $\tilde{H}$  which neighbor the hexagon  $H$ ; similarly for  $\beta_H$  and  $\gamma_H$ .

**Proof:** We will provide a demonstration only for the case of the  $\alpha_H$ 's, since the situation for the  $\beta$ 's and  $\gamma$ 's are analogous. An explicit calculation yields

$$\begin{aligned} \alpha_H &= [(u_2^* - u_1^*) + (u_1^* - u_6^*) + (u_3^* - u_4^*) + (u_4^* - u_5^*)] \\ &\quad + [(v_1^* - v_6^*) + (v_6^* - v_5^*) + (v_2^* - v_3^*) + (v_3^* - v_4^*)], \end{aligned}$$

where, by the addition and subtraction of terms, the above has been written so that each term is a derivative along some edge of the hexagon. Now we apply Lemma III.4.7 and cancel off all corresponding pieces in such a way that everything is written in terms of the Cauchy–Riemann pieces of  $u^*$ . We are then left with

$$\alpha_H = [u_5^*]_{-\hat{b}}^+ + [u_5^*]_{-\hat{c}}^+ + [u_4^*]_{\hat{c}}^+ - [u_3^*]_{-\hat{b}}^+ - [u_2^*]_{\hat{b}}^+ - [u_2^*]_{\hat{c}}^+ - [u_1^*]_{-\hat{c}}^+ + [u_6^*]_{\hat{b}}^+.$$

Associating, in a natural fashion, derivative pieces with the corresponding edge, it is seen that half of the corresponding edges are in  $H$  and half of them “invading” a neighboring hexagon. (So that in particular, there will be corresponding “invasions” from neighboring hexagons.) It is not terribly difficult to see that each of the above pieces will occur in the integration of four hexagons, twice with positive sign and twice with negative sign and therefore cancel.  $\square$

**Lemma III.4.11.** *Let  $\Lambda_{\mathfrak{F}_N}^{(N)}$  denote a floral arrangement in a simply connected, regular region which has of order  $N^2$  hexagons, and with boundary regions  $\mathcal{A}$ ,  $\mathcal{B}$  and  $\mathcal{C}$ , each of which is comprised of order  $N$  hexagons. Finally, let  $\mathcal{C}_N$*

denote a simple closed contour in  $\Lambda_{\mathfrak{S}_N}^{(N)}$  whose length is also of order  $N$ . Then there is some  $\vartheta > 0$  and some constant  $C_0 < \infty$ , such that

$$\left| \oint_{\mathcal{C}_N} [u_N^*(z) - \tau^2 v_N^*(z)] dz \right| \leq C_0 N^{-\vartheta},$$

and similarly for  $v_N^* - \tau^2 w_N^*$  and  $w_N^* - \tau^2 u_N^*$ .

**Proof:** We perform the contour integral in accord with the formula in Definition III.4.9 withholding the overall factor of  $\frac{1}{N}$  for later purposes. We may freely indent the contour one hexagon at a time, ultimately exhausting all interior hexagons. Each interior hexagon, that is to say a hexagon which does not share at least one of its edges with  $\mathcal{C}_N$ , provides zero net contribution in accord with Lemma III.4.10. What remain are the leftover Cauchy–Riemann pieces on or near the boundary, the number of terms of which is of order  $|\mathcal{C}_N|$ , which itself is of order  $N$ . However, each piece corresponds to the probability of disjoint connections to the three boundary regions, at least one of which must be of order  $N$  away. Using the 4<sup>th</sup> item in Theorem III.3.10 the result follows.  $\square$

### III.4.4 Proof of Theorem III.2.4

For  $\mathcal{Z} \in \mathcal{D}$  let us denote by  $U_N(\mathcal{Z})$  the function  $u_N(N\mathcal{Z})$ , and similarly for  $V_N(\mathcal{Z})$  and  $W_N(\mathcal{Z})$ . While the statement of the theorem concerns the blue and yellow versions of these functions, here, for obvious reasons, we deploy the color–neutral objects. In Corollary III.7.4, we will show that

$$\lim_{N \rightarrow \infty} |u_N^B(z) - u_N^Y(z)| = 0,$$

for all  $z$ , so that the various limiting objects may be identified. As has been discussed, the discrete derivatives have been displayed as (differences of) probabilities of events which require connections between  $\mathcal{Z}$  and all three boundary components. Thus, regardless of the particulars of the position of  $\mathcal{Z}$ , the discrete derivative always requires at least one long arm emanating from (the lattice location of)  $\mathcal{Z}$ . By Theorem III.3.10, item four, this vanishes with an inverse power of  $N$ , which in terms implies a Hölder estimate which is uniform in  $\mathcal{Z}$  and  $N$ . It follows that the  $U$ ,  $V$  and  $W$  sequences are equicontinuous, and we can extract sub-sequential limits (along a mutual subsequence) which we denote by  $U(\mathcal{Z})$ ,  $V(\mathcal{Z})$  and  $W(\mathcal{Z})$ . Letting  $\mathcal{C} \subset \text{int}(\mathcal{D})$  denote any simple, closed curve which is rectifiable, we write

$$\oint_{\mathcal{C}} [U(\mathcal{Z}) - \tau^2 V(\mathcal{Z})] d\mathcal{Z} = \lim_{N \rightarrow \infty} \oint_{\mathcal{C}_N} [u_N(z) - \tau^2 v_N(z)] dz,$$

and similarly for the  $V$ ,  $W$  and  $W$ ,  $U$  pairs. We wish to make use of Lemma III.4.11, but in order to do so we must replace  $u$ ,  $v$  and  $w$  by their starred versions. On the basis of Lemma III.7.2 in the Appendix, we find that  $|u_N(z) - u_N^*(z)|$  tends to zero uniformly for any particular contour, and similarly for  $v$  and  $w$ . This allows us to bring Lemma III.4.11 into play and we may now assert that the limiting contour integrals vanish.

By Morera's Theorem, it is evident that  $U$ ,  $V$  and  $W$  are an "analytic triple", i.e. the functions  $U + i \cdot \frac{1}{\sqrt{3}}(V - W)$ ,  $V + i \cdot \frac{1}{\sqrt{3}}(W - U)$  and  $W + i \cdot \frac{1}{\sqrt{3}}(U - V)$  are all analytic. However, it is immediately clear that these functions are not independent. Indeed, upon addition of the three, the imaginary part of these vanishes, allowing us to conclude that  $U + V + W$  is a constant, which, momentarily, we will show is unity. Thus there is actually only one analytic

function in play, e.g.  $U + V + i \cdot \frac{1}{\sqrt{3}}(U - V)$ . However, we will still have occasion to exploit the symmetry of the triple.

The boundary values are inherited from the discrete lattice versions of these functions:  $U = 0$  on  $\mathcal{C}$ ,  $V = 0$  on  $\mathcal{A}$  and  $W = 0$  on  $\mathcal{B}$ ; furthermore, at the point  $e_{AB}$  which joins the  $\mathcal{A}$  and  $\mathcal{B}$  boundaries,  $U = 1$ , and similarly for  $V$  and  $W$  at the other junctures. These are readily proved by another appeal to Theorem III.3.10, item four. For example, let us consider the function  $U(\mathcal{Z})$ , with the point  $\mathcal{Z}$  in the midst of  $\mathcal{C}$ . Then back on the discrete level, for all intents and purposes, this point must be joined to some point on  $\mathcal{A}$  and another on  $\mathcal{B}$  by blue transmissions. Since  $\mathcal{Z}$  cannot be close to both boundaries, this probability tends to zero as  $N$  tends to infinity. Moreover, this argument is not confined to points that are actually on the boundary, a similar argument also demonstrates that for points near the boundary – on the macroscopic scale –  $u_N(z)$  takes on a small value. Similar arguments hold for the boundary values of  $V$  and  $W$  on  $\mathcal{A}$  and  $\mathcal{B}$ , and it is also not hard to show that as  $\mathcal{Z}$  approaches  $e_{AB}$ ,  $U(\mathcal{Z})$  must approach one.

We claim that the boundary condition (and the symmetry of the triple) is, in fact, enough to specify uniquely what the function is – namely the conformal transformation of the linear Cardy–Carleson function described in the introduction. To establish this, it is sufficient to demonstrate that a similar sort of analytic triple laden with the constraint of adding up to zero – i.e. homogenous boundary conditions – is identically zero. We proceed as follows: Since all functions described are harmonic, we may, by conformal invariance, treat the corresponding (homogeneous) problem on a triangle. On the tri-

angle we denote the three functions as  $\delta U$ ,  $\delta V$  and  $\delta W$  and, without loss of generality,  $\delta U = 0$  leg of the triangle coincides with the  $x$ -axis. Noting that  $\delta U$  is the imaginary part of an analytic function,  $\Phi_U$ , whose real part is  $-\frac{1}{\sqrt{3}}(2\delta V + \delta U)$ , we may use the Schwarz Reflection Principle to extend this analytic function across the  $x$ -axis. We will use the continuation of  $\Phi_U$  to define a  $\delta U$  and  $\delta V$  throughout the reflected domain, i.e.  $\text{Im}(\Phi_U) =_{df} \delta U$  and  $\frac{1}{2}[-\sqrt{3}\text{Re}(\Phi_U) - \text{Im}(\Phi_U)] =_{df} \delta V$ . It is found, obviously, that  $\delta U$  changes sign upon this reflection. More significantly,  $\delta V$  takes on the reflection of the value  $\delta U + \delta V$  which by the homogeneity assumption is exactly  $-\delta W$ , so  $\delta W$  is given by the negative of the reflection of  $\delta V$ . The boundary conditions on the new, reflected boundaries are therefore conditions that the (extended)  $\delta V$  and  $\delta W$  vanish. A similar phenomenon will happen when reflecting across the  $\delta V = 0$  lines and/or the  $\delta W = 0$  lines. It is therefore clear that starting from a triangle whose indefinite reflections will tile the plane, e.g. a right triangle or an equilateral triangle, we will end up with a triplet of analytic functions whose individual components are always, to within a sign, one of the original  $U$ ,  $V$  or  $W$  evaluated at the corresponding point in the original triangle. It is evident that these functions are all bounded and, often enough, zero, so they are all identically zero.

Since the subsequence led to an unambiguous limit we conclude convergence of the full sequence, and the desired result has been established.  $\square$

## III.5 Conclusion

We have studied a model which differs in no outstanding way from any other in a myriad of 2D percolation models. We demonstrated that, at least as far as the crossing probabilities are concerned, the continuum limit of the present model is identical to that of the site model on the triangular lattice. Needless to say, there are obvious similarities between the present model and the site model on the triangular lattice – in particular, vis-a-vis a hexagonal tiling problem. (Not to mention that the model without irises is the  $s = 0$  limit of the model with irises.) All in all, these similarities allowed for the development of a proof which follows closely the original derivation of [14]. Notwithstanding, a small amount – but one which is of strictly positive measure – of universality has been established. In particular, and of similarly small significance, is the fact that the parameter  $s$  may take on a range of values and needless to say, there is a good deal of leeway in the placement of flowers.

There are numerous shortcomings to this work. It is worthwhile to underscore the ones which we believe are of greater significance:

1. It has not proven feasible for us to establish these results for well-known systems. In particular, one has in mind, among the self-dual problems, the full bond triangular lattice and/or the acclaimed bond problem on the square lattice, not to mention any number of 2D critical models without self-duality. We envision that in the former sorts of systems, an approach akin to the existing techniques might be developed, while for the latter, perhaps, an entirely new approach will be required.

2. While the touted advantage of a derivation along the lines in [14] is

the demonstrated robustness of the approach, the downside is that the present work sheds no new light on the nature of the critical phenomena. For example, while anticipated that the Cauchy–Riemann equations should become manifest on a mesoscopic scale, at least as far as the authors’ current understanding goes, they appear to obscure with any deviation from the microscopic hexagonal geometry.

3. On a more specific note, the authors find it highly regrettable that a rigid flower arrangement was required. In point of fact, all of the essential results, e.g. color parity of the transmission probabilities, Cauchy–Riemann relations, etc. were established for entirely arbitrary flower arrangement. What could not be done, at least not without additional labor, was the establishment of the standard critical properties of a 2D percolation system. Here, it appears (after all these years) that some significant form of lattice symmetry is still required. Notwithstanding, the authors envision a stochastic version of the current system. For example, the presence or absence of an iris could be governed by a local random variable and the values of  $s$  within the iris may also be random variables. Under some reasonable homogeneity assumptions, such problems might be approached by methods along the lines of the present work.

Finally (and one might presume that this is eminently rectifiable) would be the completion of the preliminary description for the continuum limit of this model by making the connection to  $\text{SLE}_6$ . This topic is under consideration and may very well be the subject of a later paper.

### III.6 Appendix 1: Harris–FKG Properties and Criticality

Here we give a proof of the FKG property needed to prove Corollary III.3.10. We point out that in the strict sense our model does not enjoy positive correlations, as the following example shows:

**Example III.6.1.** Consider a single flower with the petals labeled as in Section III.2.2. Let  $S_{\{4,5\}}$  be the set containing petals 4 and 5 and let  $S_{\{1\}}$  denote the singleton set containing petal 1. Let  $\{S_{\{4,5\}} \leftrightarrow S_{\{1\}}\}$  denote the event of a connection between  $S_{\{4,5\}}$  and  $S_{\{1\}}$ . Then it is claimed:

$$\mathbb{P}(\{S_{\{4,5\}} \leftrightarrow S_{\{1\}}\} \mid S_{\{4,5\}} = S_{\{1\}} = B) < \mathbb{P}(\{S_{\{4,5\}} \leftrightarrow S_{\{1\}}\}). \quad (\text{III.6})$$

Let us start by conditioning on the state of petal 6. The conditional probability given that petal 6 is blue is 1 for both the left hand side and the right hand side of Eq. (III.6), so we might as well consider the case where petal 6 is yellow. Let us start with the unconditioned probability, i.e. the right hand side. It is claimed that, as far as the rest of the petals are concerned, there are three scenarios: predetermined transmission (i.e. a connection without use of the iris), a trigger and other. The relevant conditional probabilities are 1,  $\frac{1}{2}$  and  $a + 2s$ , respectively, with the exception of a single configuration which is in both categories (i) and (ii). The resultant tally is:

$$\mathbb{P}(\{S_{\{4,5\}} \leftrightarrow S_{\{1\}}\} \mid S_{\{6\}} = Y) = 2^{-5} \left[ 5 \cdot \frac{1}{2} + 8 + 19 \cdot (a + 2s) \right]. \quad (\text{III.7})$$

For the conditional probability, we simply calculate all four cases, with the

result:

$$\mathbb{P}(\{S_{\{4,5\}} \leftrightarrow S_{\{1\}}\} \mid \{S_{\{4,5\}} = S_{\{1\}} = B\} \cap \{S_{\{6\}} = Y\}) = \frac{1}{4} \left[ 1 + \frac{1}{2} + 2(a + 2s) \right]. \quad (\text{III.8})$$

By repeated use of the fact that  $2a + 3s = 1$ , it is seen that the right hand side of Eq. (III.7) exceeds the right hand side of Eq. (III.8) whenever  $s > 0$ .

However, for the purposes of proving criticality we in fact only need positive correlations on paths. More precisely, we have

**Lemma III.6.2.** *Let  $\Lambda_{\mathcal{F}}$  denote a flower arrangement and let*

$$A_1, B_1; A_2, B_2; \dots A_n, B_n$$

*denote sets in  $\Lambda_{\mathcal{F}}$  in the complement of irises. Let  $\mathbb{T}_1$  denote the event that  $A_1$  and  $B_1$  are blue and that  $A_1$  is connected to  $B_1$  by a blue path, with similar definitions for  $\mathbb{T}_2, \dots, \mathbb{T}_n$ . Then, under the condition that  $a^2 \geq 2s^2$ , the events  $\mathbb{T}_1, \dots, \mathbb{T}_n$  are all positively correlated, i.e., if  $J \subset \{1, 2, \dots, n\}$  and  $L \subset \{1, 2, \dots, n\}$  then*

$$\mu_{\Lambda_{\mathcal{F}}} \left( \bigcap_{j \in J} \mathbb{T}_j \cap \bigcap_{\ell \in L} \mathbb{T}_\ell \right) \geq \mu_{\Lambda_{\mathcal{F}}} \left( \bigcap_{j \in J} \mathbb{T}_j \right) \mu_{\Lambda_{\mathcal{F}}} \left( \bigcap_{\ell \in L} \mathbb{T}_\ell \right)$$

**Proof:** We consider first the binary case – multiple path cases following an nearly identical argument. Let  $\sigma$  denote a generic configuration of petals and filler and let  $I$  denote a generic configuration of irises. Our first claim is that the function

$$T_j(\sigma) = \mathbb{P}_{\Lambda_{\mathcal{F}}}(\mathbb{T}_j \mid \sigma)$$

is an increasing function of  $\sigma$ . To see this, let  $\sigma$  and  $\sigma \vee \eta$  denote configurations which differ only at the site  $\eta$  – where the latter is blue and the former is yellow.

If  $\eta$  is a filler site the claim is obvious. Similarly, if  $\eta$  is a petal site where the presence/absence of blue does not affect the trigger status of the flower, the result is also trivial. Furthermore, it is also clear that if the path event does not depend on the iris (i.e. if the iris is not a pivotal site for the event  $\mathbb{T}_j$ ) then the raise at  $\eta$  can no deleterious effect on  $\mathbb{T}_j$ . Thus we must only consider situations where the state of  $\eta$  causes or disrupts a trigger and a transmission through the iris is crucial for the event that  $\mathbb{T}_j$  occurs.

First we consider the case where raising at  $\eta$  leads to a triggering situations. In this case, the associated flower must have started with exactly two blue petals. If the two blue petals were already adjacent then it is obvious that the raise at  $\eta$  can only benefit the possibility of the event  $\mathbb{T}_j$ , i.e., assuming the cooperation of the iris, this could complete a connection. Let us consider the case where the blue petals were not adjacent. We must resort to considering the full event  $\mathbb{T}_j$  on the configuration  $\omega = (\sigma, I)$ . We must thus compare the (conditional) probability of a connection between our blue petals of  $\sigma$  (without the trigger) and our three blue petals of  $\sigma \vee \eta$  with the trigger. The latter is  $\frac{1}{2}$  while the former is  $a + s < \frac{1}{2}$ . Now we turn to the case where the raise at  $\eta$  disrupts a trigger. Before the raise, the connection probability is  $\frac{1}{2}$  whereas after the raise, the connection probability is either 1 (because the two relevant sets get connected outside the iris) or, in the two less trivial cases,  $a + 2s > \frac{1}{2}$ . So our first claim is established.

We note that the conditional measure  $\mu_{\Lambda_{\mathcal{F}}}(- \mid \sigma)$  (for whom the only degrees of freedom are represented by the iris configurations) is in fact independent – but not necessarily identically distributed – measure on the irises. In

[6] it was proved that in an analogous circumstance with parameters  $a_i, e_i, s_i$ ,  $i = 1, 2, \dots$ , that provided  $a_i e_i \geq 2s_i^2$  is satisfied for all  $i$ , the corresponding product measure has positive correlations. This is our situation where some  $a_i = e_i = \frac{1}{2}$  and otherwise  $a_i e_i = a^2 \geq 2s^2 = 2s_i^2$  by hypothesis. Since the indicator function of the event  $\mathbb{T}_j$  is manifestly increasing in the iris configurations, we have correlation inequalities for the conditional measure; so

$$\mathbb{E}(\mathbb{T}_j \mathbb{T}_l \mid \sigma) \geq \mathbb{E}(\mathbb{T}_j \mid \sigma) \mathbb{E}(\mathbb{T}_l \mid \sigma) = T_j(\sigma) T_l(\sigma).$$

The desired result follows by taking the expectation over petal/filler configurations and using the Harris–FKG property for independent percolation. The proof for multiple path events as well as a variety of other increasing events follows mutatis mutantis from the argument given.  $\square$

**Remark III.6.3.** With additional labor, it may be possible to remove the  $a^2 \geq 2s^2$  restriction. However, we shall not pursue this avenue since, in any case, we require that  $a \geq \frac{1}{5}$ .

## III.7 Appendix 2: Equivalence of the Cardy–Carleson Functions

In this appendix, we will supply the necessary details to show that the difference between our functions  $u_N^*(z)$ ,  $v_N^*(z)$  and  $w_N^*(z)$  are, for all intents and purposes, equal to the unstarred counterparts. We start with some notation:

**Definition III.7.1.** Let  $B_n$  denote the  $2n \times 2n$  box centered at the origin – that is to say all those hexagons within an  $L^1$  distance  $n$  of the origin – and

$\partial B_n$  the hexagons of  $B_n^c$  with a neighbor in  $B_n$ . While technically we should also specify the location of the origin relative to the flower arrangement, in what is to follow such amendments would only result in the adjustment of a few constants in some of the estimates. We will not pay heed to these matters in the forthcoming definitions and the various later estimates should be understood as the maximum or minimum over a single period of translations.

Let  $\Pi_1(n)$  denote the event that the origin is connected to  $\partial B_n$  by a blue transmission and let  $\pi_1(n)$  denote the corresponding probability. Similarly, we consider multiple disjoint paths of various colors and arrangements which connect the origin to  $\partial B_n$  and we use the subscript to indicate the number of paths with the color and arrangement dependence notationally suppressed. Of importance will be the five-arm event,  $\Pi_5(n)$ , the subject of some discussion in [1],[10] and [11] wherein the origin is connected to  $\partial B_n$  by three blue paths and two yellow paths, with the two yellow paths separated by blues. (In [10], it was proved that the corresponding probability,  $\pi_5(n)$ , has upper and lower bounds of a constant divided by  $n^2$ ; these arguments, at least the upper bounds, are easily adapted to the present circumstances.) Next, if  $m < n$ , we define  $\Pi_1(n, m)$  to be the event of a connection between  $\partial B_m$  and  $\partial B_n$  and we denote the corresponding probability by  $\pi_1(n, m)$ . We adapt similar notations for  $\pi$ -functions involving multiple disjoint connections in the annular region. Finally, we will consider versions of these events with a geometric restriction. Let  $\theta \in [0, 2\pi)$  and consider the ray starting from the origin that makes angle  $\theta$  with the horizontal axis. We define  $\Pi_1^{\mathbb{K},\theta}(n)$ ,  $\Pi_2^{\mathbb{K},\theta}(n)$ ,  $\dots$  to be the event that the appropriate paths occur subject to the constraint that none of the

paths intersect the ray at angle  $\theta$ . We use the same notation with a lower case  $\pi$  to denote the relevant probabilities. Similarly, we define  $\Pi_1^{\mathbb{K},\theta}(n, m), \dots$  and  $\pi_1^{\mathbb{K},\theta}(n, m), \dots$  to denote the modified versions of the above mentioned for the annular regions  $B_n \setminus B_m$ .

We will also bring into play certain events of the type described in the above paragraph that incorporate additional events defined from the space of permissions. These objects will be introduced as necessary.

We begin with the central lemma of this appendix. The proof relies heavily on asymptotic estimates of certain  $\pi$ -functions which will be proved in subsequent lemmas.

**Lemma III.7.2.** *Let  $u_N^*, u_N$  denote the functions as described previously, with domain  $\Lambda$ . Let  $\mathcal{Z}$  denote a point in the interior of  $\Lambda$ ,  $z = N\mathcal{Z}$ . Then,*

$$\lim_{n \rightarrow \infty} |u_N^*(z) - u_N(z)| = 0.$$

*In particular, on closed subsets of  $\Lambda$  that are disjoint from the boundary, the above is uniformly bounded by a constant times an inverse power of  $N$ .*

**Proof:** We claim (c.f. below) that in those configurations in which  $\mathcal{U}_N$  and  $\mathcal{U}_N^*$  differ, a rather drastic event must occur involving multiple arms connected to the boundary and encircling  $z$ . If this event occurs far away from  $z$  and the boundary, then there are many, namely greater than five, long arms emanating from a single point. By the modification of some above mentioned standard results, we can show that the instances of this event in the bulk, i.e. away from the boundary and away from  $z$ , are suppressed. On the other hand, when the path ventures near  $z$  itself, not all of these arms will be long and,

conditionally speaking, such a multi-arm event is not particularly unlikely. However, the latter cases we claim are themselves unlikely; indeed most of the configurations contributing to  $u_N$  or  $u_N^*$  stay well away from  $z$  on the microscopic scale. Finally, for points near the boundary, while there may be fewer long arms to work with, the geometric constraints prove to be sufficient for our purposes. The details are as follows:

Let us first consider the event which is contained in both the starred and unstarred versions of the  $u$ -functions, namely the event of a self-avoiding, non-self-touching path separating  $z$  from  $\mathcal{C}$ , etc. We will denote the indicator function of this event by  $\mathcal{U}_N^-$ . Similarly, let us define an event, whose indicator is  $\mathcal{U}_N^{*+}$ , that contains both the starred and unstarred versions: this is the event that a separating path of the required type exists, with no restrictions on self-touching, and is allowed to share hexagons provided that permissions are granted. It is obvious that

$$\mathbb{E}[\mathcal{U}_N^{*+} - \mathcal{U}_N^-] \geq |u_N^* - u_N|. \quad (\text{III.9})$$

We turn to a description of the configurations, technically on  $(\omega, X)$ , for which  $\mathcal{U}_N^{*+} = 1$  while  $\mathcal{U}_N^- = 0$ . In such a configuration, the only separating paths contain an *essential* lasso point which, we remind the reader, could be either a shared hexagon or a closed encounter pair. For standing notation, we denote this “point” by  $z_0$ . A variety of paths converge at  $z_0$ : certainly there is a blue path from  $\mathcal{A}$ , a blue path to  $\mathcal{B}$ , and an additional loop starting from  $z_0$  (or its immediate vicinity) which contains  $z$  in its interior. However, since the lasso point was deemed to be essential, there can be neither a blue connection between this loop and the portion of the path connecting  $z_0$  to  $\mathcal{A}$  nor a blue

connection between this loop and the portion of the path connecting  $z_0$  to  $\mathcal{B}$ . This implies two additional yellow arms emanating from the immediate vicinity of  $z_0$ . These yellow arms may themselves encircle the blue loop and/or terminate at either the two boundaries  $\mathcal{A}$  and  $\mathcal{B}$ . We remark that, specifying the lasso point under study to be the first (and by the same token the final) such point on the blue journey from  $\mathcal{A}$  to  $\mathcal{B}$ , the paths from the boundaries to  $z_0$  as well as the yellow paths mentioned have no sharings and, without loss of generality, no points of close encounter. While such claims cannot be made about the loop, it is already clear that there are “somewhat more” than five standard arms emanating from the vicinity of  $z_0$ . Turning attention to this blue loop, let us regard this as two separate paths – with possible sharings – each portion of which visits all the essential lasso points; the break between the two paths may be chosen arbitrarily after the final lasso point just prior to the capture of  $z$ . Now we may claim that on the basis of Lemma III.4.3, one of these two paths may be reduced to a self-avoiding and non-self-touching path. Thus, to summarize, there are in fact six paths emanating from  $z_0$ ; a pair of blue paths separated from another pair of blue paths by a pair of yellow paths. One of the blue pairs is completely “normal”. The other blue pair, ostensibly two halves of a loop, will be regarded as one normal path and a second path which has received permissions to share and/or experience close encounters with the first.

Notwithstanding, the blue pair which captures  $z$  along with a surrounding yellow loop cannot *a priori* be ruled as unlikely if  $z_0$  is in the vicinity of  $z$ . To handle such points we let  $0 < \lambda < 1$  denote a number to be specified

momentarily. We now define  $z_0$  to be “near”  $z$  if it is within a box of side  $N^\lambda$  centered at  $z$ . Since  $\mathcal{Z} \in \text{int}(\Lambda)$ ,  $z$  itself is a distance of order  $N$  from the boundary. Such an event would thus require a connection between the boundary of the above mentioned box to the outside of a larger box, also centered at  $z$ , which is the smallest such box that will fit in  $\Lambda$ . This, for  $N$  large enough, is a translation of the event  $\Pi_1(d_{\mathcal{Z}}N, N^\lambda)$  where  $d_{\mathcal{Z}}$  is a constant related to the distance between  $\mathcal{Z}$  and the boundary of the domain measured on the unit scale. By standard arguments employing rings in disjoint annuli (which go back to [7]) we may, on the basis of Theorem III.3.10, show that the probability of such an event is bounded above by a constant times  $(\frac{N^\lambda}{N})^{\vartheta_1}$  for some  $\vartheta_1 > 0$ .

Hence for all intents and purposes, when we examine the configurations where  $\mathcal{U}_N$  and  $\mathcal{U}_N^*$  are purported to differ, we may assume that there is no visit to the near vicinity of  $z$ . (In particular, we certainly need not worry about the fractional values of  $\mathcal{U}_N^*(z)$  when the path goes directly through  $z$ .) Furthermore we will now regard, with only small loss of generality, the expectation in Eq. (V.23) to be taking place in the conditional measure where no path from the boundary visits the near vicinity of  $z$ . It follows that for  $z_0$  located anywhere in  $\Lambda$  a distance further than  $N^\lambda$  from the boundary (and  $z$ ) all of the above mentioned paths emanating from the vicinity of  $z_0$  travel to the outside of a box of side  $N^\lambda$  centered at  $z_0$ . We denote the probability of this modified six–arm event by  $\pi_{6^*}(N^\lambda)$ .

In light of [10], it should come as no surprise that

$$\pi_{6^*}(N^\lambda) \leq \frac{C_{6^*}}{N^{\lambda(2+\vartheta_2)}} \quad (\text{III.10})$$

with  $C_{6^*}$  a number of order unity independent of  $N$  and  $\vartheta_2 > 0$ . In any case, the inequality in Eq.(III.10) is the subject of Lemma III.7.3. Thus, choosing  $\lambda$  close enough to one to ensure that the power in the denominator of the right hand side exceeds two, we may sum over all relevant values of  $z_0$  and thereby dispense with the so-called bulk terms.

This leaves us with the boundary contribution which we divide into two (technically three) types. First there are points which lie near a corner of the domain and then there is the complementary set. Along with the former, we will include the points near the juncture of the  $\mathcal{A}$ - $\mathcal{B}$  boundary i.e. the point  $e_{AB}$ . Since there are only a finite number of these sorts of boundary points and the associated nearby points are handled rather easily, let us define our “vicinity” of these points and dispose of these regions immediately.

We let  $\mu_2$  be a number larger than  $\lambda$  but still smaller than one:  $1 > \mu_2 > \lambda$ , and at each corner, we place a box of side  $N^{\mu_2}$  (with its center at the corner) and another such box at  $e_{AB}$ . If  $z_0$  lies inside one of these boxes, some of the six arms will still be long. In particular, for future reference, concerning the corner points of the  $\mathcal{A}$  boundary or the  $\mathcal{B}$  boundary that are distinct from  $e_{AB}$ , there are at least four long arms. As it turns out, the points near  $e_{AB}$  have two. Regardless of the exact tally, it is clear that, for each such point mentioned, if  $z_0$  is in the associated box, the boundary of this box must be connected a distance of order  $N$  and so the requisite event is contained in a translate of the event  $\Pi_1(kN, N^{\mu_2})$ . Here  $k$  is some constant of order unity independent of  $N$  which can again be related to various distances in unit scale domain. Hence we pick up a finite number of additional terms with the upper

bound of a constant times  $(\frac{N^{\mu_2}}{N})^{\theta_1}$ .

Finally there is the remainder of the points near the boundary: points that are within a distance  $N^\lambda$  of the boundary but further than  $N^{\mu_2}$  from any of the corners or  $e_{AB}$ . By definition, if we place a box of side exceeding  $2N^\lambda$  of any of these points, that box will intersect  $\Lambda^c$ . Thus let us cover this region with partially overlapping boxes of side, say,  $3N^\lambda$  and notice that the number of boxes is of the order  $N^{1-\lambda}$ . Further, it is noted that, on a distance scale of  $N^\lambda$ , all these boxes are well away from all the corners. Thus the boundary region near any particular box is, essentially, a straight edge and there is ample room to draw straight lines in the complement of  $\Lambda$  which start from the boundary of these boxes, are directed towards their centers, and are large compared with  $N^\lambda$  but, perhaps, small compared with  $N$ .

We now take each of the above mentioned boxes and place it at the center of a box of side  $2N^{\mu_1}$ , where  $\mu_2 > \mu_1 > \lambda$ . As indicated above, we can connect the boundaries of these boxes by a straight line which lies in  $\Lambda^c$  and is directed towards their mutual center. If  $z_0$  is inside the inner box, then, as alluded to earlier, there must be four arms which connect the boundary of the inner box to the boundary of the outer box. Two of these four arms are yellow and two of these are blue, with the pair of blue arms between the yellow arms; the yellows and one of the blues are self-avoiding and non-self-touching while the second blue interacts with the first given the requisite permissions. In short, four of the six arms that were dealt with in the context of the bulk contribution. However, clearly these arms are restricted so as not to enter the region  $\Lambda^c$ ; certainly they cannot cross the straight line described in the above paragraph.

The relevant event is therefore  $\Pi_{4^*}^{\mathbb{K},\theta}(N^{\mu_1}, \frac{3}{2}N^\lambda)$ , where  $4^*$  means pretty much what  $6^*$  meant in the earlier context.

The subject of Lemma III.7.5 is that for the usual three arm version of the above event,  $\pi_3^{\mathbb{K},\theta}(n, m)$ , has upper and lower bounds of the form a constant times  $m/n$ , where the constant is uniform in  $\theta$ . Therefore it once again should not be surprising that

$$\pi_{4^*}^{\mathbb{K},\theta}\left(N^{\mu_1}, \frac{3}{2}N^\lambda\right) \leq C_{4^*} \left(\frac{N^\lambda}{N^{\mu_1}}\right)^{1+\vartheta_3}, \quad (\text{III.11})$$

with  $\vartheta_3 > 0$  and  $C_{4^*}$  a constant. The estimate in Eq. (III.11) will be proved as a corollary to Lemma III.7.5.

Summing over all such boxes, the overall remaining contribution is therefore no more than a constant times  $N^{1+\lambda\vartheta_3-\mu_1(1+\vartheta_3)}$ . The above exponent is negative if we choose (first  $\mu_2$  and then)  $\mu_1$  sufficiently close to one. It is not difficult to ascertain that every one of the above estimates are uniform in  $z$  provided that  $z$  remains a fixed distance from the boundary. The lemma is proved.  $\square$

**Lemma III.7.3.** *Consider the event  $\Pi_{6^*}(n)$  as described in the proof of Lemma III.7.2 and let  $\pi_{6^*}(n)$  denote the corresponding probability. Then, for all  $n$ , there is a finite constant  $C_{6^*}$  which does not depend on  $n$ , such that*

$$\pi_{6^*}(n) \leq \frac{C_{6^*}}{n^{2+\vartheta_2}}.$$

**Proof:** We start with some discussions concerning the five-arm event  $\Pi_5(n)$ , which, in the present circumstances, means two yellow paths and three blue paths with the two yellow paths separated. According to the arguments of

Lemma 5 in [10], the probability of a *particular arrangement* of the five arms (certain arms ending up at certain boundaries, etc.) is easily bounded above by a constant times  $n^{-2}$ . This argument goes through intact for the systems under consideration in this work. The crux of the matter is, therefore, to show that with conditional probability of order unity the system will end up in the preferred arrangement. This rather difficult matter was first resolved for the four–arm case in [9] and indeed this resolution was the technical core of that work. Most of the intricate construction consisting of fences, corridors, etc. relies on standard critical properties of 2D percolation models, specifically the second and third items in Theorem III.3.10. We remark that there were numerous points in the derivation where the Harris–FKG inequalities were employed. In essentially all of these cases, Lemma III.6.2 applies directly, as the relevant events always involved paths and connections. A small exception consists of Lemma 3. Here the proof in [9] would go through intact provided that the disjoint regions in question were in fact “flower disjoint”, e.g. in the notation of [9], the sets “ $\mathcal{A}$ ” and “ $\mathcal{E}$ ” must contain no flower in common. These and similar conditions for related sets can be arranged in any number of ways; to be specific, in every square and rectangle on all of the various scales, one may “waste” a buffer zone layer whose thickness consist of at least one unit cell. Needless to say, certain modifications of the four–arm argument must be made for the benefit of five and further arms – here the issue being that in the five arm cases, the colors no longer alternate. These matters were discussed in Section 7 (Appendix to Lemma 5) of [10]. The arguments therein can be applied with almost no modification.

To prove Eq. (III.10) one should, ostensibly, employ some sort of disjoint occurrence argument. Unfortunately the modern versions, e.g. Reimer’s inequality, do not appear to be readily adapted to the current set up, so we must resort to old fashioned methods of conditioning. We claim that in fact  $\pi_{6^*}(n) \leq \pi_5(n)\pi_1(n)$ . Let us label the yellow arms  $Y_1$  and  $Y_2$ , as ordered counterclockwise, with the “loop arms” between them. Calling the “normal” arm of the loop  $B_1$  we envision the second loop arm as lying between  $B_1$  and  $Y_2$ . We now condition on the clockwise–most transmission for the arm  $B_1$  and counterclockwise–most transmission for the arm  $Y_2$ . We denote the region in between by  $\mathcal{R}_{B_1, Y_2}$  and, with apologies, the extreme versions of these paths by  $B_1$  and  $Y_2$ , respectively.

Were it not for the possibility of sharing, our conclusion is immediate. We underscore that there are two forms of sharing involved: the mixed hexagons in  $Y_1$  and the sharings with permission in  $B_1$ . However, in the former case (c.f. the proof of Lemma III.4.7 for non–iris sites), and certainly in the latter case, we need not reveal which hexagons are available for sharing in order to provide the conditioning. The content of Lemma III.3.19 is that any path event, blue or yellow, has a greater probability in an unused flower than in a flower which has some parts conditioned on, notwithstanding that its iris may be available for sharing. It is therefore manifest that in the region  $\mathcal{R}_{B_1, Y_2}$  expanded by all the flowers of  $B_1$  and  $Y_2$ , the probability of an additional blue transmission is, in fact, greater than the requisite transmission which actually has to receive permission (and does not get rejected for illicit close encounters). However the probability in the above stated region is obviously less than  $\pi_1(n)$ ;

summing over all partitions – and using the standard power law bounds on  $\pi_1(n)$  – provides us with the desired result.  $\square$

**Corollary III.7.4.** *Let  $u_N^B(z)$  and  $u_N^Y(z)$  denote the blue and yellow components of the function  $u_N$ . Then for all  $z \in \mathcal{D}$ ,*

$$\lim_{N \rightarrow \infty} |u_N^B(z) - u_N^Y(z)| = 0,$$

*with similar results for  $v$  and  $w$ .*

**Proof:** While ostensibly it would seem that under the auspices of Lemma III.3.6, the equality of  $u_N^B(z)$  and  $u_N^Y(z)$  is a forgone conclusion, it is conceivable that a difference might arise due to the disparity between the geometry of a path designate and the geometry of the transmission which achieves this designation. However, the conditions under which this disparity might emerge are akin to the conditions which were shown to be vanishingly small in Lemma III.7.3. In particular, this might happen if the designate goes directly through  $z$  – which happens to be in a flower, or, more pertinently, the path designate may contain a long loop capturing  $z$  which is achieved by a realization making no use of this essential loop. However, if this is to happen *and* the underlying realization does not achieve the event  $\mathcal{U}_N(z)$ , then we are back to a  $\Pi_{6^*}$ -type event.

To be specific, let  $\mathcal{T}_{u_N^B(z)}$  denote the collection of path designates which may be realized by a path from  $\mathcal{A}$  to  $\mathcal{B}$  separating  $z$  from  $\mathcal{C}$ . By our usual abuse of notation, we also use  $\mathcal{T}_{u_N^B(z)}$  to denote the event that some designate in this set is achieved by a blue transmission. We define a similar quantity for yellow and, as a consequence of the arguments which were used in the proof

of Lemma III.3.6,

$$\mathbb{P}(\mathcal{T}_{u_N^B}(z)) = \mathbb{P}(\mathcal{T}_{u_N^Y}(z)).$$

On the one hand, it is clear that

$$u_N^B(z) \leq \mathbb{P}(\mathcal{T}_{u_N^B}(z)).$$

Now let  $\Xi_N(z)$  denote the complement of the events that were treated in Lemma III.7.3; e.g. no blue path from the boundary visits the near vicinity of  $z$ , no  $\Pi_{6^*}$ -type events, etc. Then, on the other hand, from the above discussion, it is not difficult to see that

$$u_N^B(z) \geq \mathbb{P}(\mathcal{T}_{u_N^B}(z) \mid \Xi_N(z)).$$

The preceding pair of inequalities also hold with  $B$  replaced by  $Y$ . On the basis of the arguments used in the proof of Lemma III.7.3, we have  $\mathbb{P}(\Xi_N(z)) \rightarrow 1$  as  $N \rightarrow \infty$  and the desired result follows.  $\square$

**Lemma III.7.5.** *Consider the events  $\pi_3^{\mathbb{K},\theta}(n, m)$  as described in the proof of Lemma III.7.2 with  $\pi_3^{\mathbb{K},\theta}(n, m)$  the corresponding probability. Then*

$$C'_3 \frac{m}{n} \leq \pi_3^{\mathbb{K},\theta}(n, m) \leq C_3 \frac{m}{n},$$

where  $C_3$  and  $C'_3$  are constants independent of all parameters, including  $\theta$ .

**Remark III.7.6.** While the proof below is tailored to the system at hand, these ideas can obviously be generalized to a variety of critical 2D percolation models.

**Proof:** We first assert that for fixed  $r \in (0, 1)$ , as  $n \rightarrow \infty$ , there exists a  $\phi(r)$  such that

$$\pi_3^{\mathbb{K},\theta}(n) \leq \phi(r) \pi_3^{\mathbb{K},\theta}(rn), \tag{III.12}$$

where the argument of the  $\pi$  on the right-hand side is understood to mean a convenient integer value. This can be established by making use of Kesten's fences ([9]); however with only three arms it is not terribly difficult to construct an argument directly.

Now consider the box  $B_n$  with a line segment at angle  $\theta$  cutting through the center of the box. Let us assume for simplicity that the segment touches only two boundaries; one of these boundaries we will denote by  $\mathbf{c}$  and the rest of the boundary will be split into two parts by the ray, and we denote these parts by  $\mathbf{a}$  and  $\mathbf{b}$ . We parametrize the line segment by  $\lambda$ , where  $\lambda = 0$  corresponds to the joining of the  $\mathbf{a}$  and  $\mathbf{b}$  boundaries and  $\lambda = 1$  corresponds to the  $\mathbf{c}$  boundary. Furthermore, we discretize the parametrization:  $\lambda \in (\lambda_1, \dots, \lambda_k)$  so that the portion of the line segment corresponding to  $\lambda_{j+1}$  contains one more hexagon than the the portion corresponding to  $\lambda_j$ . We now define the event

$$\mathbb{F}(\lambda) = \{\omega \mid \exists \text{ blue transmit from } \mathbf{a} \text{ to } \mathbf{b} \text{ which does} \\ \text{not cross the portion of the line segment} \\ \text{corresponding to parameter values in } [0, \lambda]\},$$

and we further define

$$f(\lambda) = \mathbb{P}(\mathbb{F}(\lambda)).$$

It is obvious that  $f$  is monotone non-increasing in  $\lambda$ . In fact, it is readily established that  $f$  is *strictly* decreasing since if  $1 > \lambda' > \lambda > 0$ , it is possible, using corridors, to produce configurations of uniformly positive probability for which the  $\mathbb{F}(\lambda)$  occurs while the event  $\mathbb{F}(\lambda')$  does not. We next observe that any  $\omega \in \mathbb{F}(\lambda_{j-1}) \setminus \mathbb{F}(\lambda_j)$  for all intents and purposes lies in the restricted three-arm event in question. In particular, in light of Eq. (III.12) and another

relocation of arms argument, for  $\lambda_j$  not too close to zero or one,

$$L_3 \pi_3^{\mathbb{K}, \theta}(n) \leq f(\lambda_{j-1}) - f(\lambda_j) \leq K_3 \pi_3^{\mathbb{K}, \theta}(n),$$

where  $K_3$  and  $L_3$  maybe regarded as independent of  $\lambda$  for, say,  $\lambda \in (\frac{1}{4}, \frac{3}{4})$ .

Summing up over the values of  $\lambda$  in the above specified range, we learn that  $\pi_3^{\mathbb{K}, \theta}(n)$  has upper and lower bounds of a constant times  $n^{-1}$ .

To obtain the full stated result, we note that, clearly,

$$\pi_3^{\mathbb{K}, \theta}(n) \leq \pi_3^{\mathbb{K}, \theta}(m) \cdot \pi_3^{\mathbb{K}, \theta}(n, m).$$

However, invoking the techniques of [9], this may be supplement with a bound of the opposite type augmented by constants, which establishes the desired result.  $\square$

**Corollary III.7.7.** *Consider the function  $\pi_{4^*}^{\mathbb{K}, \theta}(n, m)$  as described in the proof of Lemma III.7.2, then*

$$\pi_{4^*}^{\mathbb{K}, \theta}(n, m) \leq c_{4^*} \left( \frac{m}{n} \right)^{1+\vartheta_3},$$

for some  $\vartheta_3 > 0$ .

**Proof:** We use the result of Lemma III.7.5 in conjunction with a conditioning argument of the sort used in the proof of Lemma III.7.3 to obtain this result.  $\square$

# Bibliography

- [1] M. Aizenman. *The Geometry of Critical Percolation and Conformal Invariance*. In STATPHYS 19 (Xiamen, 1995), 104–120. World Sci. Publishing, River Edge, NJ, 1996.
- [2] F. Camia and C. M. Newman. *The Full Scaling Limit of Two-Dimensional Critical Percolation*. Available at <http://front.math.ucdavis.edu/math.PR/0504036>.
- [3] F. Camia, C. M. Newman and V. Sidoravicius. *Cardy's Formula for Some Dependent Percolation Models*. Bull. Braz. Math. Soc. (N. S.), **33**, 147-156 (2002).
- [4] F. Camia, C. M. Newman and V. Sidoravicius. *A Particular Bit of Universality: Scaling Limits of Some Dependent Percolation Models*. Comm. Math. Phys. **246**, 311-332 (2004).
- [5] J. L. Cardy. *Critical Percolation in Finite Geometries*. J. Phys. A, **25**, L201–L206 (1992).
- [6] L. Chayes and H. K. Lei. *Random Cluster Models on the Triangular Lattice*. Journal of Statistical Physics **122**, no. 4, 647–670 (2006).

- [7] T. E. Harris. *A Lower Bound for the Critical Probability in a Certain Percolation Process*. Proceedings of the Cambridge Philosophical Society **56**, 13–20 (1960).
- [8] H. Kesten. *Percolation Theory for Mathematicians*. Boston, Basel, Stuttgart: Birkhauser (1982).
- [9] H. Kesten. *Scaling Relations for 2D-Percolation*. Comm. Math. Phys. **109**, 109–156 (1987).
- [10] H. Kesten, V. Sidoravicius and Y. Zhang. *Almost All Words are Seen in Critical Site Percolation on the Triangular Lattice*. Electronic Journal of Probability, **3** (10), 1-75 (1998).
- [11] G. Lawler, O. Schramm and W. Werner. *One-Arm Exponent for Critical 2D Percolation*. Electronic Journal of Probability, **7** 13 pages (electronic) (2002).
- [12] L. Russo. *A Note on Percolation*. Z. Wahrscheinlichkeitstheorie und Verw. Gebiete **43** no. 1, 39-48 (1978).
- [13] P. D. Seymour, D. J. A. Welsh. *Percolation Probabilities on the Square Lattice*. Advances in Graph Theory (B. Bollobas, ed.), Annals of Discrete Mathematics 3, North-Holland, Amsterdam, 227-245 (1978).
- [14] S. Smirnov. *Critical Percolation in the Plane: Conformal Invariance, Cardy's Formula, Scaling Limits*. C. R. Acad. Sci. Paris Sr. I Math. **333**, 239-244 (2001).

Also available at <http://www.math.kth.se/stas/papers/index.html>.

- [15] S. Smirnov. Public Communication.
- [16] S. Smirnov and W. Werner. *Critical Exponents For Two-Dimensional Percolation*. Mathematical Research Letters **8**, 729-744 (2001).
- [17] W. Werner. *Critical Exponents, Conformal Invariance and Planar Brownian Motion, 2000*. Proceedings of the 3<sup>rd</sup> Europ. Congress of mathematics, Birkhauser.

# Chapter IV

## Discrete Approximations and Extraction of Cardy's Formula for General Domains

**Abstract:** Following the approach outlined in [26], convergence to  $\text{SLE}_6$  of the Exploration Processes for the correlated bond-triangular type models studied in [11] is established in [3] and the present work. In this installment, we focus on establishing Cardy's Formula for general domains.

**Keywords:** Universality, conformal invariance, percolation, Cardy's Formula.

## IV.1 Introduction

In this note we wish to establish the validity of Cardy’s Formula for crossing probabilities in a general (finite) domain  $\Omega \subset \mathbb{C}$ , clarifying certain notions concerning discretization and extraction of appropriate boundary values. While these issues have been addressed to various extents in e.g., [13], [14], [9], [6], [23], and may seem quite self-evident – at least for nice (i.e., Jordan) domains, a complete and unified treatment for general domains appears to be absent. Moreover, aside from æsthetic appeal, the generality that appears here is certainly needed for the approach of proving convergence to  $\text{SLE}_6$  outlined in [26] (see also [14]) and carried out in [3]. Our efforts will culminate in the establishment of Theorem IV.5.7 and Corollary IV.5.10 (which is stated in [3] as Lemma 2.6).

Since it is our intention that this note be self-contained, let us first review the methodology – introduced in [13] and adapted to the models in [11] (see also [3], §4.1) – by which Cardy’s Formula can be extracted. At the level of the continuum we are interested in a domain  $\Omega \subset \mathbb{C}$  which is a conformal triangle with boundary components  $\{\mathcal{A}, \mathcal{B}, \mathcal{C}\}$  and marked prime ends (boundary points)  $\{a, b, c\}$  – all in counterclockwise order – which represent the intersection of neighboring components. At the level of the lattice, at spacing  $\varepsilon$ , we consider an approximate domain  $\Omega_\varepsilon$ , in which the percolation process occurs and which tends – in some sense – to  $\Omega$  as  $\varepsilon \rightarrow 0$ . At the  $\varepsilon$ -scale, the competing (dual) percolative forces will be denoted, as is traditional, by “yellow” and “blue”.

Let  $z$  be an interior point (e.g., a vertex) in  $\Omega_\varepsilon$ . We define the discrete

crossing probability function  $u_\varepsilon^B(z)$  to be probability that there is a blue path connecting  $\mathcal{A}$  and  $\mathcal{B}$ , separating  $z$  from  $\mathcal{C}$ , with similar definitions for  $v_\varepsilon^B(z)$  and  $w_\varepsilon^B(z)$  along with yellow versions of these functions. For these objects, standard arguments show that subsequential limits exist; two seminal ingredients are required: First, they converge to harmonic functions with a particular conjugacy relation between them in the interior and second they satisfy certain (“obvious”) boundary values. With these ingredients in hand it can be shown that the limiting functions are the so called Carleson–Cardy functions. E.g.,

$$\lim_{\varepsilon \rightarrow 0} u_\varepsilon^Y = u,$$

and similarly for the  $v$ ’s and  $w$ ’s where, e.g., according to [4], the functions  $u, v, w$  are such that

$$F := u + e^{2\pi i/3}v + e^{-2\pi i/3}w$$

is the unique conformal map from  $\Omega$  to the equilateral triangle formed by the vertices  $1, e^{\pm 2\pi i/3}$ . This is equivalent to Cardy’s formula.

We enable this program for a general class of domains *and* their discrete approximations which is suitable for our uses in [3], Lemma 2.6/Corollary IV.5.10.

**Remark.** *The appropriate discrete conjugacy relations for the  $u_\varepsilon, v_\varepsilon$  and  $w_\varepsilon$  have only been established for the models in [13] and [11]. However, since the RSW estimates are purportedly universal and actually hold for any reasonable critical 2D percolation model, in principle we always have limiting functions  $u, v, w$  with some boundary values. Hence most of the content of the present*

*work should apply. However, certain provisos and clarifications will be required; see Remark IV.5.6.*

In the ensuing arguments we will have many occasion to make use of the uniformization map  $\varphi : \mathbb{D} \rightarrow \Omega$  (where  $\mathbb{D}$  denotes the unit disk) normalized so that say  $\varphi(0) = z_0 \in \Omega$  for some point  $z_0$  well in the interior of  $\Omega$  and  $\varphi'(0) > 0$ . We will also identify points on  $\partial\mathbb{D}$  with boundary prime ends of  $\partial\Omega$ , via the Prime End Theorem. We refer the reader to e.g., [22] for such issues. Finally, the reader may wish to keep in mind that the reason for addressing most of the issues herein is for application to the case where the curves/slits under consideration are percolation interfaces/explorer paths; for discussions on this topic we refer the reader to [3].

## IV.2 The Carathéodory Minimum

We start by dissecting the well-known Carathéodory convergence, mainly to phrase it in terms of more elementary conditions more suitable for our purposes. The reader can find similar conditions/discussions in e.g., Section 1.4 of [22].

Our general situation concerns a sequence of domains  $(\Omega_n)$  which converge in some sense to the limiting  $\Omega$  along with functions  $(u_n, v_n, w_n)$  converging to a harmonic triple  $(u, v, w)$  satisfying the appropriate conjugacy relations. As a minimal starting point let us consider the following pointwise (geo)metric conditions for domain convergence:

( $i_I$ ) If  $z \in \Omega$ , then  $z \in \Omega_n$  for all  $n$  sufficiently large.

(*i<sub>II</sub>*) If  $z_n \in \Omega_n^c$ , then all subsequential limits of  $(z_n)$  must lie in  $\Omega^c$ .

(*e*) For all  $z \in \Omega^c$  (including, especially  $\partial\Omega$ ) there exists some sequence

$$z_{n_k} \in \Omega_{n_k}^c \text{ such that } z_{n_k} \rightarrow z.$$

Conditions (*i<sub>I</sub>*) and (*i<sub>II</sub>*) ensure that limiting values of  $u$ ,  $v$  and  $w$  in (the interior of)  $\Omega$  can be retrieved and are defined by values of  $u_n$  inside  $\Omega_n$  whereas condition (*e*) implies that  $\Omega_n$ 's don't converge to a domain strictly larger than  $\Omega$ , so that the boundary values of  $u$  on  $\partial\Omega$  might actually correspond to (the limit of) boundary values of  $u_n$  on  $\Omega_n$ . Indeed, these preliminary conditions turn out to be equivalent to Carathéodory convergence (see e.g., [12]; although in our context we will actually not have occasion to use convergence of the relevant uniformization maps). More precisely, first we have the following result, whose proof is elementary (and we include for completeness):

**Proposition IV.2.1.** *Consider domains  $\Omega_n, \Omega \subset \mathbb{C}$  all containing some point  $z_0$ . Then the following are equivalent:*

1. *If  $K$  is compact and  $K \subset \Omega$ , then  $K \subset \Omega_n$  for all but finitely many  $\Omega_n$ .*

2. (*i<sub>I</sub>*) *For all  $z \in \Omega$ ,  $z \in \Omega_n$  for all but finitely many  $\Omega_n$ .*

(*i<sub>II</sub>*) *If  $z_n \in \Omega_n^c$ , then all subsequential limits of  $(z_n)$  must lie in  $\Omega^c$ .*

3. *If  $z \in \Omega$ , and  $\delta < d(z, \partial\Omega)$ , then  $B_\delta(z) \subset \Omega_n$ , for all but finitely many  $\Omega_n$ .*

*Proof.* 1  $\Rightarrow$  2) To see (*i<sub>I</sub>*) suppose  $z \in \Omega$  and  $d(z, \partial\Omega) > \delta$ , then  $\overline{B_\delta(z)} \subset \Omega$  and is compact and hence we have  $\overline{B_\delta(z)} \subset \Omega_n$  for all  $n$  sufficiently large and hence

$z \in \Omega_n$  for all  $n$  sufficiently large; conversely, To see (i<sub>II</sub>), suppose  $z_n \rightarrow z$  with  $z_n \in \Omega_n^c$  and suppose towards a contradiction that  $z \in \Omega$ . Then again arguing as before,  $\overline{B_\delta(z)} \subset \Omega_n$  for  $n$  sufficiently large, but then  $z_n \in B_\delta(z)$  also for  $n$  even larger, which implies that these  $z_n \in \Omega_n$ , a contradiction.

2  $\Rightarrow$  3) Again suppose  $d(z, \partial\Omega) > \delta$  so that  $\overline{B_\delta(z)} \subset \Omega$ . If it is not the case that  $B_\delta(z) \subset \Omega_n$  for  $n$  sufficiently large, then we can find a sequence  $z_n \in B_\delta(z) \cap \Omega_n^c$ . Since  $\overline{B_\delta(z)}$  is compact, there exists a subsequential limit point  $z_{n_k} \rightarrow z_*$ , but then by (i<sub>II</sub>),  $z_* \notin \Omega$ , contradicting  $\overline{B_\delta(z)} \subset \Omega$ .

3  $\Rightarrow$  1) Let  $K \subset \Omega$  be compact. We can cover  $K$  by  $K \subset \bigcup_{x \in K} B_{\delta_x}(x)$ , with  $\delta_x < d(x, \partial\Omega)$ . By the assumed compactness, there is a finite subcover  $K \subset \bigcup_{i=1}^k B_{\delta_{x_i}}(x_i)$ . By 3), for  $1 \leq i \leq k$ , there exists  $N_i$  such that  $B_{\delta_{x_i}}(x_i) \subset \Omega_n$  for all  $n \geq N_i$ , and hence it is the case that  $K \subset \Omega_m$  for all  $m > \max\{N_1, N_2, \dots, N_k\}$ .  $\square$

Now the notion of *kernel convergence* – which in our setting of bounded, simply connected domains is, by the theorem of Carathéodory equivalent to Carathéodory convergence, i.e., convergence uniformly on compact sets of the corresponding uniformization maps (see e.g., [12], Theorem 3.1) – requires, in addition (specifically to condition 1 in the above Proposition), that  $\Omega$  is the *largest* (simply connected) domain satisfying the above conditions. The addition of condition (e) indeed correspond to maximality; arguments similar to those just presented easily lead to the following (whose proof is elementary and is also included for completeness):

**Proposition IV.2.2.** *The conditions (i<sub>I</sub>), (i<sub>II</sub>), (e) are equivalent to  $\Omega_n$  converging to  $\Omega$  in the sense of kernel convergence.*

*Proof.* In light of the above discussion, it is sufficient to show that the condition (e) is equivalent to the maximality condition on  $\Omega$  required by kernel convergence.

$\Rightarrow$ ) Suppose  $\Omega$  is not maximal and hence  $\Omega \subsetneq \Omega'$  where  $\Omega'$  satisfies (i<sub>I</sub>) and (i<sub>II</sub>). It must be the case then there is a point  $z \in \partial\Omega \cap \Omega'$ . By condition (e) there exists  $z_{n_k} \rightarrow z$  with  $z_{n_k} \in \Omega_{n_k}^c$ , but condition (i<sub>II</sub>) for  $\Omega'$  implies that  $z \in (\Omega')^c$ , a contradiction.

$\Leftarrow$ ) Conversely, suppose  $\Omega$  is maximal and assume towards a contradiction that  $\Omega$  does not satisfy (e), so that there exists some point  $z \in \Omega^c$  and some  $\delta > 0$  such that  $B_\delta(z) \subset \Omega_n$  for all  $n$  sufficiently large. By the maximality of  $\Omega$ , it must be the case that  $\overline{B_\eta(z)} \subset \Omega$  for any  $\eta < \delta$ , which implies in particular that  $z \in \Omega$ , a contradiction.  $\square$

As is perhaps already clear, Carathéodory convergence is insufficient for our purposes: Since the functions  $u, v, w$  must acquire prescribed boundary values on separate pieces of  $\partial\Omega$ , it is manifest that (some notion of) separate convergence of the corresponding pieces of the boundary in  $\partial\Omega_n$  will be required. Special attention is needed for the cases of domains with slits – which are of seminal importance when we consider the problem of convergence to  $\text{SLE}_\kappa$ . The situation is in fact rather subtle: Note that in both Figure IV.1 and Figure IV.3, we have that  $\Omega_\varepsilon$  Carathéodory converges to  $\Omega$ , but whereas the situation in Figure IV.1 disrupts establishment of the proper boundary value, the situation in Figure IV.3 is perfectly acceptable (see Remarks IV.3.2 and IV.4.3).

### IV.3 Interior Approximations

We will begin by considering the *interior* approximations, where  $\Omega_\varepsilon \subset \Omega$  for all  $\varepsilon$ . For earlier considerations along these lines, see [8] and [10]. Here, the crucial advantage is that all domains can be viewed under a *single* uniformization map; this allows for relatively simple resolution of all concerns of a geometric/topological nature. Moreover, this appears to be the simplest setting for the purposes of establishing Cardy's Formula in a fixed (static) domain (see especially Example IV.3.3 below). In particular, for circumstances where this is all that is of interest, the reader is invited to skip the next section altogether.

We start with

**Definition IV.3.1** (Interior Approximations). We call  $(\Omega_\varepsilon^\bullet)$  an *interior approximation* to  $\Omega$  if:

(I) The domains  $\Omega_\varepsilon^\bullet$  consist of one or more (graph) connected components, each of which is bounded by a closed polygonal path, and the union of all such polygonal paths we identify as the boundary  $\partial\Omega_\varepsilon^\bullet$ . In particular,  $\partial\Omega_\varepsilon^\bullet$  consists exclusively of polygonal edges each of which is a portion of the border of an element in  $(\Omega_\varepsilon^\bullet)^c$ .

(II) The boundary  $\partial\Omega_\varepsilon^\bullet$  is divided disjoint segments, denoted by  $\mathcal{A}_\varepsilon, \mathcal{B}_\varepsilon, \dots$  in (rough) correspondence with the (finitely many) boundary components  $\mathcal{A}, \mathcal{B}, \dots$  of the actual domain  $\Omega$ . In case  $\Omega_\varepsilon$  is a single component, these are joined at vertices  $a_\varepsilon, b_\varepsilon, \dots$  corresponding to the appropriate marked prime ends. In the multi-component case, if necessary, a similar procedure may be implemented, implying the possible existence of several  $a_\varepsilon$ 's etc. When re-

quired, *the*  $a_\varepsilon, b_\varepsilon, \dots$ , etc., will be the one corresponding to the “principal” component of  $\Omega_\varepsilon$ , namely, the component which contains the point  $z_0$ , which, we recall, served to normalize the uniformization map. Here it is tacitly assumed that  $\varepsilon$  is small enough so that this component has a representative of each type.

Further, we require the following:

(i) It is always the case that  $\Omega_\varepsilon^\bullet \cup \partial\Omega_\varepsilon^\bullet \subset \Omega$ . That is,  $\Omega_\varepsilon^\bullet$  is in fact a *strictly* inner approximation.

This property ensures that indeed all of  $\bar{\Omega}_\varepsilon$  can be viewed under the (single) conformal map  $\varphi : \mathbb{D} \rightarrow \Omega$  in the ensuing arguments.

(ii) Each  $z \in \Omega$  lies in  $\Omega_\varepsilon^\bullet$  for all  $\varepsilon$  sufficiently small.

It can be seen that conditions (i) and (ii) imply that for any  $z \in \partial\mathcal{A}$ , there exists some sequence  $z_\varepsilon \rightarrow z$  with  $z_\varepsilon \in \mathcal{A}_\varepsilon$ , and similarly for  $\mathcal{B}$ , etc.

(iii) Given any sequence  $(z_\varepsilon)$  with  $z_\varepsilon \in \mathcal{A}_\varepsilon$  for all  $\varepsilon$ , any subsequential limit must lie in  $\mathcal{A}$ . Moreover, this must be true in the stronger sense that for any subsequential limit  $\varphi^{-1}(z_{\varepsilon_n}) \rightarrow \zeta \in \partial\mathbb{D}$  then  $\zeta \in \varphi^{-1}(\mathcal{A})$ . Similarly for  $\mathcal{B}$ , etc.

In particular, any subsequential limit of the  $(a_\varepsilon)$ 's will converge to a point in  $a$ , and similarly for  $b$ , etc.

**Remark IV.3.2.**

- To avoid confusion, by the above method, an interior approximation to any slit domain – no matter how smooth the slit – necessarily consist of at least a small cavity of a few lattice spacings. It is noted that the explorer

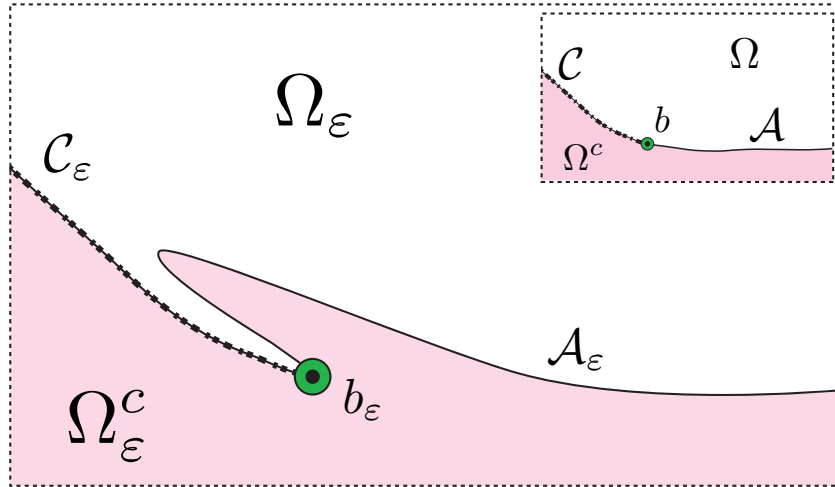


Figure IV.1: Violation of condition ii) in Definition IV.3.1, which would lead to incorrect (limiting) boundary values.

process itself produces just such a cavity.

- It is easy to check that interior approximations satisfy conditions  $(i_I)$ ,  $(i_{II})$ ,  $(e)$ .

- Condition (iii) is indeed used to ensure that the limiting boundary values are unambiguous and correspond to the desired result (see Lemma IV.5.2). A simple scenario where careless approximation leads to the wrong boundary value is illustrated in Figure IV.1.

- Note that even though for convenience we have assumed in (iii) that  $z_\varepsilon \in \mathcal{C}_\varepsilon$  and have used the uniformization map  $\varphi$ , what is sufficient is that if  $z_k \rightarrow z \in \mathcal{C}$ , then for all but finitely many  $k$ ,  $z_k$  should be close to  $\mathcal{C}_\varepsilon$ , in some appropriate sense. Indeed, we shall have occasion to formulate such a definition later, for the statement of Lemma IV.4.4.

**Example IV.3.3.** An example of an interior approximation is what we will call the *canonical approximation*, constructed as follows. To be definitive, consider a tiling problem with finitely many types of tiles. We formally define

the scale  $\varepsilon$  to be the maximum diameter of any tile. As usual, we may regard all of  $\mathbb{C}$  as having been tiled – “ $\mathbb{C}_\varepsilon$ ”. The domain  $\Omega_\varepsilon$  is defined as precisely those tiles in  $\mathbb{C}_\varepsilon$  which are entirely (including their boundary) in  $\Omega$ . Clearly then this construction satisfies (i); condition (ii) is also satisfied: if  $z \in \Omega$  is such that  $d(z, \partial\Omega) > \varepsilon_0$ , then  $z \in \Omega_\varepsilon$  for all  $\varepsilon < \varepsilon_0$ .

At this stage  $\partial\Omega_\varepsilon$  is just one or more closed polygonal paths. The boundary component types are determined as follows: For the marked points, e.g.,  $a$ , consider the neighborhood  $Q_\delta(a)$  defined as follows: Let  $\mathbf{c}_\varepsilon$  denote a sequence of crosscuts of  $\varphi^{-1}(a)$  with the property that  $\varphi(\mathbf{c}_\varepsilon)$  contains a  $\delta$  neighborhood of  $a$  with  $\delta/\varepsilon \rightarrow \infty$  and  $\delta(\varepsilon) \rightarrow 0$ ;  $Q_\delta(a)$  is then the set bounded by  $\varphi(\mathbf{c}_\varepsilon)$  and the relevant portion of  $\partial\Omega$ . It is clear, for  $\varepsilon$  small, that “outside” these neighborhoods, the assignment of boundary component type is unambiguous. Here we say a boundary segment is “outside”  $Q_\delta(a)$  etc., if all tiles (intersecting  $\Omega$ ) touching the segment in question lie in the complement of  $Q_\delta(a)$ . Indeed, each segment of  $\partial\Omega_\varepsilon$  belongs to a tile that intersects the boundary. For a fixed element of  $\partial\Omega_\varepsilon$  satisfying the above definition of “outside”, *some* of the external tile is in  $\Omega$  and therefore under  $\varphi^{-1}$ , the image of this portion of the tile joins up with  $\partial\mathbb{D}$ ; furthermore, it joins with a unique boundary component image due to the size of the obstruction provided by  $Q_\delta(a)$ . Finally, inside these neighborhoods  $Q_\delta(a)$ , etc., all that must be specified are the points  $a_\varepsilon$ , etc., which as discussed above, may have multiple designations (due to the possibility of multiple components for  $\Omega_\varepsilon$ ). The rest of the boundary is then assigned accordingly.

Finally, let us establish (iii):

**Claim IV.3.4.** *The canonical approximation satisfies (iii).*

*Proof.* Let  $z_\varepsilon \in \mathcal{A}_\varepsilon$  with some subsequential limit  $z$ . It is clear that  $z \notin \Omega$  since all  $z \in \Omega$  are a finite distance from the boundary while  $d(z_\varepsilon, \partial\Omega) \leq \varepsilon$  by construction. Moreover,  $z \in \mathcal{A}$  since  $d(z_\varepsilon, \mathcal{A})$  is (generally less than  $\varepsilon$  but certainly) no larger than  $\delta(\varepsilon)$ . It remains to show the stronger statement that any subsequential limit of  $\varphi^{-1}(z_\varepsilon)$  is in  $\varphi^{-1}(\mathcal{A})$ . If  $\zeta_\varepsilon = \varphi^{-1}(z_\varepsilon)$  converges to the image of a *marked* point in  $\varphi^{-1}(\mathcal{A})$  there is nothing to prove. Thus we may assume that, eventually,  $\zeta_\varepsilon$  is outside any  $\kappa$ -neighborhood of the marked points  $\alpha_1, \alpha_2 \in \varphi^{-1}(\mathcal{A})$  for some  $\kappa$ . Now let  $\eta < \kappa$  such that the  $\eta$  neighborhood of  $\partial\mathbb{D} \setminus [B_\kappa(\alpha_1) \cup B_\kappa(\alpha_2)]$  consist of two disjoint components, one containing all of the rest of  $\varphi^{-1}(\mathcal{A})$  and the other associated with  $\varphi^{-1}(\partial\Omega \setminus \mathcal{A})$ . Finally consider the neighborhood (here  $\mathcal{N}_\eta(\cdot)$  denotes the Euclidean  $\eta$  neighborhood of  $(\cdot)$ )

$$M_\eta := \mathcal{N}_\eta(\mathcal{A}) \cap \varphi[\mathcal{N}_\eta(\varphi^{-1}(\mathcal{A}))].$$

Since it is agreed that  $z_\varepsilon$  stays outside  $\varphi(B_\kappa(\alpha_1) \cup B_\kappa(\alpha_2))$  it is clear that, for all  $\varepsilon$  sufficiently small,  $z_\varepsilon \in M_\eta$  and therefore  $\zeta_\varepsilon \in \mathcal{N}_\eta(\varphi^{-1}(\mathcal{A})) \setminus [B_\kappa(\alpha_1) \cup B_\kappa(\alpha_2)]$  and not in the complementary  $\eta$  band described above. It follows that the limit must be in  $\varphi^{-1}(\mathcal{A})$ .

□

## IV.4 Sup-Approximations

Unfortunately, for various purposes, e.g., certain proofs of convergence to  $\text{SLE}_6$ , we will need slightly more generality than the internal approximations as provided in Definition IV.3.1. Specifically, we shall have to consider slit

domains where (in a certain sense) the slit is evolving dynamically and where, at the  $\varepsilon$ -level, the slit is determined stochastically. In particular, we are not at liberty to approximate the domains in the most convenient fashion; more generality will be required.

Here, informally, we will describe the two additional properties which are essential in this context:

- Actual sup-norm convergence of separate sides of the slits (which in the discrete approximations may well be separate curves): This is to prevent the masking of one boundary value by another near the joining of boundaries.
- The *well-organization* property: This is to prevent confusion of boundary values that could be caused by intermingling (crisscrossing) of the two curves approximating the opposite sides of the slit.

Scenarios in violation of these properties are depicted in Figure IV.2.

**Remark IV.4.1.** If  $\gamma_1$  and  $\gamma_2$  are two curves, then as usual the sup distance between them is given as

$$\text{dist}(\gamma_1, \gamma_2) = \inf_{\varphi_1, \varphi_2} \sup_t |\gamma_1(\varphi_1(t)) - \gamma_2(\varphi_2(t))|.$$

For certain purposes, it is pertinent to consider weighting the sup-norms of portions of the curves in accord with the particular crosscut in which the portion resides. We will denote the associated distance by **Dist**; see [3], §3.2 for the definition and discussions. However, our ensuing arguments will not be sensitive as to whether we are using the original sup-norm or the weighted version and thus we will continue to use the sup-norm.

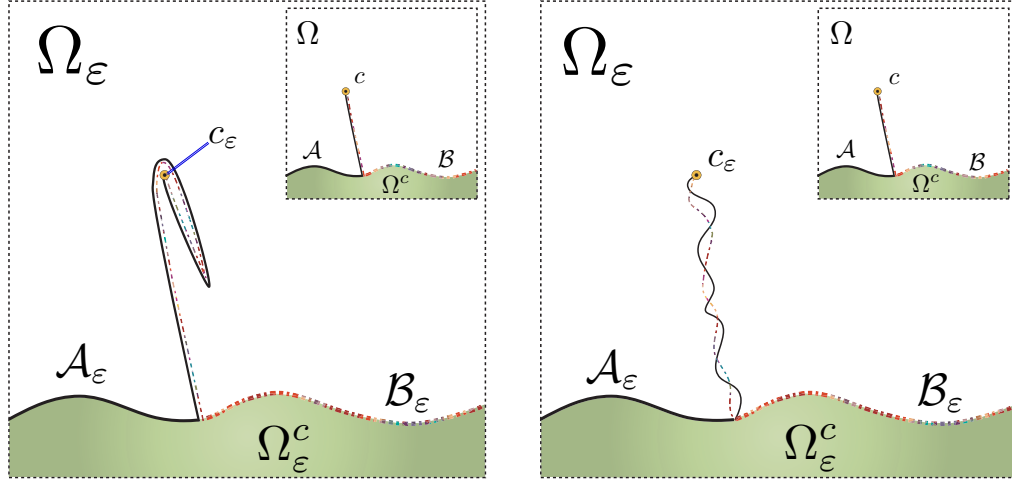


Figure IV.2: Masking and intermixing of boundary values.

**Definition IV.4.2** (Sup-approximations). Suppose  $\partial\Omega$  can be further divided (perhaps by other marked boundary points) with the boundary between *these* points described by Jordan arcs or, more generally, Löwner curves. We shall label the new points  $J_1, J_2$ , etc. and between certain pairs, e.g.,  $J_k$  &  $J_{k+1}$  will be a Löwner curve denoted by  $[J_k, J_{k+1}]$ . The marked prime ends  $a, b, \dots$  may serve as an endpoints of (some of) these segments, but it is understood that they do not reside *inside* these arcs.

Some of this curve (often enough all of it) will be part of the boundary  $\partial\Omega$ . (On the other hand, it can be envisioned that a portion of this curve lives in a “swallowed” region and is part of  $\Omega^c$ .) At the discrete level, we recall that  $\partial\Omega_\varepsilon$  is automatically a union of closed self-avoiding curves. It will be supposed that  $\Omega_\varepsilon$  has corresponding  $J_1^\varepsilon, J_2^\varepsilon, \dots$  and the relevant portion of the curve between the relevant  $J$ -pair converges in sup-norm to the corresponding portions in  $\partial\Omega$  – or  $\Omega^c$ , as the case may be – at rate  $\eta(\varepsilon)$ .

We assume that all of this transpires in such a way that the following property, which we call *well organized*, holds: For any curve of interest  $[J_k^\varepsilon, J_{k+1}^\varepsilon]$ ,

pick points  $p$  and  $p'$  on this arc. Consider  $\delta$ -neighborhoods around  $p$  and  $p'$  and consider the portion of the arc joining these neighborhoods (last exit from neighborhood around  $p$  to first entrance to neighborhood around  $p'$ ), which we label  $\mathcal{L}$ . Let  $\mathcal{P}$  be any path connecting the boundaries of these neighborhoods to one another in the complement of all  $\partial\Omega_\varepsilon$ . Then the relevant portions of the  $\partial B_\delta(p)$ ,  $\partial B_\delta(p')$ ,  $\mathcal{P}$  and  $\mathcal{L}$  clearly form a Jordan domain, whose interior we denote by  $\mathcal{O}$ . Let  $\mathcal{O}' \subset \mathcal{O}$  denote the connected component of  $\mathcal{P}$  in  $\overline{\mathcal{O}} \setminus \partial\Omega_\varepsilon$ . Then,  $\partial\mathcal{O}' \cap \partial\Omega_\varepsilon$  is *monochrome*, i.e., it cannot intersect both  $[J_k^\varepsilon, J_{k+1}^\varepsilon]$  and  $[J_\ell^\varepsilon, J_{\ell+1}^\varepsilon]$  for  $k \neq \ell$ . While this may sound overly complicated, what we have in mind is actually a simple topological criterion, c.f., Remark IV.4.3.

The rest of the domain and boundary is approximated by interior approximation. Thus, for those  $J_k$ 's which divide arc-portions of  $\partial\Omega$  from "other", we require *commensurability* at the joining points. In particular, in order that the interior approximation be implementable, it is clear that we must require  $J_k^\varepsilon \in \Omega$ .

**Remark IV.4.3.**

- While at first glance it is difficult to imagine that  $\partial\mathcal{O}'$  is anything except, say  $\mathcal{L}$ , what we have in mind is when  $\mathcal{L}$  and a neighboring curve are some approximation to a two-sided slit. The well-organized property does not permit the sides of the approximation to crisscross one another. Alternatively, this is a simple topological criterion which can be phrased as saying that under say the uniformization map (in fact any homeomorphism onto a Jordan domain would do) the image of each of these  $J$ -pieces occupies a single contiguous piece of the boundary. This sort of monochromaticity property is required for

well-behaved convergence of relevant boundary conditions we shall need later. Then a crisscrossing approximation can very well lead to altogether different limiting values – or none at all. It is clear that this well-organized property is satisfied by the trace of any discrete percolation explorer process.

- Sup-approximations satisfy conditions  $(i_I)$ ,  $(i_{II})$ ,  $(e)$ .
- The added difficulty here is that since the approximation is no longer interior, we can no longer determine the “topological situation” by looking under a single conformal map. E.g., for a point close to the boundary, we can no longer determine which boundary piece it is “really” close to. This is exemplified by the case of a slit domain: If, say, part of  $\mathcal{C}$  is one side of a two-sided slit  $\gamma$ , then points close to  $\gamma$  on one side (corresponding to  $\mathcal{C}$ ) will have small  $u$  value which tends to 0 whereas points close to  $\gamma$  on the other side (corresponding to say  $\mathcal{B}$ ) will tend to non-trivial boundary values. In the case of interior approximation all such ambiguities were resolved by looking under the conformal map  $\varphi^{-1}$ .

- It is worth noting that the important case in point where the boundary consist of an original  $\Omega$  with a (Löwner) slit – which might be two sided – falls into the setting under consideration. In particular, we will have occasion to consider cases where we have  $\gamma_n \rightarrow \gamma$  in the sup-norm with  $\gamma_n$  being discrete explorer paths. In this case to check condition  $(i_{II})$ , we observe that if  $\gamma_n \rightarrow \gamma$  in sup-norm and  $z_n \in \gamma_n$  and  $z_n \rightarrow z$ , then  $z \in \gamma$  and hence certainly in the complement of the the domain of interest  $\Omega \setminus \mathbb{I}(\gamma)$  (i.e.,  $\Omega$  delete  $\gamma$  together with components “swallowed” by  $\gamma$ ). For an illustration see Figure IV.3. These circumstances may be readily approximated by a hybrid

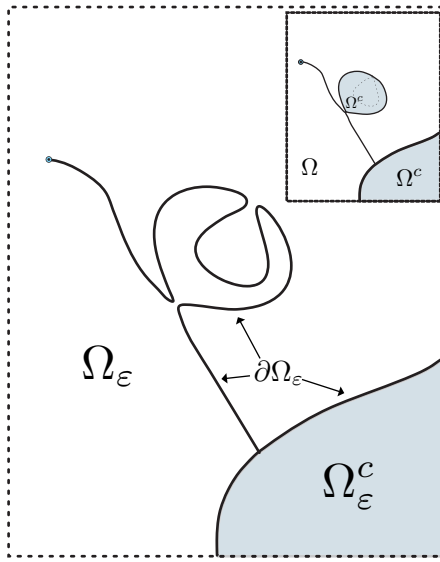


Figure IV.3: A case where the limiting domains does not contain a component present in approximating domains. Due to frequent self-touching, such (limiting) domains are in fact typical of  $\text{SLE}_6$ .

of sup- and canonical approximations and, as is not hard to see, satisfy the condition of commensurability.

The main addition is the following lemma which serves the role of condition (iii) in Definition IV.3.1 to ensure unambiguous retrieval of boundary values (see Lemma IV.5.3). That is, if  $w \in \Omega$  is close to  $\mathcal{C}$  in the “homotopical sense” that any *short* walk from  $w$  which hits  $\partial\Omega$  must hit the  $\mathcal{C}$  portion of  $\partial\Omega$  then  $w$  is close to  $\mathcal{C}_n$  by the same criterion. A precise statement of this intuitive notion is, unfortunately, much more involved.

**Lemma IV.4.4** (Homotopical Consistency). *Consider a domain  $\Omega$  with marked boundary prime ends  $a, b \in \partial\Omega$ . Let us focus on boundary  $\mathcal{C}$  with end points  $a$  and  $b$  which we consider to be the bottom of the boundary. (Note that  $\mathcal{C}$  may consist of Jordan arcs together with arbitrary parts – if double-sided slits are involved, such that not both sides belong to  $\mathcal{C}$ , then the corresponding arc(s) must be connected all the way up to  $b$  and/or  $a$ ). Let us denote the sup-*

approximation to  $\Omega$  by  $\Omega_n$  and the portion of the boundary approximating  $\mathcal{C}$  by  $\mathcal{C}_n$ .

Suppose we have a point  $q$  which is more than  $\Delta$  away from  $a$  and  $b$  and  $\delta^*$  away from  $\mathcal{C}$  with  $\Delta \gg \delta^*$ , such that  $\vartheta = \varphi^{-1}(q)$  is close to  $\varphi^{-1}(\mathcal{C})$ . Then there exists  $\eta > 0$  with  $\eta \ll \delta^*$  such that if  $\text{dist}(\mathcal{C}_n, \mathcal{C}) < \eta$  (here  $\text{dist}$  denotes e.g., the sup-norm distance where appropriate, and otherwise the Hausdorff distance) then there exists some path  $\mathcal{P}$  from (some point in)  $\varphi^{-1}(B_\Delta(a))$  to (some point in)  $\varphi^{-1}(B_\Delta(b))$  (we denote this by  $\varphi^{-1}(B_\Delta(a)) \rightsquigarrow \varphi^{-1}(B_\Delta(b))$ ) such that in the sup-approximation  $\Omega_n$ ,  $q$  is in the bottom component of  $\Omega_n \setminus \varphi(\mathcal{P} \cup B_\Delta(a) \cup B_\Delta(b))$  and further, any walk from  $q$  in the bottom component which hits  $\partial\Omega_n$  must hit  $\mathcal{C}_n$ .

*Proof.* For clarity, we divide the proof into four parts.

1. We let  $\eta \ll \Delta \ll 1$  and consider, under the uniformization map, the set

$$\mathcal{B} := \mathbb{D} \setminus [\varphi^{-1}(B_\Delta(a)) \cup \varphi^{-1}(B_\Delta(b))].$$

Let us now draw a path  $\mathcal{P}' : \partial\varphi^{-1}(B_\Delta(a)) \rightsquigarrow \partial\varphi^{-1}(B_\Delta(b))$  which defines top and bottom components in  $\mathcal{B}$  with  $\omega$  in the bottom component, and hence also the bottom component of  $\varphi(\mathcal{B}) \setminus \varphi(\mathcal{P}')$ . Further,  $\mathcal{P} := \varphi(\mathcal{P}')$  is some finite distance  $\delta \gg \eta > 0$  away from  $q$ . (In essence,  $\delta$  will now play the role of  $\delta^*$  in the statement of the Lemma.)

2. We now look at the domain

$$\mathcal{V}_n = \Omega_n \setminus [B_\Delta(a) \cup B_\Delta(b) \cup \mathcal{P}].$$

We claim that for  $n$  sufficiently large, all of the above is well-defined: Indeed,  $\mathcal{P}$  is a compact set in  $\Omega$  and hence for  $n$  sufficiently large, is contained in

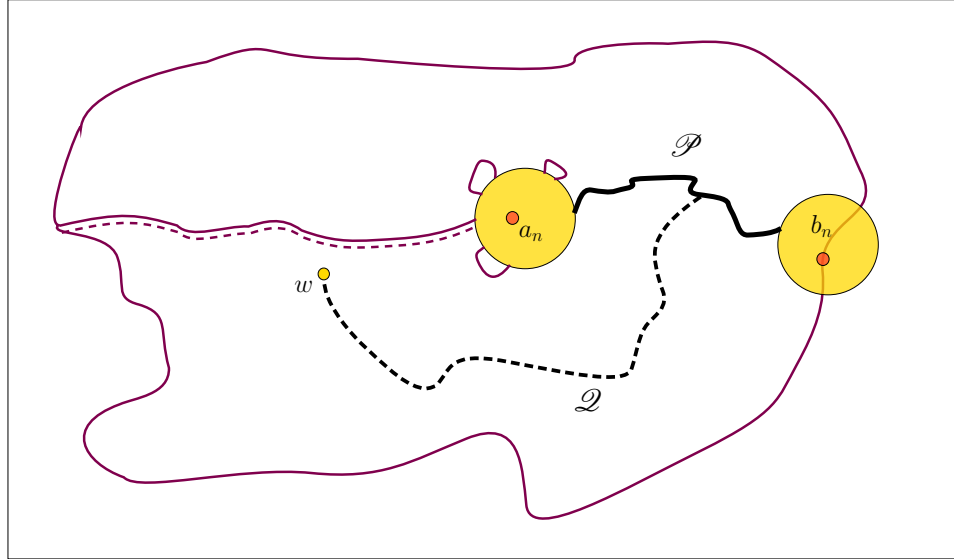


Figure IV.4: The domain  $\mathcal{V}_n$ , etc.

$\Omega_n$ , by Proposition IV.2.1. Of course,  $\Omega_n$  itself may have many components; we are focusing on the principal component. Even so, with the above setup,  $\mathcal{V}_n$  may also have many components, e.g., near the boundaries of  $B_\Delta(a)$  and  $B_\Delta(b)$  (see Figure IV.4).

However, we claim that it has the analogue of a top and bottom component: Indeed, it is clear that “large” compact sets in  $\mathcal{B}$  well away from the boundaries continue to lie in large connected components of  $\mathcal{V}_n$ . More quantitatively, while at the scale  $\Delta$ ,  $\partial\Omega_n$  may create various components by entering and re-entering  $B_\Delta(a)$  and  $B_\Delta(b)$ , since  $\mathcal{C}_n$  and  $\mathcal{C}$  are  $\eta$ -close (say in the Hausdorff distance), if we shrink these neighborhood balls to scale  $\Delta - 2\eta$ , then such components merge into (the) two principal components, leaving only  $\eta$ -scale small components in the vicinity of the neighborhood balls.

Finally, we claim that  $q$  is in the bottom component of  $\mathcal{V}_n$ . First, since

$B_\delta(q)$  must all be in the same component of  $\mathcal{V}_n$ ,  $q$  cannot be in a small  $\eta$ -scale component. The argument can be finished by any number of means. For example we may choose to regard  $\mathcal{P}$  as two-sided; the component of  $q$  is determined by which side of  $\mathcal{P}$  it may be connected to. For future reference, let  $\mathcal{Q}' \subset \mathbb{D}$  denote a simple path (staying well away from  $\partial\mathcal{B}$ ) connecting  $\vartheta$  to  $\mathcal{P}'$  and  $\mathcal{Q}$  the image of  $\mathcal{Q}'$  under  $\varphi$ . Then, again, by Proposition IV.2.1, for all  $n$  sufficiently large, the entirety of  $\mathcal{Q}$  is found in  $\Omega_n$  and the appropriate component – bottom – for  $q$  is determined for once and all. The relevant domains, etc., are illustrated in Figure IV.4.

3. It is clear that  $q$  is close to  $\mathcal{C}_n$ . We further claim that it is not obstructed from  $\mathcal{C}_n$  by other portions of  $\partial\Omega_n$ , as may be the worry when a portion of  $\mathcal{C}$  is (one side of) a two-sided slit. We need to divide into a few cases. First if the only portion of  $\mathcal{C}$  which is close to  $q$  is approximated interiorly, then by an investigation of the situation under the uniformization map, it is clear that no obstruction is possible. So now we suppose that  $q$  is close to some Jordan arc  $\mathcal{J} := [J_k, J_{k+1}]$ . If  $\mathcal{J}$  is one-sided, then there is no problem, since then  $q$  is not close in anyway to any other portion of the boundary except near the endpoints, which we may assume, by shrinking relevant scales if necessary, that  $q$  is far away from.

4. We are down to the main issue where  $\mathcal{J}$  is a two-sided slit, which is being sup-norm approximated by  $\mathcal{J}_n$ . Since at least one of the end points must be  $a$  or  $b$ , let us assume without loss of generality that  $J_k = a$ . We will need to do some refurbishing, starting with the neighborhood balls around  $a$  (and  $b$ , if necessary). Let  $\mathfrak{q}$  be a point on  $\mathcal{J}$  near  $a$ . It is manifestly the

case that  $\mathfrak{q}$  has two images under  $\varphi^{-1}$  – which are near  $\varphi^{-1}(a)$ ; consider a crosscut between these two images; the image of this crosscut under  $\varphi$  then defines the relevant neighborhood, which we will denote by e.g.,  $B(a)$ . We note that i) by construction,  $B(a)$  has the property that  $\mathcal{J}$  enters exactly once and terminates at  $a$ , and ii) being slightly more careful if necessary to ensure the relevant crosscut is contained in  $\varphi^{-1}(B_\Delta(a))$ , we can also ensure that  $B(a) \subset B_\Delta(a)$ . Here we will consider  $\eta \ll \text{dist}(a, \partial B(a))$ , so that in particular, e.g.,  $a_n \in B(a)$ .

Now let us return attention to  $\Omega_n$ . We will now refurbish  $\mathcal{P}$  so that it directly joins  $a_n$  to  $b_n$  and avoids all of  $\partial\Omega_n$ ; we will call the resultant path  $\mathcal{P}_r$ . We claim that it is possible to draw such a  $\mathcal{P}_r$  by suitably extending  $\mathcal{P}$ , under the above stipulations concerning  $B(a)$ ,  $B(b)$ , and  $\eta$ . Focusing attention on  $B(a)$ , if this were not possible, then it must have been the case that a portion of  $\mathcal{J}_n$  or a portion of  $\partial\Omega_n \setminus \mathcal{J}_n$  which is approximating the other side of  $\mathcal{J}$ , is obstructing. This scenario implies an inner domain inside  $B(a)$  surrounding the tip  $a_n$  with boundary e.g.,  $\mathcal{J}_n$ . Since  $\eta \ll \text{dist}(a, \partial B(a))$ , this violates sup–norm  $\eta$  closeness. (Here it appears that the sup–norm closeness property is crucial. For an illustration see Figure IV.5.)

Having achieved all this, it is again clear that the principal component of  $\Omega_n$  is divided into two disjoint Jordan domains. Indeed by the fact that the approximation is well–organized, there are two circuits – both using  $\mathcal{P}_r$ , passing through  $a_n$  and  $b_n$ , such that one (which again is the bottom one) contains  $\mathcal{C}_n$  and the other contains (the principal component of)  $\Omega_n \setminus \mathcal{C}_n$ , with no possibility of mixing via crisscrossing. Since  $\mathcal{P}_r$  is an extension of  $\mathcal{P}$ , it is

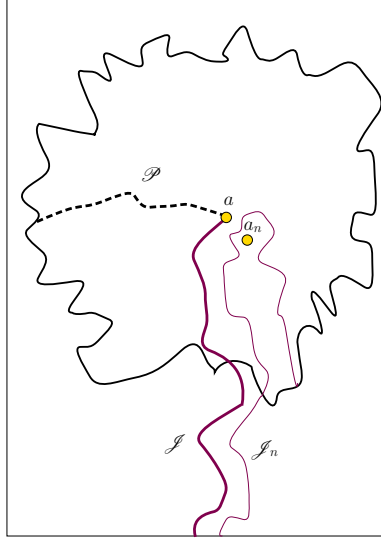


Figure IV.5: Failure to continue  $\mathcal{P}$  to  $\mathcal{P}_r$  inside  $B(a)$ .

clear from the closing argument of 3) that  $q$  is in the bottom component and hence must be closed to  $\mathcal{C}_n$  without obstruction from any portion of  $\partial\Omega_n \setminus \mathcal{C}_n$ .

□

## IV.5 Verification of Boundary Values for $u, v, w$

We are now in a position to verify boundary values for  $u, v, w$  using RSW estimates. Let us begin with a more detailed recapitulation/clarification of how we take the scaling limit of  $u_\varepsilon, v_\varepsilon, w_\varepsilon$  (see [13] and [11]). Consider some exhaustion  $K_n \nearrow \Omega$ , with  $K_n$  compact. The RSW estimates imply equicontinuity, and hence we have  $u_{\varepsilon_k}^{(n)} \rightarrow u^{(n)}$  uniformly on  $K_n$  and, at least for the models in [13] and [11],

$$F^{(n)} := u^{(n)} + e^{2\pi i/3}v^{(n)} + e^{-2\pi i/3}w^{(n)}$$

is analytic there with

$$u^{(n)} + v^{(n)} + w^{(n)} = \text{const.}$$

We may take  $(\varepsilon_k^{(n+1)}) \subset (\varepsilon_k^{(n)})$  as a subsequence which implies that

$$u_{\varepsilon_k}^{(n+1)} \rightarrow u^{(n+1)}$$

etc., so that  $F^{(n+1)}$  is analytic in  $K_{n+1}$  with values agreeing with the old  $F^{(n)}$  in  $K_n$ . The diagonal sequence  $(u_{\varepsilon_n}^{(n)})$  converges uniformly on compact sets to some  $u$ ; together with similar statements for  $v$  and  $w$ , we obtain that the limiting  $F$  is analytic on  $\Omega$ . In the sequel for simplicity we will drop the  $(n)$  superscripts and e.g., simply denote  $u_\varepsilon \rightarrow u$ .

We begin with a lemma which provides us with the RSW technology which is necessary for establishing boundary values.

**Lemma IV.5.1.** *Let  $\Omega$  and  $\varphi$  be as described. The pre-image of  $\partial\Omega$  under  $\varphi$  is divided into a finite number of disjoint (connected) closed arcs the intersection of any adjacent pair of which is the corresponding (pre-image of the) prime end. Then for  $z \in \partial\Omega \setminus \{a, b, c, \dots\}$ , we identify  $z$  with a single  $\varphi^{-1}(z)$  and similarly identify its corresponding boundary component.*

(I) *There exists an infinite sequence of (“square”) neighborhoods  $(S_\ell)$  centered at  $z$  such that  $S_\ell \cap \Omega \neq \emptyset$  for all  $\ell$  and  $S_{\ell+1}$  is strictly contained in  $S_\ell$  with  $\partial S_\ell$  containing portions of the boundary component containing  $z$  and*

(II) *In each  $S_\ell \setminus S_{\ell+1}$ , there is a “yellow” circuit and/or a “blue” circuit which separates  $z$  from all other boundary components with probability that is uniformly positive as  $\varepsilon \rightarrow 0$  (provided that  $\varepsilon$  is sufficiently small depending*

on  $\ell$ ). By separation it is meant that in the pre-image in  $\mathbb{D}$ ,  $\zeta$  is separated from all other boundary components along any path in  $\mathbb{D}$  whose image under  $\varphi$  tends to  $z$ .

Finally, for  $z \in \{a, b, c, \dots\}$ , a similar statement holds, except for the fact that here the relevant circuits separate  $z$  from all other boundary points and boundary components to which  $z$  does not belong.

*Proof.* Let  $z \in \partial\Omega$  and let  $\zeta = \varphi^{-1}(z)$  denote its corresponding pre-image. First suppose  $z \notin \{a, b, c, \dots\}$  so that  $\zeta$  is some finite distance from the corresponding points on  $\partial\mathbb{D}$ . Next we consider a sufficiently small crosscut  $\Gamma$  of  $\mathbb{D}$  surrounding  $\zeta$  (a finite distance away from  $\zeta$ ) whose end points on  $\partial\mathbb{D}$ , denoted  $\alpha$  and  $\beta$ , are such that  $\alpha$  and  $\beta$  are in the (interior of the) boundary component of  $\zeta$ . We also denote by  $Q$  the image of the interior of the region bounded by  $\Gamma$  and the relevant portion of  $\partial\mathbb{D}$ ; we note that  $z \in \partial Q$ . Let  $S_0 \subset \mathbb{C}$  be a small square centered at  $z$  whose intersection with  $\Omega$  lies entirely inside  $Q$ . Then by construction,  $\partial(S_0 \cap \Omega)$  can contain at most boundary pieces from the boundary component of  $z$ . Now the sequence  $S_n$  will be constructed similarly, with the stipulation that the linear scale of  $S_{\ell+1}$  is reduced by half.

By standard RSW estimates for the percolation problem in all of  $\mathbb{C}$ , there is a blue and/or yellow Harris ring inside each annulus  $S_\ell \setminus S_{\ell+1}$  with probability uniformly bounded from below for  $\varepsilon$  sufficiently small (depending on  $n$ ). Now consider any path  $\mathcal{P}$  in  $\mathbb{D}$  which originates at  $\zeta$  and ends outside  $\varphi^{-1}(Q)$  such that the image of the path originates at  $z$ . Such a path stays in  $\Omega$  and therefore must intersect the said circuit.

Identical arguments hold for  $z \in \{a, b, c, \dots\}$  except for the fact that the

original crosscut will now originate and end on two distinct boundary components.  $\square$

It is noted that in the presence of a circuit in  $S_\ell \setminus S_{\ell+1}$ , the above separation argument also applies to points in  $\partial(S_m \cap Q)$  if  $m \geq \ell + 1$ .

**Lemma IV.5.2** (Establishment of Boundary Values for Interior Approximations). *Let  $\Omega$  and  $\varphi$  be as described. We recall that  $u_\varepsilon^B(z)$  is the probability at the  $\varepsilon$  level that there is a blue crossing from  $\mathcal{A}_\varepsilon$  to  $\mathcal{B}_\varepsilon$ , separating  $z$  from  $\mathcal{C}_\varepsilon$ , and let  $u$  denote the limiting function. Then  $u = 0$  on  $\mathcal{C}$  in the sense that if  $z_k \rightarrow z \in \mathcal{C}$  in such a way that  $\varphi^{-1}(z_k) = \zeta_k \rightarrow \zeta \in \varphi^{-1}(\mathcal{C})$ , then  $\lim_{k \rightarrow \infty} u(z_k) = 0$ . Similarly, in the vicinity of the point  $c$ ,  $u$  tends to one. Analogous statements hold for  $v_\varepsilon^B$  and  $w_\varepsilon^B$  and for the yellow versions of these functions.*

*Proof.* Suppose a yellow Harris circuit has occurred in  $S_\ell \setminus S_{\ell+1}$  and let  $z_k \rightarrow z$  as described. Then, in the language of the proof of Lemma IV.5.1, for  $k$  sufficiently large  $z_k \in Q \cap S_m$  for some  $m = m(k)$  tending to  $\infty$  as  $k \rightarrow \infty$ . For  $\varepsilon$  sufficiently small, it follows from (iii) in Definition IV.3.1 that  $\mathcal{A}_\varepsilon$  and  $\mathcal{B}_\varepsilon$  are disjoint from  $(S_m \cap Q \cap \Omega_\varepsilon^\bullet)$  and since  $\Omega_\varepsilon^\bullet$  is an interior approximation, the relevant portion of the circuit evidently joins with  $\partial\mathcal{C}_\varepsilon$  to separate  $\partial S_m \cap Q \cap \Omega_\varepsilon^\bullet$  from  $c$ , as for  $z$  as discussed near the end of the proof of Lemma IV.5.1. This separation would preclude the crossing event corresponding to  $u_\varepsilon^B(z_k)$  since – as is clear if we look on the unit disc via the conformal map  $\varphi^{-1}$  – the latter necessitates (two) blue connections between the relevant portions of  $\partial S_m$  and other boundaries. Now consider  $k$  with  $m(k)$  very large; then for all

$\varepsilon$  sufficiently small, the probability of at least one yellow circuit is, uniformly (in  $\varepsilon$ ), close to some  $p(m)$  where  $p(m) \rightarrow 1$  as  $m \rightarrow \infty$ . It therefore follows that  $u(z_k) \leq 1 - p(m(k)) \rightarrow 0$  as  $z_k \rightarrow z$ . Finally, boundary value of  $c$  follows the same argument: Here the blue Harris ring events accomplish the required connection between  $\mathcal{A}_\varepsilon$  and  $\mathcal{B}_\varepsilon$ . Arguments for other functions/boundaries are identical.

□

**Lemma IV.5.3** (Establishment of Boundary Values for Sup-approximations).

*Let  $\Omega$  and  $\varphi$  be as described. We recall that  $u_\varepsilon^B(z)$  is the probability at the  $\varepsilon$  level that there is a blue crossing from  $\mathcal{A}_\varepsilon$  to  $\mathcal{B}_\varepsilon$ , separating  $z$  from  $\mathcal{C}_\varepsilon$ , and let  $u$  denote the limiting function. Then  $u = 0$  on  $\mathcal{C}$  in the sense that if  $z_k \rightarrow z \in \mathcal{C}$  in such a way that  $\varphi^{-1}(z_k) = \zeta_k \rightarrow \zeta \in \varphi^{-1}(\mathcal{C})$ , then  $\lim_{\varepsilon \rightarrow 0} u_\varepsilon^B(z_k) \rightarrow 0$ . Similarly, in the vicinity of the point  $c$ ,  $u$  tends to one. Analogous statements hold for  $v_\varepsilon^B$  and  $w_\varepsilon^B$ .*

*Proof.* We recall that we have three boundary pieces  $\mathcal{A}, \mathcal{B}, \mathcal{C}$  in counterclockwise order, where we assume without loss of generality that  $\mathcal{C}$  is on the bottom. We also label the relevant marked prime ends  $a, b, c$ , in counterclockwise order, such that e.g.,  $c$  is opposite to  $\mathcal{C}$ . Thus if we draw a path  $\mathcal{P}$  between  $a_\varepsilon$  and  $b_\varepsilon$  inside  $\Omega_\varepsilon$ , and  $z_k \in \Omega_\varepsilon$  is inside the region formed by  $\mathcal{P}$  and  $\mathcal{C}_\varepsilon$  then to prevent events which contribute to  $u_\varepsilon^B$ , it is sufficient to seal  $z_k$  off from  $c_\varepsilon$  by a yellow Harris ring together with the bottom boundary  $\mathcal{C}_\varepsilon$ . This is precisely the setting of Lemma IV.4.4 (with  $w = z_k$ ) and so we conclude that for  $k$  sufficiently large, for  $\varepsilon$  sufficiently small depending on  $k$ , in order to prevent events contributing to  $u_\varepsilon^B$ , it is indeed sufficient to seal  $z_k$  off with a yellow

Harris ring.

We are now in a position to invoke Lemma IV.5.1. The proof follows closely as in the last part of the proof of Lemma IV.5.2 except for one difference: For  $k$  sufficiently large,  $z_k \in S_m$  for some  $m = m(k)$  which increases as  $k$  increases; however, in the case of sup-approximation, it is no longer quite so automatic that arbitrarily small Harris rings will hit the boundary  $\mathcal{C}_\varepsilon$ . However, given  $\varepsilon$ , we have that  $\mathcal{C}_\varepsilon$  is at most a distance  $\eta(\varepsilon)$  from  $\mathcal{C}$ , and thus, for fixed  $\varepsilon_0$ , there is some  $M(\varepsilon_0)$  such that  $m(k) \nearrow M(\varepsilon_0)$  as  $k \rightarrow \infty$  (and  $M(\varepsilon_0) \rightarrow \infty$  as  $\varepsilon_0 \rightarrow 0$ ). So we still have that uniformly for all  $\varepsilon \leq \varepsilon_0$ ,  $U_\varepsilon(z) \leq 1 - p(M(\varepsilon_0))$ , where  $p(M(\varepsilon_0))$  as before denotes the probability of at least one yellow Harris ring in the annulus  $S_1 \setminus S_{M(\varepsilon_0)}$ , and tends to 1 as  $M(\varepsilon_0)$  tends to infinity.

□

**Remark IV.5.4.** Our arguments in fact show that the function  $u$  is continuous up to the boundary: Given any sequence  $z_k \rightarrow z \in \mathcal{C}$ , we have that given any  $\kappa > 0$ , for  $k$  sufficiently large,  $|u_{\varepsilon_n}^{(n)}(z_k)| < \kappa$ , uniformly in  $n$ , for  $n$  sufficiently large (or  $\varepsilon$  sufficiently small) and hence  $u(z_k) < \kappa$  (c.f., the end of the proof of Theorem IV.5.5). We have similar statements for  $v$  and  $w$  on the corresponding boundaries.

To check that  $F$  is indeed the appropriate conformal map and thereby uniquely determine it and retrieve Cardy's Formula, we follow the arguments in [4]. We remark that while there exists certain literature on discrete complex analysis (see e.g., [10] and [7] and references therein) our situation is less straightforward since e.g., none of the functions  $u_N, v_N, w_N$  are actually discrete harmonic. Moreover, due to the fact that we are considering gen-

eral domains (versus Jordan domains) and  $\partial\Omega$  may not be so well-behaved, to obtain conformality requires some extra work. In any case, we will now amalgamate all ingredients to prove the following result:

**Theorem IV.5.5.** *For the models described in [11] (which includes the triangular site problem studied in [13]), consider the function  $F = u + e^{2\pi i/3}v + e^{-2\pi i/3}w$ , where  $u, v, w$  are the limits of  $u_\varepsilon, v_\varepsilon, w_\varepsilon$ . Then  $F$  is the unique conformal map between  $\Omega$  and the equilateral triangle  $\mathbf{T}$  with vertices at  $1, e^{2\pi i/3}, e^{-2\pi i/3}$ .*

*Proof.* We claim that the following seven conditions hold:

1.  $F$  is nonconstant and analytic in  $\Omega$ ,
2.  $u, v, w$  (and hence  $F$ ) can be continued (continuously) to  $\partial\Omega$ ,
3.  $u + v + w$  is a constant,
4.  $u(c) = 1$ , with similar statements for  $v$  and  $w$  at  $a$  and  $b$ ,
5.  $u \equiv 0$  on  $\mathcal{C}$  with similar statements for  $v$  and  $w$  on  $\mathcal{A}$  and  $\mathcal{B}$ ,
6.  $F \circ \varphi$  maps  $\partial\mathbb{D}$  bijectively onto  $\partial\mathbf{T}$ ,
7.  $(F \circ \varphi)(\mathbb{D}) \cap (F \circ \varphi)(\partial\mathbb{D}) = \emptyset$ ;

from which the proposition follows immediately. Indeed, from conditions 7 and 6,  $F \circ \varphi : \mathbb{D} \rightarrow \mathbf{T}$  is a conformal map (this follows directly from e.g., Theorem 4.3 in [18]). But clearly, conditions 5, 4, 3 imply that  $F$  maps  $\Omega$  into  $\mathbf{T}$ , and further, conditions 2 and 1 imply that  $F$  maps  $\Omega$  onto  $\mathbf{T}$  (this follows from e.g., Theorem 4.1 in [18]). Altogether, conformality of  $F$  itself now follows: It

is enough to show that  $F'$  never vanishes, but this follows from the fact that  $0 \neq (F \circ \varphi)'(z) = F'(\varphi(z))\varphi'(z)$ .

We now turn to the task of verifying conditions 1 – 7. It follows from [13], [11], and [4] that  $F$  is analytic and that  $u + v + w$  is constant. On this basis, the real part of  $F$  is proportional to  $u$  plus a constant and it is seen from Lemma IV.5.2 (or Lemma IV.5.3) that  $u$  is *not* constant, i.e., it is close to 1 near  $c$  and close to 0 near  $\mathcal{C}$ . We have conditions 1 and 3. Conditions 2, 4, 5 follow from Lemma IV.5.2 (or Lemma IV.5.3) and Remark IV.5.4.

To demonstrate condition 7, let us write  $\operatorname{Re}(F) = (3/2)u - 1/2$ . Then if we show that  $u \neq 0$  in  $\Omega$ , then we have demonstrated that  $F(\Omega)$  does not intersect  $F(\mathcal{C})$ . The latter follows since once  $z \in \Omega$ , we can construct a tube of bounded conformal modulus connecting  $\mathcal{A}$  to  $\mathcal{B}$  going underneath  $z$ , and within this tube, by standard percolation arguments which go back to [2], we can construct a monochrome path separating  $z$  from  $\mathcal{C}$ . Condition 6 follows in a similar spirit: E.g., on the  $\mathcal{A}$  boundary, if  $z \neq q$ , but  $|z - q| \ll 1$ , then by the argument of Lemma IV.5.1,  $u(z)$  is close to  $u(q)$  (since both can be surrounded by many annuli in which e.g., a blue circuit occurs). Similar arguments for  $v$  and  $w$  and other boundaries directly imply continuity of all functions on all boundaries of  $\Omega$ . Moreover, this implies, e.g.,  $u \circ \varphi^{-1}(\mathcal{A})$  is continuous on the relevant portion of the circle starting (at  $\varphi^{-1}(c)$ ) with the value 1 and ending (at  $\varphi^{-1}(b)$ ) with the value 0 and thus achieving all values in  $[0, 1]$ . Similarly statements hold for the other functions on the other boundaries. Condition 6 now follows directly.

□

**Remark IV.5.6.** It is worth noting that while using only arguments involving RSW bounds, we have determined that 1) the  $u, v, w$ 's can be continued to the boundary and 2) partial boundary values, e.g.,  $u \equiv 0$  on  $\mathcal{C}$ , sufficient determination of boundary values requires additional ingredients. In particular, we also needed that e.g.,  $v + w \equiv 1$  on  $\mathcal{C}$ ; this would follow from  $u + v + w \equiv 1$  which at present seems only to be derivable from analyticity considerations. Duality implies e.g.,  $v_\varepsilon^B + w_\varepsilon^Y \equiv 1$  on  $\mathcal{C}$ , but we cannot go any further without color symmetry as in the site percolation on the triangular lattice case ([13]) or some (asymptotic) color symmetry restoration as was established for the models in [11].

Recalling that  $C_0(\Omega, a, b, c, d)$  is equal to e.g.,  $u(d)$  with  $d \in \mathcal{A}$ , we now have

**Theorem IV.5.7.** *For the models described in [11] with the assumption  $M(\partial\Omega) < 2$  (which includes the triangular site problem studied in [13], where the assumption on  $\partial\Omega$  is unnecessary) Cardy's Formula can be established via an interior or sup-approximation, i.e.,*

$$C_\varepsilon(\Omega_\varepsilon, a_\varepsilon, b_\varepsilon, c_\varepsilon, d_\varepsilon) \rightarrow C_0(\Omega, a, b, c, d)$$

if  $(\Omega_\varepsilon)$  is an interior or sup-approximation to  $\Omega$ .

*Proof.* For the site percolation model, this follows from [13], [11], [4], and Theorem IV.5.5. For the model described in [11], the interior analyticity statement in sufficient generality is verified in [3], §4.4. □

Finally, let us single out the cases that will be used in the proof of the Main Theorem in [3].

**Corollary IV.5.8.** *Consider the models described in [11] (which includes the triangular site problem studied in [13]) on a bounded domain  $\Omega$  with boundary Minkowski dimension less than two (if necessary) and two marked boundary points  $a$  and  $c$ . Suppose we have  $\mathbb{X}_{[0,t]}^\varepsilon \rightarrow \mathbb{X}_{[0,t]}$  in the **Dist** norm where  $\mathbb{X}_{[0,t]}^\varepsilon$  is the trace of a discrete Exploration Process starting at  $a$  and aiming towards  $c$ , stopped at some time  $t$ , then*

$$C_\varepsilon(\Omega_\varepsilon \setminus \mathbb{X}_{[0,t]}^\varepsilon, \mathbb{X}_t^\varepsilon, b_\varepsilon, c_\varepsilon, d_\varepsilon) \rightarrow C_0(\Omega \setminus \mathbb{X}_{[0,t]}, \mathbb{X}_t, b, c, d).$$

Further, it is possible to extract a slightly stronger statement which will be used in the proof of the Main Theorem in [3]. For the sake of [3] we will state these results in the **Dist** norm (c.f., Remark VI.1). For purposes of clarity, we first state a lemma:

**Proposition IV.5.9.** *Let us denote the type of (slit) domain under consideration by  $\Omega^\gamma$  and abbreviate, by abuse of notation, e.g.,  $C_\varepsilon((\Omega^\gamma)_\varepsilon) := C_\varepsilon(\Omega_\varepsilon \setminus \gamma_\varepsilon([0,t]), \gamma_\varepsilon(t), b_\varepsilon, c_\varepsilon, d_\varepsilon)$  (but here,  $\gamma$  could stand for other boundary pieces as detailed in Definition IV.4.2). Then for any sequence  $\gamma_n \rightarrow \gamma$  in the **Dist** norm and any sequence  $(\varepsilon_m)$  converging to zero,*

$$\lim_{n,m \rightarrow \infty} C_{\varepsilon_m} [(\Omega^{\gamma_n})_{\varepsilon_m}] = C_0(\Omega^\gamma),$$

*regardless of how  $n$  and  $m$  tend to infinity.*

*Proof.* From Lemma IV.5.3 we have that e.g., if  $\gamma_{\varepsilon_m}^{(n)} \rightarrow \gamma_n$  is any sup-approximation, then  $C_{\varepsilon_m} [(\Omega^{\gamma_n})_{\varepsilon_m}] \rightarrow C_0(\Omega^{\gamma_n})$ . The result follows by noting that  $\gamma_{\varepsilon_m}^{(n)}$  is also a sup-approximation to  $\gamma$  as *both*  $m, n \rightarrow \infty$ . We emphasize that the reason for such robustness of Lemma IV.5.3 is because the proof is completely insensitive

to how  $\gamma_\varepsilon$  converges to  $\gamma$  as  $\varepsilon \rightarrow 0$ . All that is needed is that  $\gamma_\varepsilon$  is sufficiently close to  $\gamma$  and  $\varepsilon$  is sufficiently small, which is inevitable if  $\varepsilon$  is tending to zero and  $\gamma_\varepsilon$  is tending to  $\gamma$ .  $\square$

**Corollary IV.5.10.** *Considered the models described in [11] (which includes the triangular site problem studied in [13]) on a bounded domain  $\Omega$  with boundary Minkowski dimension less than two (if necessary) and two marked boundary points  $a$  and  $c$ . Consider  $\mathcal{C}_{a,c,\Delta}$ , the set of Löwner curves which begin at  $a$ , are aiming towards  $c$  but have not yet entered the  $\Delta$  neighborhood of  $c$  for some  $\Delta > 0$ . Suppose we have  $\gamma_\varepsilon \rightarrow \gamma$  e.g., in the **Dist** norm, then*

$$C_\varepsilon(\Omega_\varepsilon \setminus \gamma_\varepsilon([0, t]), \gamma_\varepsilon(t), b_\varepsilon, c_\varepsilon, d_\varepsilon) \rightarrow C_0(\Omega \setminus \gamma([0, t]), \gamma(t), b, c, d)$$

*pointwise equicontinuously in the sense that*

$$\forall \kappa > 0, \quad \forall \gamma \in \mathcal{C}_{a,c,\Omega}, \quad \exists \delta(\gamma) > 0, \quad \exists \varepsilon_\gamma,$$

*such that*

$$\forall \gamma' \in \mathcal{B}_{\delta(\gamma)}(\gamma), \quad \forall \varepsilon \leq \varepsilon_\gamma,$$

$$|C_\varepsilon((\Omega \setminus \gamma)_\varepsilon([0, t]), (\gamma(t))_\varepsilon, b_\varepsilon, c_\varepsilon, d_\varepsilon) - C_\varepsilon((\Omega \setminus \gamma')_\varepsilon([0, t]), (\gamma'(t))_\varepsilon, b_\varepsilon, c_\varepsilon, d_\varepsilon)|$$

$$< \kappa.$$

(IV.1)

Here  $B_\delta(\gamma)$  denotes the **Dist** neighborhood of  $\gamma$ .

*Proof.* This is immediate from Proposition IV.5.9. Negation of the conclusion in the statement means that there exists a sequence  $\gamma_n \rightarrow \gamma$  and  $\varepsilon_n \rightarrow 0$  such

that  $|C_{\varepsilon_n}((\Omega^{\gamma^n})_{\varepsilon_n}) - C_{\varepsilon}((\Omega^{\gamma})_{\varepsilon_n})| > \kappa > 0$  for all  $\varepsilon_n$ , which clearly contradicts the fact that both of these objects converge to the limit  $C_0(\Omega^{\gamma})$ .

□

**Remark IV.5.11.** We remark that (V.2) holds even if “ $\varepsilon = 0$ ” and thus implies continuity of Cardy’s Formula in the “**Dist** norm”. However, we note that Lemma IV.5.3, being merely a limiting statement, would be highly inadequate if one had in mind some uniformity of the convergence or uniformity of the continuity.

# Bibliography

- [1] M. Aizenman, J. T. Chayes, L. Chayes, J. Frohlich, and L. Russo. *On a Sharp Transition From Area Law to Perimeter Law in a System of Random Surfaces*. Comm. Math. Phys. **92**, no. 1, 19–69 (1983).
- [2] V. Beffara. *Cardy’s Formula on the Triangular Lattice, the Easy Way*. Universality and Renormalization, vol. 50 of the Fields Institute Communications, 39–45 (2007).
- [3] I. Binder, L. Chayes and H. K. Lei. *On Convergence to SLE<sub>6</sub> I: Conformal Invariance for Certain Models of the Bond–Triangular Type*.
- [4] B. Bollobás and O. Riordan. *Percolation*. Cambridge: Cambridge University Press (2006).
- [5] F. Camia and C. M. Newman. *Two-Dimensional Critical Percolation: The Full Scaling Limit*. Comm. Math. Phys. **268**, no. 1, 1–38 (2006).  
*Critical Percolation Exploration Path and SLE<sub>6</sub>: a Proof of Convergence*.  
Available at <http://arxiv.org/list/math.PR/0604487> (2006)

- [6] L. Chayes and H. K. Lei. *Cardy's Formula for Certain Models of the Bond-Triangular Type*. *Reviews in Mathematical Physics*. **19**, 511–565 (2007).
- [7] D. Chelkak and S. Smirnov. *Discrete Complex Analysis on Isoradial Graphs*. arXiv:0810.2188v1
- [8] R. J. Duffin. *Potential Theory on a Rhombic Lattice*. *J. Combinatorial Theory*. **5**, 258–272 (1968).
- [9] P. L. Duren. *Univalent Functions*. Berlin, New York: Springer Verlag (1983).
- [10] J. Ferrand. *Fonctions préharmoniques et fonctions préholomorphes*. *Bull. Sci. Math.* **2**, vol. 68, 152–180 (1944).
- [11] S. Lang. *Complex Analysis*. Berlin, New York: Springer (1999).
- [12] G. F. Lawler. *Conformally Invariant Processes in the Plane*. *Mathematical Surveys and Monographs*, 114. American Mathematical Society, Providence, RI, 2005. xii+242 pp. ISBN: 0-8218-3677-3
- [13] C. Pommerenke. *Univalent Functions*. Gottingen: Vandenhoeck and Ruprecht (1975).
- [14] C. Pommerenke. *Boundary Behavior of Conformal Maps*. Berlin, New York: Springer (1992).
- [15] B. Ráth. *Conformal Invariance of Critical Percolation on the Triangular Lattice*. Available at: <http://www.math.bme.hu/~rathb/rbperko.pdf>

- [16] O. Schramm. *Conformally Invariant Scaling Limits (an overview and a collection of problems)*. arXiv:math.PR/0602151
- [17] S. Smirnov. *Towards Conformal Invariance of 2D Lattice Models*. Proceedings of the International Congress of Mathematicians, Madrid, Spain, 2006.
- [18] S. Smirnov. *Critical Percolation in the Plane: Conformal Invariance, Cardy's Formula, Scaling Limits*. C. R. Acad. Sci. Paris Sr. I Math. **333**, 239–244 (2001).  
Also available at <http://www.math.kth.se/~stas/papers/percras.ps>.
- [19] W. Werner. *Lectures on Two-Dimensional Critical Percolation*. arXiv:0710.0856

# Chapter V

## Convergence to $\text{SLE}_6$

**Abstract:** Following the approach outlined in [26], convergence to  $\text{SLE}_6$  of the Exploration Processes for the correlated bond-triangular type models studied in [11] is established. This puts the said models in the same universality class as the standard site percolation model on the triangular lattice [13]. In the context of these models, the result is proven for all domains with boundary Minkowski dimension less than two. Moreover, the proof of convergence applies in the context of general critical 2D percolation models and for general domains, under the stipulation that Cardy's Formula can be established for domains in this generality.

**Keywords:** Universality, conformal invariance, percolation, Cardy's Formula.

## V.1 Introduction

In recent years, the scaling behavior of critical 2D percolation systems have been the subject of attention. While the results proved in this note amount to a statement concerning the scaling limit of the specific percolation models defined in [11], the purpose of this work is actually three-fold: 1) Following the framework described in [26], we provide a general proof that (the law of) the “interface” of essentially *any* critical 2D percolation model converges to  $\text{SLE}_6$ , whenever Cardy’s Formula can be verified. 2) Rigorous extraction of Cardy’s Formula for general domains – including slit domains, given interior analyticity of the Cardy–Carleson functions; this includes clarification of the necessary discretization schemes. 3) Finally, we provide a generalization of Cardy’s Formula to an extended class of domains for the specific class of models described in [11], and also establish additional “typical” (critical) percolation properties which are required, in accord with 1) and 2) above. We accomplish 1) and 3) in the current installment of this work; item 2) will be tended to in a separate (companion) note [6].

It is already well-known [13] that site percolation on the 2D triangular lattice satisfies these sorts of properties. While in [9] an elaborate proof of convergence to  $\text{SLE}_6$  has been detailed, and while it is possible that the proof therein applies in more generality than claimed, the present approach is manifestly applicable to a variety of systems and in a variety of domains. As a result we have, in complete accordance with the ideology espoused since the 1960s, demonstrated a non-trivial example of universality: Via the common continuum limit, various aspects of the long distance behavior for the models

defined in [11] are asymptotically identical to those of the critical triangular site percolation model.

We remark that in principle, our proof applies in the general context of any critical 2D percolation model. The required conditions are summarized as follows:

- Russo–Seymour–Welsh (RSW) theory: Uniform estimates for probabilities of crossings (of either type) on all scales plus the ability to stitch smaller crossings together without substantial degradation of the estimates – FKG–type inequalities.
- A self–replicating definition of an Exploration Process and a class of *admissible* domains with the property that this class is preserved under the operation of deleting the beginning of a typical explorer path in an admissible domain.
- The validity of Cardy’s Formula for the above–mentioned admissible domains.
- BK–type inequalities whereby probabilities of separated path type events can be estimated in terms of the individual probabilities.
- Explicit (“superuniversal”) “bounds” on full–space multiple colored five–arm events and half–space multiple colored three–arm events: The probability of observing disjoint crossings of an annulus with aspect ratio  $a$  is, on all scales, bounded above by a constant times  $a^{-2}$ .

The rest of this paper is organized as follows: In Section V.2, we assemble the necessary ingredients into the proof of convergence to  $\text{SLE}_6$  (providing

some minor proofs of an analytical nature along the way). These ingredients amount to a number of technical lemmas, a few of which require a sustained effort and whose proofs are provided in Section V.3 and, for one of them, a result imported from [6]. Finally, Section V.4 is devoted to shoring up the required properties of the models defined in [11] to the appropriate level for the program in Section V.2.

## **V.2 Conformal Invariance of the Scaling Limit**

### **V.2.1 2D Percolation: Criticality and Interfaces**

#### **(a Brief Discussion)**

In this subsection, we shall elucidate, to some extent, the first and second (bullet) items in the penultimate paragraph of the introduction. For brevity – and purposes of clarity – we will not attempt to axiomatize the relevant notions. In general, the percolation process consists of two competing species, conveniently denoted by “blue” and “yellow”. The condition of criticality implies that the two species have roughly equal parity; it need not be the case that the two are exactly equivalent, but neither species is dominant at large scales. In particular, there is no percolation of either species – with probability one, all monochrome connected clusters are finite. As it turns out, this is (more or less) equivalent to the statement that for both species, at all scales, the probability of crossing “rectangles” of fixed ratio is bounded above and below uniformly. Moreover, with some notion of positive correlations for crossing type events of the same color, we may patch together the appropriate crossings

to conclude that there are scale-invariant bounds on the existence of circuits in annuli; since *Bernoulli percolation* is supposed to imply independence beyond some fixed scale, this also implies similar estimates for circuits in “partial annuli” and approximate independence in disjoint layered annuli. Typically, the way such estimates are applied is as follows: There is a large outside scale and a small inside scale separated by logarithmically many intermediate scales; the probability of monochrome connections between the inner and outer scale is therefore a power of the ratio. This is the basis of the so-called Russo–Seymour–Welsh (RSW) theory which will be used throughout this work. For the standard percolation models, these concepts are discussed in the books [10], [8] and [6]; see also Sections 2.2 and 2.3 of [7] and the paper [9]. For the particular model of interest in this work, such results are not quite automatic, but anyway have been established in [11], the relevant portions of which will be cited as necessary.

In a similar spirit, let us now discuss critical interfaces for these models (although strictly speaking, criticality plays no rôle). The general setup is as follows: For any finite connected lattice domain, let us fix two “boundary points”  $a$  and  $c$  and impose boundary conditions so that the portion of the boundary going from  $a$  to  $c$  one way is colored blue and the complementary portion of the boundary is yellow. The precise lattice-mechanics depend, of course, on the model at hand (and indeed may involve different procedures on the yellow and blue sides). In any case, if this procedure has been implemented successfully, then in any percolation configuration there will be an *interface* stretching from  $a$  to  $c$ , which separates the blue connected component of the

blue boundary from the yellow component of the yellow boundary. The explicit construction for our model will be provided in Section V.4.2; well known examples include the triangular site percolation problem and the bond model on  $\mathbb{Z}^2$ . In the former case, the interface can be realized as boundary segments of hexagons and in the latter, interface consists of segments which connect sites of the so-called medial lattice.

The seminal ingredient is the Domain Markov Property: The full percolation model with the above boundary setup conditioned on an initial portion of the Exploration Process is identical to the problem in the “slit” domain with additional (two-colored) boundary formed by the corresponding curve segment. It seems manifest, at least for planar models, that all 2D percolation systems have this property. Whereas the preceding may seem rather vague and discursive, what is actually needed is somewhat less and succinctly formulated: The precise requirement is the content of Equation (V.3), which is the restriction of these notions to crossing events.

## V.2.2 SLE: Definitions and Notations

As the title of this subsection indicates, we will briefly review the relevant notions of Löwner evolution – mostly for the purpose of fixing notation. Let  $\Omega$  be a domain with two boundary prime ends  $a$  and  $c$ .

**Definition V.2.1.** Let  $\{\Omega_t\}_{t=0}^\infty$  be a strictly decreasing family of subdomains of  $\Omega$  ( $t \in [0, \infty)$ ) which is Carathéodory continuous with respect to  $c$ , such that  $\Omega_0 = \Omega$  and  $c \in \bigcap_{t=0}^\infty \overline{\Omega}_t$ . Then we call  $\{\Omega_t\}_{t=0}^\infty$  a Löwner chain.

Let  $\mathbb{H}$  denote the upper-half plane of  $\mathbb{C}$ . We can select some conformal map

$g_0 : \Omega \rightarrow \mathbb{H}$  such that  $g_0(a) = 0$  and  $g_0(c) = \infty$ . The family of conformal maps  $g_t : \Omega_t \rightarrow \mathbb{H}$  normalized such that  $g_t(c) = \infty$  and  $g_t \circ g_0^{-1}(z) = z + \frac{A(t)}{z} + o(1/z)$  are continuous in  $t$ . We now reparameterize time so that  $A(t)$ , the capacity at time  $t$ , is equal to  $2t$ .

We call  $\gamma$  a *crosscut* in  $\Omega$  from  $a$  to  $c$  if it is the preimage of a non-self-crossing curve from  $0$  to  $\infty$  in  $\mathbb{H}$  under  $g_0$ . Note that  $\gamma$  is allowed to touch itself but not to cross itself. We define  $\Omega_t$  to be the connected component of  $\Omega \setminus \gamma_{[0,t]}$  containing  $c$ . It's easy to see that  $\Omega_t$  is a Löwner chain if and only if the following two conditions are satisfied for every  $t > 0$ :

$$(L1) \quad \gamma_t \in \overline{\Omega_{t-\varepsilon}}, \quad \forall \varepsilon > 0$$

and

$$(L2) \quad \exists \delta_n \rightarrow 0, \quad \forall \varepsilon > 0, \quad \gamma_{t-\delta_n} \in \Omega_{t-\delta_n-\varepsilon}.$$

If  $\gamma$  satisfies (L1) and (L2), then we say that  $\gamma$  is a *Löwner curve*. Under these conditions, we can reparametrize  $\gamma$  so that the maps  $g_t$ 's satisfy the following celebrated Löwner equation:

$$\partial_t g_t(z) = \frac{2}{g_t(z) - \lambda_t},$$

where  $\lambda_t = g_t(\gamma(t))$  is a continuous real function. On the other hand, the solution of the Löwner equation for any initial conformal map  $g_0 : \Omega \rightarrow \mathbb{H}$  and any continuous real function  $\lambda(t)$  defines a Löwner chain, but not necessarily a curve (see [19] for a complete discussion). The object  $\lambda_t$  is called the *driving function* of  $\Omega_t$ .

If we take the very special function  $\lambda_t = B(\kappa t)$ , where  $B(t)$  is one-dimension Brownian motion started at zero, then the corresponding random Löwner chain is called the Stochastic (or Schramm) Löwner Evolution with parameter  $\kappa$ ,

SLE $_{\kappa}$ . We will be particularly interested in the case  $\kappa = 6$ .

### V.2.3 Statement of the Main Theorem and Lemmas

We start with a bounded and connected domain  $\Omega \subset \mathbb{C}$ . We will sometimes assume that  $\Omega$  has “boundary dimension”  $M(\partial\Omega) < 2$ . Here  $M(S)$  denotes the (upper) *Minkowski* dimension of the set  $S$  which, as usual, is defined as

$$M(S) = \limsup_{\vartheta \rightarrow 0} \frac{\log \mathcal{N}(\vartheta)}{\log(1/\vartheta)},$$

where  $\mathcal{N}(\vartheta)$  is the number of boxes of side length  $\vartheta$  needed to cover the set. We will tile  $\Omega$  with the discrete lattice of interest (which may require detail, c.f. §V.4.2 and, especially, the discussion in [6]) at scale  $\varepsilon > 0$  and denote the resulting object by  $\Omega_{\varepsilon}$ . Critical percolation is then performed in  $\Omega_{\varepsilon}$ , with  $\varepsilon$  tending to zero.

While the principal result of this note has more general applicability, for simplicity let us state it for the particular model under consideration:

**Main Theorem.** *Let  $\Omega$  be as described above with  $M(\partial\Omega) < 2$ , let  $\Omega_{\varepsilon}$  be some suitable discretization (see [6] for discussions and results) and consider the percolation model described in [11] (see §V.4.1). Let  $a$  and  $c$  denote two prime ends at the boundary of  $\Omega$  and let us set the boundary conditions on  $\Omega_{\varepsilon}$  in such a way that the Exploration Process, as defined in §V.4.2, runs between  $a$  and  $c$ . Let  $\mu_{\varepsilon}$  be the probability measure on random curves induced by the Exploration Process on  $\Omega_{\varepsilon}$ , and let us endow the space of curves with the appropriate weighted sup-norm metric as described in Definition V.3.12.*

Then,

$$\mu_\varepsilon \xrightarrow[\mathcal{L}]{} \mu_0,$$

where  $\mu_0$  has the law of chordal  $SLE_6$  from  $a$  to  $c$ .

We remark that while the above statement appears to require a number of “future specifics”, these are merely technicalities. The central requisites are captured in the items listed in the penultimate paragraph of the introduction and will be detailed as the proof of the Main Theorem unfolds. (In particular, here and throughout, the requirement  $M(\partial\Omega) < 2$  is for the specific benefit of the model defined in [11].)

The key ingredient which will be used in the proof of the Main Theorem is Cardy’s Formula:

**Lemma V.2.2** (Cardy’s Formula). *Let  $(\Omega, a, b, c, d)$  be a conformal rectangle – that is to say, a domain with boundary prime ends  $a, b, c, d$ , listed in counter-clockwise order, and let us assume that  $M(\partial\Omega) < 2$ . Let  $C_\varepsilon(\Omega, a, b, c, d)$  denote the probability that there exists a blue crossing from  $[a, b]$  to  $[c, d]$  on the  $\varepsilon$ -lattice approximation of  $\Omega$ . Consider the (unique) conformal map which takes  $(\Omega, a, b, c, d)$  to  $(\mathbb{H}, 1 - x, 1, \infty, 0)$ , where, clearly,  $0 < x < 1$  and  $x = x(\Omega, a, b, c, d)$ . Then, for the model described in §V.4.1 (or without the restriction  $M(\partial\Omega) < 2$  for the site percolation model)*

$$\lim_{\varepsilon \rightarrow 0} C_\varepsilon(\Omega, a, b, c, d) = F(x) := \frac{\int_0^x (s(1-s))^{-2/3} ds}{\int_0^1 (s(1-s))^{-2/3} ds}. \quad (\text{V.1})$$

*Proof.* This, modulo the formula (V.1), is the content of [6], Theorem 4.7. For the particular model at hand, this was established for a restricted class of

domains in [11]. The necessary generalization of the work in [11] to domains with  $M(\partial\Omega) < 2$  will be proved in §V.4.4 (see Lemma V.4.8).  $\square$

Using general estimates in §V.3.1, we establish the following important properties of any weak\*-limiting point  $\mu'$ . The proofs can be found in §V.3.2 and §V.3.3.

**Lemma V.2.3** (Tightness). *Let  $\mu'$  be any limit point, in the weak\* Hausdorff topology on compact sets, of  $\mu_\varepsilon$ . Then  $\mu'$  gives full measure to Löwner curves in  $\Omega$  from  $a$  to  $c$ .*

Furthermore, we have

**Lemma V.2.4** (Admissibility). *The limit point  $\mu'$  gives full measure to curves with upper Minkowski dimension less than  $2 - \psi'$  for some  $\psi' > 0$ .*

We note that in Lemma V.2.3 (and Lemma V.2.4), a stronger notion of convergence is available. Indeed, for domains which are regular enough, the results of [2] provide weak\* convergence to  $\mu'$  in the distance provided by the sup-norm:

$$\text{dist}(\gamma_1, \gamma_2) = \inf_{\varphi_1, \varphi_2} \sup_t |\gamma_1(\varphi_1(t)) - \gamma_2(\varphi_2(t))|,$$

where the infimum is over all possible parametrizations. For our purposes – where prime ends are a concern – we will consider a weighted sum of the distances within various regions between the curves. We will denote the appropriate distance by **Dist**; see Definition V.3.12. We can easily extend the result of [2] to the following:

**Lemma V.2.5** (**Dist** Topology). *The measure  $\mu'$  is a limit point in the weak\* **Dist** topology on curves of  $\mu_\varepsilon$ .*

Finally, we will use the following continuity result for crossing probabilities, whose proof can be found in [6] (stated as Corollary 5.10):

**Lemma V.2.6.** *Consider the models described in [11] (which includes the triangular site problem studied in [13]) on a bounded domain  $\Omega$  with boundary Minkowski dimension less than two (if necessary) and two marked boundary points  $a$  and  $c$ . Consider  $\mathcal{C}_{a,c,\Delta}$ , the set of Löwner curves which begin at the point  $a$  and are aiming towards the point  $c$  but have not yet entered the  $\Delta$  neighborhood of  $c$  for some  $\Delta > 0$ . Suppose we have  $\gamma^\varepsilon \rightarrow \gamma$  in the **Dist** norm, then*

$$C_\varepsilon(\Omega_\varepsilon \setminus \gamma_\varepsilon([0, t]), \gamma_\varepsilon(t), b_\varepsilon, c_\varepsilon, d_\varepsilon) \rightarrow C_0(\Omega \setminus \gamma([0, t]), \gamma(t), b, c, d)$$

*pointwise equicontinuously in the sense that*

$$\forall \sigma > 0, \quad \forall \gamma \in \mathcal{C}_{a,c,\Omega}, \quad \exists \delta(\gamma) > 0, \quad \exists \varepsilon_\gamma,$$

*such that*

$$\forall \gamma' \in \mathcal{B}_{\delta(\gamma)}(\gamma), \quad \forall \varepsilon \leq \varepsilon_\gamma,$$

$$\begin{aligned} & |C_\varepsilon((\Omega \setminus \gamma)_\varepsilon([0, t]), (\gamma(t))_\varepsilon, b_\varepsilon, c_\varepsilon, d_\varepsilon) - C_\varepsilon((\Omega \setminus \gamma')_\varepsilon([0, t]), (\gamma'(t))_\varepsilon, b_\varepsilon, c_\varepsilon, d_\varepsilon)| \\ & < \sigma. \end{aligned} \tag{V.2}$$

Here  $\mathcal{B}_\delta(\gamma)$  denotes the **Dist** neighborhood of  $\gamma$ .

## V.2.4 Proof of the Main Theorem

Let us show how to derive our Main Theorem from the preceding lemmas. We closely follow the strategic initiative outlined in the expositions of [26] (for a slightly different and more probabilistic perspective on the subject, also see the exposition in [14]); moreover, the “expansion at infinity” technique we will use here first appeared in [20] in the proof of the convergence of the loop-erased random walk to  $\text{SLE}_2$ .

Let us fix  $\Omega$  with  $M(\partial\Omega) < 2$  and two boundary prime ends  $a$  and  $c$ . We start with an informal list of the key steps.

- I. Extract some limiting measure  $\mu'$ .
- II. Show that any limiting measure is supported on Löwner curves.
- III. Establish the discrete domain (crossing) Markov property.
- IV. Löwner parameterize all curves under consideration.
- V. Obtain the limiting martingale.
- VI. Show that  $\kappa = 6$ .

◊ I.] Let us note that the collection of measures  $(\mu_\varepsilon)$  defined by the Exploration Processes on  $\varepsilon$ -lattice is weakly precompact as a set of regular measures defined on the space of compact subsets of  $\bar{\Omega}$  with the Hausdorff metric. Thus to prove the Main Theorem it is enough to show that any weak limit point  $\mu'$ , of  $\mu_\varepsilon$ , has the law of  $\text{SLE}_6$  from  $a$  to  $c$  in  $\Omega$ .

◇ II.] By Lemma V.2.3,  $\mu'$  gives full measure to Löwner curves. Let  $w_t$  be the random driving function of the curve. To finish the proof, we need to show that  $w_t$  has the law of  $B_{6t}$ , where  $B_t$  is the standard one dimensional Brownian Motion started at 0.

◇ III.] Let us add two boundary prime ends  $b$  and  $d$  so that  $(a, b, c, d)$  are listed counter-clockwise. Given a discrete Exploration Process, we may parametrize it in any convenient fashion and denote the resulting curve by  $\mathbb{X}_t^\varepsilon$ . Let us assume, temporarily, that  $\mathbb{X}_t^\varepsilon$  does not “explore” the boundary,  $\partial\Omega_\varepsilon$ . Now, by convention/definition, the faces on the right side of the Exploration Process are blue, and the faces on the left side are yellow. In general, a blue crossing from  $[a, b]$  to  $[c, d]$  can either touch the blue portion of the exploration path  $\mathbb{X}_{[0,t]}^\varepsilon$ , or avoid it. It is thus a fact that the blue crossing in  $\Omega_\varepsilon$  of the described type implies a blue crossing between  $[\mathbb{X}_t^\varepsilon, b]$  to  $[c, d]$  in  $\Omega_\varepsilon \setminus \mathbb{X}_{[0,t]}^\varepsilon$ . And vice versa: It is clear (at least modulo cases where  $\mathbb{X}_{[0,t]}^\varepsilon$  touches  $\partial\Omega_\varepsilon$ ) that any blue crossing between  $[\mathbb{X}_t^\varepsilon, b]$  to  $[c, d]$  in  $\Omega_\varepsilon \setminus \mathbb{X}_{[0,t]}^\varepsilon$  produces a blue crossing from  $[a, b]$  to  $[c, d]$  in  $\Omega_\varepsilon$ .

Under these conditions, we can write the following *Markov identity* for the crossing probabilities

$$C_\varepsilon \left( \Omega_\varepsilon \setminus \mathbb{X}_{[0,t]}^\varepsilon, \mathbb{X}_t^\varepsilon, b, c, d \right) = C_\varepsilon \left( \Omega_\varepsilon, a, b, c, d \mid \mathbb{X}_{[0,t]}^\varepsilon \right). \quad (\text{V.3})$$

and further,

$$\mathbb{E}_{\mu_\varepsilon} \left[ C_\varepsilon \left( \Omega_\varepsilon \setminus \mathbb{X}_{[0,t]}^\varepsilon, \mathbb{X}_t^\varepsilon, b, c, d \right) \right] = C_\varepsilon \left( \Omega_\varepsilon, a, b, c, d \right). \quad (\text{V.4})$$

Now let  $0 < s < t$ , then given some  $\mathbb{X}_{[0,s]}^\varepsilon$ , the same reasoning as above applied to  $\Omega_\varepsilon \setminus \mathbb{X}_{[0,s]}^\varepsilon$  and the conditional measure  $\mu_\varepsilon \left( \cdot \mid \mathbb{X}_{[0,t]}^\varepsilon \right)$  gives the *martingale*

equation

$$\mathbb{E}_{\mu_\varepsilon} [C_\varepsilon (\Omega_\varepsilon \setminus \mathbb{X}_{[0,t]}^\varepsilon, \mathbb{X}_t^\varepsilon, b, c, d) \mid \mathbb{X}_{[0,s]}^\varepsilon] = C_\varepsilon (\Omega_\varepsilon \setminus \mathbb{X}_{[0,s]}^\varepsilon, \mathbb{X}_s^\varepsilon, b, c, d). \quad (\text{V.5})$$

We will later establish a continuum version of this equation (see Equation (V.9)).

**Remark V.2.7.** Here, let us focus briefly on circumstances where  $\mathbb{X}_{[0,t]}^\varepsilon$  has touched  $\partial\Omega_\varepsilon$  – which turns out to be highly likely – or has even “already determined” the crossing game in  $\Omega_\varepsilon$  – which must happen eventually. In case of the former but not the latter, the above equations require no further discussion provided we interpret  $\Omega_\varepsilon \setminus \mathbb{X}_{[0,t]}^\varepsilon$  as the connected component of  $c$  in  $\Omega_\varepsilon \setminus \mathbb{X}_{[0,t]}^\varepsilon =: \text{Comp}_{\Omega \setminus \mathbb{X}_{[0,t]}^\varepsilon}(c)$ . As for the latter, it is not difficult to see that this occurs precisely when either  $b$  or  $d$  fail to lie in the boundary of  $\text{Comp}_{\Omega_\varepsilon \setminus \mathbb{X}_{[0,t]}^\varepsilon}(c)$ . As such, the notation  $C_\varepsilon (\Omega_\varepsilon \setminus \mathbb{X}_{[0,t]}^\varepsilon, \mathbb{X}_t^\varepsilon, b, c, d)$  can no longer be literally read as “the crossing probability in said domain with these marked boundary points” since at least one of the relevant points is not actually in the boundary of the relevant domain. Notwithstanding, we can and will use the notation  $C_\varepsilon (\Omega_\varepsilon \setminus \mathbb{X}_{[0,t]}^\varepsilon, \mathbb{X}_t^\varepsilon, b, c, d)$  even when  $b$  or  $d$  is not in  $\text{Comp}_{\Omega_\varepsilon \setminus \mathbb{X}_{[0,t]}^\varepsilon}(c)$  with the understanding that in this case the relevant crossing probability is given by

$$\begin{cases} 1; & \text{if } \mathbb{X}_t^\varepsilon \text{ has hit } [c, d] \text{ before } [b, c] \\ 0; & \text{if } \mathbb{X}_t^\varepsilon \text{ has hit } [b, c] \text{ before } [c, d]. \end{cases}$$

We will continue with this convention in the  $\varepsilon \rightarrow 0$  case.

It is noted that for  $\varepsilon > 0$ , we are dealing with a discrete system and the above holds regardless of the parameterization scheme (provided that no

overcounting is engendered); however, some care will be needed as we take the continuum limit. In particular, the above equation with all  $\varepsilon$  removed does not really make sense unless all curves  $\mathbb{X}_{[0,t]}$  are endowed with a “common” parameterization. The natural choice is the Löwner parameterization, but this requires some argument since the relevant topology for convergence is in the sup–norm (or **Dist** norm).

◊ IV.] Now we show that it is possible to re–parameterize by the Löwner parameterization. What will suffice for us is a statement to the effect that every “Löwner parameterization neighborhood” in the support of  $\mu'$  contains a **Dist**–neighborhood. (By the former it is meant that if  $\gamma$  and  $\gamma'$  are endowed with the Löwner parameterization, then the distance between them is taken to be  $d_{\mathcal{L}}(\gamma, \gamma') = \sup_t |\gamma(t) - \gamma'(t)|$ ; thus the converse of the above claim is obvious.) We remark that the statement is essentially deterministic; we put in the proviso that we are in the support of  $\mu'$  just to ensure that the curves can be Löwner parameterized in the first place.

Hereafter we shall restrict attention to the portion of the curves which have not yet entered the  $\Delta$  neighborhood of  $c$ . Our first claim is that (for  $\eta \ll \Delta$ ), in fact, these portions of all curves in the same  $\eta$ –**Dist** neighborhood are in fact close in the *Löwner* parameterization. Indeed,

**Lemma V.2.8.** *Consider curves  $\gamma$  emanating from  $a$  which stay outside of the  $\Delta$  neighborhood of  $c$ . If  $\mathbf{Dist}(\gamma_1, \gamma_2) < \eta$ , then*

$$|\mathrm{Cap}_{\mathbb{H}}(\gamma_1) - \mathrm{Cap}_{\mathbb{H}}(\gamma_2)| < C(\Omega, \Delta)\eta^\alpha$$

for some  $\alpha > 0$  and some  $\Omega$  and  $\Delta$  dependent constant  $C(\Omega, \Delta)$ . Here  $\mathrm{Cap}_{\mathbb{H}}(\cdot)$

denotes the half plane capacity.

*Proof.* On  $\mathbb{H}$ , if two (compact) sets  $A_1$  and  $A_2$  are  $\sigma$  close (even) in the Hausdorff metric, then by for example the Beurling estimates (see e.g., Corollary 3.80 in [19])

$$|\text{Cap}_{\mathbb{H}}(A_1) - \text{Cap}_{\mathbb{H}}(A_2)| \leq C\sqrt{\sigma} \cdot \text{diam}(\mathcal{N}_{\sigma}(A_1))^{3/2}, \quad (\text{V.6})$$

where  $\mathcal{N}_{\sigma}(A_1)$  denotes the Hausdorff- $\sigma$  neighborhood of  $A_1$  and  $C$  is some constant (the estimate is equally good if we replace  $\mathcal{N}_{\sigma}(A_1)$  by  $\mathcal{N}_{\sigma}(A_2)$ ). In our case, we are only assuming  $\sigma$ -closeness in the original domain  $\Omega$  and therefore one could *a priori* be concerned about distortions near the boundary. However, this can be rectified with the aid of some distortion theorems. Let us decompose  $\Omega = \mathcal{N}_{\delta}(\partial\Omega) \cup [\Omega \setminus \mathcal{N}_{\delta}(\partial\Omega)]$  and similarly given two curves  $\gamma_1$  and  $\gamma_2$ , we will write e.g.,  $\gamma_1 = \hat{\gamma}_1 \cup \bar{\gamma}_1$ , where  $\hat{\gamma}_1 = \gamma_1 \cap [\Omega \setminus \mathcal{N}_{\delta}(\partial\Omega)]$  and  $\bar{\gamma}_1 = \gamma_1 \cap \mathcal{N}_{\delta}(\partial\Omega)$ .

First by the Distortion Theorems (for a more detailed argument along these lines, see the proof of Lemma VI.2.6) we know that if  $\varphi : \Omega \rightarrow \mathbb{H}$ , then

$$\varphi(\mathcal{N}_{\delta}(\partial\Omega)) \subset \mathcal{N}_{C'\sqrt{\delta}}(\partial\mathbb{H})$$

for some ( $\Omega$  dependent) constant  $C'$  and hence bounding the capacity via the area of the corresponding strip, we have

$$\text{Cap}_{\mathbb{H}}(\bar{\gamma}_1), \text{Cap}_{\mathbb{H}}(\bar{\gamma}_2) \lesssim D\sqrt{\delta}$$

where  $D$  is the diameter of the image of the complement of the  $\Delta$ -neighborhood of  $c$  under  $\varphi$  and we use  $\lesssim$  to denote implied universal/ $\Omega$ -dependent constants.

Next we note that by the subadditive property of capacities, it is clear that

$$|\text{Cap}_{\mathbb{H}}(\gamma_1) - \text{Cap}_{\mathbb{H}}(\gamma_2)| \leq \text{Cap}_{\mathbb{H}}(\tilde{\gamma}_1) + \text{Cap}_{\mathbb{H}}(\tilde{\gamma}_2) + |\text{Cap}_{\mathbb{H}}(\hat{\gamma}_1) - \text{Cap}_{\mathbb{H}}(\hat{\gamma}_2)|$$

so we now estimate  $|\text{Cap}_{\mathbb{H}}(\hat{\gamma}_1) - \text{Cap}_{\mathbb{H}}(\hat{\gamma}_2)|$ . But first, by another distortion estimate (see e.g., Corollary 3.19 in [19]) we have

$$|\varphi'(z)| \lesssim 1/\sqrt{\delta}$$

and hence  $d(\varphi(z_1), \varphi(z_2)) \lesssim \frac{\eta}{\sqrt{\delta}}$  if  $z_1, z_2 \in \Omega \setminus \mathcal{N}_{\delta}(\partial\Omega)$  with  $d(z_1, z_2) < \eta$  and we conclude that

$$d_H(\hat{\gamma}_1, \hat{\gamma}_2) \lesssim \frac{\eta}{\sqrt{\delta}}$$

where  $d_H$  denotes the Hausdorff distance, from which it follows by (V.6) that

$$|\text{Cap}_{\mathbb{H}}(\hat{\gamma}_1) - \text{Cap}_{\mathbb{H}}(\hat{\gamma}_2)| \lesssim \frac{\sqrt{\eta}}{\delta^{1/4}}.$$

Combining the above estimates, we see that with proper choice of  $\delta$  (which vanishes with  $\eta$ ), the difference in capacities indeed differs by a fractional power of  $\eta$ . □

We may thus safely replace all parameterizations by the Löwner parameterization:

**Corollary V.2.9.** *Let  $\gamma$  be a Löwner curve emanating from  $a$  and staying outside of the  $\Delta$  neighborhood of  $c$ , and let  $\mathcal{L}_{\sigma}(\gamma)$  denotes the  $\sigma$  Löwner parameterization neighborhood of  $\gamma$ . Then there exists  $\eta = \eta(\sigma, \Delta, \gamma) > 0$  such that the **Dist** neighborhood of size  $\eta$  is contained in  $\mathcal{L}_{\sigma}(\gamma)$ .*

*Proof.* Suppose towards a contradiction that this is not the case. Then there exists  $\gamma_n \rightarrow \gamma$  in the **Dist** norm such that  $d_{\mathcal{L}}(\gamma_n, \gamma) > \sigma$ . It is clear that we

may endow each  $\gamma_n$  – as well as  $\gamma$  – with some (uniform) parameterization so that  $\sup_t |\gamma_n(t) - \gamma(t)| = \eta_n$ , which tends to zero; further, we can and will without loss of generality assume that  $\gamma$  is in fact parameterized by capacity (this does *not* imply that  $\gamma_n$ 's are parameterized by capacity; indeed, they are parameterized by  $\gamma$ 's capacity). But this implies that there is a sequence of capacities  $\mathbf{c}_n$ , which occur for  $\gamma_n$  at time  $s_n$  (in this parameterization) such that

$$|\gamma_n(s_n) - \gamma(\mathbf{c}_n)| > \sigma.$$

Taking a subsequence if necessary, we may assume that  $s_n \rightarrow s$ . Our first claim is that  $\gamma_n([0, s_n])$  converges in the **Dist** norm to  $\gamma([0, s])$ . Indeed,

$$\begin{aligned} & \mathbf{Dist}(\gamma_n([0, s_n]), \gamma([0, s])) \\ & \leq \mathbf{Dist}(\gamma([0, s_n]), \gamma([0, s])) + \mathbf{Dist}(\gamma([0, s_n]), \gamma_n([0, s_n])). \end{aligned}$$

The second term is clearly bounded by  $\eta_n$ ; as for the first term, it is clearly bounded by  $\text{diam}(\gamma([s_n \wedge s, s_n \vee s]))$  which tends to zero since  $\gamma$  is continuous. We may assume without loss of generality (taking a subsequence if necessary) that  $\mathbf{c}_n \rightarrow \mathbf{c}$ . By Lemma V.2.8 we then have

$$\mathbf{c} = \lim_{n \rightarrow \infty} \text{Cap}_{\mathbb{H}}(\gamma_n[0, s_n]) = \text{Cap}_{\mathbb{H}}(\gamma[0, s]).$$

So using the fact that capacity is strictly increasing (which follows from the definition of Löewner curves) the above display implies that  $s = \mathbf{c}$  which is a contradiction since **Dist**-convergence necessitates that  $\gamma_n(s_n) \rightarrow \gamma(s)$ .  $\square$

◇ V.] As a first step towards obtaining a martingale observable in the continuum, our next goal is to remove all  $\varepsilon$ 's from (V.4). On the basis of the

previous step, it is clear that we may now interpret (V.4) in terms of Löwner parameterization. Further, we set  $t > 0$  to be such that the relevant curves have not yet entered the  $\Delta$  neighborhood of  $c$ . First, the right hand side of (V.3) converges to the continuum counterpart  $C_0(\Omega, a, b, c, d)$  by Lemma V.2.2, so we focus on the left hand side.

First, recalling that  $\mu'$  is a weak\* limit with respect to the **Dist** norm, and that the space of all possible continuous curves is, in fact, separable, it follows that there are countably many curves  $\gamma_n$  such that the space,  $\mathcal{C}_{a,c,\Delta}$ , of Löwner curves which begin at  $a$  aiming towards  $c$  but having not yet entered the  $\Delta$  neighborhood of  $c$ , can be written as

$$\mathcal{C}_{a,c,\Delta} = \bigcup_{n=1}^{\infty} B_{\delta_n}(\gamma_n) \cap \mathcal{L}_{\sigma}(\gamma_n) := \bigcup_{n=1}^{\infty} \mathcal{N}_n^*.$$

In the above,  $\delta_n$  has been chosen in accord with Lemma V.2.6 (and also, for the model in [11], described in §V.4.1, Lemma V.2.4 ensures that Cardy's Formula is viable for domains slit by the Explorer Process) so that

$C_{\varepsilon} \left( \Omega_{\varepsilon} \setminus \mathbb{X}_{[0,t]}^{\varepsilon}, \mathbb{X}_t^{\varepsilon}, b, c, d \right)$  for any  $\mathbb{X}_{[0,t]}^{\varepsilon}$  in  $B_{\delta_n}(\gamma_n)$  is  $\vartheta$  close to the corresponding object with argument  $\gamma_n([0, t])$  (for  $\varepsilon < \varepsilon(\gamma_n)$  sufficiently small), where  $\vartheta \ll 1$  is small, and  $\sigma$  is also envisioned to be small. Further, modifying the neighborhoods to be mutually disjoint, we can now reduce to a finite number,  $N$ , of these neighborhoods which carries all but  $\alpha$  (with  $\alpha \ll 1$ ) of the measure of  $\mu'$ . For what follows, we will sometimes abbreviate, e.g.,

$$K_{\varepsilon}(Y_t^{\varepsilon}) := C_{\varepsilon} \left( \Omega_{\varepsilon} \setminus \mathbb{Y}_{[0,t]}^{\varepsilon}, \mathbb{Y}_t^{\varepsilon}, b, c, d \right).$$

In the above display, it is understood that the right hand side is interpreted in accord with Remark V.2.7 above.

We first observe that (for  $\varepsilon$  sufficiently small)

$$\begin{aligned} \left| \mathbb{E}_{\mu_\varepsilon}(K_\varepsilon(X_t^\varepsilon)) - \sum_{n=1}^N \mu_\varepsilon(\mathcal{N}_n^*) K_\varepsilon(\gamma_n) \right| &\leq \alpha + \sum_{n=1}^N \sum_{X_t^\varepsilon \in \mathcal{N}_n^*} |K_\varepsilon(X_t^\varepsilon) - K_\varepsilon(\gamma_n)| \mu_\varepsilon(X_t^\varepsilon) \\ &\leq \alpha + \vartheta \end{aligned}$$

and similarly

$$\begin{aligned} \left| \mathbb{E}_{\mu'}(K_0(X_t)) - \sum_{n=1}^N \mu'(\mathcal{N}_n^*) K_0(\gamma_n) \right| &\leq \alpha + \sum_{n=1}^N \int_{X_t \in \mathcal{N}_n^*} |K_0(X_t) - K_0(\gamma_n)| d\mu'(X_t) \\ &\leq \alpha + \vartheta \end{aligned}$$

Therefore, it is enough to control the difference of the relevant sums over neighborhoods:

$$\begin{aligned} &\left| \sum_{n=1}^N \mu_\varepsilon(\mathcal{N}_n^*) K_\varepsilon(\gamma_n) - \sum_{n=1}^N \mu'(\mathcal{N}_n^*) K_0(\gamma_n) \right| \\ &\leq \sum_{n=1}^N |\mu_\varepsilon(\mathcal{N}_n^*) K_\varepsilon(\gamma_n) - \mu'(\mathcal{N}_n^*) K_0(\gamma_n)| \\ &\leq \sum_{n=1}^N |\mu_\varepsilon(\mathcal{N}_n^*) (K_\varepsilon(\gamma_n) - K_0(\gamma_n))| + |(\mu'(\mathcal{N}_n^*) - \mu_\varepsilon(\mathcal{N}_n^*)) K_0(\gamma_n)| \\ &\leq \vartheta + \alpha \end{aligned}$$

Thus, taking  $N \rightarrow \infty$  and  $\varepsilon \rightarrow 0$ , etc., we may now upgrade Eq. (V.3) with

$$\mathbb{E}_{\mu'} [C_0(\Omega \setminus \mathbb{X}_{[0,t]}, \mathbb{X}_t, b, c, d)] = C_0(\Omega, a, b, c, d). \quad (\text{V.7})$$

**Remark V.2.10.** The demonstration of Equation (V.7) (or some version thereof) *in the continuum* represents the key issue in this approach to proving convergence. In the present work, this has been achieved via a robust convergence to Cardy's Formula in general (i.e., slit) domains via the sup-approximations; see e.g., [6], Corollary 4.10. In any case, the authors strongly believe that *some* analytical statement along these lines cannot be avoided.

Next we recast Equation (V.7) in terms of conditional expectation:

$$\mathbb{E}_{\mu'}(\mathbf{1}_{\mathcal{C}_\Omega} \mid \sigma([0, t])) \equiv \mathbb{E}_{\mu'}(\mathbf{1}_{\mathcal{C}_\Omega} \mid \mathbb{X}_{[0, t]}) = K_0(\mathbb{X}_{[0, t]}), \quad (\text{V.8})$$

where  $\sigma([0, t])$  denotes the  $\sigma$ -algebra generated by  $\mu'$  supported curves up to time  $t$  and  $\mathbf{1}_{\mathcal{C}_\Omega}(\cdot)$  is the indicator function of the crossing event. (The latter can be realized as

$$\mathbf{1}_{\mathcal{C}_\Omega}(\gamma) = \begin{cases} 1 & \text{if } \gamma \text{ hits } [c, d] \text{ before } [b, c] \\ 0 & \text{if } \gamma \text{ hits } [b, c] \text{ before } [c, d] \end{cases}$$

and hence is a  $\mu'$  measurable function.) Note that e.g.,  $\mathbf{1}_{\mathcal{C}_\Omega} \equiv 1$  if  $\mathbb{X}_{[0, t]}$  has already hit the  $[c, d]$  boundary of  $\Omega$  and, in this vein, Equation (V.8) is of course interpreted in accord with Remark V.2.7 above. We see that Equation (V.8) follows immediately: For  $\mathcal{B} \in \sigma([0, t])$ ,

$$\begin{aligned} \int_{\mathcal{B}} [\mathbb{E}_{\mu'}(\mathbf{1}_{\mathcal{C}_\Omega} \mid \sigma([0, t]))](\gamma) \, d\mu'(\gamma) &= \int_{\mathcal{B}} \mathbf{1}_{\mathcal{C}_\Omega}(\gamma) \, d\mu'(\gamma) \\ &= \mu'(\mathcal{C}_\Omega \cap \mathcal{B}) \\ &= \int_{\mathcal{B}} K_0(\mathbb{X}_{[0, t]}) \, d\mu'. \end{aligned}$$

Here the first two equalities are definitions and the third equality can be established by a straightforward modification of the argument used to establish Equation (V.7) – which corresponds to the case where  $\mathcal{B}$  is the full sample space.

From Equation (V.8) and the defining properties of conditional expectation, we can deduce that 1) the random variable  $K_0(\mathbb{X}_{[0, t]})$  is  $\sigma([0, t])$  measurable and 2)  $K_0(\mathbb{X}_{[0, t]})$  is a continuous time martingale, i.e., if  $0 < s < t$ , then

$$\mathbb{E}_{\mu'} [C_0(\Omega \setminus \mathbb{X}_{[0, t]}, \mathbb{X}_t, b, c, d) \mid \mathbb{X}_{[0, s]}] = C_0(\Omega \setminus \mathbb{X}_{[0, s]}, \mathbb{X}_s, b, c, d). \quad (\text{V.9})$$

In particular, Equation (V.9) is simply Equations (V.7) and (V.8) with  $\Omega$  replaced by  $\Omega \setminus \mathbb{X}_{[0,s]}$  – along with the interpretation of the latter in terms of conditional expectations – and  $\mu'$  averaging over  $\mathbb{X}_{[s,t]}$ . More specifically, since  $\sigma([0, s]) \subset \sigma([0, t])$ , if  $\mathcal{B} \in \sigma([0, s])$ , then

$$\begin{aligned} \int_{\mathcal{B}} \mathbb{E}_{\mu'}(\mathbf{1}_{\mathcal{E}_\Omega} \mid \sigma([0, s])) \, d\mu' &= \int_{\mathcal{B}} \mathbf{1}_{\mathcal{E}_\Omega} \, d\mu' \\ &= \int_{\mathcal{B}} \mathbb{E}_{\mu'}(\mathbf{1}_{\mathcal{E}_\Omega} \mid \sigma([0, t])) \, d\mu' \\ &= \int_{\mathcal{B}} \mathbb{E}_{\mu'} [\mathbb{E}_{\mu'}(\mathbf{1}_{\mathcal{E}_\Omega} \mid \sigma([0, t]) \mid \sigma([0, s]))] \, d\mu', \end{aligned}$$

which is the content of (V.9).

◇ VI.] We will now finish the proof and show that  $\kappa = 6$ . Notice that the map

$$h_t(z) = \frac{g_t(z) - g_t(d)}{g_t(b) - g_t(d)},$$

where  $g_t(z)$  is the Löwner map, maps the rectangle  $(\Omega \setminus \mathbb{X}_{[0,t]}, \mathbb{X}_t, b, c, d)$  conformally onto

$$\left( \mathbb{H}, \frac{\lambda_t - g_t(d)}{g_t(b) - g_t(d)}, 1, \infty, 0 \right).$$

By Cardy's identity (Lemma V.2.2),

$$C_0(\Omega \setminus \mathbb{X}_{[0,t]}, \mathbb{X}_t, b, c, d) = F \left( \frac{g_t(b) - \lambda_t}{g_t(b) - g_t(d)} \right), \quad (\text{V.10})$$

where we recall that the relevant domain is really the connected component of  $c$  in  $\Omega \setminus \mathbb{X}_{[0,t]}$  and it is tacitly assumed that  $b$  and  $d$  are both (still) in the boundary of this component.

Using Eq. (V.10), we can rewrite Eq. (V.9), accounting for such errors, via

$$\begin{aligned}
& \left| F \left( \frac{g_s(b) - \lambda_s}{g_s(b) - g_s(d)} \right) \mathbf{1}_{\{b, d \in \partial(\Omega \setminus \mathbb{X}_{[0, s]})\}} \right. \\
& \quad \left. - \mathbb{E}_{\mu'} \left( F \left( \frac{g_t(b) - \lambda_t}{g_t(b) - g_t(d)} \mid \mathbb{X}_{[0, s]} \right) \cap \{b, d \in \partial(\Omega \setminus \mathbb{X}_{[0, t]})\} \right) \right| \\
& \leq \mathbb{P} (b \notin \partial(\Omega \setminus \mathbb{X}_{[0, t]}) \text{ or } d \notin \partial(\Omega \setminus \mathbb{X}_{[0, t]})) . \quad (\text{V.11})
\end{aligned}$$

Let us now consider  $|g_t(b)|$  and  $|g_t(d)|$  both large compared with  $\lambda_t$  and  $t$ , which may be enabled by considering  $t$  fixed and  $b, d \rightarrow c$ . In particular, let us define  $b_0 = g_0(b)$  and  $d_0 = g_0(d)$ ; the object  $b_0$  will be our large parameter and since  $b_0 > 0$  while  $d_0 < 0$ , we may as well defined  $d_0$  via  $d_0 = -rb_0$  with  $r > 0$  of order unity. It turns out that  $r = 1$  is slightly peculiar (which is anyway easily understood) and we will assume that this is *not* the case.

Let us observe right now that (for fixed  $t$ ) the right hand side of Equation (V.11) tends to zero as we take  $b_0$  to infinity: Since the capacity of the curve at time  $t$  is, by definition,  $2t$ , it is clear that the image of the curve must stay within a distance  $\approx \sqrt{t}$  of the real axis. The asymptotic expansion for  $g_t(g_0^{-1})$  directly implies that for  $t \ll b_0$ , e.g.,  $b_t \approx b_0$  and hence, the image of the Exploration Process up to time  $t$  under the map  $g_0$  will be forced to cross a box of large aspect ratio, which by (conformal invariance of) Cardy's Formula, tends to zero exponentially like  $e^{-\mathbf{O}(b_0/\sqrt{t})}$ . Hence it is sufficient to complete the proof under the assumption that  $b, d \in \partial\Omega_t$ .

We now carry out the promised asymptotic expansion in  $1/b_0$ . Recall that by the Löwner parameterization in the half plane,  $g_t(g_0^{-1}(z)) = z + 2t/z +$

$\mathbf{O}(1/z^2)$  for  $z \rightarrow \infty$ . Thus,

$$g_t(b) = b_0 + \frac{2t}{b_0} + \dots$$

Therefore (assuming  $b$  and  $d$  are in  $\partial\Omega \setminus \mathbb{X}_{[0,s]}$ ) we may write, for the first term on the left hand side of Eq. (V.11)

$$F \left( \frac{g_t(b) - \lambda_t}{g_t(b) - g_t(d)} \right) = A(r) + B(r) \left[ \frac{\lambda_t}{b_0} \right] + C(r) \left[ \frac{\lambda_t^2 - 6t}{b_0^2} \right] + \mathbf{O}(b_0^{-3}). \quad (\text{V.12})$$

We will need to take expectation of all terms; provided that each term in the expansion is well-defined, we may examine coefficients of various powers of  $b_0$  and draw conclusions. The necessary moment estimates appear in Lemma V.2.11 below.

First let us take expectations and note that Equation (V.7) implies that the average over  $\mathbb{X}_{[0,t]}$  and hence  $\lambda_{[0,t]}$  must provide the same result as in the original setup (corresponding to  $t = 0$ ). This implies, from the first two terms, that

$$\mathbb{E}(\lambda_t) = \lambda_0 = 0 \quad (\text{V.13})$$

and

$$\mathbb{E}(\lambda_t^2 - 6t) = 0. \quad (\text{V.14})$$

Finally, we reiterate that the entirety of  $\mathbb{X}_{[0,t]}$  is determined by  $\lambda_{[0,t]}$  (the history of the driving function up to time  $t$ ). Now, conditioning on  $\mathbb{X}_{[0,s]}$  – which is equivalent to conditioning on  $\lambda_{[0,s]}$  – Equation (V.9) gives us that the conditional expectation of Equation (V.12) must (term by term) give us what we would have gotten with  $s$  replacing  $t$ , namely,

$$\mathbb{E}(\lambda_t \mid \lambda_s) = \lambda_s, \quad \mathbb{E}(\lambda_t^2 - 6t \mid \lambda_s) = \lambda_s^2 - 6s.$$

Therefore both  $\lambda_t$  and  $\lambda_t^2 - 6t$  are continuous martingales, which, by Lévy's characterization of Brownian Motion, implies that  $\lambda_t$  has the law of  $B_{6t}$ . Modulo the moment estimates for  $\lambda_t$ , this completes the proof of the Main Theorem.  $\square$

Finally, as promised, we will now prove an *a priori* estimate on  $\lambda_t$ .

**Lemma V.2.11** (*A priori Estimate*).

$$\mathbb{P}[\lambda_t > n] \leq C_1 \exp\left(-C_2 \frac{n}{\sqrt{t}}\right),$$

for some absolute constants  $C_1$  and  $C_2$ .

To prove Lemma V.2.11 let us first observe that:

**Lemma V.2.12.** *Let  $\gamma(t)$  be the chordal SLE generated by  $\lambda_t$ . Then*

- $\text{Im}(\gamma(t)) \leq 2\sqrt{t}$ .
- $\sup_{s \leq t} |\gamma(s)| \geq \frac{|\lambda_t|}{4}$ .

*Proof.* We remark that the first statement (perhaps with a different constant) can be attained by capacity estimates, but in any case, let us observe that

$$\partial_t(\text{Im}(g_t)) = -2\text{Im}(g_t)/|g_t - \lambda_t|^2 \geq -2/\text{Im}(g_t),$$

so  $\partial_t(\text{Im}(g_t))^2/4 \geq -1$ . Integrating, we get  $(\text{Im}(g_t))^2 \geq (\text{Im}(z))^2 - 4t$ . The conclusion is now clear if we plug in  $z = \gamma(t)$  in the previous expression and note that  $g_t(\gamma(t)) \in \mathbb{R}$ .

For the second part, let us denote  $R_t = \sup_{s \leq t} |\gamma(s)|$ . From e.g., Corollary 3.44 of [19], we have that  $|g_t(z) - z| \leq 3R_t$ , for all  $z \in \mathbb{H} \setminus \gamma([0, t])$ . The result follows by considering  $z = \gamma(t)$  (or an approximating sequence).  $\square$

Now we are in a position to prove Lemma V.2.11.

*Proof of Lemma V.2.11.* On the basis of the above lemma,  $|\lambda_t| > n$  implies that in the half plane a rectangle of aspect ratio of the order  $n/\sqrt{t}$  has been crossed by  $g_0(\gamma_{[0,t]})$ . But this means that  $\gamma_{[0,t]}$  itself crossed a *conformal* rectangle with conformal modulus  $n/\sqrt{t}$ . Invoking Lemma V.2.2, the probability of such an event is bounded by  $C_1 e^{-C_2 \frac{n}{\sqrt{t}}}$  for some  $C_1, C_2 > 0$ .  $\square$

## V.3 Properties of Typical Explorer Paths

We will now provide proofs for the properties of a typical explorer path. Recall that  $\mu_\varepsilon$  is a measure generated by the percolation Exploration Process on the  $\varepsilon$ -lattice scale in a domain  $\Omega$  with two distinguished boundary prime ends  $a$  and  $c$  and  $\mu'$  is any limit point of  $\mu_\varepsilon$  in the weak\*-Hausdorff topology.

### V.3.1 Estimates for Explorer Paths

Here in this subsection, we collect some estimates for the explorer paths deduced from the underlying percolation systems. These estimates represent – at the  $\varepsilon$  level – exactly the behavior that ensures that the limiting objects in the support of  $\mu'$  are precisely Löwner curves. We start with

**Definition V.3.1.** Let  $\Omega$  be a domain. Let  $\delta \gg \eta > 0$  and let  $\gamma : [0, 1] \rightarrow \Omega$  be a parametrized curve. We say that  $\gamma$  has a  $\delta$ - $\eta$  doubleback if there exists disjoint subsegments  $I_1$  and  $I_2$  of  $[0, 1]$ , with  $\text{diam}(\gamma(I_1)) \geq \delta$ ,  $\text{diam}(\gamma(I_2)) \geq \delta$ , and such that the segments  $\gamma(I_1)$  and  $\gamma(I_2)$  are  $\eta$ -close in the sup-norm.

**Lemma V.3.2** (No Doubleback). *Let  $\Omega$  be a domain and let  $\gamma \in \text{supp}(\mu')$ . Let  $\delta, \eta > 0$  satisfy  $\eta < c_1\delta$ , with a particular  $c_1$  of order unity. Then for all  $\delta$  sufficiently small, there are additional constants  $c_2$  and  $c_3$  of order unity such that for all  $\varepsilon$  sufficiently small, the  $\mu_\varepsilon$ -probability of a  $\delta$ - $\eta$  doubleback is bounded above by*

$$\frac{c_2}{\delta^2} \cdot e^{-c_3\delta/\eta},$$

*with the same result inherited by  $\mu'$ .*

*Proof.* It is sufficient to verify the statement in the measures  $\mu_\varepsilon$  for  $\varepsilon$  sufficiently small. Thus let  $\delta \ll 1$  and  $\eta$  small as desired and then  $\varepsilon$  much smaller than the scale set by  $\eta$ . Thus we are back to percolation estimates which reduce to crossing estimates for large boxes. Proofs of similar results have appeared in the literature (many times) before so we shall be succinct. In summary, the probability of a percolation path crossing a fixed box with aspect ratio of order  $\delta : \eta$  is of order  $e^{-[\text{const.}]\delta/\eta}$ . The event in question implies such a crossing (somewhere) and the factor of  $\delta^{-2}$  accounts for all possible locations. We now proceed.

For  $k$  large but of order unity, let us grid the domain  $\Omega$  into pixels of scale  $k^{-1}\delta$ . It's not difficult to see that the event in question necessitates an easy-way  $\eta$ -close double-crossing of some rectangle of this scale with aspect ratio of order unity. Let us now consider a particular such  $\delta : k\delta$  rectangle, denoted by  $R_\delta$  and let us consider the event of at least two disjoint blue crossings of  $R_\delta$  that are within distance  $\eta$  of each other. If  $g_0$  is such a (single) crossing,

let

$$N(g_0) = \{\exists \text{ a blue crossing of } R_\delta$$

in the region *above*  $g_0$  that is within distance  $\eta$  of  $g_0\}$ .

Our first claim is that, uniformly in  $\varepsilon$ , for all  $\varepsilon$  sufficiently small,  $\mathbb{P}(N(g_0)) \leq e^{-c_3 \frac{\delta}{\eta}}$ , for all  $\eta, \delta$ . To see this, let us cover  $g_0$  with disjoint annuli of scale  $3\eta : \eta$ , with the center of each annulus centered on a point of  $g_0$ . Clearly, there are at least of the order  $\delta/\eta$  such annuli. If in the region above  $g_0$ , in any one of these annuli there is a yellow circuit, then  $N(g_0)$  cannot possibly occur. For future reference, we note that in fact these preventative steps take place in the intersection of the relevant annuli with  $R_\delta$ . Since the probability of such a yellow circuit is uniformly positive, we have so far indeed shown that

$$\mathbb{P}(N(g_0)) \leq e^{-c_3 \frac{\delta}{\eta}}.$$

Letting  $\mathbf{G}_0$  denoting the event that  $g_0$  is the lowest crossing, one obtains the same estimate as the above for  $\mathbb{P}(N(g_0) \mid \mathbf{G}_0)$ . The estimates will hold if we now let  $\mathbf{G}_k$  denote the event that the curve  $g_k$  is the  $k^{\text{th}}$  to lowest crossing, e.g., out of a total of  $\ell \geq k$  disjoint crossings. Thus, by subadditivity, conditioned on the existence of say  $\ell$  disjoint crossings, the ultimate double-crossing event of interest has probability bounded above by  $\ell e^{-d_3 \frac{\delta}{\eta}}$ . However, if  $r_\ell$  denotes the probability of  $\ell$  disjoint crossings in  $R_\delta$ , then by a BK-type inequality (which for the model at hand is provided in Lemma V.4.7) it is clear that  $\sum_\ell \ell r_\ell < \infty$ . Hence the probability of two disjoint blue crossings (or two disjoint yellow crossings) in  $R_\delta$  is bounded above by

$$c_2 e^{-c_3 \frac{\delta}{\eta}}. \tag{V.15}$$

To finish we note that there are only of order  $\delta^{-2}$  such rectangles in  $\Omega$  and hence summing over them, we have finished proving the lemma.  $\square$

In the above and in what is to follow, results are shown to hold “uniformly in  $\varepsilon$  for  $\varepsilon$  sufficiently small” – which, ultimately, always follows from scale invariance of the RSW estimates. Hereafter we shall be somewhat less explicit concerning this matter.

**Lemma V.3.3** (Multi-Arm Estimates). *Let  $D(\eta, l)$  denote the circular annulus with inner radius  $\eta$  and outer radius  $l$ . Consider the events of a (i) 5-arm crossing of  $D(\eta, l)$  and (ii) 6-arm crossing of  $D(\eta, l)$ . Then the 5-arm event has probability bounded above by  $(\eta/l)^2$  while the 6-arm event has probability bounded above by  $(\eta/l)^{2+\sigma}$  for some  $\sigma > 0$ .*

*Proof.* Let us rescale back so that the lattice spacing is of order unity and the diameter of  $\Omega_\varepsilon$  is of order  $N$ . Then the five arm event in  $D(\eta, l)$  is the event of five crossings between circles of radius  $\eta N$  and  $lN$ . Approximating by appropriate “square” annular regions, the arguments of [11] may be used in generic circumstances (of course some degree of reflection symmetry for the underlying lattice has to be employed and in addition it has been checked that the fencing/corridor arguments in [11] apply) and so the probability of the five arm event in  $D(\eta, l)$  is bounded above by a constant times  $(\eta/l)^2$ . For the particular percolation model at hand, such issues were dispensed with in the proof of Lemma 7.3 in [11]. To bound the 6-arm event (also the subject of Lemma 7.3 in [11] but not handled with ease) we note that if we let  $A$  denote the event of one crossing in the annular region, then the probability of

$A$  is bounded by  $(\frac{\eta}{l})^\sigma$ , for some  $\sigma > 0$ , by standard Russo–Seymour–Welsh arguments. Then letting  $B$  be the event of 5 crossings in the annular region and applying a BK–type inequality to  $A \circ B$  (which for the model at hand is given as Lemma V.4.7) we obtain the desired result.  $\square$

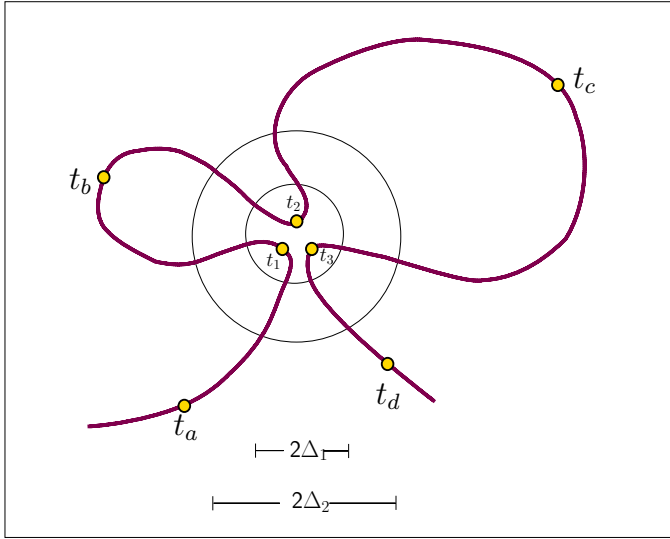
**Definition V.3.4.** Let  $\Delta_2 > \Delta_1$  (with  $\Delta_2 \gg \Delta_1$  envisioned) and let  $\gamma : [0, 1] \rightarrow \Omega$  be a curve. We say that  $\gamma$  has a  $\Delta_2$ – $\Delta_1$  *triple visit* if there are times  $t_a < t_1 < t_b < t_2 < t_c < t_3 < t_d$  such that  $\gamma(t_1), \gamma(t_2)$  and  $\gamma(t_3)$  all lie within a single  $\Delta_1$ –neighborhood while  $\gamma(t_a), \dots, \gamma(t_d)$  each lie a distance at least  $\Delta_2$  from some point in this neighborhood. For an illustration see Figure VI.1(a).

A direct consequence of Lemma VI.2.1 is the absence of triple visits of the type described in the above definition as the ratio  $\Delta_1/\Delta_2$  tends to zero:

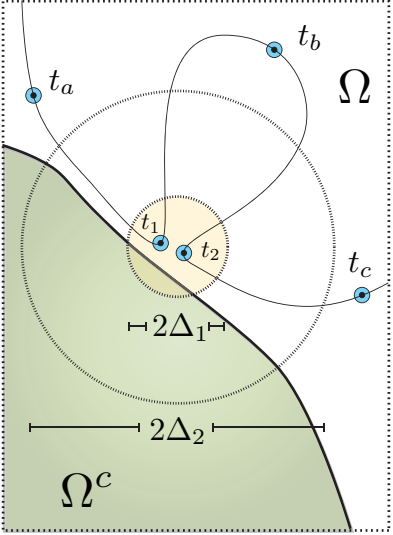
**Lemma V.3.5.** *Let  $\Omega$  be a domain and let  $\Delta_2 \gg \Delta_1 > 0$ . The  $\mu'$ –probability of a  $\Delta_2$ – $\Delta_1$  triple visit tends to zero as  $\Delta_1/\Delta_2 \rightarrow 0$ .*

*Proof.* A quick sketch of a triple visit scenario in  $D(\eta, l)$  yields immediately 6 long disjoint passages of  $\gamma(t)$  across the annulus. Note this can occur in two topologically distinct fashions. For  $\gamma(t)$  a two–sided Exploration Process, naïve counting would yield as many as twelve long arms, but adjacent sides of “disjoint” long arms can lead to sharing of (boundary) elements of the process; in the worst possible case, entire adjacent arms can “collapse”. However, in either topology, even taking into account all these sharings and collapses, we are still left with six genuinely *disjoint* long arms.

We have established, in the continuum or lattice approximation, that the



(a) Triple visit in the interior



(b) Double visit near the boundary

Figure V.1: Atypical behavior of  $\mu_\varepsilon$  curves.

six arm event in an annulus  $D(\eta, l)$  has probability bounded above by  $(\frac{\eta}{l})^{2+\sigma}$ . We may divide  $\Omega$  (or  $\Omega_\varepsilon$ ) into an overlapping grid of scale  $\eta$ . The probability that such an event happens anywhere is therefore bounded above by  $(\eta/l)^{2+\sigma} \left(\frac{1}{\eta^2}\right) = \frac{1}{l^2} \left(\frac{\eta}{l}\right)^\sigma$ , so ultimately, the probability of an actual triple visit is zero and the probability of a  $\Delta_2$ - $\Delta_1$  triple visit indeed tends to zero as  $\frac{\Delta_1}{\Delta_2} \rightarrow 0$ .  $\square$

**Remark V.3.6.** We make the following observation for intrinsic interest and for possible future reference: Observe that in one of the topological alternatives, after the second visit to the inner circle, the Exploration Process can immediately delve into the sack created between this visit and the first. As an *Exploration Process*,  $\gamma(t)$  is now forced to perform its third visit *and* escape  $D(\eta, l)$  altogether. The observation of interest is that these forced future visitation events provide, at least on the level of arm estimates, no additional decay after the (deep) visit into the cul-de-sac. Indeed, six arms are already present at this juncture (all potential additional arms may undergo collapse).

**Definition V.3.7.** Let  $\Omega$  be a domain. Let  $\Delta_2 > \Delta_1$  (with  $\Delta_2 \gg \Delta_1$  envisioned) and let  $\gamma : [0, 1] \rightarrow \Omega$  be a curve. We say that  $\gamma$  has a  $\Delta_2$ - $\Delta_1$  *double visit to the boundary* by the obvious modification of Definition VI.2.2 (using only  $t_a, t_1, t_b, t_2, t_c$  along with the stipulation that at least one of the points  $\gamma(t_1)$  or  $\gamma(t_2)$  is within distance  $\Delta_1$  of  $\partial\Omega$ ). For an illustration see Figure VI.1(b).

**Lemma V.3.8** (No Double Visits Near the Boundary). *For any  $\Delta_2 > 0$ , the probability of a  $\Delta_2$ - $\Delta_1$  double visit to (anywhere on) the boundary tends to zero as  $\Delta_1 \rightarrow 0$ .*

*Proof.* First we observe that if the Exploration Process has a  $\Delta_2$ - $\Delta_1$  double visit to the boundary, then this implies at least a 3-arm event on the scale of  $\Delta_2 : \Delta_1$  near the boundary. This three-arm event can be viewed as the difference of crossing probabilities of certain conformal rectangles, all of which are contained in  $\Omega$ ; the limiting probabilities of these events are therefore *conformally invariant* and, furthermore, can be viewed under a single conformal map.

The problem on the unit disc follows from well-known estimates: If  $\mathcal{N}_{\mathbb{D},p}$  denotes the  $p$  neighborhood of the boundary in  $\mathbb{D}$  then, as  $\varepsilon \rightarrow 0$ , the probability of a three-arm event between  $\mathcal{N}_{\mathbb{D},p_1}$  and  $\mathcal{N}_{\mathbb{D},p_2}^c$  is of the order  $(p_1/p_2)^2$ . For percolation domains with smooth boundaries, this follows from the *a priori*  $1/N^2$  power law estimates described in [1] and [12]. (The idea of proof is straightforward. In brief: Consider the easy way crossing of an  $N$  by  $2kN$  box. This probability is markedly larger than the similar probability in an  $N$  by  $kN$  box with both probabilities of order unity. The difference between these two probabilities can be written as a telescoping sum, with each increment corresponding to a single site distortion, the vast majority of which leading to a three arm event in the half space – the contributions from sites near the boundary are negligible. This implies on the order of  $N^2$  three arm events, each of which can be shown to happen with comparable probability by the rearrangement arguments of Kesten [11]. Since the sum of all these probabilities is of order unity, the result follows).

Let us then consider the uniformization map  $\varphi : \mathbb{D} \rightarrow \Omega$ . We denote by  $p_2 = p_2(\Delta_2, \Omega)$  the distance between  $[\varphi^{-1}(\mathcal{N}_{\Omega, \Delta_2})]^c$  and  $\partial\mathbb{D}$ . Obviously  $p_2$  is

independent of  $\Delta_1$ , therefore it is sufficient that the image of  $\mathcal{N}_{\Omega, \Delta_1}$  is contained in a neighborhood of  $\partial\mathbb{D}$  whose girth vanishes as  $\Delta_1 \rightarrow 0$ . In particular and more than adequate it can be shown that  $f(\mathcal{N}_{\Omega, \Delta_1}) \subset \mathcal{N}_{\mathbb{D}, C(\Omega)\sqrt{\Delta_1}}$ : Indeed, by the Bieberbach Distortion theorem,  $|\varphi'(z)| \geq |\varphi'(0)|(1 - |z|)/4$ . By the Koebe 1/4-theorem,  $\text{dist}(\varphi(z), \partial\Omega) \geq 1/4(1 - |z|)|\varphi'(z)| \geq 1/16|\varphi'(0)|(1 - |z|)^2$ . This implies the required estimate with  $C(\Omega) = 4/\sqrt{|\varphi'(0)|}$ .

□

**Remark V.3.9.** The above estimates apply equally to the situation when the tip of the Exploration Process has “just” performed a double visit; i.e., the time  $t_c$  in Definition VI.2.6 is in fact superfluous. This situation is analogous to the forced future triple visitations discussed in Remark VI.2.4. As in these cases, the ostensible extra arms that the continuation of the journey might generate are susceptible to collapse and cannot be counted, while the estimates are already sufficient without these arms.

### V.3.2 Limit is Supported on Löwner Curves

Here we provide a proof of Lemma V.2.3, i.e., any limit point of the  $\mu_\varepsilon$ 's is supported on Löwner curves. Our proof will utilize three additional lemmas, but first we must discuss crosscuts.

As alluded to several times before, we envision  $\Omega$  as the conformal image of the upper half plane via some map  $\phi : \mathbb{H} \rightarrow \Omega$ . The prime end  $a$  is defined in the usual fashion as the set of all limit points of sequences  $\phi(z_n)$ ,  $z_n \rightarrow z_a$ , where  $z_a \in \mathbb{R}$  is fixed. Alternatively, consider

$$A_k = \overline{\phi(\{|z - z_a| \leq 1/k, \text{Im}z > 0\})},$$

then the prime end  $a$  can be defined as  $\cap_k A_k$ . We define similar quantities for  $c$  and call them  $C_k$ . Finally let us also define  $\gamma_\varepsilon^k$  to be the curve formed by  $\gamma_\varepsilon$  from the last exit from  $A_k$  to the first entrance into  $C_k$  after this last exit from  $A_k$  (here  $\gamma_\varepsilon$  denotes a generic  $\mu_\varepsilon$  curve). We remark that for finite  $k$ , with non-zero probability,  $\gamma_\varepsilon$  will form multiple crossings of the region  $\Omega_k \equiv \Omega \setminus (A_k \cup C_k)$ , but this probability tends to zero as  $k \rightarrow \infty$ , as can be seen by applying Cardy's Formula (or by using Russo–Seymour–Welsh type arguments, c.f. the proof of Lemma V.2.4).

**Lemma V.3.10.** *Consider the domain  $\Omega_k$  and let  $\mu'_k$  be a limit point of the measures on the curves  $\gamma_\varepsilon^k$ . Then the  $\mu'_k$ 's are supported on Hölder continuous curves. Moreover, the weak convergence to  $\mu'_k$  can be taken with respect to the topology defined by the sup-norm distance between curves.*

*Proof.* These claims follow from the result of [2]. We claim that on  $\Omega_k$ , the curves  $\{\gamma_\varepsilon^k\}$  satisfy hypothesis H1 of [2], namely: The probability of multiple crossings of circular shells (intersected with  $\Omega_k$ ) goes to zero as the multiplicity gets large. This is clear if we consider circular shells with the outer radius sufficiently small, dependent on  $k$ . Indeed, for  $R$  less than some  $R_k$ , there is no possibility of both blue and yellow boundary inside  $\Omega_k$  intersected with the corresponding circular shell. Thus we must only rule out many crossings of  $\gamma_\varepsilon^k$  of the circular shell either in the presence of no boundary or in the presence of a monochrome boundary – with the rate of decay which increases to infinity with the number of traversals. These estimates follow from straightforward repeated applications of the BK type inequality, which, for the model at hand, is proved in Lemma V.4.7. □

For the next lemma, we need another definition. We say that we have a *jump* of magnitude (at least)  $\ell$  if

$$\gamma_\varepsilon^{k+\ell} \cap (\Omega_\varepsilon \setminus (A_k \cup C_k)) \neq \gamma_\varepsilon \cap (\Omega_\varepsilon \setminus (A_k \cup C_k)).$$

For an illustration see Figure V.2.

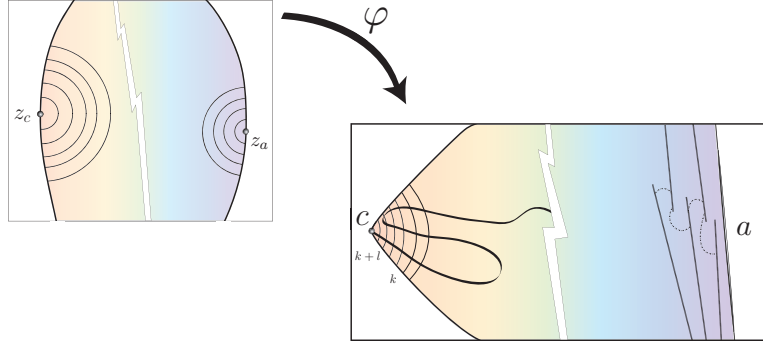


Figure V.2: A jump of magnitude  $l$  occurring in the vicinity of the prime end  $c$ .

**Lemma V.3.11.** *For every  $k$ , as  $\varepsilon \rightarrow 0$ , the magnitude of the jumps stay bounded with probability one.*

*Proof.* The modulus of the conformal rectangle  $(A_k \setminus A_{k+\ell})^\circ$  tends to infinity as  $\ell \rightarrow \infty$  (with  $\ell \gg k$  envisioned). We observe that in the event of a jump there must be a crossing of this conformal rectangle. As  $\varepsilon \rightarrow 0$ , we may utilize Cardy's formula to show that the probability of such a crossing is bounded by some constant  $\delta_{k,\ell}$  which tends to zero as  $\ell \rightarrow \infty$ , i.e., as  $\varepsilon \rightarrow 0$ , the probability of jumps of unbounded magnitude is zero. Analogous arguments hold for the  $C_k$ 's. □

We are now ready to prove that  $\mu'$  is supported on Löwner curves.

*Proof of Lemma V.2.3.* We first establish that any limiting measure  $\mu'$  is supported on curves from  $a$  to  $c$ . By Lemma V.3.11, a  $\mu'$  generic set intersected with  $\Omega \setminus (A_k \cup C_k)$  is the same as  $\mu'_{k+\ell}$  generic curves (these objects are curves by Lemma V.3.10) intersected with  $\Omega \setminus (A_k \cup C_k)$  for some  $\ell$ . The family of domains  $\Omega \setminus (A_k \cup C_k)$  is monotone and exhaustive, and hence  $\mu'$  is concentrated on curves. By Lemma V.3.11 again, these curves are crosscuts from  $a$  to  $c$ .

To show that these are Löwner crosscuts it is enough to show that they almost surely satisfy conditions (L1) and (L2). Consider a parametrization of  $\gamma$  with non-vanishing speed. It is not difficult to see that a violation of (L1) implies that there exists some point  $z_0$  which is visited at least three times if  $z_0$  is in the bulk or twice if  $z_0$  is on the boundary. We remind the reader that this is in the continuum; at the lattice level, our collisions could represent approaches which are microscopically large but macroscopically small e.g., a sublinear power of  $N$ .

Such an encounter in the interior leads to a triple visit and thus has vanishing probability, by Corollary VI.2.3. If  $z_0$  is  $\eta(\varepsilon)$ -close to the boundary,  $\eta \rightarrow 0$ , violation of (L1) implies a double visit below/at  $z_0$ . As  $\varepsilon \rightarrow 0$ , this has vanishingly small probability, by Lemma VI.2.6. Finally, a violation of (L2) is equivalent to the existence of some severe doubling back (e.g. at scales  $\delta(\varepsilon)$ ,  $\eta(\varepsilon)$ , with  $\eta/\delta \rightarrow 0$ ), as defined in Definition VI.2.8 and therefore is forbidden by Lemma VI.2.9. □

We are now prepared to define the **Dist** function alluded to in the previous section.

**Definition V.3.12.** Let  $\lambda_\ell > 0$  be fixed numbers that satisfy  $\sum_\ell \lambda_\ell = 1$ , e.g.,  $\lambda_\ell = 2^{-\ell}$ . If  $\gamma_r$  and  $\gamma_g$  are two curves in  $\Omega$  from  $a$  to  $c$ , we denote, as before,  $\gamma_r^\ell$  (or  $\gamma_r^{\ell,\varepsilon}$ ) the appropriate portion of the curve in  $\Omega_\ell$ , etc. Let  $d_\ell(\gamma_r, \gamma_g)$  denote the usual sup norm distances between  $\gamma_r^\ell$  and  $\gamma_g^\ell$ . Then we define

$$\mathbf{Dist}(\gamma_r, \gamma_g) = \sum_\ell \lambda_\ell d_\ell(\gamma_r, \gamma_g).$$

As a corollary, we have weak\* convergence of  $\mu^\varepsilon$  to  $\mu'$  with respect to the topology provided by the **Dist** norm:

*Proof of Lemma V.2.5.* For any finite  $k$ , we have by the result of [2] that  $\mu'_k$  is the weak\* sup–norm limit of the objects  $\mu_{k,\varepsilon}$ , which are measures on the curves  $\{\gamma_\varepsilon^k\}$ . It only remains to be seen that once two curves in  $\Omega_k$  are close for  $k$  large, then they remain close uniformly in  $k$ , but this is a property which follows directly from the definition of **Dist**. □

### V.3.3 Preservation of $M(\partial\Omega) < 2$

Here we show that if we start with some domain  $\Omega$  with boundary Minkowski dimension less than two, then the Exploration Process also yields a curve with Minkowski dimension less than two.

*Proof of Lemma V.2.4.* Let  $z \in \text{Int}(\Omega)$  and  $g_\delta(z)$  the box of radius  $\delta$  surrounding  $z$  and  $D(z)$  denote the distance between  $z$  and  $\partial\Omega$ . We claim that there is some  $\psi > 0$  such that for all  $\varepsilon$  sufficiently small,

$$\mathbb{P}_\varepsilon(\mathbb{X}_t^\varepsilon \in g_\delta(z)) < C_2 \left(\frac{\delta}{D}\right)^\psi$$

where  $C_2$  is a constant.

This follows from Russo–Seymour–Welsh theory, which we do here in some detail. Indeed, if  $r < s$ , let  $A_{s,r}(z) \equiv B_s(z) \setminus B_r(z)$  denote the annulus centered at  $z$ , where, if necessary, the sides are approximated, within  $\varepsilon$ , by the lattice structure. Assume temporarily that  $A_{s,r}(z) \subset \text{Int}(\Omega)$ . Clearly, if there is both a yellow and a blue ring in  $A_{s,r}$ , then  $\mathbb{X}_t^\varepsilon$  cannot possibly visit  $B_r(z)$  (since the yellow portion of  $\mathbb{X}_t^\varepsilon$  cannot penetrate the blue ring and similarly with yellow  $\leftrightarrow$  blue). Now by the Russo–Seymour–Welsh estimates alluded to (Theorem 3.10, item (iii) in [11] for the model at hand) the probability of a blue ring in  $A_{M,\lambda M}$  is bounded below uniformly in  $\varepsilon$  by a strictly positive constant that depends only on  $\lambda$ . Let  $\eta > 0$  denote a lower bound on the probability that in  $A_{4L,3L}$  there is a blue ring and in  $A_{3L,2L}$  a yellow. Now let  $k$  satisfy  $2^k > \varepsilon^{-1}D > 2^{k-1}$  and similarly  $2^\ell > \varepsilon^{-1}\delta > 2^{\ell-1}$ . Then, give or take, there are  $k - \ell$  independent annuli in which the pair of rings described can occur. The probability that all such ring pair events fail is less than  $C_1(1 - \eta)^{k-\ell} \leq C_2 \left(\frac{\delta}{D}\right)^\psi$ , where  $C_1$  and  $C_2$  are constants and  $\psi > 0$  is defined via  $\eta$ .

Let us fix a square grid of scale  $\delta$  with  $\varepsilon \ll \delta \ll 1$ . Let  $\mathcal{N}_\delta$  denote the number of boxes of scale  $\delta$  that are visited by the process. We claim that for all  $\varepsilon$  sufficiently small

$$\mathbb{E}_\varepsilon(\mathcal{N}_\delta) \leq C_{\psi'} \left(\frac{1}{\delta}\right)^{2-\psi'} = C_{\psi'} n^{2-\psi'}, \quad (\text{V.16})$$

where  $\psi' > 0$  is a constant and  $n = n_\delta = \delta^{-1}$  represents the characteristic scale of  $\Omega$  on the grid of size  $\delta^{-1}$ . In particular we may take  $\psi' < \min\{\psi, \theta\}$ , where  $\theta \in [0, 1]$  describes the roughness of the boundary:  $M(\partial\Omega) = 2 - \theta$ .

Let  $n_k$  denote the number of boxes a distance  $k\delta$  (i.e.,  $k$  boxes distant)

from  $\partial\Omega$  and

$$N_l = \sum_{k \leq l} n_k.$$

Our first claim is that for all  $\delta$ ,

$$N_l < C_{\theta'} n^{2-\theta'} l^{\theta'}, \quad (\text{V.17})$$

for any  $\theta' < \theta$ , where  $C_{\theta'}$  is a constant. To see this, let us estimate the total area of boxes on a grid of size  $\sigma$  intersected by or within one unit of  $\partial\Omega$ . It is not hard to see that this is bounded by  $C_{\theta'} \times \left(\frac{1}{\sigma}\right)^{2-\theta'} \times \sigma^2 = C_{\theta'} \sigma^{\theta'}$ , where  $C_{\theta'}$  is a constant which is uniform for a fixed  $\theta' < \theta$ . Taking  $\sigma = l\delta$  and noting that *these* boxes contain all of the  $n_1 + \dots + n_l$  boxes of scale  $\delta$  (i.e., boxes within  $l$  units of  $\partial\Omega$ ), the claim follows.

Now, clearly,

$$\mathbb{E}_\varepsilon(\mathcal{N}_\delta) \leq C_2 \sum_{k=1}^{l_{\max}} n_k \cdot \left(\frac{1}{k}\right)^\psi.$$

Let us now dispense with the sum in the display. Summing by parts, we get

$$\sum_{k=1}^{l_{\max}} n_k \left(\frac{1}{k}\right)^\psi = N_{l_{\max}} l_{\max}^{-\psi} + \sum_{k=1}^{l_{\max}-1} N_k \left(\frac{1}{k^\psi} - \frac{1}{(k+1)^\psi}\right).$$

Now if  $\psi > \theta$ , then  $\psi > \theta'$ . Using Eq. (VI.4) and pulling out an  $n^{2-\theta'}$ , the sum is convergent. Meanwhile, the first term (again using the estimate in Eq. (VI.4)) is smaller. Conversely, if  $\psi \leq \theta$ , then both terms are of order  $n^{2-\theta'} l_{\max}^{\theta'-\psi}$  and the result follows if we take  $l_{\max} = n$ . It is re-emphasized that the estimate in Eq. (VI.3) is uniform in  $\varepsilon$ ; by further sacrifice of the constant, we may claim that Eq. (VI.3) holds for all box-scales in the range  $[\delta, 2\delta]$ .

The remaining argument is now immediate. Letting  $\delta_k = 2^{-k}$  we have that for any  $\delta \in [\delta_{k+1}, \delta_k]$  and  $s > 0$

$$\mathbb{P}_\varepsilon(\mathcal{N}_\delta > C_{\psi'} n_\delta^{2-\psi'+s}) \leq \frac{1}{2^{ks}}. \quad (\text{V.18})$$

The result follows, for any  $s > 0$ , by taking  $\varepsilon \rightarrow 0$  and summing over  $k$ .  $\square$

## V.4 The Model

### V.4.1 Review of Model

Here we give a quick description of the model under study. For more details see Section 2.2 of [11]. The model takes place on the hexagon tiling of the 2D triangular site lattice: hexagons are yellow, blue and sometimes split; half and half. Connectivity for us is defined by adjacent shapes (of the same color) sharing an edge segment in common. Our description of the model starts with a particular local arrangement of hexagons:

**Definition V.4.1.** A *flower* is the union of a particular hexagon with its six neighbors. The central hexagon we call an *iris* and the outer hexagons we call *petals*. We number the petals from 1 to 6, starting from the one directly to the right of the iris. All hexagons which are not flowers will be referred to as *filler*.

Let  $\Omega \subset \mathbb{C}$  be a domain, which for simplicity we may regard as being a finite connected subset of the hexagon lattice. A *floral arrangement*, symbolically denoted  $\Omega_{\mathfrak{F}}$ , is a designation of certain hexagons as irises (this determines the flowers). There are three restrictions on placement of irises: (i) no iris is a boundary hexagon, (ii) there are at least two non-iris hexagons between each pair of irises, and (iii) ultimately in infinite volume the irises have a periodic structure with  $60^\circ$  symmetries.

We are now ready to define the statistical properties of our model.

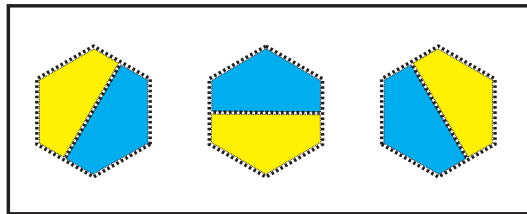


Figure V.3: The three allowed “split” states of the hexagon. Note that these correspond to single bond occupancy events in the corresponding up-pointing triangle in the bond-triangular lattice percolation problem.

**Definition V.4.2.** Let  $\Omega$  be a domain with floral arrangement  $\Omega_{\mathfrak{F}}$ .

- Petals and hexagons in the complement of flowers are only allowed to be blue or yellow, each with probability  $1/2$ .
- For “most” configurations of petals, irises can be blue, yellow, or mixed (one of three ways c.f., Figure V.3) with probabilities  $a$ ,  $a$ , or  $s$ , so that  $2a + 3s = 1$  and in addition,

$$a^2 \geq 2s^2.$$

- The exceptional configurations of petals, which we call *triggers*, are configurations where there are three yellow and three blue petals, with one pair of blue (and hence also yellow) petals contiguous. In these configurations, the irises can now only be blue or yellow, each with probability  $1/2$ .

Note that triggering is the only source of (very short range) correlation in this model; everything else is configured independently. It is worth noting that for each floral arrangement, we have a one-parameter family of critical models with  $s = 0$  reducing to the usual site percolation on the triangular lattice.

Finally, it is remarked that the total of five possible configurations on a hexagon correspond to the eight possible configurations on (up-pointing) triangles – of which there are five distinct connectivity classes. It is not hard to see, by checking local connectivity properties, that the model described is a representation of a correlated percolation model on the triangular bond lattice.

It was shown in [11] Theorem 3.10 that our model exhibits all the typical properties of a 2D percolation model at criticality. Cardy’s formula for this model was the main result of [11] (Theorem 2.4). More specifically, let  $\Omega \subset \mathbb{C}$  be a domain with piecewise smooth boundary which is conformally equivalent to a triangle. Let us denote the three boundaries and “prime ends” of interest by  $\mathcal{A}, c, \mathcal{B}, a, \mathcal{C}, b$ , in counterclockwise order. We endow  $\Omega$  with an approximate discretization (with hexagons) on a lattice of scale  $\varepsilon = 1/N$  and a floral arrangement  $\Omega_{\mathfrak{F}_\varepsilon}$ . Let  $z$  be the vertex of a hexagon in  $\Omega_{\mathfrak{F}_\varepsilon}$ . We define the discrete crossing probability function  $u_\varepsilon^Y(z)$  to be the indicator function of the event that there is a blue path connecting  $\mathcal{A}$  and  $\mathcal{B}$ , separating  $z$  from  $\mathcal{C}$ , with similar definitions for  $v_\varepsilon^Y(z)$  and  $w_\varepsilon^Y(z)$  and the blue versions of these functions. Then taking the scaling limit in an appropriate fashion (for more details see Section 2.3 of [11]), we have, e.g.

$$\lim_{\varepsilon \rightarrow 0} u_\varepsilon^Y = u,$$

where  $u$  is one of the so-called Carleson–Cardy function: It is harmonic, and on the up-pointing equilateral triangle with base  $\mathcal{C}$  being the unit interval, it is equal to  $\frac{2}{\sqrt{3}} \cdot y$  – this is equivalent to Cardy’s formula. The functions  $v$  and  $w$  are defined similarly.

## V.4.2 The Exploration Process

We now give a (microscopic) definition of the percolation Exploration Process tailored to our system at hand. We must start with a precise prescription of how to construct our domains. Let  $\Omega$  be a domain as described. Let  $a$  and  $c$  be two prime ends and consider hexagons of the  $\varepsilon$ -tiling of  $\mathbb{C}$ . It is assumed that within this tiling (with fixed origin of coordinates) the locations of all irises/flowers/fillers are predetermined. We define  $\Omega_\varepsilon$  to be the union of all fillers and flowers whose closure lies in the interior of  $\Omega$ . It is assumed that  $\varepsilon$  is small enough that both  $a$  and  $c$  are in the same lattice connected component of the tiling. Other components, if any, will not be discarded but will only play a peripheral rôle. With the exception of flowers, the boundary of the domain will be taken as the usual internal lattice boundary, which consists of the points of the set which have neighbors not belonging to the set. If the lattice boundary cuts through a flower, then the whole flower is included as part of the boundary. The notation for this lattice boundary will be  $\partial_\varepsilon\Omega_\varepsilon$ .

Consider points  $a_\varepsilon, c_\varepsilon$  which are on  $\partial_\varepsilon\Omega_\varepsilon$  and are vertices of hexagons. We call  $(\Omega_\varepsilon, \partial\Omega_\varepsilon, a_\varepsilon, c_\varepsilon)$  *admissible* if

- $\Omega_\varepsilon$  contains no partial flowers.
- $\partial_\varepsilon\Omega_\varepsilon$  can be decomposed into two lattice connected sets consisting of hexagons and/or halves of boundary irises, one of which is colored blue and one of which is colored yellow, such that  $a_\varepsilon$  and  $c_\varepsilon$  lie at the points where the two sets join and such that the blue and yellow paths are valid paths following the connectivity and statistical rules of our model; in

particular, the coloring of these paths do not lead to flower configurations that have probability zero.

- $a_\varepsilon$  and  $c_\varepsilon$  lie at the vertices of hexagons, such that of the three hexagons sharing the vertex, one of them is blue, one of them is yellow, and the third is in the interior of the domain. (See Figure V.4.)

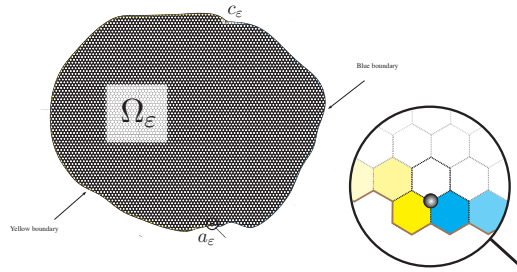


Figure V.4: The setup for the definition of the Exploration Process.

We remark that in the case of boundary flowers (and other sorts of clusters on the boundary) it is not necessary to color *all* the hexagons/irises. Indeed the coloring scheme need not be unique – it is only required that a boundary coloring of the requisite type can be selected.

It is not hard to see that the domains  $(\Omega_\varepsilon, \partial_\varepsilon \Omega_\varepsilon, a_\varepsilon, c_\varepsilon)$  converges to  $(\Omega, \partial\Omega, a, c)$  in the sense that  $\partial_\varepsilon \Omega_\varepsilon$  and  $\Omega_\varepsilon$  converge respectively to  $\partial\Omega$  and  $\Omega$  in the Hausdorff metric and in the Caratheodory metric with respect to any point inside  $\Omega$ . Also, there exists  $a_\varepsilon$  and  $c_\varepsilon$  which converge respectively to  $a$  and  $c$  as  $\varepsilon \rightarrow 0$ . Notice that the latter convergence is really in terms of the preimages under the uniformization map of the relevant domain. In some sense we have chosen the “simplest” discretization scheme, which, in the companion work [6] will be called the *canonical* approximation; of course other discretizations are

possible, but in the interest of brevity we shall not discuss these in the present work.

Geometrically, the *Exploration Process* produces, in any percolation configuration on  $\Omega_\varepsilon$ , the unique interface connecting  $a_\varepsilon$  to  $c_\varepsilon$ , i.e., the curve separating the blue lattice connected cluster of the boundary from that of the yellow. We denote this interface by  $\gamma_\varepsilon$ . Dynamically, the exploration *process* is defined as follows: Let  $\mathbb{X}_0^\varepsilon = a_\varepsilon$ . Given  $\mathbb{X}_{t-1}^\varepsilon$ , it may be necessary to color new hexagons in order to determine the next step of the process. (In particular,  $\mathbb{X}_{t-1}^\varepsilon$  is “usually” at the vertex of a hexagon which has not yet been colored.) We color any necessary undetermined hexagons according to the following rules:

- If the undetermined hexagon is a filler hexagon, we color it blue or yellow with probability  $1/2$ .
- If the undetermined hexagon is a petal or an iris, we color it blue or yellow or mixed with the conditional distribution given by the hexagons of the flower which are already determined.
- If a further (petal) hexagon is needed, it is colored according to the conditional distribution given by the iris and the other hexagons of the flower which have already been determined.

We are now ready to describe how to determine  $\mathbb{X}_t^\varepsilon$ :

- If  $\mathbb{X}_{t-1}^\varepsilon$  is not adjacent to an iris,  $\mathbb{X}_t^\varepsilon$  will be equal to the next hexagon vertex we can get to in such a way that blue is always on the right of the segment  $[\mathbb{X}_{t-1}^\varepsilon, \mathbb{X}_t^\varepsilon]$ .

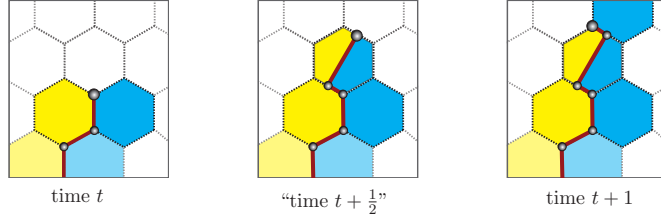


Figure V.5: “Multistep” procedure by which the Exploration Process gets through a mixed hexagon.

- If  $\mathbb{X}_{t-1}^\varepsilon$  is adjacent to an iris, then the state of the iris is determined as described above, after which the exploration path can be continued (keeping blue on the right) until a petal is hit. The color of the petal will now be determined (according to the proper conditional distribution) and  $\mathbb{X}_t^\varepsilon$  will equal one of the two possible vertices common to the iris and the new petal which keeps the blue region to the right of the final portion of the segments joining  $\mathbb{X}_{t-1}^\varepsilon$  to  $\mathbb{X}_t^\varepsilon$ .

In particular, it is noted that at the end of each step, we always wind up on the vertex of a hexagon (see Figure V.5). We denote by  $(\gamma_\varepsilon)_t$  the actual value taken by the random variable  $\mathbb{X}_t^\varepsilon$ .

We state without proof some properties of our Exploration Process.

**Proposition V.4.3.** *Let  $\gamma_\varepsilon([0, t])$  be the line segments formed by the process up till time  $t$ , and  $\Gamma_\varepsilon([0, t])$  the hexagons revealed by the Exploration Process. Let  $\partial_\varepsilon \Omega_\varepsilon^t = \partial_\varepsilon \Omega_\varepsilon \cup \Gamma_\varepsilon([0, t])$  and let  $\Omega_\varepsilon^t = \Omega_\varepsilon \setminus \Gamma_\varepsilon([0, t])$ . Then, the quadruple  $(\Omega_\varepsilon^t, \partial_\varepsilon \Omega_\varepsilon^t, \mathbb{X}_t^\varepsilon, c_\varepsilon)$  is admissible. Furthermore, the Exploration Process in  $\Omega_\varepsilon^t$  from  $\mathbb{X}_t^\varepsilon$  to  $c_\varepsilon$  has the same law as the original Exploration Process from  $a_\varepsilon$  to  $c_\varepsilon$  in  $\Omega_\varepsilon$  conditioned on  $\Gamma_\varepsilon([0, t])$ .*

### V.4.3 A Restricted BK–Inequality

Here we will prove an inequality that will be needed for proofs in several other places.

Suppose  $A$  and  $B$  are two events. Then the BK inequality [5] states that (for suitable probability spaces) the probability of the *disjoint* occurrence of  $A$  and  $B$  is bounded above by the product of their probabilities. The most general version of this is Reimer’s inequality [24] (see also [8] for more background and a self-contained proof), which holds for arbitrary product probability spaces. For the model at hand, we do not have a product probability space; Reimer’s inequality would, in the present context, yield the desired result only for *flower* disjoint events. Unfortunately, we have need of a stronger statement; specifically, for disjoint path-type events where the individual paths may use the same flower. In fact, as the following example demonstrates, a general BK inequality does not hold in our system. However, as we later show, an abridged version holds for path-type events.

**Example V.4.4.** Let  $A$  be the event of a blue connection between petals 1, 4, and 5 (without any requirement on the color of the petals 1, 4, and 5), and let  $B = \{\text{petals 1, 4, 5 are blue}\}$ . Observe that  $B$  and  $B^c$  are defined entirely on the petals 1, 4, 5, whereas  $A$  is defined on the complementary set. Therefore we have  $A \cap B^c = A \circ B^c$ . By Example 6.1 of [11], we know that  $\mathbb{P}(A \cap B) < \mathbb{P}(A)\mathbb{P}(B)$ . But this immediately implies that  $\mathbb{P}(A \circ B^c) > \mathbb{P}(A)\mathbb{P}(B^c)$ .

Before tending to the detailed analysis of flowers, let us first introduce the notion of disjoint occurrence for non-negative random variables.

**Definition V.4.5.** Let  $a_i, b_j \geq 0$  and let

$$X = \sum_1^n a_i \mathbf{1}_{A_i}, \quad Y = \sum_1^m b_j \mathbf{1}_{B_j},$$

where  $A_i \cap A_k = \emptyset$  for  $i \neq k$  and  $B_j \cap B_l = \emptyset$  for  $j \neq l$ . We define

$$X \circ Y = \sum_{i,j} a_i b_j \mathbf{1}_{A_i \circ B_j}.$$

If the usual BK inequality holds then linearity immediately gives

$$\mathbb{E}(X \circ Y) \leq \mathbb{E}(X)\mathbb{E}(Y).$$

We will be working with this slight generalization; what we have in mind is the hexagon disjoint occurrence of paths, and in the case of paths of different colors, sharing of the iris may occur. To be precise, we have the following definition:

**Definition V.4.6.** Let  $\Omega_{\mathfrak{F}}$  denote a flower arrangement and let  $S$  and  $T$  denote sets in  $\Omega_{\mathfrak{F}}$  which contain no irises. Let  $X_{S,T}^b$  denote the indicator of the event that all hexagons in  $S$  and  $T$  are blue and that there is a blue path – possibly including irises – connecting  $S$  and  $T$ . Similarly we define  $X_{S,T}^y$  to be the yellow version of this event. Now if  $S'$  and  $T'$  are two other sets of  $\Omega_{\mathfrak{F}}$  which are disjoint from  $S$  and  $T$  and also do not contain irises, then we may define  $X_{S,T}^b \circ X_{S',T'}^b$  in accord with the usual fashion. However, for present purposes, in the event corresponding to  $X_{S,T}^b \circ X_{S',T'}^y$ , the two paths may share a mixed iris.

**Lemma V.4.7.** Let  $X_{S_1,T_1}^{\ell_1}, X_{S_2,T_2}^{\ell_2}, \dots, X_{S_n,T_n}^{\ell_n}$  be the indicator functions of path-type events as described in Definition V.4.6, where  $\ell_i \in \{b, y\}$ , then

$$\mathbb{E}(X_{S_1,T_1}^{\ell_1} \circ X_{S_2,T_2}^{\ell_2} \circ \dots \circ X_{S_n,T_n}^{\ell_n}) \leq \mathbb{E}(X_{S_1,T_1}^{\ell_1})\mathbb{E}(X_{S_2,T_2}^{\ell_2}) \dots \mathbb{E}(X_{S_n,T_n}^{\ell_n}).$$

*Proof.* Our proof is slightly reminiscent of the proof of Lemma 6.2 in [11]. Let  $\sigma$  denote a configuration of petals and filler and let  $I$  denote a configuration of irises. We will use induction; first we prove the statement for the case of exactly one flower (i.e., supposing there is only one flower in all of  $\Omega_{\mathfrak{F}}$ ) and two path events, whose indicator functions we denote by  $X$  and  $Y$ . We write

$$\mathbb{E}(X \circ Y) = \mathbb{E}_{\sigma}[\mathbb{E}_I(X \circ Y|\sigma)].$$

If we can show that  $\mathbb{E}_I(X \circ Y|\sigma) \leq \mathbb{E}_I(X|\sigma) \circ \mathbb{E}_I(Y|\sigma)$ , then we may apply the BK-inequality to the outer expectation to yield the desired result since, on the outside, the measure is independent. It is clear that the function  $\mathbb{E}(X \circ Y|\sigma)$  can only take on five different values; we write

$$\begin{aligned} \mathbb{E}(X \circ Y|\sigma) &= 1 \cdot \mathbf{1}_{\mathcal{O}(X \circ Y)}(\sigma) \\ &\quad + (a + s) \cdot \mathbf{1}_{A_1(X \circ Y)}(\sigma) \\ &\quad + (1/2) \cdot \mathbf{1}_{A_2(X \circ Y)}(\sigma) \\ &\quad + (a + 2s) \cdot \mathbf{1}_{A_3(X \circ Y)}(\sigma) \\ &\quad + s \cdot \mathbf{1}_{\mathcal{F}(X \circ Y)}(\sigma), \end{aligned} \tag{V.19}$$

where e.g.

$$\mathcal{O}(X \circ Y) = \{\sigma \mid \mathbb{E}(X \circ Y|\sigma) = 1\}.$$

It is not difficult to see that  $\mathcal{O}(X \circ Y)$  is the set of  $\sigma$  configurations where  $X \circ Y$  has occurred on the complement of the iris. The remaining terms warrant some discussion. We first point out that these terms correspond to configurations where the flower is pivotal for the achievement of at least one of  $X$  and  $Y$ , and, due to the nature of the events in question, petal arrangements in these configurations satisfy certain constraints. For instance, configurations

in  $A_3$  must exhibit a petal arrangement such that one of the paths is in a position where it must transmit through the iris, which can be accomplished by the preferred color or two of the split configurations; the flower must *not* be in a triggering configuration and, needless to say, the other path has already occurred (independent of the iris).

Finally we observe that  $\sigma \in \mathcal{F}(X \circ Y)$  implies that both paths must use the iris and therefore can only occur when the paths in question have different colors. It is not hard to see, via petal counting, that  $\mathcal{F}(X \circ Y)$  forces the alternating configuration of petals and that indeed, we have a situation of a “parallel transmission” through the iris, with exactly one iris configuration which achieves both desired transmissions. We also note that in similar expressions for  $\mathbb{E}(X|\sigma)$  and  $\mathbb{E}(Y|\sigma)$ , the corresponding terms  $\mathcal{F}(X)$  and  $\mathcal{F}(Y)$  will be empty, since e.g., if the path is blue and some iris is capable of achieving the transmission, then certainly the pure blue iris will achieve the transmission.

Let us expand  $\mathbb{E}(X|\sigma) \circ \mathbb{E}(Y|\sigma)$  in the sense defined above:

$$\begin{aligned}
\mathbb{E}(X|\sigma) \circ \mathbb{E}(Y|\sigma) &= 1 \cdot \mathbf{1}_{\mathcal{O}(X) \circ \mathcal{O}(Y)}(\sigma) \\
&\quad + (a + s) \cdot [\mathbf{1}_{\mathcal{O}(X) \circ A_1(Y)}(\sigma) + \mathbf{1}_{A_1(X) \circ \mathcal{O}(Y)}(\sigma)] \\
&\quad + (1/2) \cdot [\mathbf{1}_{\mathcal{O}(X) \circ A_2(Y)}(\sigma) + \mathbf{1}_{A_2(X) \circ \mathcal{O}(Y)}(\sigma)] \\
&\quad + (a + 2s) \cdot [\mathbf{1}_{\mathcal{O}(X) \circ A_3(Y)}(\sigma) + \mathbf{1}_{A_3(X) \circ \mathcal{O}(Y)}(\sigma)] \\
&\quad + (a + s)^2 \cdot [\mathbf{1}_{A_1(X) \circ A_1(Y)}(\sigma)] \\
&\quad + \mathcal{R}(a, s, \sigma),
\end{aligned} \tag{V.20}$$

where  $\mathcal{R}(a, s, \sigma)$  contains all the remaining terms in the expansion, e.g. the terms

$$(1/2)(a + s) \cdot [\mathbf{1}_{A_1(X) \circ A_2(Y)}(\sigma) + \mathbf{1}_{A_2(X) \circ A_1(Y)}(\sigma)] \tag{V.21}$$

and

$$(a + s)(a + 2s) \cdot [\mathbf{1}_{A_1(X) \circ A_3(Y)}(\sigma) + \mathbf{1}_{A_3(X) \circ A_1(Y)}(\sigma)]. \quad (\text{V.22})$$

We claim that Eq.(V.21) will evaluate to zero for each  $\sigma$ : In the first term,  $A_1(X)$  requires that the petals exhibit a configuration which precludes a trigger and  $A_2(Y)$  requires the petals to exhibit a configuration which leads to a trigger, and similarly for the second term. The terms in Eq.(V.22) may or may not evaluate to zero for all  $\sigma$  *a priori*, but in any case will not be needed.

Now we match up the terms in Eq.(V.19) and (V.20) and demonstrate that indeed  $\mathbb{E}(X \circ Y|\sigma) \leq \mathbb{E}(X|\sigma) \circ \mathbb{E}(Y|\sigma)$ . First note that  $\mathcal{O}(X \circ Y) = \mathcal{O}(X) \circ \mathcal{O}(Y)$ . Next, as discussed previously, we see that  $A_i(X \circ Y) \subset (A_i(X) \circ \mathcal{O}(Y)) \cup (\mathcal{O}(X) \circ A_i(Y))$ ,  $1 \leq i \leq 3$ . Finally, and this is the key case, we claim that  $\mathcal{F}(X \circ Y) \subset A_1(X) \circ A_1(Y)$ . This follows from the observation we made before, which is that if  $\sigma \in \mathcal{F}(X \circ Y)$ , then we must see the alternating configuration on the flower, requiring next to nearest neighbor transmissions through the iris for both paths; such a  $\sigma$  certainly lies in  $A_1(X) \circ A_1(Y)$ . Thus we are done, assuming that  $(a + s)^2 \geq s$  – but this is equivalent to the statement that  $a^2 \geq 2s^2$ .

We have established the claim for the case of a single flower and two paths. Next we may induct on the number of flowers, as follows. Suppose now the claim is established for  $K - 1$  flowers. We can now let  $\sigma$  denote the configuration of all petals, filler, and irises of the first  $K - 1$  flowers. We condition on  $\sigma$  as above and adapt the notation so that the sets  $\mathcal{O}$ ,  $A_i$ 's, and  $\mathcal{F}$  correspond to the  $K^{\text{th}}$  flower. The argument can then be carried out exactly as above to yield the result for  $K$  flowers and two paths. Finally we induct on the number

of paths. Suppose the claim is true for  $n - 1$  paths. Since the  $\circ$  operation is associative, we consider  $(X_1 \circ \cdots \circ X_{n-1}) \circ X_n$ , where the  $X_i$ 's are indicator functions of the  $n$  paths. We simply view  $(X_1 \circ \cdots \circ X_{n-1})$  as a single path-type event and repeat the proof (note that the analogue of equation (V.20) may now contain non-trivial  $\mathcal{F}$ -type terms; these are immaterial since what is listed is already enough for an upper bound). This argument is sufficient since no more than two paths may share an iris under any circumstance.  $\square$

#### V.4.4 On the Generalization of Cardy's Formula for $M(\partial\Omega) < 2$

Here we provide the necessary interior analyticity statement required to extract Cardy's Formula for the model in [11] (the actual, full proof requires additional ingredients found in the companion work [6]). As described in §V.4.1, [11] contains a proof of Cardy's formula for piecewise smooth domains, so what is needed here is a generalization to domains  $\Omega$  with  $M(\partial\Omega) < 2$ . What we will prove is the following:

**Lemma V.4.8.** *Let  $\Omega$  denote any conformal triangular domain with  $M(\partial\Omega) < 2$ . Let  $u_\varepsilon^Y$ ,  $v_\varepsilon^Y$  and  $w_\varepsilon^Y$  denote the crossing probability functions as defined in  $\Omega$  for the lattice at scale  $\varepsilon$ . Then for the model as defined in §V.4.1, we have*

$$\lim_{\varepsilon \rightarrow 0} u_\varepsilon^Y = u,$$

*with similar results for  $v_\varepsilon^Y$  and  $w_\varepsilon^Y$  and the corresponding blue versions of these functions, where  $u$ ,  $v$  and  $w$  are the Cardy–Carleson functions.*

To prove the current statement, we start by repeating the proof in [11] up to Lemma 7.2 and Corollary 7.4 – the one place where the assumption on a piecewise smooth boundary is used. We now give a quick exposition of the (relevant portions of the) strategy of proof in [11]. The idea (directly inherited from [13]) is to represent the derivative of the crossing probability functions as a “three–arm” event, e.g., two blue paths and one yellow path from some point to the boundaries, with all paths disjoint, and then derive Cauchy–Riemann type identities by switching the color of one of the arms.

In order to accomplish this color switching in our model, it was necessary to introduce a *stochastic* notion of disjointness. This amounted to the introduction of a large class of random variables which indicate whether or not a percolation configuration contributes to the event of interest (e.g., a blue path from  $\mathcal{A}$  to  $\mathcal{B}$ , separating  $z$  from  $\mathcal{C}$ ). We call the restrictions and permissions given by these random variables *\*–rules*. The \*–rules may at times call a self–avoiding path illegitimate if it contains *close encounters*, i.e., comes within one unit of itself; on the other hand, the \*–rules may at other times permit a path which is not self–avoiding but in fact shares a hexagon. Thus the \*–rules are invoked only at shared hexagons and close encounter points of a path. When a close encounter or sharing at a hexagon is required to achieve the desired path event it is called an *essential lasso point*.

The fact that these \*–rules may be implemented by random variables in a fashion which allows color switching is the content of Lemma 3.17 in [11]. The strategy was then to first prove that the \*–version of e.g., the function  $u_\varepsilon$ , denoted  $u_\varepsilon^*$ , converges to  $u$ , then show that in the limit the starred and

unstarred versions of the function coincide. For the current work, the precise statement is as follows:

**Lemma V.4.9.** *Let  $\Omega$  be a domain such that*

$$M \equiv M(\partial\Omega) < 2.$$

*Let  $z$  denote a point in  $\Omega$ . Consider the (blue version of the) function  $u_\varepsilon(z)$  as defined in §V.4.1. Let  $u_\varepsilon^*(z)$  denote the version of  $u_\varepsilon$  with the  $*$ -rules enforced. Then,*

$$\lim_{\varepsilon \rightarrow \infty} |u_\varepsilon^*(z) - u_\varepsilon(z)| = 0.$$

*In particular, on closed subsets of  $\Omega$ , the above is uniformly bounded by a constant times a power of  $\varepsilon$ .*

Before we begin the proof we need some standard percolation notation.

**Definition V.4.10.** Back on the unit hexagon lattice, if  $L$  is a positive integer, let  $B_L$  denote a box of side length  $L$  centered at the origin. Further, let  $\Pi_5(L)$  denote the event of five disjoint paths, not all of the same color, starting from the origin and ending on  $\partial B_L$ . Now let  $m < n$  be positive integers, and let  $\Pi(n, m)$  denote the event of five long arms, not all of the same color, connecting  $\partial B_m$  and  $\partial B_n$ . We use the notation  $\pi_5(n)$  and  $\pi_5(n, m)$  for the probabilities of  $\Pi_5(n)$  and  $\Pi_5(n, m)$ , respectively.

*Proof of Lemma V.4.9.* We set  $N = \varepsilon^{-1}$  and, without apology, we will denote the relevant functions by  $u_N$ . For convenience we recap the proof of Lemma 7.2 in [11] (with one minor modification). Let us first consider the event which is contained in both the starred and unstarred versions of the  $u$ -function, namely

the event of a self-avoiding, non-self-touching path separating  $z$  from  $\mathcal{C}$ , etc. We will denote the indicator function of this event by  $\mathfrak{U}_N^-$ . Similarly, let us define an event, whose indicator is  $\mathfrak{U}_N^{*+}$ , that contains both the starred and unstarred versions: This is the event that a separating path of the required type exists, with no restrictions on self-touching, and is allowed to share hexagons provided that permissions are granted. It is obvious that

$$\mathbb{E}[\mathfrak{U}_N^{*+} - \mathfrak{U}_N^-] \geq |u_N^* - u_N|. \quad (\text{V.23})$$

We turn to a description of the configurations, technically on  $(\omega, X)$  (the enlarged probability space which include the permissions), for which  $\mathfrak{U}_N^{*+} = 1$  while  $\mathfrak{U}_N^- = 0$ . In such a configuration, the only separating paths contain an *essential* lasso point which, we remind the reader, could be either a shared hexagon or a closed encounter pair. Let us specify the lasso point under study to be the last such point on the journey from  $\mathcal{A}$  to  $\mathcal{B}$  (i.e., immediately after leaving this point, the path must capture  $z$  without any further sharing or self-touching, then return to this point and continue on to  $\mathcal{B}$ ). For standing notation, we denote this “point” by  $z_0$ . A variety of paths converge at  $z_0$ : certainly there is a blue path from  $\mathcal{A}$ , denoted  $B_{\mathcal{A}}$ , a blue path to  $\mathcal{B}$ , denoted  $B_{\mathcal{B}}$ , and an additional loop starting from  $z_0$  (or its immediate vicinity) which contains  $z$  in its interior. The loop we may view as two blue paths of comparable lengths, denoted  $L_z^1$  and  $L_z^2$ . However, since the lasso point was deemed to be essential, there are two additional yellow arms emanating from the immediate vicinity of  $z_0$ . These yellow arms may themselves encircle the blue loop and/or terminate at the boundary  $\mathcal{C}$ . We denote these yellow paths  $Y_{\mathcal{C}}^1$  and  $Y_{\mathcal{C}}^2$ .

Since  $z_0$  is the last lasso point on the blue journey from  $\mathcal{A}$  to  $\mathcal{B}$ , we auto-

matically get that the two loop arms are *strictly* self-avoiding. Also, without loss of generality, we may take the yellow arms to be strictly self-avoiding. Further, by Lemma 4.3 of [11], we may take either the portion of the path from  $\mathcal{A}$  to  $z_0$  to be strictly self-avoiding or the portion of the path from  $\mathcal{B}$  to  $z_0$  to be strictly self-avoiding. To summarize, we have six paths emanating from  $z_0$ , four blue and two yellow, with all paths disjoint except for possible sharings between  $B_{\mathcal{A}}$  and  $B_{\mathcal{B}}$ . For simplicity, let us start with the connected component of  $z$  in  $\Omega \setminus (\alpha_k \cup \beta_k \cup \gamma_k)$  where  $\alpha_k, \beta_k, \gamma_k$  are short crosscuts defining the prime ends  $a, b, c$ , respectively. It is noted that in this restricted setting, the various portions of the boundary are at a finite (macroscopic) distance from one another. Thus, on a mesoscopic scale, we are always near only a single boundary.

The case where  $z_0$  is close to  $z$  is handled by RSW-type bounds (see proof of Lemma 7.2 in [11]). The terms where  $z_0$  is in the interior follow from the  $5^+$  arm estimates; these arguments are the subject of Lemma 7.2 and Lemma 7.3 in [11]. We are left with the case where say  $z_0$  is within a distance  $N^\lambda$  of the boundary but outside some box of side  $N^{\mu_2}$  separating  $c$  from  $z$ .

Let  $\delta > 0$ . For  $N$  large enough,  $\partial\Omega$  can be covered by no more than  $J_\delta N^{M+\delta-\lambda}$  boxes of side  $N^\lambda$ . Now we take these boxes and expand by a factor of, say, two and we see that the region within  $N^\lambda$  of the boundary can be covered by  $J_\delta N^{M+\delta-\lambda}$  boxes of side  $2N^\lambda$ . We surround each of these boxes by a box of side  $N^{\mu_1}$ , where  $\mu_2 > \mu_1 > \lambda$ .

Now suppose  $z_0$  is inside the inner box. We still have the six arms  $B_{\mathcal{A}}$ ,  $B_{\mathcal{B}}$ ,  $L_z^1$ ,  $L_z^2$ ,  $Y_c^1$  and  $Y_c^2$ , but since  $z_0$  is now close to some boundary, we expect

some arm(s) to be short (i.e., shorter than  $N^\lambda$ ). We note that the box of side  $\mu_1$  is still away from  $c$ , and therefore we cannot have more than one of  $B_{\mathcal{A}}$  and  $B_{\mathcal{B}}$  be short due to being close to the boundary. Also, since  $z$  must be a distance of order  $N$  away from the boundary,  $z$  is outside of both of these boxes and therefore both  $L_z^1$  and  $L_z^2$  are long. The upshot is that regardless of which boundary  $z_0$  is close to, one and only one of the six arms will be short: If  $z_0$  is close to  $\mathcal{A}$  (respectively  $\mathcal{B}$ ), then  $B_{\mathcal{A}}$  (respectively  $B_{\mathcal{B}}$ ) will be short, and if  $z_0$  is close to  $\mathcal{C}$ , then a moment's reflection will show that only one of the yellow arms will be short.

What we have is then five long arms and one short arm emanating from the immediate vicinity of  $z_0$ , and these arms either end on some boundary or the boundary of the outer box of side  $N^{\mu_1}$ . For reasons which will momentarily become clear, we will now perform a color switch. Topologically, the two yellow arms separate  $L_z^1$  and  $L_z^2$  from  $B_{\mathcal{A}}$  and  $B_{\mathcal{B}}$ . Denote the outer box by  $B_{\mu_1}$  and consider now the region  $T \equiv \Omega \cap B_{\mu_1}$ . The two yellow arms together form a ‘‘crosscut’’ (in the sense of Kesten [17]) of  $T$ . This crosscut separates  $T$  into two disjoint regions  $T_b$  and  $T_l$ , where  $T_b$  contains  $B_{\mathcal{A}}$  and  $B_{\mathcal{B}}$  and  $T_l$  contains  $L_z^1$  and  $L_z^2$ . We condition on the crosscut which minimizes the area of  $T_l$ . Next we apply Lemma 4.3 of [11] to reduce the blue arm adjacent to the longer of the two yellow arms – which we take to be  $Y_{\mathcal{C}}^1$  – to be strictly self-avoiding, which without loss of generality we assume to be  $B_{\mathcal{A}}$ . Since  $B_{\mathcal{A}}$  forms a crosscut of  $T_b$ , there is a crosscut which maximizes the region which contains  $B_{\mathcal{B}}$ , which we denote  $\Omega_B$ . The region  $\Omega_B$  is now an unconditioned region, and we may apply Lemma 3.17 of [11] to switch the color of  $B_{\mathcal{B}}$  from

blue to yellow, while preserving the probability. The resulting yellow path we will denote  $Y_{\mathcal{B}}$ .

We now have three blue paths and three yellow paths. The blue paths are now all strictly self-avoiding.  $Y_{\mathcal{C}}^1$  is still strictly self-avoiding, but the path  $Y_{\mathcal{B}}$  may very well interact with (i.e., share hexagons with, due to the \*-rules)  $Y_{\mathcal{C}}^2$ . If indeed there is sharing, then let  $\hat{Y} = Y_{\mathcal{B}} \cup Y_{\mathcal{C}}^2$  be the geometric union of the two paths.  $\hat{Y}$  can then be reduced to be a strictly self-avoiding path, which we now denote  $Y$ . In any case, we now have (at least) five long paths emanating from  $z_0$ , three blue and two yellow, with the yellow paths separating the blue paths, and with all paths strictly self-avoiding. The probability of such an event is certainly bounded above (possibly strictly since the boxes will most likely intersect  $\Omega^c$ ) by the full space event  $\Pi_5(N^{\mu_1}, 2N^\lambda)$  – see Definition V.4.10. The upshot of Lemma 5 of [17] is that

$$\pi_5(N^{\mu_1}, 2N^\lambda) \leq C \left( \frac{N^\lambda}{N^{\mu_1}} \right)^2, \quad (\text{V.24})$$

where  $C$  is a constant. This result can, almost without modification, be taken verbatim from [17]; the proviso therein which concerned “relocation of arms” was discussed in the first paragraph of the proof of Lemma 7.3 in [11]. We consider (V.24) to be established.

If we sum over all such boxes of side  $2N^\lambda$ , we find that the contribution from the near boundary regions is a constant times

$$N^{M+\delta-\lambda+2\lambda-2\mu_1} = N^{M+\delta+\lambda-2\mu_1}.$$

Since  $M < 2$ , we may first choose  $\delta$  and  $\lambda$  such that  $M + \delta + \lambda < 2$ , and next we will choose  $\mu_2$  and then  $\mu_1$  large enough so that the exponent is negative.

Finally let us take care of the crosscuts. We shall show that for large  $k$ , the event that a path emanates from the crosscut e.g.,  $\beta_k$  and goes to  $\mathcal{B}$  tends to 0 as  $k \rightarrow \infty$  (uniformly in  $N$  for all  $N$  sufficiently large): Indeed, although the prime end  $b$  may be a continua, the probability of a path emanating from  $b$  is “as small” as though  $b$  were a point. Let us begin by looking at the conformal rectangle  $B_k \setminus B_{2k}$  defined by the relevant crosscuts. We now mollify  $B_k \setminus B_{2k}$  so that the resulting domain has smooth boundary and lies strictly in  $\Omega$ : This is easily accomplished by deleting from  $B_k \setminus B_{2k}$  the image under the conformal map  $\phi : \mathbb{H} \rightarrow \Omega$  of some  $\delta$  neighborhood of  $\partial\mathbb{H}$ , where  $\delta_k > 0$  is chosen so small that the said image is within some (Euclidean distance)  $\eta_k$  of  $\partial\Omega$ . Let us denote the resulting domain by  $R_k$ . Since  $R_k$  has smooth boundary, the result of [11] applies and we may apply Cardy’s Formula inside  $R_k$  to see that the probability of a “lateral” yellow crossing (i.e., one “parallel” to  $\beta_k$  and  $\beta_{2k}$ ) is uniformly bounded from below, independently of  $k$ , if  $\eta_k$  is properly chosen. We may even assume that the crossing takes place in the “bottom” half of  $R_k$ , which will allow us to construct Harris annuli of order  $\eta_k$  enabling a connection to the actual boundary. Thus, having achieved all this, looking at the lowest such crossing, we may RSW continue the crossing to the actual  $\partial\Omega$ , with probability uniformly bounded from below. It is now straightforward to observe that in the presence of such a yellow crossing, no blue path may emanate from  $\beta_k$ . Performing this construction on a multitude of scales, it is clear, as  $\varepsilon \rightarrow 0$  that with probability tending to one, no blue path emanates from this prime end.

All estimates described above are uniform in  $z$  provided  $z$  remains a fixed

non-zero (Euclidean) distance from the boundary. And, finally, the proof of Lemma V.4.9 for  $v_N$  and  $w_N$  are the same.  $\square$

*Proof of Lemma V.4.8.* Corollary 7.4 of [11] concerned the difference between the blue and yellow versions of these functions (Cauchy–Riemann relations are only established for color-neutral sums). However, the argument of Corollary 7.4 in [11] reduced the difference between the two colored versions to six arm events in the bulk and five arm events near the boundary, to which the above arguments can be applied. Replacing Lemma 7.2 (and Lemma 7.3) in [11] with Lemma V.4.9 gives a proof of Lemma V.4.8.  $\square$

# Bibliography

- [1] M. Aizenman. *The Geometry of Critical Percolation and Conformal Invariance*. Proceedings STATPHYS19 (Xiamen 1995), H. Bai-lin (ed.), World Scientific (1995).
- [2] M. Aizenman, J. T. Chayes, L. Chayes, J. Frohlich, and L. Russo. *On a Sharp Transition From Area Law to Perimeter Law in a System of Random Surfaces*. Comm. Math. Phys. **92**, no. 1, 19–69 (1983).
- [3] M. Aizenman and A. Burchard. *Hölder Regularity and Dimension Bounds for Random Curves*. Duke Math. J. **99**, no. 3, 419–453 (1999).
- [4] V. Beffara. *Cardy’s Formula on the Triangular Lattice, the Easy Way*. Universality and Renormalization, vol. 50 of the Fields Institute Communications, 39–45 (2007).
- [5] J. van den Berg and H. Kesten. *Inequalities with Applications to Percolation and Reliability*. J. Appl. Probab. **22**, 556–569 (1985).
- [6] I. Binder, L. Chayes and H. K. Lei. *On Convergence to SLE6 II: Discrete Approximations and Extraction of Cardy’s Formula for General Domains*.

- [7] B. Bollobás and O. Riordan. *Percolation*. Cambridge: Cambridge University Press (2006).
- [8] C. Borgs, J. T. Chayes and D. Randall. *The van den Berg–Kesten–Reimer Inequality: a Review*. Perplexing Problems in Probability: Festschrift in honor of Harry Kesten, Birkhauser (M. Bramson and R. Durrett, editors): 159-173 (1999). Also available at <http://www.math.gatech.edu/randall/reprints.html>.
- [9] F. Camia and C. M. Newman. *Two-Dimensional Critical Percolation: The Full Scaling Limit*. Comm. Math. Phys. **268**, no. 1, 1–38 (2006).  
*Critical Percolation Exploration Path and  $SLE_6$ : a Proof of Convergence*. Available at <http://arxiv.org/list/math.PR/0604487> (2006)
- [10] J. T. Chayes and L. Chayes. *Percolation and Random Media*. In: Osterwalder, K., Stora, R. (eds.) Les Houches Session XLIII: Critical Phenomena, Random Systems and Gauge Theories, pp. 1001–1042. Amsterdam: Elsevier (1986).
- [11] L. Chayes and H. K. Lei. *Cardy’s Formula for Certain Models of the Bond–Triangular Type*. Reviews in Mathematical Physics. **19**, 511–565 (2007).
- [12] P. L. Duren. *Univalent Functions*. Berlin, New York: Springer Verlag (1983).
- [13] G. Grimmett. *Percolation*. Berlin, New York: Springer Verlag (1999).

- [14] H. Kesten. *Analyticity Properties and Power Law Estimates of Functions in Percolation Theory*. J. Stat. Phys., **25**, no. 4, 717–756 (1981).
- [15] H. Kesten. *Percolation Theory for Mathematicians*. Boston, Basel, Stuttgart: Birkhauser (1982).
- [16] H. Kesten. *Scaling Relations for 2D-Percolation*. Comm. Math. Phys. **109**, 109–156 (1987).
- [17] H. Kesten, V. Sidoravicius and Y. Zhang. *Almost All Words are Seen in Critical Site Percolation on the Triangular Lattice*. Electronic Journal of Probability, **3** (10), 1–75 (1998).
- [18] S. Lang. *Complex Analysis*. Berlin, New York: Springer (1999).
- [19] G. F. Lawler. *Conformally Invariant Processes in the Plane*. Mathematical Surveys and Monographs, 114. American Mathematical Society, Providence, RI, 2005. xii+242 pp. ISBN: 0-8218-3677-3
- [20] G. F. Lawler, O. Schramm, W. Werner. *Conformal Invariance of Planar Loop-Erased Random Walks and Uniform Spanning Trees*. Ann. Probab. **32** no. 1B, 939–995 (2004).
- [21] G. F. Lawler, O. Schramm, W. Werner. *One-Arm Exponent for Critical 2D Percolation*. Electronic Journal of Probability, **7**, 13 pages (electronic) (2002).
- [22] C. Pommerenke. *Boundary Behavior of Conformal Maps*. Berlin, New York: Springer (1992).

- [23] B. Ráth. *Conformal Invariance of Critical Percolation on the Triangular Lattice*. Available at: <http://www.math.bme.hu/~rathb/rbperko.pdf>
- [24] D. Reimer. *Proof of the van den Berg–Kesten Conjecture*. *Combin. Probab. Comput.* **9** no. 1, 27–32 (2000).
- [25] O. Schramm. *Conformally Invariant Scaling Limits (an overview and a collection of problems)*. arXiv:math.PR/0602151
- [26] S. Smirnov. *Towards Conformal Invariance of 2D Lattice Models*. Proceedings of the International Congress of Mathematicians, Madrid, Spain, 2006.
- [27] S. Smirnov. *Critical Percolation in the Plane: Conformal Invariance, Cardy’s Formula, Scaling Limits*. *C. R. Acad. Sci. Paris Sr. I Math.* **333**, 239–244 (2001).  
Also available at <http://www.math.kth.se/~stas/papers/percras.ps>.
- [28] W. Werner. *Lectures on Two–Dimensional Critical Percolation*. arXiv:0710.0856

# Chapter VI

## Restricted Uniform Continuity of Crossing Probabilities

In this chapter we establish a rather technical result quantifying uniform continuity of critical percolation crossing probabilities in domains slit by Explorer Process typical curves and discuss some first consequences. For discussions about critical percolation, interfaces, etc., we refer the reader to discussions in [5]. Here we will state and establish the result in the simplest setting possible (e.g., smooth boundary).

The arguments used herein are “elementary” given *a priori* percolation estimates on properties of interface typical curves. It is possible that one may simplify the arguments using a proof along the lines of Lemma 4.4 in [4] (since the bulk of the difficulty both here and there is some “topological consistency” result), which uses conformal maps, etc., but to obtain a statement with some uniformity would still require more careful quantification: The proof of Lemma

4.4 takes advantage of the pointwise nature of the statement to shrink many relevant scales, i.e., the size of the relevant scales depend on the nature of the particular approximating slit under consideration, whereas here we make some statement which is almost uniform provided the slits are less than some *fixed* sup-norm distance away from the reference slit. Along the same lines, we also remark that the pointwise convergence result of [4] does indeed already provide pointwise continuity of crossing probabilities, but again, no uniformity.

As a consequence of this result, we can obtain that the limiting crossing probability in the domain slit by the interface up to time  $t$  is in fact a martingale. (In [5] we obtained the same statement via different means, i.e., by a robust convergence to Cardy's Formula, but the arguments there do not offer any uniformity.) We point out, of course, no conformal invariance is available from such arguments (indeed, the only way we have obtained conformal invariance so far is via establishing Cardy's Formula, i.e., knowing *exactly* what the limiting crossing probability is; see [4], [5]).

Secondly, it appears that this result can perhaps contribute to establishing some rate of convergence to  $\text{SLE}_6$ . On the latter point we note that thus far, the convergence arguments have been quite weak in the sense that we first extract some abstract limiting point then work to establish appropriate properties of the limit. (In fact, so far, the only explicit rate of convergence result for convergence of lattice models to any SLE appears to be [3] for the convergence of loop-erased random walk to  $\text{SLE}_2$ .)

## VI.1 Preliminaries

The key tool we will use are the so-called Russo–Seymour–Welsh estimates, and thus the arguments here should apply for any model satisfying such typical critical percolation estimates (again we refer the reader to discussions in [5]). Since this estimate plays such a key role in what follows, let us state it now in the form we will use. The proof of the following statement in approximately the form stated can be found in e.g., [8], §11.7.

**Lemma VI.1.1** (RSW Estimate). *Let  $B_L$  denote a square of side length  $L$  and  $P_{\ell_r}^{(p)}(B_L)$  the probability of a left right crossing of  $B_L$  in say blue at parameter  $p$ . If it is the case that  $0 < P_{\ell_r}^{(p)}(B_L) < 1$ , then*

$$P(A_{L,3L}) \geq \alpha > 0$$

*for some constant  $c$  depending on  $P_{\ell_r}^{(p)}(B_L)$ . Here  $A_{L,3L}$  denotes event of a blue circuit inside the annulus  $B_{3L} \setminus B_L$ .*

*Consequently, if  $\eta < \delta$  and  $\varepsilon \ll \eta, \delta$ , then setting up logarithmically many annuli between the concentric squares of side length  $\eta$  and side length  $\delta$  and performing percolation at scale  $\varepsilon$ , we obtain*

$$P(A_{\eta,\delta}^c) \leq c'(\eta/\delta)^\alpha$$

*for some constant  $c'$  (here  $A^c$  denotes the complementary event: There is no blue circuit in  $B_\delta \setminus B_\eta$ ).*

We note that the above estimates are scale-invariant, i.e., they do not depend on  $L$ , but only on the aspect ratio, but only the relevant aspect ratios.

Next let us describe our setting: Recall that  $\mu_\varepsilon$  is a measure generated by the percolation Exploration Process (a.k.a. the interface) on the  $\varepsilon$ -lattice scale in a domain  $\Omega$  with two distinguished boundary prime ends  $a$  and  $c$  and  $\mu'$  is a weak limit point of  $\mu_\varepsilon$  where space of curves is equipped with the sup-norm topology (this is the setting of [2]) given by

$$\text{dist}(\gamma_1, \gamma_2) = \inf_{\varphi_1, \varphi_2} \sup_t |\gamma_1(\varphi_1(t)) - \gamma_2(\varphi_2(t))|. \quad (\text{VI.1})$$

## VI.2 Properties of Slits Under Consideration

We will now provide proofs for the properties of a typical explorer path (a lot of what appears here has already appeared [5], but for convenience and completeness we have reproduced them here). We remark that these estimates represent – at the  $\varepsilon$  level – the behavior that ensures that the limiting objects in the support of  $\mu'$  are precisely Löwner curves. A lot of the estimates which follow are uniform in  $\varepsilon$  (for  $\varepsilon$  sufficiently small) and hence we may be rather lackadaisical at times about whether we are talking about  $\mu_\varepsilon$  or  $\mu'$ . We start with the fairly familiar multi-arm estimates.

### VI.2.1 Multi-Arm Estimates

In this section we establish the multi-arm estimates and establish (a) typical behavior of the curves under consideration.

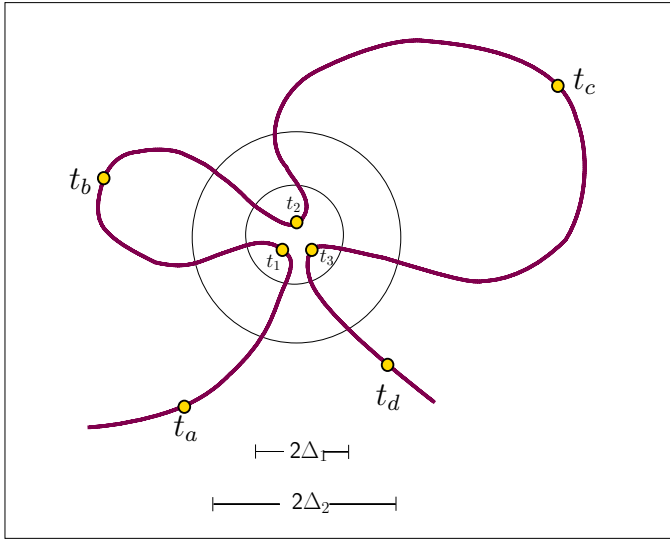
**Lemma VI.2.1** (Multi-Arm Estimates). *Let  $D(\eta, l)$  denote the circular annulus with inner radius  $\eta$  and outer radius  $l$ . Consider the events of a (i) 5-arm crossing of  $D(\eta, l)$  and (ii) 6-arm crossing of  $D(\eta, l)$ . Then the 5-arm event*

has probability bounded above by  $(\eta/l)^2$  while the 6–arm event has probability bounded above by  $(\eta/l)^{2+\sigma}$  for some  $\sigma > 0$ .

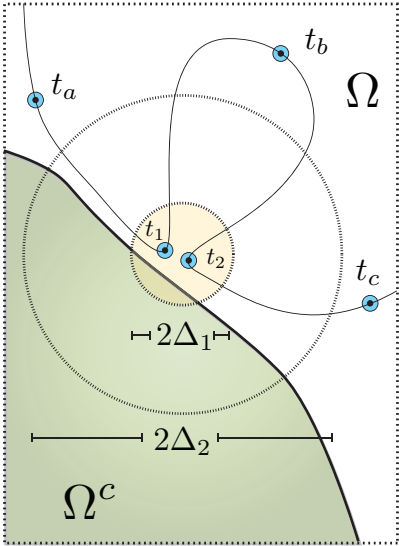
*Proof.* Let us rescale back so that the lattice spacing is of order unity and the diameter of  $\Omega_\varepsilon$  is of order  $N$ . Then the five arm event in  $D(\eta, l)$  is the event of five crossings between circles of radius  $\eta N$  and  $lN$ . Approximating by appropriate “square” annular regions, the arguments of [11] may be used in generic circumstances (of course some degree of reflection symmetry for the underlying lattice has to be employed and in addition it has been checked that the fencing/corridor arguments in [11] apply) and so the probability of the five arm event in  $D(\eta, l)$  is bounded above by a constant times  $(\eta/l)^2$ . To bound the 6–arm event we note that if we let  $A$  denote the event of one crossing in the annular region, then the probability of  $A$  is bounded by  $(\frac{\eta}{l})^\sigma$ , for some  $\sigma > 0$ , by standard Russo–Seymour–Welsh arguments. Then letting  $B$  be the event of 5 crossings in the annular region and applying a BK–type inequality to  $A \circ B$  we obtain the desired result.  $\square$

**Definition VI.2.2.** Let  $\Delta_2 > \Delta_1$  (with  $\Delta_2 \gg \Delta_1$  envisioned) and let  $\gamma : [0, 1] \rightarrow \Omega$  be a curve. We say that  $\gamma$  has a  $\Delta_2$ – $\Delta_1$  *triple visit* if there are times  $t_a < t_1 < t_b < t_2 < t_c < t_3 < t_d$  such that  $\gamma(t_1), \gamma(t_2)$  and  $\gamma(t_3)$  all lie within a single  $\Delta_1$ –neighborhood while  $\gamma(t_a), \dots, \gamma(t_d)$  each lie a distance at least  $\Delta_2$  from some point in this neighborhood. For an illustration see Figure VI.1(a).

A direct consequence of Lemma VI.2.1 is the absence of triple visits of the type described in the above definition as the ratio  $\Delta_1/\Delta_2$  tends to zero:



(a) Triple visit in the interior



(b) Double visit near the boundary

Figure VI.1: Atypical behavior of  $\mu_\epsilon$  curves

**Lemma VI.2.3.** *Let  $\Omega$  be a domain and let  $\Delta_2 \gg \Delta_1 > 0$ . The  $\mu'$ -probability of a  $\Delta_2$ - $\Delta_1$  triple visit tends to zero as  $\Delta_1/\Delta_2 \rightarrow 0$ .*

*Proof.* A quick sketch of a triple visit scenario in  $D(\eta, l)$  yields immediately 6 long disjoint passages of  $\gamma(t)$  across the annulus. Note this can occur in two topologically distinct fashions. For  $\gamma(t)$  a two-sided Exploration Process, naïve counting would yield as many as twelve long arms, but adjacent sides of “disjoint” long arms can lead to sharing of (boundary) elements of the process; in the worst possible case, entire adjacent arms can “collapse”. However, in either topology, even taking into account all these sharings and collapses, we are still left with six genuinely *disjoint* long arms.

We have established, in the continuum or lattice approximation, that the six arm event in an annulus  $D(\eta, l)$  has probability bounded above by  $(\frac{\eta}{l})^{2+\sigma}$ . We may divide  $\Omega$  (or  $\Omega_\varepsilon$ ) into an overlapping grid of scale  $\eta$ . The probability that such an event happens anywhere is therefore bounded above by  $(\eta/l)^{2+\sigma} \left(\frac{1}{\eta^2}\right) = \frac{1}{l^2} \left(\frac{\eta}{l}\right)^\sigma$ , so ultimately, the probability of an actual triple visit is zero and the probability of a  $\Delta_2$ - $\Delta_1$  triple visit indeed tends to zero as  $\frac{\Delta_1}{\Delta_2} \rightarrow 0$ . □

**Remark VI.2.4.** We make the following observation for intrinsic interest and for possible future reference: Observe that in one of the topological alternatives, after the second visit to the inner circle, the Exploration Process can immediately delve into the sack created between this visit and the first. As an *Exploration Process*,  $\gamma(t)$  is now forced to perform its third visit *and* escape  $D(\eta, l)$  altogether. The observation of interest is that these forced future visitation events provide, at least on the level of arm estimates, no additional

decay after the (deep) visit into the cul-de-sac. Indeed, six arms are already present at this juncture (all potential additional arms may undergo collapse).

**Definition VI.2.5.** Let  $\Delta_2 > \Delta_1$  (with  $\Delta_2 \gg \Delta_1$  envisioned) and let  $\gamma : [0, 1] \rightarrow \Omega$  be a curve. We say that  $\gamma$  has a  $\Delta_2$ - $\Delta_1$  *double visit to the boundary* by the obvious modification of Definition VI.2.2 (using only  $t_a, t_1, t_b, t_2, t_c$  along with the stipulation that at least one of the points  $\gamma(t_1)$  or  $\gamma(t_2)$  is within distance  $\Delta_1$  of  $\partial\Omega$ ). For an illustration see Figure VI.1(b).

**Lemma VI.2.6** (No Double Visits Near the Boundary). *For any  $\Delta_2 > 0$ , the probability of a  $\Delta_2$ - $\Delta_1$  double visit to (anywhere on) the boundary tends to zero as  $\Delta_1 \rightarrow 0$ .*

*Proof.* First we observe that if the Exploration Process has a  $\Delta_2$ - $\Delta_1$  double visit to the boundary, then this implies at least a 3-arm event on the scale of  $\Delta_2 : \Delta_1$  near the boundary.

For percolation domains with smooth boundaries, this follows from the *a priori*  $1/N^2$  power law estimates described in [1] and [12]. (The idea of proof is straightforward. In brief: Consider the easy way crossing of an  $N$  by  $2kN$  box. This probability is markedly larger than the similar probability in an  $N$  by  $kN$  box with both probabilities of order unity. The difference between these two probabilities can be written as a telescoping sum, with each increment corresponding to a single site distortion, the vast majority of which leading to a three arm event in the half space – the contributions from sites near the boundary are negligible. This implies on the order of  $N^2$  three arm events, each of which can be shown to happen with comparable probability

by the rearrangement arguments of Kesten [11]. Since the sum of all these probabilities is of order unity, the result follows). □

**Remark VI.2.7.** The above estimates apply equally to the situation when the tip of the Exploration Process has “just” performed a double visit; i.e., the time  $t_c$  in Definition VI.2.6 is in fact superfluous. This situation is analogous to the forced future triple visitations discussed in Remark VI.2.4. As in these cases, the ostensible extra arms that the continuation of the journey might generate are susceptible to collapse and cannot be counted, while the estimates are already sufficient without these arms.

## VI.2.2 Double-Back Estimates

Next we provide double-back estimates for the curves under consideration.

**Definition VI.2.8.** Let  $\Omega$  be a domain. Let  $\delta \gg \eta > 0$  and let  $\gamma : [0, 1] \rightarrow \Omega$  be a parametrized curve. We say that  $\gamma$  has a  $\delta$ - $\eta$  doubleback if there exists disjoint subsegments  $I_1$  and  $I_2$  of  $[0, 1]$ , with  $\text{diam}(\gamma(I_1)) \geq \delta$ ,  $\text{diam}(\gamma(I_2)) \geq \delta$ , and such that the segments  $\gamma(I_1)$  and  $\gamma(I_2)$  are  $\eta$ -close in the sup-norm.

**Lemma VI.2.9** (No Doubleback). *Let  $\Omega$  be a domain and let  $\gamma \in \text{supp}(\mu')$ . Let  $\delta, \eta > 0$  satisfy  $\eta < c_1\delta$ , with a particular  $c_1$  of order unity. Then for all  $\delta$  sufficiently small, there are additional constants  $c_2$  and  $c_3$  of order unity such that for all  $\varepsilon$  sufficiently small, the  $\mu_\varepsilon$ -probability of a  $\delta$ - $\eta$  doubleback is bounded above by*

$$\frac{c_2}{\delta^2} \cdot e^{-c_3\delta/\eta},$$

with the same result inherited by  $\mu'$ .

*Proof.* It is sufficient to verify the statement in the measures  $\mu_\varepsilon$  for  $\varepsilon$  sufficiently small. Thus let  $\delta \ll 1$  and  $\eta$  small as desired and then  $\varepsilon$  much smaller than the scale set by  $\eta$ . (We are envisioning that  $\eta/\delta$  actually tends to zero.) For  $k$  large but of order unity, let us grid the domain  $\Omega$  into pixels of scale  $k^{-1}\delta$ . It's not difficult to see that the event in question necessitates an easy-way  $\eta$ -close double-crossing of some rectangle of this scale with aspect ratio of order unity. Let us now consider a particular such  $\delta : k\delta$  rectangle, denoted by  $R_\delta$  and let us consider the event of at least two disjoint blue crossings of  $R_\delta$  that are within distance  $\eta$  of each other. If  $g_0$  is such a (single) crossing, let

$$N(g_0) = \{ \exists \text{ a blue crossing of } R_\delta \text{ in the region above } g_0 \\ \text{that is within distance } \eta \text{ of } g_0 \}.$$

Our first claim is that, uniformly in  $\varepsilon$ , for all  $\varepsilon$  sufficiently small,  $\mathbb{P}(N(g_0)) \leq e^{-c_3 \frac{\delta}{\eta}}$ , for all  $\eta, \delta$ . To see this, let us cover  $g_0$  with disjoint annuli of scale  $3\eta : \eta$ , with the center of each annulus centered on a point of  $g_0$ . Clearly, there are at least of the order  $\delta/\eta$  such annuli. If in the region above  $g_0$ , in any one of these annuli there is a yellow circuit, then  $N(g_0)$  cannot possibly occur. For future reference, we note that in fact these preventative steps take place in the intersection of the relevant annuli with  $R_\delta$ . Since the probability of such a yellow circuit is uniformly positive, we have so far indeed shown that

$$\mathbb{P}(N(g_0)) \leq e^{-c_3 \frac{\delta}{\eta}}.$$

Letting  $\mathbf{G}_0$  denoting the event that  $g_0$  is the lowest crossing, one obtains the same estimate as the above for  $\mathbb{P}(N(g_0) \mid \mathbf{G}_0)$ . The estimates will hold if we

now let  $\mathbf{G}_k$  denote the event that the curve  $g_k$  is the  $k^{\text{th}}$  to lowest crossing, e.g., out of a total of  $\ell \geq k$  disjoint crossings. Thus, by subadditivity, conditioned on the existence of say  $\ell$  disjoint crossings, the ultimate double-crossing event of interest has probability bounded above by  $\ell e^{-d_3 \frac{\delta}{\eta}}$ . However, if  $r_\ell$  denotes the probability of  $\ell$  disjoint crossings in  $R_\delta$ , then by a BK-type inequality it is clear that  $\sum_\ell \ell r_\ell < \infty$ . Hence the probability of two disjoint blue crossings (or two disjoint yellow crossings) in  $R_\delta$  is bounded above by

$$c_2 e^{-c_3 \frac{\delta}{\eta}}. \tag{VI.2}$$

To finish we note that there are only of order  $\delta^{-2}$  such rectangles in  $\Omega$  and hence summing over them, we have the lemma.  $\square$

For our purposes, we will need a related property of a  $\mu'$ -typical explorer path.

**Definition VI.2.10.** Let  $\vartheta > 0$  (but with  $\vartheta \ll 1$ ) and consider a gridding of  $\Omega$  with boxes of scale  $\vartheta$ . Let  $\delta > \vartheta$  and let  $b_\vartheta$  denote one such box which is a distance greater than  $\delta$  away from both  $a$  and  $c$ . Let  $\vartheta_\ell = 3^\ell \vartheta$  and consider the 3:1 annulus of scale  $\vartheta_\ell$  with  $b_\vartheta$  at the center of the annulus. Let  $\kappa > 0$  (considered small) and, if the Exploration Process double crosses the annulus (here crossing means a connection from the inner to the outer square), we shall say that it has had a  $\kappa$ -weak doubleback if the two disjoint crossings of the annulus are, in the sup-norm, closer than a distance  $\kappa \vartheta_\ell$  to each other. Let  $v > 0$ . Then, we say that, for  $b_\vartheta$ , the Exploration Process has the  $v$ -persistent  $\kappa$ -weak doubleback property if a fraction in excess of  $(1-v)$  of the  $k$  disjoint 3:1 annuli of scale  $\vartheta_\ell, \ell = 1, 2, \dots, q; 3^q \vartheta < \delta < 3^{q+1} \vartheta$  house a  $\kappa$ -weak doubleback.

**Lemma VI.2.11.** *Let  $\Omega$  denote a domain of the type described, and let  $\gamma \in \text{supp}(\mu')$ . With definitions and notation as in the previous definition, we have that given  $v > 0$ , and any  $\alpha > 0$  there exists  $\kappa > 0$  such that the probability that  $\gamma$  has a  $v$ -persistent  $\kappa$ -weak doubleback for any box  $b_\vartheta$  is bounded above by*

$$\frac{C_1}{\vartheta^2} \left( \frac{\vartheta}{\delta} \right)^\alpha$$

for some constant  $C_1 < \infty$ .

*Proof.* The key point here is the observation that in each of the four (overlapping) rectangles of aspect ratio 3 which comprise the relevant  $\vartheta_\ell$  scale annuli, the absence of preventative steps (as described in the previous lemma) which would forbid such  $\vartheta_\ell : \kappa\vartheta_\ell$  encounters only occurs with probability as in the display (VI.2), with  $\delta$  replaced by  $\vartheta_\ell$  and  $\eta$  replaced by  $\kappa\vartheta_\ell$ . Notice that as  $\kappa \rightarrow 0$ , this quantity gets exponentially small with  $\kappa^{-1}$ . For fixed  $v$ , using independence of the preventative steps in each annulus, the probability of having a fraction in excess of  $1 - v$  of the close encounters will, for  $v < 1$ , be bounded above by  $\exp[-q(r_1\kappa^{-1} - r_2)]$  where  $r_1 > 0$  and  $r_2 < \infty$ , for all  $q$  sufficiently large (where  $3^q\vartheta < \delta < 3^{q+1}\vartheta$ ). This implies a bound of the stated form without the  $\vartheta^{-2}$  prefactor for any given box; the prefactor accounts for all possible boxes via subadditivity.  $\square$

### VI.2.3 Minkowski Dimension

Finally, for completeness we include here a result on the Minkowski dimension of a  $\mu'$ -typical curve.

**Lemma VI.2.12.** *If the upper Minkowski dimension of  $\partial\Omega$  is less than two, then the limit point  $\mu'$  gives full measure to curves with upper Minkowski dimension less than  $2 - \psi'$  for some  $\psi' > 0$ .*

*Proof.* Let  $z \in \text{Int}(\Omega)$  and  $g_\delta(z)$  the box of radius  $\delta$  surrounding  $z$  and  $D(z)$  denote the distance between  $z$  and  $\partial\Omega$ . We claim that there is some  $\psi > 0$  such that for all  $\varepsilon$  sufficiently small,

$$\mathbb{P}_\varepsilon(\mathbb{X}_t^\varepsilon \in g_\delta(z)) < C_2 \left(\frac{\delta}{D}\right)^\psi$$

where  $C_2$  is a constant.

This follows from Russo–Seymour–Welsh theory, which we do here in some detail. Indeed, if  $r < s$ , let  $A_{s,r}(z) \equiv B_s(z) \setminus B_r(z)$  denote the annulus centered at  $z$ , where, if necessary, the sides are approximated, within  $\varepsilon$ , by the lattice structure. Assume temporarily that  $A_{s,r}(z) \subset \text{Int}(\Omega)$ . Clearly, if there is both a yellow and a blue ring in  $A_{s,r}$ , then  $\mathbb{X}_t^\varepsilon$  cannot possibly visit  $B_r(z)$  (since the yellow portion of  $\mathbb{X}_t^\varepsilon$  cannot penetrate the blue ring and similarly with yellow  $\leftrightarrow$  blue). Now by the Russo–Seymour–Welsh estimates, the probability of a blue ring in  $A_{M,\lambda M}$  is bounded below uniformly in  $\varepsilon$  by a strictly positive constant that depends only on  $\lambda$ . Let  $\eta > 0$  denote a lower bound on the probability that in  $A_{4L,3L}$  there is a blue ring and in  $A_{3L,2L}$  a yellow. Now let  $k$  satisfy  $2^k > \varepsilon^{-1}D > 2^{k-1}$  and similarly  $2^\ell > \varepsilon^{-1}\delta > 2^{\ell-1}$ . Then, give or take, there are  $k - \ell$  independent annuli in which the pair of rings described can occur. The probability that all such ring pair events fail is less than  $C_1(1 - \eta)^{k-\ell} \leq C_2 \left(\frac{\delta}{D}\right)^\psi$ , where  $C_1$  and  $C_2$  are constants and  $\psi > 0$  is defined via  $\eta$ .

Let us fix a square grid of scale  $\delta$  with  $\varepsilon \ll \delta \ll 1$ . Let  $\mathcal{N}_\delta$  denote the number of boxes of scale  $\delta$  that are visited by the process. We claim that for all  $\varepsilon$  sufficiently small

$$\mathbb{E}_\varepsilon(\mathcal{N}_\delta) \leq C_{\psi'} \left(\frac{1}{\delta}\right)^{2-\psi'} = C_{\psi'} n^{2-\psi'}, \quad (\text{VI.3})$$

where  $\psi' > 0$  is a constant and  $n = n_\delta = \delta^{-1}$  represents the characteristic scale of  $\Omega$  on the grid of size  $\delta^{-1}$ . In particular we may take  $\psi' < \min\{\psi, \theta\}$ , where  $\theta \in [0, 1]$  describes the roughness of the boundary:  $M(\partial\Omega) = 2 - \theta$ .

Let  $n_k$  denote the number of boxes a distance  $k\delta$  (i.e.,  $k$  boxes distant) from  $\partial\Omega$  and

$$N_l = \sum_{k \leq l} n_k.$$

Our first claim is that for all  $\delta$ ,

$$N_l < C_{\theta'} n^{2-\theta'} l^{\theta'}, \quad (\text{VI.4})$$

for any  $\theta' < \theta$ , where  $C_{\theta'}$  is a constant. To see this, let us estimate the total area of boxes on a grid of size  $\sigma$  intersected by or within one unit of  $\partial\Omega$ . It is not hard to see that this is bounded by  $C_{\theta'} \times \left(\frac{1}{\sigma}\right)^{2-\theta'} \times \sigma^2 = C_{\theta'} \sigma^{\theta'}$ , where  $C_{\theta'}$  is a constant which is uniform for a fixed  $\theta' < \theta$ . Taking  $\sigma = l\delta$  and noting that *these* boxes contain all of the  $n_1 + \dots + n_l$  boxes of scale  $\delta$  (i.e., boxes within  $l$  units of  $\partial\Omega$ ), the claim follows.

Now, clearly,

$$\mathbb{E}_\varepsilon(\mathcal{N}_\delta) \leq C_2 \sum_{k=1}^{l_{\max}} n_k \cdot \left(\frac{1}{k}\right)^\psi.$$

Let us now dispense with the sum in the display. Summing by parts, we get

$$\sum_{k=1}^{l_{\max}} n_k \left(\frac{1}{k}\right)^\psi = N_{l_{\max}} l_{\max}^{-\psi} + \sum_{k=1}^{l_{\max}-1} N_k \left(\frac{1}{k^\psi} - \frac{1}{(k+1)^\psi}\right).$$

Now if  $\psi > \theta$ , then  $\psi > \theta'$ . Using Eq. (VI.4) and pulling out an  $n^{2-\theta'}$ , the sum is convergent. Meanwhile, the first term (again using the estimate in Eq. (VI.4)) is smaller. Conversely, if  $\psi \leq \theta$ , then both terms are of order  $n^{2-\theta'} l_{\max}^{\theta'-\psi}$  and the result follows if we take  $l_{\max} = n$ . It is re-emphasized that the estimate in Eq. (VI.3) is uniform in  $\varepsilon$ ; by further sacrifice of the constant, we may claim that Eq. (VI.3) holds for all box-scales in the range  $[\delta, 2\delta]$ .

The remaining argument is now immediate. Letting  $\delta_k = 2^{-k}$  we have that for any  $\delta \in [\delta_{k+1}, \delta_k]$  and  $s > 0$

$$\mathbb{P}_\varepsilon(\mathcal{N}_\delta > C_{\psi'} n_\delta^{2-\psi'+s}) \leq \frac{1}{2^{ks}}. \quad (\text{VI.5})$$

The result follows, for any  $s > 0$ , by taking  $\varepsilon \rightarrow 0$  and summing over  $k$ .  $\square$

## VI.3 Statement and Proof of Main Result

**Lemma VI.3.1.** *[Restricted Uniform Continuity] Let  $\Omega$  be a domain with smooth boundary and  $a, b, c, d$  be four points on  $\partial\Omega$ . Let  $\theta, \Delta > 0$  and consider curves which start at  $a$  and end at  $c$ . Then there exists a set  $\Xi_{\theta, \Delta}$  of such curves and  $\eta > 0$ , with*

$$\eta = C\theta^{1/\alpha}$$

*for some constants  $C, \alpha > 0$ , such that if  $\gamma_1 \in \Xi_{\theta, \Delta}$  and  $\text{dist}(\gamma_1, \gamma_2) < \eta$ , then  $\forall T \geq 0$  such that  $\gamma_1([0, T])$  and  $\gamma_2([0, T])$  do not visit the  $\Delta$  neighborhood of  $c$  and provided that  $b, c, d$  are all in the same connected component in both the domains  $\Omega \setminus \gamma_1((0, T])$  and  $\Omega \setminus \gamma_2((0, T])$ ,*

$$|C_\varepsilon(\Omega \setminus \gamma_1([0, T]), \gamma_1(T), b, c, d) - C_\varepsilon(\Omega \setminus \gamma_2([0, T]), \gamma_2(T), b, c, d)| < \frac{1}{2}\theta$$

and for all  $\varepsilon$  sufficiently small,

$$\mu_\varepsilon(\Xi_{\theta,\Delta}) > 1 - \frac{1}{2}\theta,$$

with the same for  $\mu'$ .

**Remark VI.3.2.** While the result in the statement of this lemma may seem perfectly obvious, and the ultimate proof not too terribly arduous, it is worth pointing out the obstructions to an immediate proof:

- The relevant curves are “two-sided” – i.e., a yellow and blue side. If we wish to meaningfully *connect* a particular curve to a given boundary via a path in the background, it is important to ensure that the path strike the appropriate side of  $\gamma$ . The simplest counterexample is perhaps given by two curves  $\gamma_1$  and  $\gamma_2$  which are sup-norm close, both doubleback on themselves, but in *opposite* directions.
- Even if an appropriate continuation has been satisfied, care must be taken to ensure that *later* portions of  $\gamma$  do not “cut” the connection by presenting an obstruction to the connecting path with its opposite colored side.
- The topological problems will in fact happen on many scales, necessitating a multi-scale version of no-doublingback estimates (Lemma VI.2.11).

The proof of this lemma will therefore involve 1) first making some logical reductions to reduce to considering only certain set of percolation configurations (which rids us of the second difficulty) 2) establishing a suitable “topological” picture to ensure the troublesome scenarios described in the previous

paragraph has small probability (which rids us of the first difficulty) and finally 3) carry out the appropriate percolation construction to continue the crossing (where we will resolve the third difficulty).

**Remark VI.3.3.** In what follows we are not very explicit about whether  $\gamma_1, \gamma_2$  are continuum curves or their discrete approximations. Strictly speaking, we should really be talking about  $\gamma_1^\varepsilon, \gamma_2^\varepsilon$ , which are sup-approximations (e.g.,  $\gamma_1^\varepsilon$  converges to  $\gamma_1$  in the sup-norm as given in (VI.1); see [4]) to  $\gamma_1$  and  $\gamma_2$ . Indeed, the arguments that follow really only concerns this setting: I.e.,  $\text{dist}(\gamma_1^\varepsilon, \gamma_2^\varepsilon) < \eta$ .

However, once the lemma has been established, we do obtain as a consequence that the crossing probability is, up to an error, fairly independent of discretization. (A similar line of reasoning is used in [6], §7.) On the other hand, some care may be required if one demands more precise quantification: It may very well be the case that  $\eta$  is quite different from  $\varepsilon$ , e.g.,  $\eta = \varepsilon^{1/a}$ , for some  $a > 1$ .

*Proof. Scales and Properties of  $\gamma$ .*

We envision  $\Omega$  to be rectangular, with  $a$  as the bottom right corner, and

$$\eta \ll \vartheta' \lesssim \vartheta \ll \delta_3 \ll \delta_2 \ll \delta_{3/2} \ll \delta_1 \ll \Delta_4 \ll \tilde{\Delta} \lesssim \Delta \ll \Delta_1 \ll 1. \quad (\text{VI.6})$$

We remark that, perhaps, not all these separate scales are strictly necessary for the proof, but we shall utilize them to facilitate the exposition. Here  $\Xi_{\theta, \Delta}$  denotes the set of curves  $\gamma$  emanating from  $a$  which have the following properties:

1.  $\gamma$  has neither  $\frac{1}{2}\delta_2-3\delta_3$  nor  $\frac{1}{2}\vartheta'-3\eta$  double backs ( $\vartheta' \lesssim \vartheta$ );
2.  $\gamma$  satisfies the conclusion of Lemma VI.2.11 concerning  $v$ -persistent- $\kappa$ -weak doubleback at scales  $\frac{1}{2}\delta_2 > 3\vartheta$ ;
3.  $\gamma$  has neither  $\frac{1}{2}\delta_1-2\delta_2$  nor  $\frac{1}{2}\delta_3-2\eta$  triple visits; moreover, c.f. Remark VI.2.4, at these scales, there are no “forced future triple visits” with  $\gamma(t)$  inside a cul-de-sac;
4.  $\gamma$  has neither  $\frac{1}{2}\Delta_4-\delta_1$  nor  $\frac{1}{2}\delta_{3/2}-2\delta_2$  (nor  $\frac{1}{2}\delta_4-2\delta_2$ ) double visit to the boundary; moreover, c.f. Remark VI.2.7, at these scales, there are no “none fully developed” double visits;
5.  $\gamma$  stays a distance  $2\Delta$  away from the corners  $b$  and  $d$ ;
6.  $\gamma$  does not return to the  $2\Delta$  neighborhood of  $a$  after having left a  $\frac{1}{2}\Delta_1$  neighborhood of  $a$ , i.e., if

$$t_0 = \inf_t \{\text{dist}(a, \gamma(t)) > \frac{1}{2}\Delta_1\},$$

then for  $t > t_0$ ,  $\text{dist}(a, \gamma(t)) > 2\Delta$ ; similarly at the scales  $2\delta_3-\frac{1}{2}\delta_1$ .

By Lemmas VI.2.9, VI.2.6, Russo–Seymour–Welsh arguments, Corollary VI.2.3, Lemma VI.2.11, respectively, we have that  $\mu_\varepsilon(\Xi_{\theta,\Delta}) > 1 - \frac{1}{2}\theta$ . (Here we have assumed the domain to have smooth boundary, so the conformal invariance argument from the proof of Lemma VI.2.6 is not needed.) Notice that since  $\gamma_1 \in \Xi_{\theta,\Delta}$  and  $\gamma_2$  is  $\eta$ -close to  $\gamma_1$  in the sup-norm, both curves satisfy properties 1 – 6 without the numerical factors. We emphasize that while  $\gamma_1$  was supposed to be Exploration Process typical, this curve will not interact with

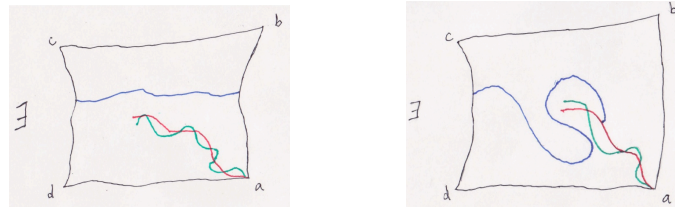
the background configuration of  $\Omega$ ; the above mentioned are the *only* properties of the  $\gamma$ 's which will be used.

We let  $R_1$  denotes the (conformal) rectangle  $\Omega \setminus \gamma_1([0, T])$ , and similarly for  $R_2$ . Let us start by assuming that there is a blue crossing for  $R_1$ ; to prove the lemma in this case it is enough to show that with high probability there is a blue crossing for  $R_2$ . Since “blue” and “yellow” are interchangeable and  $(\gamma_1, R_1) \leftrightarrow (\gamma_2, R_2)$  are interchangeable (since we only use properties 1 – 6 modulo factors of two) this is in fact enough to prove the entire lemma. Under the present circumstances, let us separate into three disjoint cases:

1. There is a blue crossing of  $\Omega_\varepsilon$  *itself* which passes through neither  $\gamma_1([0, T])$  nor  $\gamma_2([0, T])$ .
2. The criterion of case 1 is not satisfied; there is a blue crossing of  $R_1$  which hits  $\gamma_1([0, T])$  but does not pass through  $\gamma_2([0, T])$ .
3. Any blue crossing of  $R_1$  passes through  $\gamma_2([0, T])$ .

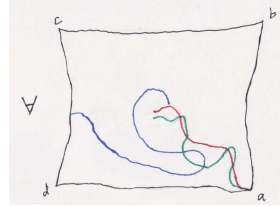
For illustration of these cases, see Figures VI.2.

**Remark.** In the above, we only need appeal to the heuristic interpretation of curves “hitting” or “passing through” one another. This is unambiguous if we consider discrete curves (see Remark VI.3.3). More precisely, in the present context, we may consider the map (conformal or otherwise) which takes e.g.,  $R_1$  to a rectangle. Here the tip,  $\gamma_1(T)$ , constitutes the lower right corner and there are two images of  $a$ ; the yellow side of  $\gamma_1$  joins with the original  $[d, a]$  boundary of  $\Omega$  while the blue side joins with the corresponding  $[a, b]$  boundary (it is often useful to think of the above “unzipped” domain as  $R_1$  itself). In the



(a) Case 1

(b) Case 2



(c) Case 3

Figure VI.2: Division of configurations containing a left–right blue crossing for  $R_1$  into cases.

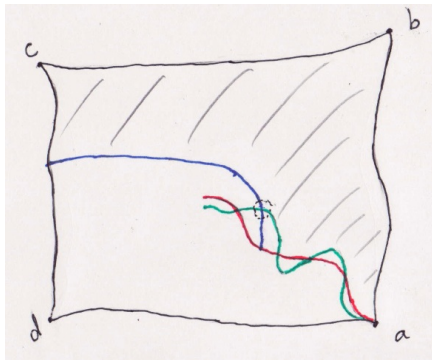
context of *this* rendition of  $R_1$ , the blue crossing “passing through”  $\gamma_1$  means that it is no longer a single contiguous curve but if it only hits  $\gamma_1$ , it remains a curve (which happens to have touched the boundary).

Our next goal is to show that:

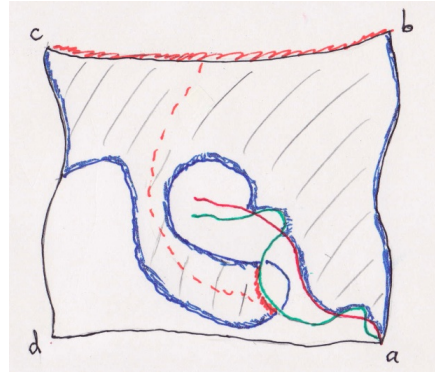
*Without loss of generality, we may assume we are in case 2.*

Aside from the obvious – one case fewer – the reduction to case 2 has succinct tactical advantages. In particular, the positioning of  $\gamma_2$  relatively to “the” crossing (ultimately, the *highest* crossing) of  $R_1$  will enable continuation of the crossing up to the blue side of  $\gamma_2$ . Then, by the stipulations of this case, we are assured (c.f. remarks in the opening paragraph of this proof) that the later portions of  $\gamma_2$  will *not* override the established connection which renders this connection a genuine crossing of  $R_2$ .

***Reduction to Case 2.***



(a) Either blue crossing for  $R_2$



(b) Or case 2 with yellow  $\leftrightarrow$  blue,  $2 \leftrightarrow 1$

Figure VI.3: Reduction of case 3 to case 2.

In case 1, we clearly have a blue crossing of both  $R_1$  and  $R_2$  and there is nothing to prove, so let us examine case 3. Our general claim about case 3 is that either there will also be a blue crossing for  $R_2$  or we are back in case 2 with the reversal of yellow  $\leftrightarrow$  blue,  $2 \leftrightarrow 1$ . Indeed, suppose in general there is a blue crossing in  $R_1$ . This creates a new domain  $\mathbb{B}$ , which is the region bounded by the said blue crossing,  $[b, c]$ , and the relevant portions of  $[c, d]$ ,  $[a, b]$  and  $\gamma_1$ . We remark that while  $\mathbb{B}$  still has a yellow “top”, namely  $[b, c]$ , it no longer constitutes an arena for crossing problems since there is no other yellow boundary. However, let us consider  $\tilde{\mathbb{B}}$  which is the connected component of  $[c, b]$  in  $\mathbb{B} \setminus \gamma_2([0, T])$ . Now  $\tilde{\mathbb{B}}$  still has a yellow top (not necessarily topologically connected) and *may* have additional pieces of yellow boundary at places where  $\gamma_2$  presented its yellow side into the interior of  $\mathbb{B}$ . In  $\tilde{\mathbb{B}}$  there is either a top to “bottom” (presumed to be non-empty) yellow crossing or not. If there is no such yellow crossing (this includes the case that the bottom of  $\tilde{\mathbb{B}}$  is empty), then certainly there is a blue type crossing in  $R_2$  (any other scenario would lead to a violation of the assumption that we are in case 3); here we conclude that we got into case 3 because the pass through of the said initial blue crossing

of  $R_1$  happened on the blue side of  $\gamma_2$  *before* reaching the blue side of  $R_1$ . But, if there is a top–bottom yellow crossing in  $\tilde{B}$ , it emanates from a portion of  $\gamma_2$  and it certainly asserts itself in the complement of the boundary of  $\tilde{B}$  and thus manifestly does not pass through  $\gamma_1$ ; this is the blue  $\leftrightarrow$  yellow reverse of case 2 and the reduction is complete. These scenarios are illustrated in Figure VI.3.

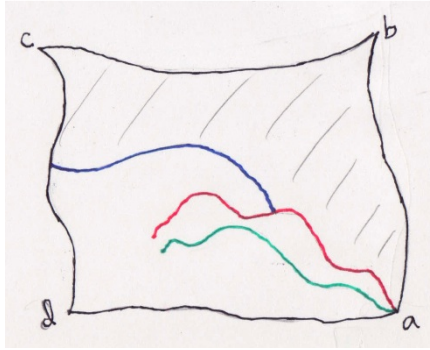
***Reduction to Highest Crossing.***

Now we let  $B_{\delta_1}(\gamma_1(T))$  denote the ball of radius  $\delta_1$  around  $\gamma_1(T)$ , and note that  $B_{\delta_1}(\gamma_1(T))$  is well away from  $c$ . Let us also assume that  $B_{\delta_1}(\gamma_1(T))$  is well away from all the other corners and the boundary; the corner and boundary cases will be handled at the very end of the proof. By Russo–Seymour–Welsh arguments, we can safely assume that any blue or yellow paths we will discuss stay away from  $B_{2\delta_1}(\gamma_1(T))$ .

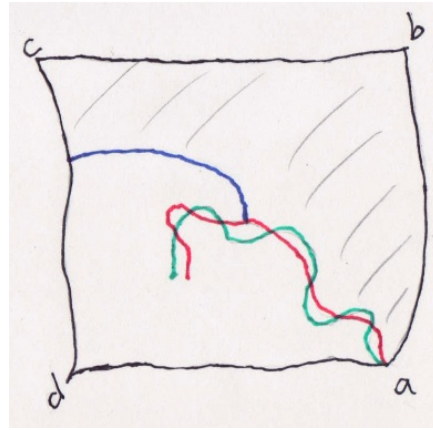
Our next claim is (assuming  $\gamma_1 \in \Xi_{\theta,\Delta}$ ):

*If  $\beta_0$  is a blue crossing of  $R_1$  manifesting the conditions of case 2, i.e., “ $\beta_0$  is a blue crossing of  $R_1$  which hits  $\gamma_1([0, T])$  but does not pass through  $\gamma_2([0, T])$ ”, and  $\beta_1$  is a “higher” crossing in  $R_1$ , then either  $\beta_1$  provides a blue crossing in  $R_2$ , or  $\beta_1$  also manifests the conditions of case 2 [in particular this will allow us to focus on the highest blue crossing for  $R_1$ ].*

This step is needed as to actually continue the crossing requires us to use the fact that (conditioned on the highest crossing) we again have independent percolation in the region below the highest crossing.



(a) Case where  $\beta_0$  lies entirely in  $\mathbb{B}_0$



(b) Case where  $\gamma_2$  weaves in and out of  $\mathbb{B}_0$  in a “regular” fashion

Figure VI.4: Scenarios where it is easy to reduce to the highest crossing.

To see this, let  $m_0$  denote the time along  $\gamma_1$  where  $\beta_0$  meets  $\gamma_1$  to produce the purported crossing. It is clear that  $\beta_0, \gamma_1([0, m_0])$ , and the relevant portion of  $\partial\Omega$  form a Jordan domain containing  $b$  which will be denoted  $\mathbb{B}_0$ . We first remark that if  $\gamma_2 \subset \mathbb{B}_0^c$ , then the claim is in fact trivial: Any higher blue crossing than  $\beta_0$  lies entirely in  $\mathbb{B}_0$  and therefore there is no possibility of it hitting  $\gamma_2$  at all. Moreover, if  $\gamma_2$  weaves in and out of  $\mathbb{B}_0$  and  $\mathbb{B}_0^c$  in a “regular” fashion, the result is equally plausible. For illustrations of these well-behaved scenarios, see Figure VI.4.

However, due to contortions in which the curve bends back on itself, the situation is much more complicated (see Figure VI.5) and we will need to employ, in a measured fashion, Assumption 1. To this end, let us first define  $\tau^*$  to be the last time  $\gamma_2$  enters  $B_{\delta_1}(\gamma_2(T))$  before reaching  $\gamma_2(T)$ . Next let us apply Assumption 1 to produce a point  $\gamma_2(t^*) \in B_{\delta_1}(\gamma_2(T))$  (with  $t^* > \tau^*$ ) which is a distance (at least)  $2\delta_3$  from all boundaries of  $\mathbb{B}_0$  (recall that  $\beta_0$  is assumed to stay outside  $B_{2\delta_1}(\gamma_2(T))$ ).

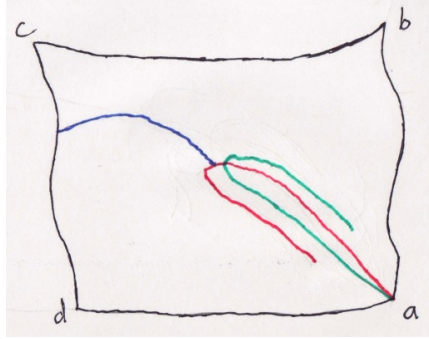


Figure VI.5: Case where  $\beta_0$  is manifesting the conditions of case 2 but a higher crossing may not be.

***Reduction to Highest Crossing: “Topological” Description***

The key observation is that if there exists some path  $\Gamma : \gamma_2(t^*) \rightarrow d$  inside  $\mathbb{B}_0^c$  which avoids  $\gamma_2([0, \tau^*])$ , then we are in fact done. Indeed, in the simplest case where  $\Gamma$  can be made to avoid all of  $\gamma_2([0, t^*])$ ,  $\Gamma$  together with  $\gamma_2([0, t^*])$  and  $[d, a]$  form a Jordan domain with the property that the external boundary (of the  $\gamma_2$  part) is blue; if somehow collisions of  $\Gamma$  with portions of  $\gamma_2([\tau^*, t^*])$  are unavoidable, the relevant domain may be constructed by running  $\gamma_2$  until its first collision point with  $\Gamma$  and then proceeding along  $\Gamma$ . We will not distinguish between these two cases, nor their underlying domains, since no blue connection emanating from  $[c, d]$  will ever enter  $B_{\delta_1}(\gamma_2(T))$ . Now any higher crossing  $\beta_1$  must initiate outside this domain, so if it hits the boundary of this domain, then it must hit the blue side of  $\gamma_2$  and hence form a crossing for  $R_2$  (it cannot hit  $\Gamma$  since  $\Gamma \subset \mathbb{B}_0^c$  and  $\beta_1 \subset \mathbb{B}_0$ ); on the other hand, if  $\beta_1$  fails to hit the boundary of the domain, then it fails to hit any part of  $\gamma_2$ , and we remain in Case 2, since  $\gamma_2([\tau^*, T]) \subset B_{\delta_1}(\gamma_2(T))$  which by assumption is not entered by any blue crossing of interest.

***Reduction to Highest Crossing: Multiply Connected Components, etc.***

**Remark.** *The sort of arguments here concerning multiply connected components also appear later under “The Bulk Case: Multiply Connected Components, etc.” and are in fact simpler there. The reader may wish to skip this section on a first reading.*

For technical reasons, we will not have much occasion to working with  $\gamma_2(\tau^*)$ , but instead with another point  $V$ , which is defined to be the last point on  $\gamma_2$  before it enters  $\mathbb{B}_0^c$  before time  $\tau^*$  and we let  $\gamma_2(v) = V$  (so that  $\tau^* \geq v$ ). For definitiveness, let us assume that  $v \geq m_0$ . Indeed, if  $V$  occurs before  $\gamma_2$  enters the  $\eta$ -ball about  $M_0$ , the point  $V$  – along with various associated considerations – is not really necessary and the proof is, overall, slightly easier. However, even in this case, much of the forthcoming is required so we shall not provide a completely separate argument, but instead indicate the necessary modifications/simplifications when the occasion arises. Note that  $V$  exists, since we have ruled out the trivial case where  $\gamma_2 \subset \mathbb{B}_0^c$ . Let us now define a few multiply-connected domains. For standing notation, if  $\omega \in \Omega$  and  $\mathbb{L} \subset \Omega$  is a domain, then  $C_{\mathbb{L}}(\omega)$  is notation for the connected component of  $\omega$  in  $\mathbb{L}$ . Let

$$G_r = \Omega \setminus [\beta_0 \cup \gamma_1([0, v]) \cup B_\eta(V) \cup B_\eta(M_0)]$$

and let  $G_g$  denote the corresponding domain with  $\gamma_1$  replaced by  $\gamma_2$ :

$$G_g = \Omega \setminus [\beta_0 \cup \gamma_2([0, v]) \cup B_\eta(V) \cup B_\eta(M_0)].$$

Both of these domains have “principal” components, namely, the connected component of  $d$  and the connected component of  $b$ , and, possibly, other com-

ponents. To simplify matters, note that  $\gamma_1(t^*)$  and  $\gamma_2(t^*)$  are both far away from  $\partial G_r$  and  $\partial G_g$  and therefore for all intents and purposes, we may identify them as the same point and denote it by  $\gamma(t^*)$ . Our claim is that now we are done if we can show  $\gamma(t^*) \in C_{G_r \cap G_g}(d)$  (more precisely, it is meant that  $\gamma(t^*)$  can be connected to  $d$  by a path which does not pass through any of the boundaries – but it is conceivable that it may touch these boundaries). Indeed, in terms of the existence of the  $\Gamma$  of interest, we are in fact forcing  $\Gamma$  to avoid more of  $\gamma_1$  than is strictly necessary. On the other hand, it is the case that  $v \leq \tau^*$ , so we avoid less of  $\gamma_2$  *a priori*, but this is of no concern, since the portion of  $\gamma_2$  after time  $v$  is either inside  $\mathbb{B}_0^c$  or inside  $B_{\delta_1}(\gamma_2(T))$ , and hence cannot interfere with the higher crossing  $\beta_1$  (as per the explanation right after the definition of  $\Gamma$ ).

First it is clear that  $\gamma(t^*) \notin C_{G_r \cap G_g}(b)$  since it is not even in  $\mathbb{B}_0$ . It remains to handle the cases where  $\gamma(t^*)$  is in one of the “smaller” components (which ultimately, since we are discrete on the scale  $\varepsilon$ , there are only a finite number of). We will begin by showing  $\gamma(t^*) \in C_{G_r}(d)$ . We point out that  $\gamma(t^*) \in \mathbb{B}_0^c$ , which means that without the deletion of the  $\eta$ -neighborhoods of  $M_0$  and  $V$ , there *is* a path  $\Gamma^*$  which connects  $\gamma(t^*)$  to  $d$ . If it is the case that  $\gamma(t^*) \notin C_{G_r}(d)$ , then it must have been the case that any such  $\Gamma^*$  went through either  $B_\eta(M_0)$  or  $B_\eta(V)$ . Let us first consider the case of  $B_\eta(M_0)$ . Here the implication is that  $\gamma(t^*)$  has been trapped inside a sack formed by (some portion of)  $\gamma_1([0, v])$  and  $\partial B_\eta(M_0)$ . In particular  $\gamma_1([0, v])$  must have made a double visit to  $B_\eta(M_0)$ . It is noted that by Russo–Seymour–Welsh arguments applied to  $\beta$ , with probability close to unity,  $M_0$  is a distance more than  $\delta_1 > \delta_3$

from  $a$ . Thus  $\gamma_1(t^*)$  is in a deep cul-de-sac of the type which “would” force a future triple visit at  $B_\eta(M_0)$ . The relevant parameters for the cul-de-sac are  $\delta_3$  and  $\eta$  (since  $\gamma(t^*)$  is a distance at least  $2\delta_3$  from all boundaries and the initial path to  $M_0$  is at least  $\delta_1$ ). This is ruled out by Assumption 3.

The case where  $\Gamma^*$  goes through  $B_\eta(V)$  is nearly identical. Foremost, if  $v$  occurs before  $\gamma_2$  enters  $B_\eta(M_0)$ , we may omit  $B_\eta(V)$  altogether from the definitions of  $G_g$  and  $G_r$  since  $\gamma_2([m_0, t^*])$  is not actually obstructed by  $\gamma_1([0, m_0])$ . That is, we replace the definition of e.g.  $G_g$  with

$$G_g = \Omega \setminus [\beta_0 \cup \gamma_2([0, m_0]) \cup B_\eta(M_0)],$$

and similarly for  $G_r$ . The cases  $v \gtrsim m_0$  follow identically, the only relevant modification being the observation that the first visit to  $B_\eta(V)$  (coming from  $a$ ) must be at least of scale  $\delta_3$ , according to Assumption 6, since otherwise the later visits would be precluded.

Next we turn attention to  $G_g$  and reduce to the case that  $\gamma(t^*) \in [C_{G_g}(b) \cup C_{G_g}(d)]$ . This will be done by reducing to the case as described above in the domain  $G_r$ . We first note that in the absence of  $B_\eta(M_0)$  and  $B_\eta(V)$ ,  $\gamma(t^*)$  is in both the connected component of  $b$  and the connected component of  $d$ . (This is because  $\beta_0$  is a crossing which gets us into case 2 and therefore does not pass through  $\gamma_2$ . Here we are using the phrase “connected component” in the sense as described before. Note that this does not apply to the domain  $\mathbb{B}_0$  whose boundary is taken to be the union of  $\beta_0$  and  $\gamma_1([0, m])$ , regarded as a single curve, so in particular, a path is not allowed to slip through the juncture at  $M_0$ ). In particular, there exists  $\Gamma^* : \gamma(t^*) \rightarrow d$ . Again  $\Gamma^*$  must pass through say  $B_\eta(M_0)$  (or it may pass through  $B_\eta(V)$ , just as before). The same argument

as in the previous paragraph now shows that  $\gamma(t^*)$  must be contained in a  $\delta_3$  sack formed by  $\gamma_2([0, v])$ . Doubling the radius of  $B_\eta(M_0)$  if necessary, this also implies  $\gamma(t^*)$  is contained in a large sack formed by  $\gamma_1([0, v])$ , since  $\gamma_1$  and  $\gamma_2$  are  $\eta$ -close, and hence we would again be in contradiction of Assumption 3.

Next we will show that  $\gamma(t^*) \in C_{G_r}(d)$  and  $\gamma(t^*) \in [C_{G_g}(b) \cup C_{G_g}(d)]$  in fact implies that  $\gamma(t^*) \in C_{G_g}(d)$ . Suppose towards a contradiction that  $\gamma(t^*) \in C_{G_g}(b)$  (i.e.,  $\gamma(t^*) \notin C_{G_g}(d)$ ). This implies that  $\gamma(t^*) \notin C_{G_r \cap G_g}(d)$  and  $\gamma(t^*) \notin C_{G_r \cap G_g}(b)$ . Due to the previously noted components of  $d$  (and  $b$ ) in  $G_r$  (respectively  $G_g$ ) to which  $\gamma(t^*)$  belongs it is clear that the obstructions in the intersected domain are the  $\gamma$  curves themselves.

For technical reasons, if  $m_0 \leq v$ , let us join  $\gamma_1(v)$  to  $\gamma_2(v)$  by a straight line segment (if it were the case that  $m_0 > v$ , then we would make the argument with  $m_0$  instead of  $v$ ) – half of which is adjoined to  $\gamma_1$  and the other half to  $\gamma_2$ , in the obvious fashion. We now omit from consideration all other portions of the boundary and consider only the closed curve formed by the  $\gamma$ 's, etc in the punctured domain  $\mathbb{C} \setminus \gamma(t^*)$ . We now claim that the closed curve in question is contractible to a point in  $\mathbb{C} \setminus \gamma(t^*)$ . Indeed, since the ‘‘puncture’’ is far away ( $\delta_3$  away) from the e.g., the straight line segments of length less than  $\eta$  joining  $\gamma_1(t)$  to  $\gamma_2(t)$ , one curve can be deformed onto the other in  $\mathbb{C} \setminus \gamma(t^*)$ . It is thus evident that  $\gamma(t^*)$  is in the connected component of either  $b$  or  $d$  in  $G_r \cap G_g$ . (Recall that we have already ruled out the possibilities of  $\gamma(t^*)$  being caught in a sack formed by  $\gamma_1$  or  $\gamma_2$  and the neighborhoods being cut out; regardless, the preceding argument in fact would show that  $\gamma(t^*)$  would actually end up in the ‘‘same’’ sack in  $G_r$  and  $G_g$ .) Thus, so far, we have

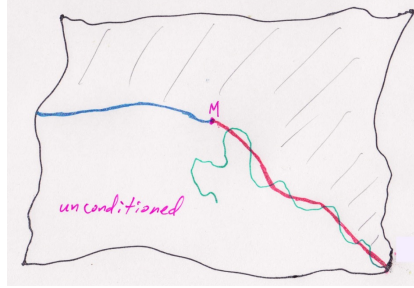


Figure VI.6: The region  $\mathbb{B}$  and  $\mathbb{B}^c$  – the unconditioned region.

that  $\gamma(t^*) \in C_{G_g}(d)$ . But now we claim that the above homotopy argument also implies that  $\gamma(t^*) \in C_{G_g \cap G_r}(d)$  (and hence the required  $\Gamma$  exists). Indeed, in the intersected domain, the options for the connected component of  $\gamma(t^*)$  are limited and the above demonstrates that they do not change under the homotopic distortion.

### ***The Bulk Case: Description***

As the title indicates, we shall be treating cases where relevant portions of  $\gamma_1$  and  $\gamma_2$  are well away from  $\partial\Omega$ . These relevant portions are, in fact, the tips ( $\gamma_1(T)$  and  $\gamma_2(T)$ ), and a point,  $M \in \gamma_1$ , which is the analogue of the point  $M_0$  in *Reduction to Case 2*; these distance scales will turn out to be  $\delta_1$  respectively, and, in addition, we shall assume that *all* portions of the  $\gamma$ 's are outside the  $\Delta$  neighborhoods of  $b, c, d$  (as in accord with the statement of the Lemma and Assumption 5).

Let us then select the highest blue crossing for  $R_1$ ; we denote this crossing by  $\beta$ . Let us further denote by  $M$  the point where it hits  $\gamma_1$ ; moreover we shall define the time  $m$  via  $\gamma_1(m) = M$ . In accord with the preceding notation, we shall denote by  $\mathbb{B}$  the region which is above  $\beta$  in  $R_1$ , i.e., the domain bounded

by the union of  $\beta$ ,  $\gamma_1([0, m])$  and the relevant portions of  $\partial\Omega$ . An important observation which will be used time and again in the forthcoming paragraphs is that having selected the highest crossing, it is precisely – no more and no less – the region  $\mathbb{B}^c$  which may be considered “unconditioned”. For an illustration see Figure VI.6.

Let  $s$  denotes the last time  $\gamma_2$  exits the ball  $B_{\delta_2}(M)$ . Suppose we have the following claims:

**Claim 1.** *With high probability  $\gamma_2(s)$  can be connected to  $d$  by a curve  $\Gamma$  inside  $\Omega$  not intersecting the blue crossing,  $B_{\delta_2}(M)$  or  $\gamma_2([0, s])$ .*

**Claim 2.** *With high probability,  $\beta$  can be continued to hit  $\gamma_2([0, s])$  inside  $B_{\delta_2}$  via a circuit (or portion thereof) which encircles  $M$ .*

Then we are done, since given Claim 1, if  $D$  denotes the domain below  $\gamma_2([0, s]) \cup \Gamma$ , then 1) the  $\gamma_2$  portion of the boundary of  $D$  presents its blue side to the outside and 2)  $M \in D^c$  since  $\gamma_2$  does not cross  $\beta$ .

**Remark VI.3.4.** In fact, a weaker condition than Claim 1 will already do, since we do not need  $\Gamma$  to avoid all of  $B_{\delta_2}(M)$ : It is sufficient that  $M \in D^c$  and it can be guaranteed that all continuations of  $\beta$  will hit  $\gamma_2$  *first* – and not  $\Gamma$ .

Claim 2 then gives the required continuation of  $\beta$  to hit  $\gamma_2$ , with high probability, and the two observations imply that this continuation must hit the blue side of  $\gamma_2$ . The “correct” topological picture just described is illustrated in Figure VI.7.



Figure VI.7: Outcome of Claims 1 and 2.

***The Bulk Case: Multiply Connected Components, etc.***

Let us first establish Claim 1, i.e., it is highly unlikely that  $\Gamma$  as described doesn't exist. The curve  $\gamma_2$  has no  $\delta_1$ - $\delta_3$  double back, by assumption. So, there exists a point  $\gamma_2(t^*)$  in  $B_{\delta_1}$  which is at least  $\delta_3$  away from  $\gamma_2([0, s])$ . Now let us observe that  $\gamma_2(s)$  is connected to  $d$  as described above if the same happens with  $\gamma_2(t^*)$ , since  $\gamma_2(s)$  can be connected to  $\gamma_2(t^*)$  by  $\gamma_2$  itself. We work with  $\gamma_2(t^*)$  from now on (although  $\Gamma$  need only avoid  $\gamma_2([0, s])$ ).

We now define the domain

$$E = \Omega \setminus [\gamma_2([0, s]) \cup B_{\delta_2}(M) \cup \beta],$$

where we remind the reader that  $M$  is at least  $\delta_1$  away from the boundary. Recall the notation  $C_E(x)$  which denotes the connected component of  $x$  in the domain  $E$  (for a drawing of such a domain see Figure VI.8). It is observed, possibly, that in addition to  $C_E(d) \neq \emptyset$  and  $C_E(b) \neq \emptyset$ ,  $E$  may have other connected components due to loops formed by  $\beta$  or  $\gamma_2$  running in and out of  $B_{\delta_2}(M)$ . In this language:

*The existence of  $\Gamma$  (with high probability) is equivalent to the state-*

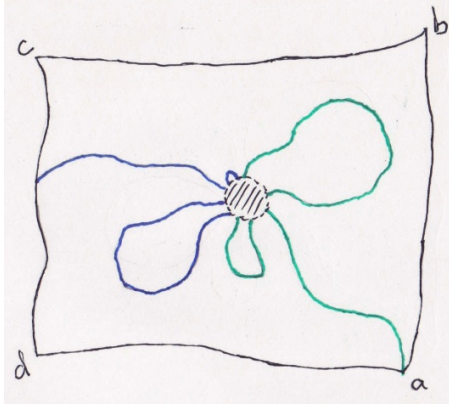


Figure VI.8: Multiply connected domain.

ment that  $\gamma_2(t^*) \in C_E(d)$  (with high probability).

Further, by minor abuse of notation, we use  $C_{\mathbb{B}}(x)$  to denote the component of  $x$  in  $\Omega \setminus [\beta \cup \gamma_1([0, m])]$ . Once again, it is observed then that since  $\gamma_1(t^*)$  and  $\gamma_2(t^*)$  are within  $\eta$  of each other and both of these points are at least  $\delta_3 \gg \eta$  from any other boundary of  $\mathbb{B}$  or  $E$ ,  $C_{\mathbb{B}}(\gamma_1(t^*)) = C_{\mathbb{B}}(\gamma_2(t^*))$  and  $C_E(\gamma_1(t^*)) = C_E(\gamma_2(t^*))$ ; indeed, the entire  $\delta_3$  neighborhood of  $\gamma_2(t^*)$  resides in the same component of  $E$  and in the same “component of  $\mathbb{B}$ ”. Thus both (either) of these points will be denoted by  $\gamma(t^*)$ . The relevant scales are illustrated in Figure VI.9.

Our next goal is to show that under the stated conditions,  $\gamma(t^*) \notin C_E(b)$ . Suppose towards a contradiction that  $\gamma(t^*) \in C_E(b)$ . Now let us consider a simpler domain, designed to be similar to the domain  $\mathbb{B}$ :

$$F_g = \Omega \setminus [\gamma_2([0, m]) \cup B_{2\eta}(M) \cup \beta].$$

We notice that  $E \subset F_g$  and hence under our current assumption,  $\gamma(t^*) \in C_{F_g}(b)$ . Furthermore, we also consider  $F_r = \Omega \setminus [\gamma_1([0, m]) \cup B_{2\eta}(M) \cup \beta]$ ,

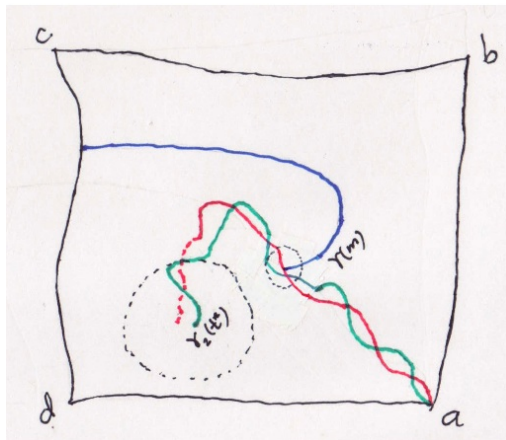
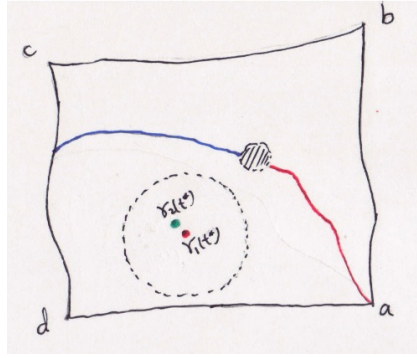


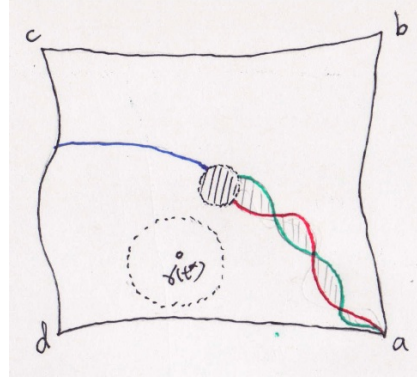
Figure VI.9: The point  $\gamma^*$ .

the  $\gamma_1$  version of the above display. We assert that  $\gamma(t^*) \in C_{F_r}(d)$  with high probability: Since  $\gamma(t^*) \in C_{\mathbb{B}}(d)$ , the only thing that can go wrong is if all paths from  $\gamma(t^*)$  to  $d$  must go through  $B_{2\eta}(M)$ , i.e., a long portion of  $\gamma_1$  or  $\beta$  together with  $B_{2\eta}(M)$  form a domain with  $\gamma(t^*)$  in its interior. As it turns out, this case is essentially a “minor” version of the cases where  $\gamma(t^*) \notin C_E(b) \cup C_E(d)$  and hence will be treated later. Since  $b$  and  $d$  are clearly in separate connected components in both  $F_r$  and  $F_g$ , it is clear that  $\gamma(t^*) \notin C_{F_r \cap F_g}(b)$  and  $\gamma(t^*) \notin C_{F_r \cap F_g}(d)$  – and that the obstructions in the intersected domain are the  $\gamma$  curves themselves.

For technical reasons, let us join  $\gamma_1(m)$  to  $\gamma_2(m)$  by a straight line segment – half of which is adjoined to  $\gamma_1$  and the other half to  $\gamma_2$ , in the obvious fashion. We now omit from consideration all other portions of the boundaries – including  $\partial\Omega$  – and consider only the closed curve formed by the  $\gamma$ 's, etc. in the punctured domain  $\mathbb{C} \setminus \gamma(t^*)$ . We now claim that the closed curve in question is contractible to a point in  $\mathbb{C} \setminus \gamma(t^*)$ . Indeed, since the “puncture” is far away



(a)  $\gamma_1, \gamma_2 \in C_{F_r}(d)$



(b) Homotopy argument

Figure VI.10:  $\gamma(t^*)$  cannot be trapped between  $\gamma_1$  and  $\gamma_2$ .

from e.g., the straight line segments joining  $\gamma_1(t)$  to  $\gamma_2(t)$  (of length  $\eta$ ), one curve can be deformed onto the other in  $\mathbb{C} \setminus \gamma(t^*)$ . It is thus evident that  $\gamma(t^*)$  is in the connected component of either  $b$  or  $d$  in  $F_r \cap F_g$ , a contradiction, and hence  $\gamma(t^*) \notin C_E(b)$ . The relevant scales, etc., are illustrated in Figure VI.10.

To finish the bulk case, we recall that  $E$  may have several connected components other than  $C_E(b)$  and  $C_E(d)$  and therefore we must rule out the possibility that  $\gamma(t^*)$  belongs to these components. These components can come about either because 1) a portion of  $\beta$  connects two points of  $\partial B_{\delta_2}(M)$  in the complement of  $B_{\delta_2}(M)$  or 2) a portion of  $\gamma_2([0, s])$  connects two points of  $\partial B_{\delta_2}(M)$  in the complement of  $B_{\delta_2}(M)$ . For obvious reasons, these components will be called blue pseudo-pods and  $\gamma_2$  pseudo-pods, respectively. Recall also that the  $\gamma(t^*) \notin C_{F_r}(d)$  assertion in the previous portion of the proof suffers a similar description (albeit with a smaller neighborhood around  $M$  cut out) as 2), except with the curve  $\gamma_1$  instead of  $\gamma_2$  (and also  $\gamma_1$  truncated at an earlier time than  $s$ ). For technical reasons, it will be more convenient to treat  $\gamma_1$ -type pseudo-pods; since the two  $\gamma$  curves are  $\eta$ -close, we can always “convert”  $\gamma_2$ -type pseudo-pods to  $\gamma_1$ -type pseudo-pods by cutting out

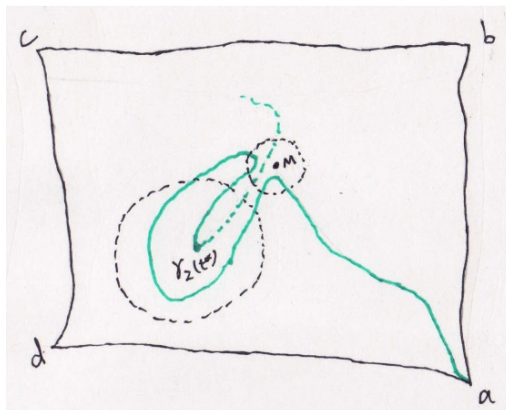


Figure VI.11:  $\gamma_2$  pseudo-pods.

a neighborhood around  $M$  of slightly larger radius.

Let us first consider  $\gamma_1$  pseudo-pods. In this case, the curve  $\gamma_1$  itself must visit  $B_{\delta_2}(M)$  itself twice, traveling a distance  $\delta_1$  in between, before reaching  $\gamma(t^*)$ , leaving it deep in a cul-de-sack (where in the future it would be forced to visit  $B_{\delta_2}(M)$  on its way to  $c$ ), in violation of Assumption 3 (for an illustration see Figure VI.11). It is worth remarking that this scenario we must estimate away: In effect what is happening in this case is that the curve is reversing its orientation at the  $\delta_1$ - $\delta_2$  scale (and since we are establishing a uniform estimate, we are not at liberty to expand/shrink the relevant scales) and as can be seen in Figure VI.11, it is very likely that a possible RSW continuation inside  $B_{\delta_2}(M)$  can hit the portion of  $\gamma_2$  after its re-entrance into  $B_{\delta_2}(M)$ , and hence hit the *yellow* side of  $\gamma_2$ , failing to constitute a valid continuation (note that most of the dashed portion of  $\gamma_2$  in this figure may very well not be present since we are only considering the curve up to time  $T$ ).

### ***The Bulk Case: Blue Pseudo-Pods***

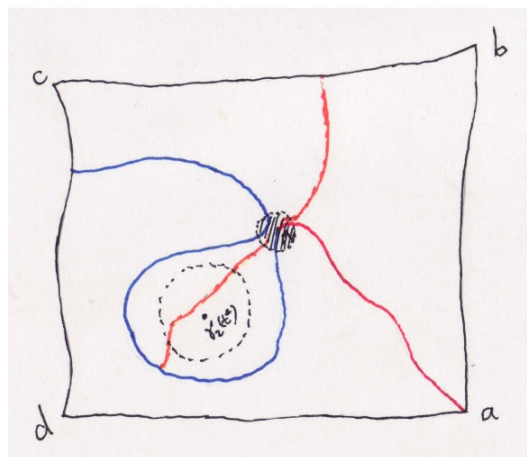
We finally turn attention to blue pseudo-pods. We will present two argu-

ments.

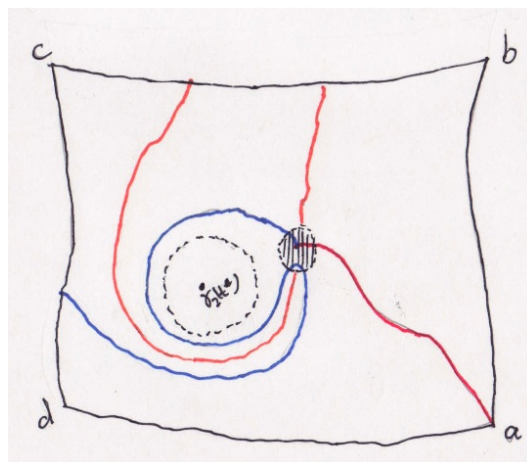
**First Argument:** In this case,  $\beta$  must have the following property:  $\beta$  visits  $B_{\delta_2}(M)$ , goes around  $B_{\delta_1}$  and revisits  $B_{\delta_2}(M)$ , since it separates  $\gamma(t^*) \in B_{\delta_1}$  from  $d$ . Since  $\beta$  is the *highest* crossing of  $R_1$ , it leads to the existence of 3 blue and 2 yellow  $\delta_1$ - $\delta_2$  long arms emanating from  $B_{\delta_2}(M)$  (both yellow arms come from the fact that  $\beta$  is the highest crossing; see Figure VI.12). Such an event has probability proportional to  $(\delta_1/\delta_2)^2$  by Lemma VI.2.1, and hence happens with probability tending to 0 as  $\delta_1/\delta_2$  tends to 0, because the Minkowski dimension of  $\gamma_1$  is less than 2 by Lemma VI.2.12.

**Second Argument:** Alternatively, we may argue that in fact blue pseudo-pods do not present any difficulty – instead of estimating such configurations away, as follows: Let us note that, running  $\beta$  starting from  $M$ , there are two types of blue pseudo-pods, clockwise and counterclockwise, or, alternatively, this corresponds to  $\gamma(t^*)$  being in  $C_{\mathbb{B}}(b)$  or  $C_{\mathbb{B}}(d)$ , respectively (here  $\mathbb{B} = \Omega \setminus [\gamma_1([0, m]) \cup \beta]$ ). For an illustration see Figure VI.12 (where the yellow arms forcing the blue pseudo-pod are also drawn). First we claim that a clockwise blue pseudo-pod as described is impossible: In this case,  $\gamma(t^*)$  (actually all of  $\gamma_1([m, T])$ ) lies in the connected component of  $\mathbb{B}$  with blue boundary, but this necessarily implies that  $\beta$  actually hit the *yellow* side of  $\gamma_1$ , contrary to assumption.

It remains to consider the case where  $\gamma(t^*)$  is in a counterclockwise blue pseudo-pod. Having handled all other possibilities (especially  $\gamma_2$  pseudo-pods), we may assume it is the case that there is some path  $\Gamma$  connecting  $\gamma_2(t^*)$  to  $d$  which avoids  $\beta$  and  $\gamma_2([0, t^*])$ , but goes through  $B_{\delta_2}(M)$ . Now as



(a) Clockwise blue pseudo-pod.



(b) Counterclockwise blue pseudo-pod.

Figure VI.12: Two possible orientations of blue pseudo-pods.

explained in Remark VI.3.4, for our purposes it is in fact already sufficient to show that  $M \in C_D(b)$ , where  $D = \Omega \setminus [\gamma_2([0, t^*]) \cup \Gamma]$ , and it can be guaranteed that all possible continuations inside  $B_{\delta_2}(M)$  will hit  $\gamma_2$  first.

The fact that  $M \in C_D(b)$  is clear: The curve  $\gamma_2([0, t^*])$  starts at  $a$  and must end up in  $C_{\mathbb{B}}(d)$  and since it cannot cross  $\beta$ , it must cross into  $C_{\mathbb{B}}(d)$  before  $\gamma_1$  joins  $\beta$  (which occurs at the point  $M$ ) and thus, since  $\Gamma$  also cannot cross  $\beta$ , the entirety of  $\Gamma$  must also lie in  $C_{\mathbb{B}}(d)$ . Since  $\beta$  starts (from the  $[c, d]$  boundary) outside of  $D$  and by the above arguments cannot cross  $\partial D$ , we have that  $M \in C_D(b)$ . Finally, it is easy to check that in this case (especially since  $\gamma(t^*)$  is not trapped in a  $\gamma_2$  pseudo-pod) one can draw a  $\Gamma$  so that it does not “block”  $\gamma_2$  from a possible continuation. It is worthwhile to compare this with the scenario of  $\gamma(t^*)$  being trapped inside a  $\gamma_2$  pseudo-pod, since there, as one can envision from Figure VI.11, it can easily be the case that any possible  $\Gamma$  will cut a continuation of  $\beta$ .

In any case, we have established some version of Claim 1 (c.f. Remark VI.3.4).

***The Bulk Case: Multiscale No-Doublingback, etc.***

Recall that  $M$  is surrounded by a ball of radius  $\delta_2$ , denoted by  $B_{\delta_2}(M)$ . We now want to establish Claim 2, i.e., “continue”  $\beta$  in some fashion, with probability close to one, in such a way that it hits  $\gamma_2$  inside  $B_{\delta_2}(M) \cap \mathbb{B}^c$ . We first note that  $\partial B_{\delta_2}(M)$  is connected to  $M$  inside  $\mathbb{B}^c$  – namely, by the relevant portion of  $\gamma_1$  after time  $m$ . We first show that, with probability tending to one, there are a sequence of points, on disjoint scales, each containing neighborhoods comparable to their scale, inside  $B_{\delta_2}(M) \cap \mathbb{B}^c$ .

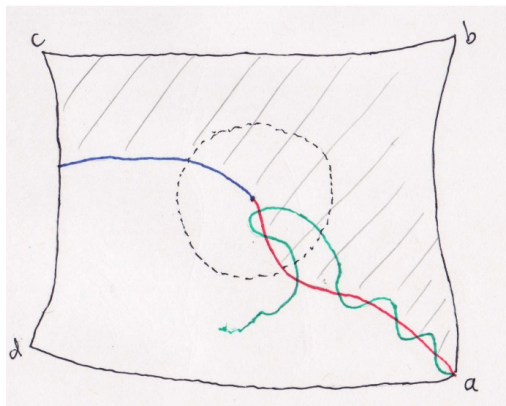


Figure VI.13: Scenario where  $\gamma_2$  “hides” behind  $\gamma_1$ .

To achieve this, we first assert the contents of Assumption 2 concerning  $v$ -persistent- $\kappa$ -weak doubling back at scales  $\delta_2$  and  $\vartheta$  with  $\eta \ll \vartheta \ll \delta_2$ . Thus, in a fraction at least as large as  $v$  of the 3:1 annuli of scale  $\vartheta_\ell (= 3^\ell \vartheta)$ , there is a point on  $\gamma_2$  – after time  $m$  – with the property that the box of scale  $\kappa \vartheta_\ell$  centered at this point does not meet  $\gamma_1([0, m])$ . We note that such a careful statement is needed since we can envision scenarios where  $\gamma_2$  “hides” behind  $\gamma_1$  in such a way that the continuation fails to hit  $\gamma_2$ . For an illustration see Figure VI.13. We note that this is the same sort of topological obstruction that concerned us shortly before, just at smaller scales.

Obviously, this box contains a segment of  $\gamma_2$  of diameter of the order  $\kappa \vartheta_\ell$ . We claim that this segment is, in fact, either entirely contained in  $\mathbb{B}$  or entirely contained in  $\mathbb{B}^c$ . Indeed, it cannot cross from  $\mathbb{B}$  to  $\mathbb{B}^c$ , because doing so necessitates crossing  $\gamma_1([0, m])$ , which it is far away from, or crossing  $\beta$ , which is *a priori* forbidden. However, if this segment were in  $\mathbb{B}$ , it is emphasized that the corresponding segment of  $\gamma_1$  which it is supposed to be  $\eta$ -close to is itself in  $\mathbb{B}^c$  (by definition) and therefore the pair must be separated by  $\beta$  – the

only available boundary, which we will now show is extremely unlikely.

Considering  $\gamma_1$  as a *fixed* object, we shall now establish the following elementary property of the active percolation configurations: For  $\eta > 0$ , let  $\vartheta' \lesssim \vartheta$  and consider the event

$$\mathbf{U}_{\vartheta'} = \{\exists \text{ a connected monochrome chain that is } \eta\text{-close} \\ \text{to any portion of } \gamma_1 \text{ of diameter } \geq \vartheta'\},$$

where in the above,  $\eta$ -close refers to the sup-norm. We claim that for  $\gamma_1$  satisfying Assumption 1

$$\mathbb{P}_\varepsilon(\mathbf{U}_{\vartheta'}) \leq c_1 \left(\frac{1}{\vartheta'}\right)^2 \left(\frac{\vartheta'}{\eta}\right)^2 e^{-c_2 \frac{\vartheta'}{\eta}}.$$

The proof of this statement involves arguments very similar to those found in the proofs of Lemmas VI.2.9 and VI.2.11, so we shall be succinct: We consider a tiling of  $\Omega$  by  $\vartheta' : k\vartheta'$  rectangles (where  $k$  is some integer) and focus attention on one of these. If the rectangle is crossed the easy way by  $\gamma_1$ , we obtain the factor  $e^{-c_2 \vartheta'/\eta}$  since on the order of  $\vartheta'/\eta$  disjoint annuli of scale  $3\eta$  can be produced along a curve of this diameter each of which has a uniform probability of containing preventative steps. This is an estimate for a single crossing which should, as a bound, be multiplied by the number of (disjoint) crossings that  $\gamma_1$  makes of the rectangle in question. While *a priori* the latter is unbounded, by invoking the no  $\vartheta'$ - $\eta$  doublebacking (Assumption 1), it is clear that each successive pass of  $\gamma_1$  must contain a point around which a box of scale  $\eta$  can be drawn which has not yet been visited by the curve. In a rectangle of the type described, there can be at most of the order  $(\vartheta'/\eta)^2$  such “pixels”, which will suffice for our estimate on the number of crossings. Finally,

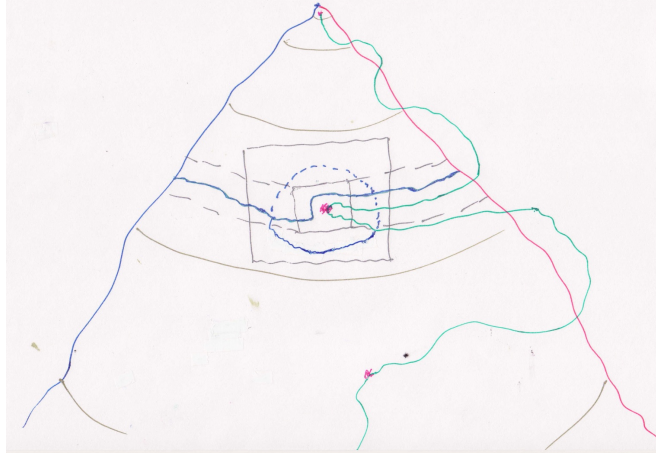


Figure VI.14: Final RSW construction to continue crossing.

$\Omega$  can be covered by of the order  $(1/\vartheta')^2$  such rectangles and, combining these considerations, we arrive at the formula in the previous display.

Thus let  $k$  denote, more or less, the total number of independent scales available:  $3^{k-1} \leq \delta_2/\vartheta \leq 3^k$  and  $v = v(\kappa)$  the parameter from Lemma VI.2.11/Assumption 2. Then we have, with high probability, a sequence of disjoint annuli on scales  $\vartheta_{\ell_1}, \dots, \vartheta_{\ell_A}$ , where  $A > vk$ , in each of which is some point  $x_{\ell_j}$ , which enjoy the following properties: 1)  $x_{\ell_j} \in \gamma_2([m, s])$ , where  $s$  is the last time  $\gamma_2$  exits the ball. 2) There is a neighborhood of scale  $\kappa\vartheta_{\ell_j}$  around  $x_{\ell_j}$  which is in the interior of  $\mathbb{B}^c$  (explicitly,  $\beta$  and  $\gamma_1([0, m])$  do not enter this neighborhood).

***The Bulk Case: Percolation Construction to Continue  $\beta$***

We finally show that by standard percolation arguments, this implies that with a uniform probability, a point on  $\gamma_2$  – in the above discussed neighborhood – is connected by a blue path to  $\beta$ , thus establishing Claim 2. Indeed, we may first construct a 3:1 annulus of scale  $\kappa\vartheta_{\ell_j}$  with  $x_{\ell_j}$  at its center. By RSW

estimates, a separating blue circuit occurs in this annulus with uniform, in  $\ell$ , probability. Next, temporarily foregoing which part of the annulus of scale  $\vartheta_{\ell_j}$  is in  $\mathbb{B}$  and which part in  $\mathbb{B}^c$ , we consider a “corridor” of width  $\kappa\vartheta/3$  running through the inner portion of our neighborhood and circling around the  $\vartheta_{\ell_j}$  annulus. Within this corridor, one can have a blue circuit with a probability that is uniform in  $\vartheta_{\ell_j}$  – albeit tending to zero as  $\kappa \rightarrow 0$ . Restricting this circuit to the region  $\mathbb{B}^c$ , it is not hard to see that the above construction connects the relevant portion of  $\gamma_2$  to  $\beta$ . Since all this happens with uniform probability on all relevant scales, the desired connection between  $\gamma_2$  and  $\beta$  has been established, with high probability. For an illustration of this construction see Figure VI.14.

***The Boundary Cases:  $M$  Close to the Boundary***

For technical reasons that shall become clear, we shall first treat the cases where  $M$  is close to the boundary, and then the tip cases (although the opposite order would seem more fundamental). So let us suppose that  $M$  is within distance  $\delta_2$  of the boundary. We first consider red pseudo-pods. The description for what  $\gamma_1$  must do in this case remain the same as in the bulk case, the only danger being that some visits may now be short; it is clear that this can only happen if  $M$  is close to  $a$  or  $M$  is close to  $c$ . The point  $M$  cannot be close to  $c$  since  $\gamma_1([0, T])$  is outside the  $\Delta$  neighborhood of  $c$ . If the point  $M$  is in the  $\delta_2$  neighborhood of  $a$ , the requirement that  $\beta$  visit this neighborhood renders the production of a blue crossing sufficiently unlikely for our purposes. Later on we will in fact assert that  $M$  is at least a distance  $\Delta_4$  away from  $a$ .

We next consider the cases of blue pseudo-pods when  $M$  is close to some

boundary. First, suppose  $M$  is close to  $[a, b]$  or  $[d, a]$ . In these cases, it is not difficult to see that all of the five long arms actually remain long and the bulk argument applies without change. Next, we consider the cases where  $M$  is within  $\delta_2$  of the  $[b, c]$  or  $[c, d]$  boundary. The case of the  $[b, c]$  boundary will be ruled out on the grounds of overall unlikelihood. Specifically, let us define a *choke point* as a point on  $\gamma_1$  within or at a distance  $\delta_2$  of the  $[b, c]$  boundary with the property that it can be connected to  $[b, c]$  by some path inside the  $\delta_2$  neighborhood of  $[b, c]$  in the complement of the earlier portion of  $\gamma_1$ . It is clear that anytime  $\gamma_1$  visits the  $\delta_2$  neighborhood of  $[b, c]$  there exists a choke point (e.g., the first time  $\gamma_1$  visits the  $\delta_2$  neighborhood of  $[b, c]$ ). As for the present circumstances, let  $Y$  be the latest choke point along  $\gamma_1$ . Let us join  $Y$  to  $[b, c]$  in the complement of  $\gamma_1$  (up to the point  $Y$ ) inside the  $\delta_1$  neighborhood of  $[b, c]$ . Observe that  $\gamma_1$  up to  $Y$ , the line joining  $Y$  to  $[b, c]$ , and the relevant portions of  $[a, b]$  and  $[b, c]$  form a Jordan domain and the “inner” boundary of this domain formed by  $\gamma_1$  is blue.

If  $M$  is indeed within  $\delta_2$  of  $[b, c]$ , then either  $M$  happened before (or at) or after  $Y$ . If  $M$  happened before  $Y$ , then by the previous observation it is on the (inner) boundary of this domain and therefore any blue crossing from  $[c, d]$  must pass “over”  $Y$  in order to reach  $M$  (note that from the perspective of the percolation configurations,  $Y$  is deterministic). Since we are well away (distance  $\Delta$ ) from the corner  $c$ , this probability vanishes as  $\delta_2/\Delta \rightarrow 0$ . (Technically, the probability will vanish as a power of  $\delta_2/\tilde{\Delta}$ , where  $\tilde{\Delta} \lesssim \Delta$  is defined as the distance between  $[b, c]$  and  $[c, d]$  outside the  $\Delta$  neighborhood of  $c$ .) On the other hand, if  $M$  happened after  $Y$ , then either  $M$  is inside  $B_{\delta_1}(Y)$  or not.

In the former case, the blue path is again rare (albeit with slightly modified estimate). In the latter case, we claim that there is a  $\delta_1$ - $\delta_2$  double-visit to the boundary: Since  $M$  is *not* a choke point, and is within  $\delta_2$  of  $[b, c]$ , it is separated from  $[b, c]$  by a previous portion of  $\gamma_1$ , which constitutes the point(s) of revisitation (some portion of  $\gamma_1$  must “travel” at least distance  $\delta_1$  in order to get to  $Y$  – from the  $\delta_2$  neighborhood of  $M$  – and must have already traveled a distance  $\delta_1$  in order to have arrived from  $a$ ).

We now turn attention to the  $[c, d]$  boundary. Here, the argument will be similar in spirit but differing in detail. As in the previous case, we define the point  $J$  to be the last choke point on the curve  $\gamma_1([0, T])$ . We first remind the reader that  $\delta_2 \ll \delta_{3/2} \ll \delta_1$ . Again we divide into two cases, the first of which is  $M$  occurring before  $J$  and/or  $M$  occurring in the  $\delta_{3/2}$  neighborhood of  $J$ . Here, in order for a blue pseudo-pod to happen, a long blue arm – of length at least  $\delta_1$  – must emanate from the  $\delta_{3/2}$  vicinity of the point  $J$ , which renders this event improbable, again because the point  $J$  is deterministic (at least as far as the active percolation configurations are concerned). The remaining case is  $M$  occurring after  $J$  and outside the  $\delta_{3/2}$  neighborhood of  $J$ . This is identical to the argument in the previous paragraph, with relabeling of scales – it now leads to a  $\delta_{3/2}$ - $\delta_2$  double visit to the boundary.

***The Boundary Cases: “Tip” Close to the Boundary***

Finally we dispense with cases where  $\gamma_1(T)$  and  $\gamma_2(T)$  are close to  $\partial\Omega$ . Again we remind the reader that separate arguments are needed for these cases, since our scales are *fixed*.

We start with situations where  $\gamma_1(T)$  and  $\gamma_2(T)$  are  $\Delta$ -close to  $a, b, c, d$ ; the

latter three corners we need not consider by the definition of  $\Xi_{\theta,\Delta}$  (property 4),  $\gamma_1(T)$  and  $\gamma_2(T)$  and/or the assumptions of the lemma. Finally let us consider the corner  $a$ . Then, again by the definition of  $\Xi_{\theta,\Delta}$  (Assumption 6),  $\gamma_1([0, T])$  and  $\gamma_2([0, T])$  are contained in a  $\Delta_1$ -neighborhood of  $a$ , but in this case, by Russo–Seymour–Welsh,  $a$  is sealed by many rings of both colors with high probability and hence neither  $\gamma_1$  nor  $\gamma_2$  actually participate in any crossing event of interest.

Next suppose  $\gamma_1(T)$  and  $\gamma_2(T)$  are  $\delta_1$  close to some boundary and not close to any corners. The case when the tip is close to  $[b, c]$  has essentially already been handled in the context of the identical argument for the cases when  $M$  is close to these boundaries. We define choke points, etc. using  $\delta_1$  as the small scale and  $\Delta_4$  as the large scale and the argument goes through *mutatis mutandis* (here we require the special clause in Assumption 4). The case when  $\gamma_1(T)$  and  $\gamma_2(T)$  are close to the  $[c, d]$  boundary follows from the color reverse of the argument for the  $[b, c]$  boundary. Finally, the cases where  $\gamma_1(T)$  and  $\gamma_2(T)$  are close to the opposite sorts of boundaries (where paths possibly terminate) can be handled by a similar argument.

**Quantification of Estimates.** The set  $\Xi_{\theta,\Delta}$  is defined by Assumptions 1 – 6 and the  $\mu_\varepsilon$  measure of  $\Xi_{\theta,\Delta}$  is given by estimates from §VI.2, which are uniform in  $\varepsilon$  for  $\varepsilon$  sufficiently small. The estimates on  $|C_\varepsilon(R_1) - C_\varepsilon(R_2)|$  follow from RSW type estimates and estimates from §VI.2, which are scale invariant, and thus with the scales in (VI.6) set, and  $\varepsilon$  much less than the relevant scales, are also uniform in  $\varepsilon$  for  $\varepsilon$  sufficiently small. Finally, we may envision the scales in (VI.6) to be power-law, e.g.,  $\eta = \delta^a$  for some  $a > 1$ ,

and since the estimates from §VI.2 are of the form e.g.,  $c(\eta/\delta)^{\alpha'}$  (for constants  $c, \alpha' > 0$ ), we may rewrite our estimates in the form  $C'\eta^\alpha := \theta$ , which gives the form of  $\eta$  described.

The proof is now complete.

□

## VI.4 Corollaries to the Main Result

In this section we discuss some consequences of Lemma VI.3.1.

### VI.4.1 Limiting Martingale

A fairly easy consequence is that we obtain (via elementary means) the statement that the limiting crossing probability in the domain slit by the some  $\mu'$ -typical curve up till some time  $t$  is a martingale (this is one key step in the proof of convergence to  $\text{SLE}_6$  in [5]).

Let us describe the setting: Let  $(\Omega, a, b, c, d)$  be a conformal rectangle,  $C_\varepsilon$  denote the crossing probability from  $[a, b]$  to  $[c, d]$  at the  $\varepsilon$ -scale,  $\Omega_\varepsilon$  denotes  $\Omega$  with some suitable discretization and  $\mathbb{X}_{[0,t]}^\varepsilon$  denotes the interface up to some time  $t$  (parametrized in some reasonable fashion), then

$$C_\varepsilon(\Omega_\varepsilon, a, b, c, d \mid \mathbb{X}_{[0,t]}^\varepsilon) = C_\varepsilon(\Omega_\varepsilon \setminus \mathbb{X}_{[0,t]}^\varepsilon, \mathbb{X}_t^\varepsilon, b, c, d), \quad (\text{VI.7})$$

(we are ignoring for the moment that  $\mathbb{X}_{[0,t]}$  has already hit  $\partial\Omega$ ) hence  $C_t^\varepsilon := C_\varepsilon(\Omega \setminus \mathbb{X}_{[0,t]}^\varepsilon, \mathbb{X}_t^\varepsilon, b, c, d)$  is a martingale for  $\varepsilon > 0$ . We will obtain a limiting version of (VI.7).

**Corollary VI.4.1.** *Consider  $\mu'$ -typical curves and parametrize them by Löwner parametrization. Define*

$$\mathbf{1}_{\mathcal{E}_\Omega}(\gamma) = \begin{cases} 1 & \text{if } \gamma \text{ hits } [c, d] \text{ before } [b, c] \\ 0 & \text{if } \gamma \text{ hits } [b, c] \text{ before } [c, d] \end{cases}$$

and

$$K_0(\mathbb{X}_{[0,t]}) = C_0(\Omega \setminus \mathbb{X}_{[0,t]}, \mathbb{X}_{[0,t]}, b, c, d),$$

where  $C_0$  denotes the limiting crossing probability (which we assume to exist).

Then

$$K_0(\mathbb{X}_{[0,t]}) = E_{\mu'}(\mathbf{1}_{\mathcal{E}_\Omega} \mid \sigma([0, t])),$$

where  $\sigma([0, t])$  denotes the  $\sigma$ -algebra generated by  $\mu'$  supported curves up to time  $t$ , so in particular  $K_0(\mathbb{X}_{[0,t]})$  is a martingale.

*Proof.* Lemma VI.3.1 gives an equicontinuity result (in  $\varepsilon$ ) outside a set with uniformly small measure, and hence we obtain a limiting (weak) version of (VI.7). For more details we refer the reader to Proof of Main Theorem in [5]. □

**Remark VI.4.2.** We have stated the above result without explicit reference to Cardy's Formula and instead assumed that there exists a limiting crossing probability function  $C_0(\Omega, a, b, c, d)$  (viewed as a function of domain and marked points). Lemma VI.3.1 implies that such a function is continuous if it exists and since  $C_\varepsilon$ 's are bounded, in a suitable setting (e.g., where we have a countable dense subset of a class of domains under consideration, equipped with a suitable norm) it is not difficult to abstractly extract a limiting func-

tion. Along these lines, we also draw the reader's attention to Remark 5.6 in [4].

## VI.4.2 Rate of Convergence to $\text{SLE}_6$ : Discussion

Let us conclude by arguing very loosely why we expect to obtain some rate of convergence from Lemma VI.3.1. In particular, we expect power law rate of convergence, i.e., at some rate  $\varepsilon^\alpha$ ,  $\alpha > 0$ .

First we recall that on the upper half plane  $\mathbb{H}$ , if we consider curves  $\gamma(t)$  to be growing from 0 to  $\infty$ , and  $g_t$  is the conformal map from  $\mathbb{H} \setminus \gamma([0, t])$  to  $\mathbb{H}$ , then  $g_t$  satisfies  $\partial_t g_t(z) = 2/(g_t(z) - w(t))$ , where

$$w(t) = g_t(\gamma(t))$$

is the *driving function*. Convergence to  $\text{SLE}_6$  means that the corresponding random driving function for limiting interfacial curves is given by  $6B_t$ , where  $B_t$  denotes standard Brownian motion.

Now let us work instead on the equilateral triangle  $\mathbb{T}$  with vertices at  $\{0, 1, e^{\frac{i\pi}{3}}\}$ . More precisely, let us conformally map our conformal rectangle  $(\Omega \setminus \gamma([0, t]), \gamma_t, b, c, d)$  to  $(\mathbb{T}, x, 1, e^{\frac{i\pi}{3}}, 0)$  via  $G_t$  so that  $x = G_t(\gamma_t) =: w(t) \in [0, 1]$ . We note that if  $\gamma_t$  is mapped to it is the case that

$$G_t(\gamma_t) = C_0(\Omega \setminus \gamma([0, t]), \gamma_t, b, c, d).$$

Here  $C_0$  denotes Cardy's Formula and one way to see this is to recall Carleson's observation about Cardy's Formula on an equilateral triangle with side length one (see [13] and also [14]).

Thus, the driving function  $w(t)$  (on the triangle) is given as Cardy's Formula in the corresponding slit domain. Therefore, if say  $\gamma_n \rightarrow \gamma$  in the sup-norm (we envision e.g.,  $\varepsilon = n^{-1}$ ), and  $w_n$  and  $w$  denote the driving functions of  $w_n$  and  $w$ , respectively, then

$$|C_0(\Omega \setminus \gamma_n([0, t]), \gamma_n(t), b, c, d) - C_0(\Omega \setminus \gamma([0, t]), \gamma(t), b, c, d)| = |w_n(t) - w(t)|.$$

The left hand side can be estimated by Lemma VI.3.1, if we can provide some knowledge of the distance between  $\gamma_n$  and  $\gamma$ , which would boil down to estimating e.g.,  $|\mu_\varepsilon(N_\eta) - \mu_{\varepsilon'}(N_\eta)|$  for  $\varepsilon \ll \varepsilon'$ , where  $N_\eta$  is some sup-norm  $\eta$  neighborhood. (Recall that so far the convergence of  $\mu_\varepsilon$  to  $\mu'$  is weak.) Given Lemma VI.3.1, it appears that the best we can hope for is some power-law rate of convergence: e.g.,  $\mathbb{P}(\sup_{t \in [0, T]} |w_n(t) - w(t)| > n^{-\alpha}) < \varphi(n)$ , where  $\varphi(n) \rightarrow 0$  as  $n \rightarrow \infty$ . We note that again, Lemma VI.3.1 would contribute a power-law to  $\varphi(n)$ .

# Bibliography

- [1] M. Aizenman. *The Geometry of Critical Percolation and Conformal Invariance*. Proceedings STATPHYS19 (Xiamen 1995), H. Bai-lin (ed.), World Scientific (1995).
- [2] M. Aizenman and A. Burchard. *Hölder Regularity and Dimension Bounds for Random Curves*. *Duke Math. J.* **99**, no. 3, 419–453 (1999).
- [3] C. Benes, F. Johansson, and M. J. Kozdron. On the rate of convergence of loop-erased random walk to SLE(2). arXiv:0911.3988v1
- [4] I. Binder, L. Chayes, and H. K. Lei. *On Convergence to  $SLE_6$  II: Discrete Approximations and Extraction of Cardy's Formula for General Domains*. Submitted.
- [5] I. Binder, L. Chayes, and H. K. Lei. *On Convergence to  $SLE_6$  I: Conformal Invariance for Certain Models of the Bond-Triangular Type*. Submitted.
- [6] B. Bollobás and O. Riordan. *Percolation*. Cambridge: Cambridge University Press (2006).

- [7] J. T. Chayes and L. Chayes. *Percolation and Random Media*. In: Osterwalder, K., Stora, R. (eds.) Les Houches Session XLIII: Critical Phenomena, Random Systems and Gauge Theories, pp. 1001–1042. Amsterdam: Elsevier (1986).
- [8] G. Grimmett. *Percolation*. Berlin, New York: Springer Verlag (1999).
- [9] H. Kesten. *Analyticity Properties and Power Law Estimates of Functions in Percolation Theory*. J. Stat. Phys., **25**, no. 4, 717–756 (1981).
- [10] H. Kesten. *Percolation Theory for Mathematicians*. Boston, Basel, Stuttgart: Birkhauser (1982).
- [11] H. Kesten. *Scaling Relations for 2D-Percolation*. Comm. Math. Phys. **109**, 109–156 (1987).
- [12] G. F. Lawler, O. Schramm, W. Werner. *One-Arm Exponent for Critical 2D Percolation*. Electronic Journal of Probability, **7**, 13 pages (electronic) (2002).
- [13] S. Smirnov. *Critical Percolation in the Plane: Conformal Invariance, Cardy’s Formula, Scaling Limits*. C. R. Acad. Sci. Paris Sr. I Math. **333**, 239–244 (2001).  
Also available at <http://www.math.kth.se/~stas/papers/percras.ps>.
- [14] W. Werner. *Lectures on Two-Dimensional Critical Percolation*. arXiv:0710.0856